WORLDSHEET MODELS AND THE SCATTERING EQUATIONS

From Strings to Quantum Field Theory and back

Ricardo Stark-Muchão

Supervised by

Dr. Ricardo Monteiro

Thesis submitted to

Queen Mary University of London

in partial fulfilment for the award of the degree of

DOCTOR OF PHILOSOPHY

SCHOOL OF PHYSICS AND ASTRONOMY
CENTRE FOR RESEARCH IN STRING THEORY

August 2021

Abstract

Through many surprising developments, the study of scattering amplitudes in quantum field theory has unearthed deeper questions into the nature of our understanding of the subject. One of these developments which has been quite successful is the culmination of two active areas of research: the colour-kinematics duality and the notion of worldsheet models. This development was first understood as the CHY formalism, which in its inception compactly described the entire tree-level S-matrix of Yang-Mills theory and gravity. The task of computing scattering amplitudes in this formalism equates to solving a set of algebraic equations denoted the scattering equations. Since then, this has been more generally understood to arise naturally from the ambitwistor string, a chiral worldsheet model that allows a straightforward extension of CHY to compute quantum corrections in terms of worldsheet formulae. In this thesis we discuss these worldsheet formulae at loop-level, emphasising the connection between the scattering equations and the resulting field theory expressions. We develop a novel form of one-loop BCFW integrand recursion in momentum space, which motivates a construction of new one-loop scattering equations which results in quadratic propagators, a feature that typical loop-level worldsheet formulae do not exhibit. We then present n-point two-loop formulae for the integrands of pure Yang-Mills and gravity, motivated by the genus-two ambitwistor string. Finally, we use the ambitwistor string as a steppingstone back to superstring theory, where we present a strategy that allows proposals for massless superstring integrands at loop-level to be computed from their field theory counterparts. Using this strategy, we show that two-loop superstring results are reproduced purely from field theory and give a proposal for the three-loop four-point superstring result.

Declaration

I, Ricardo Stark-Muchão, confirm that the research included within this thesis is my own work or that where it has been carried out in collaboration with, or supported by others, that this is duly acknowledged below and my contribution indicated. Previously published material is also acknowledged below.

I attest that I have exercised reasonable care to ensure that the work is original, and does not to the best of my knowledge break any UK law, infringe any third party's copyright or other Intellectual Property Right, or contain any confidential material. I accept that the College has the right to use plagiarism detection software to check the electronic version of the thesis.

I confirm that this thesis has not been previously submitted for the award of a degree by this or any other university. The copyright of this thesis rests with the author and no quotation from it or information derived from it may be published without the prior written consent of the author.

Signature:

Date: August 31, 2021

This thesis describes research carried out with my supervisor Ricardo Monteiro which was published in [1–3]. It also contains some unpublished material. We collaborated with Yvonne Geyer on all of the published work mentioned above. In [1] we also collaborated with Arthur Lipstein and Joe Farrow. Where other sources have been used, they are cited in the bibliography.

I have also co-authored work published in [4,5] in collaboration with Chris White and Nadia Bahjat-Abbas. This work is however not the main topic of this thesis.

Chapters 1 and 2 are dedicated as reviews of topics required to understand the material of the thesis. I attest that I strongly believe to have appropriately cited the relevant works therein.

Acknowledgements

It goes without saying that I am greatly indebted to my supervisor Ricardo Monteiro, who not only gave me the opportunity to achieve a goal of mine for many years, but for being such an inspiring guide throughout my time as a PhD student. I have learnt many things from him, not just the complex academic topics throughout my research, but also how to approach problems more effectively and efficiently, how to take opportunities, and how to conveniently address collaborators with the same name. I would also like to thank him for introducing me to many other great physicists throughout my studies.

This includes our main collaborator Yvonne Geyer, whom I would like to thank for being patient with me, and an inspiration for me throughout my studies. As well as her uplifting attitude, knowledge, and approach to physics, I will miss seeing the different exotic locations she found herself in during our Skype chats.

I owe many thanks to all of the PhD students in CRST I have encountered, and particularly to Joe Hayling and Rodolfo Panarei, who welcomed me into department with open arms and always made sure I never went long without laughter.

I owe myself to many of the members of CRST whom I have learnt from and had great conversations with, including Costis Papageorgakis, Chris White, Gabriele Travaglini, Sanjaye Ramgoolam and David Berman. I would like to give a special thanks to Andreas Brandhuber, my supervisor throughout my undergraduate, who introduced me to the advanced topics in theoretical physics, particularly scattering amplitudes.

The time throughout my studies would not have been anywhere near as great if it was not for Nadia Bahjat-Abbas, who was my partner in crime throughout my PhD. I am very lucky to have met her, and more so to have worked with her; our time working on problems in physics manifested what makes working on problems fun.

I would like to say that I owe everything to my mother Jacqueline Stark, my father Jorge Muchão, and my sister Paris Stark. Without their love and support, I could not have reached a fraction of the milestones I have; they have and always will motivate me to be try and achieve my best. I love you all with all my heart.

Finally, I would like to thank all of my other friends and family, and deeply apologise for not having the space to mention you all in great detail. Of my friends in particular, I would like to thank Deividas Gailiunas and his family, for always being there even when we started out in physics many moons ago.

Contents

Introduction

On small scales, nature appears to be described very adequately by *quantum field theory* (QFT). This theory turns out to be arguably one of the most successful scientific theories ever created. The predictions of QFT, more specifically the standard model, have been successful many times through comparison to experiments e.g. at the LHC. Of particular importance in this respect is the study of quantum chromodynamics (QCD). For example, comparing theory to high-precision experiments requires (in part) knowledge of jet processes involving gluons, the mediators of the strong force. These comparisons are possible through one of the fundamental observables of QFT, namely the cross-section. The calculation of the cross-section of a process in theory requires the *scattering amplitude*. The scattering amplitude is used for calculating the probability that a scattering process will occur a certain way and is therefore itself fundamental to QFT. The complete set of scattering amplitudes for a theory can be described by its *S-matrix*, which dictates how initial states end up in final states.

Traditionally, the scattering amplitude for a process is calculated using *Feynman diagrams*. These provide an intuitive and systematic way of calculating the amplitude, with each theory having its set of Feynman rules. However, for theories well-suited to describing nature, the use of Feynman diagrams can quickly become computationally overwhelming. An example of this can be seen in the table below, which specifies the number of Feynman diagrams required for a process involving n gluons, calculated in [6].

Number of gluons n	Number of required Feynman diagrams
4	4
6	220
8	34,300
10	10,525,900

Moreover, the size of the mathematical expression for each diagram grows as n increases. The complexity of the problem is therefore even greater than the table above indicates.

Where does this complexity stem from? Feynman diagrams are, as mentioned above, intuitive, since the Feynman rules are (typically) designed to give local expressions, since they derive from (typically) a local action. This however requires the use of many diagrams to capture all the right information. Moreover, especially in the case described in the above table, each diagram itself is not *gauge-invariant*; only the amplitude (the sum of all Feynman diagrams) is gauge-invariant. By being intuitive, they lose efficiency. The case of gravity, where processes involve the scattering of *gravitons*, is even worse.

Many techniques that have been discovered since the inception of Feynman diagrams have shown that scattering amplitudes can in fact be expressed in a more efficient and com-

pact manner. An example of this is the *Parke-Taylor* amplitude [7], which describe the scattering of gluons with a maximally helicity-violating (MHV) configuration, and are composed of only a single term for any number n of gluons. These techniques all revolve around the same question: *what is the S-matrix?* Indeed, the study of scattering amplitudes has unearthed deeper questions about quantum field theory itself, and precisely how the theories therein are related to one another.

This thesis will be focused on one of the more recent developments that is the result of (a little over) two decades of work, with origins older still. This development regards the notion of *worldsheet models*. These are based on the techniques of string theory, where the scattering of particles is obtainable by the scattering of strings (which forms a *worldsheet*) in an abstract space. It is the culmination of two lines of development in scattering amplitude techniques.

The first has origins in string theory itself, where Kawai, Lewellin, and Tye (KLT) found that closed string amplitudes can be written as a product of open string amplitudes [8]. These were come to be known as the *KLT relations* and provided the first notion of what is known today as the *double copy* between amplitudes, where gravity calculations (from closed strings) can be obtained using the results of Yang-Mills calculations (from open strings). These appeared in the context of field theory in [9], where the analogous relations were discovered by Bern, Carrasco, and Johansson (BCJ). Using these relations, it was found in the same reference one could write the tree-level scattering amplitudes of Yang-Mills theory as[1]

$$\mathcal{A}_{\rm YM} = (-1)^{n+1} \sum_{\mathrm{a}\in\Gamma_n} \frac{n_{\mathrm{a}}\, c_{\mathrm{a}}}{D_{\mathrm{a}}}\,.$$

In the above, the label 'a' runs over the set of n-point trivalent diagrams Γ_n, each one having a *colour factor* c_{a} encoding the information on the colour degrees of freedom, a *kinematic numerator* factor n_{a}, and a set of propagators D_{a} determined by the diagram. A crucial feature of this representation of the scattering amplitude introduced the notion of the *colour-kinematics duality*. Specifically, if the colour factors between a set of diagrams are related by the *Jacobi identity*, then the corresponding kinematic numerators are related in the same way,

$$c_{\mathrm{a}} + c_{\mathrm{b}} + c_{\mathrm{c}} = 0 \qquad \Leftrightarrow \qquad n_{\mathrm{a}} + n_{\mathrm{b}} + n_{\mathrm{c}} = 0\,.$$

This is a very non-trivial property of kinematic numerators in scattering amplitudes. Since the propagators and colour factors are straightforwardly obtained from the structure of the diagram, the task of obtaining the Yang-Mills amplitude equates to finding the set of *BCJ numerators* n_{a}. An even more remarkable property of this representation is that, once the BCJ numerators have been found, one can straightforwardly obtain a gravity amplitude but substituting the colour factors with another kinematic factor[2],

$$\mathcal{A}_{\rm grav} = (-1)^{n+1} \sum_{\mathrm{a}\in\Gamma_n} \frac{n_{\mathrm{a}}\, \tilde{n}_{\mathrm{a}}}{D_{\mathrm{a}}}\,.$$

[1] Throughout this thesis we will omit the coupling constants, which can easily be put back in through scaling considerations. We will also use conventions in which all external momenta are incoming. The $(-1)^{n+1}$ factor in the BCJ formulae here are placed to match normalisations with the results we obtain in the next chapter.

[2] We note here that the second set of kinematic numerators do *not* have to belong to the same theory, and in fact one can obtain amplitudes in a particular theory by 'mixing' the BCJ numerators in others. Moreover, only *one* of the sets of numerators need to obey the Jacobi identity. For more details on this see e.g. [10].

This is remarkable for a couple of reasons. First of all, expanding the Einstein-Hilbert action produces an infinite number of vertices in the Feynman rules, whereas the above formula requires only diagrams with trivalent vertices. Secondly, it means that gravity amplitude follows directly from those calculated for Yang-Mills in this representation. This is one of the signature features of *gauge/gravity duality*, and possibly hints at something more fundamental about QFT that is currently unknown. The BCJ representation of scattering amplitudes above has been proved [11] and is well-understood at tree-level, and the conjecture to loop-level [12], though not currently proven, has been quite fruitful, particularly through the method of unitarity for scattering amplitudes [10, 12–16] and the study of gravitational waves [17–20]. More detail on this and many other applications of the colour-kinematics duality can be found in the extensive review of [10].

The second line of development began when Witten discovered the *twistor string* [21], where he found that certain amplitudes in $\mathcal{N} = 4$ super Yang-Mills theory were supported on certain holomorphic curves in twistor space. This was the original worldsheet model and was further studied in [22] where it was found that the challenge of computing scattering amplitudes in this formalism equated to solving a set of algebraic equations, a feature that would carry through to the worldsheet model that is the topic of this thesis. Witten's discovery furnished developments that led to twistor-string descriptions of (super-)gravity [23–28], as well as their connections to other on-shell formalisms such as BCFW recursion and MHV diagrams [29–35]. Being twistor string descriptions, the resulting formulae were mainly for theories in four-dimensions. Ultimately, Cachazo, He and Yuan (CHY), following work by Cachazo and Skinner [36], began studying the set of algebraic equations that appeared in the twistor-string formulae, and found connections to the KLT relations [37]. This led to the inception of the *CHY formalism* [38], which represented scattering amplitudes of Yang-Mills and gravity as integrals over the moduli space of punctured Riemann surfaces. Whilst very reminiscent to traditional string theory, these integrations are localised over the solutions to this set of algebraic equations, called *the scattering equations*,

$$\sum_{j\neq i} \frac{k_i \cdot k_j}{\sigma_i - \sigma_j} = 0\,, \qquad\qquad i = 1, 2, \cdots, n\,.$$

Unlike their predecessors, these *worldsheet formulae* give results in D-dimensions and clearly manifest a double-copy structure. The success of this formalism has led to worldsheet formulae for many other theories, such as the biadjoint scalar theory [39], ϕ^n theory [40], and a large variety of others related by the double copy [41, 42]. Due to its clear resemblance with string scattering amplitudes, it was not long after the discovery of CHY that a string-like description was found. This was done by Mason and Skinner in [43], where they found that defining a string theory in *ambitwistor space*, the space of null geodesics in complexified spacetime, not only naturally produces the scattering equations, but furthermore results precisely in the CHY formulae for gravity. Moreover, an ambitwistor string description for these theories allows an alternative study in non-trivial backgrounds [44–49], and importantly for us, a natural extension to loop-level, first performed rigorously at one-loop in [50] and two-loops in [51].

In this thesis, we will discuss these worldsheet models and the scattering equations at loop-level, primarily focusing on the role that the scattering equations play and their relationship with the resulting loop-integrands.

Chapter 1 is dedicated to a review of the CHY formalism, where we introduce its basic ingredients and discuss the structure of the integrands that will be of primary concern to

us. We will review two algorithms present in [52] and [39] that will allow one to evaluate a vast number of formulae we present in later chapters, and understand how this formalism leads directly to the BCJ representation of scattering amplitudes.

We also dedicate chapter 2 to a review of the ambitwistor string at genus zero and one, showing the origins of the scattering equations, how the ambitwistor string leads directly to gravity in CHY, and the role of the scattering equations at one-loop. A particular feature of the one-loop formulae will be that it exhibits an unorthodox representation of the loop integrand, which can be described as a type of forward-limit.

We study this description in chapter 3 in two different contexts The first, applicable to field theory, will be a new interpretation of BCFW recursion for the one-loop integrand in momentum space. The second, applicable to worldsheet formulae, will be a new set of scattering equations that give rise to quadratic propagators more akin to conventional field theory. We demonstrate their applications in both cases with a number of examples and discuss their extension to non-planar theories.

In chapter 4 we extend this forward-limit interpretation to two-loops and obtain formulae for the two-loop n-point integrand of pure Yang-Mills and gravity in this unorthodox representation. These follow from the modification of a naive guess based on worldsheet formulae; we derive this modification and postulate its origin from the genus-two ambitwistor string after discussing the case with supersymmetry, following the work of [51].

In chapter 5 we attempt to come full circle with the superstring, and propose a strategy to obtain superstring loop integrands for massless states from the field theory limit, using the ambitwistor string as a steppingstone. We demonstrate that this strategy works at two-loops and use it to give a proposal for the genus-three superstring amplitude for four massless states.

Finally, we end with some concluding remarks and an outlook regarding future work.

Chapter 1

The CHY formalism and the scattering equations

As mentioned in the introduction, the CHY formalism is the natural successor to previous twistor string models, and its form provides the basis of all worldsheet formulae we will present in this thesis. This section is dedicated to a review of the CHY formalism, and how precisely it can reproduce the BCJ representation of scattering amplitudes in field theory. A simple and systematic way of doing the latter requires knowledge of two algorithms, which we will discuss in detail. They are also added for completeness, since they can be used to explicitly evaluate the formulae we will present throughout the thesis, particularly for non-supersymmetric theories at loop-level.

1.1 CHY amplitudes and their primary ingredients

In the CHY formalism, n-point tree-level amplitudes for massless particles are represented as integrals over the moduli space of an n-punctured Riemann sphere [38],

$$\mathcal{A}_n^{(0)} = \int_{\mathfrak{M}_{0,n}} d\mu_n \, \mathcal{I}_n \, . \tag{1.1.1}$$

As one can see, it is formed of two essential ingredients. The first is the CHY *measure*,

$$d\mu_n = \frac{d^n\sigma}{\text{vol SL}(2,\mathbb{C})} \prod_i{}' \bar{\delta}\left(\mathcal{E}_i\right) \, , \tag{1.1.2}$$

which provides the measure for the locations of the punctures $\sigma_i \in \mathbb{CP}^1$, which are to be integrated over. The vol $\text{SL}(2,\mathbb{C})$ factor is a symmetry factor; sets of locations for the punctures are related to others by $\text{SL}(2,\mathbb{C})$ transformations, a residual symmetry from the group of diffeomorphisms on the sphere. Dividing by this factor ensures that there is no over-counting when one integrates over these locations. In practice, this is achieved by fixing the location of any three punctures σ_r, σ_s, σ_t and multiplying the integrand by $\sigma_{rs}\sigma_{st}\sigma_{tr}$, where[1] $\sigma_{ij} := \sigma_i - \sigma_j$. That three punctures are fixed means there are essentially $(n-3)$ integrals to perform in (1.1.2).

[1] This notation will be used throughout this thesis.

The complex delta functions[2] enforce the *scattering equations*

$$\mathcal{E}_i = \sum_{j\neq i} \frac{k_i \cdot k_j}{\sigma_{ij}}\,, \tag{1.1.3}$$

which play an essential role in this formalism. These equations were first discovered in [53–55] in the context of dual resonance models, and in [56] in the context of high-energy scattering of strings. They were first noticed in the context of field theory explicitly in [37], based on formulae for the tree-level S-matrix of maximally supersymmetric Yang-Mills and gravity [22, 36] inspired by the twistor string [21]. Whilst the amplitude (1.1.1) looks more familiar from string theory, where the n-punctured Riemann sphere is essentially the worldsheet, it is the scattering equations (1.1.3) which make the amplitudes inherently correspond to field theory; we will discuss this in more detail in the next section.

The scattering equations also exhibit an $\mathrm{SL}(2,\mathbb{C})$ symmetry on the support of momentum conservation, which can be summarised through the following identities

$$\sum_i \mathcal{E}_i = 0\,, \qquad \sum_i \sigma_i\,\mathcal{E}_i = 0\,, \qquad \sum_i \sigma_i^2\,\mathcal{E}_i = 0\,. \tag{1.1.4}$$

As a result, not all n scattering equations are linearly independent, and so only $(n-3)$ of them need to be enforced. In (1.1.2) this is precisely what the prime on the product entails: for any three particle labels r', s' and t', the primed product omits their scattering equations and compensates with a factor $\sigma_{r's'}\sigma_{s't'}\sigma_{t'r'}$,

$$\prod_i{}' \bar{\delta}(\mathcal{E}_i) := \sigma_{r's'}\sigma_{s't'}\sigma_{t'r'} \prod_{i\neq r',\,s',\,t'} \bar{\delta}(\mathcal{E}_i)\,. \tag{1.1.5}$$

In practice, whilst the scattering equations (1.1.3) look simple, solving them is notoriously difficult at high multiplicities, which can more easily be seen by placing them in a polynomial form [57]. For any n, they admit $(n-3)!$ solutions, first proven for four-dimensions in [58] and for any dimension in [37]. There has been work which has provided ways to solve these equations at higher points [37, 59, 60], but analytic solutions quickly become increasingly involved. This however will not be an issue for us, as we will discuss.

The measure given in (1.1.2) is *universal*, in the sense that it is the same regardless of the theory under consideration. Unlike the original developments from the twistor string, which were based in four-dimensions, it is used to describe tree-level amplitudes for massless particles in any spacetime dimension.

What characterises the theory in the expression (1.1.1) is the particular CHY *integrand* $\mathcal{I}_n$. In its original inception, the CHY formalism described n-point formulae for Yang-Mills and gravity, based off previous developments found for their maximally supersymmetric counterparts in four-dimensions, and formulae presented by Hodges [61,62]. Fundamentally, the CHY integrands for these theories naturally exhibit a double-copy structure, which follows from the KLT relations and so-called KLT orthogonality [37]. In this way they are expressed with the colour-kinematics duality manifest,

$$\mathcal{I}_{\mathrm{YM}} = \mathcal{I}_{\mathrm{kin}}\,\mathcal{I}_{\mathrm{SU}(N)}\,, \qquad \mathcal{I}_{\mathrm{grav}} = \mathcal{I}_{\mathrm{kin}}\,\tilde{\mathcal{I}}_{\mathrm{kin}}\,. \tag{1.1.6}$$

[2]Precisely, these are defined as $2\pi i\,\bar{\delta}(f(z)) := \bar{\partial}(1/f(z))$, with $\bar{\partial}(\cdots) = d\bar{z}\,\partial_{\bar{z}}(\cdots)$.

The objects $\mathcal{I}_{\text{kin}}$ and $\mathcal{I}_{\text{SU}(N)}$ are thus referred to as *half-integrands*. The 'colour' half-integrand, which captures the colour dependence of Yang-Mills amplitudes, is defined as

$$\mathcal{I}_{\text{SU}(N)} = \sum_{\gamma\in S_n/\mathbb{Z}_n} \frac{\text{tr}(T^{a_{\gamma(1)}}T^{a_{\gamma(2)}}\cdots T^{a_{\gamma(n)}})}{\sigma_{\gamma(1)\gamma(2)}\sigma_{\gamma(2)\gamma(3)}\cdots\sigma_{\gamma(n)\gamma(1)}}\,, \tag{1.1.7}$$

which depends on the puncture locations $\{\sigma_i\}$ and the generators of the gauge group $\text{SU}(N)$, given by T^a. The trace structures follow from the colour-decomposition of Yang-Mills amplitudes, which is therefore embedded into the formalism from the outset. Throughout this thesis, we will refer to the cyclic products of the σ_{ij} (that is, the coefficients of the traces in (1.1.7)) as *Parke-Taylor factors*[3]. They will form the basis of most integrands we will consider as their structure makes them most conveniently related to the diagrams obtained in field theory, as we will see.

The 'kinematic' half-integrand is expressed in terms of a reduced Pfaffian of a $2n\times 2n$ matrix M,

$$\mathcal{I}_{\text{kin}} = \text{Pf}'(M) := \frac{(-1)^{i+j}}{\sigma_{ij}}\text{Pf}\,(M^{ij}_{ij}) \tag{1.1.8}$$

where the notation M^{ij}_{ij} signifies that we remove the rows and columns i and j from the matrix M. Specifically, this matrix has the form

$$M = \begin{pmatrix} A & -C^T \\ C & B \end{pmatrix}\,, \tag{1.1.9}$$

where the $n\times n$ block matrices A, B and C are defined as

$$A_{ij} = \frac{k_i\cdot k_j}{\sigma_{ij}}\,, \qquad B_{ij} = \frac{\epsilon_i\cdot\epsilon_j}{\sigma_{ij}}\,, \qquad C_{ij} = \frac{\epsilon_i\cdot k_j}{\sigma_{ij}}$$

for $i\neq j$, and

$$A_{ii} = 0\,, \qquad B_{ii} = 0\,, \qquad C_{ii} = -\sum_{j\neq i}\frac{\epsilon_i\cdot k_j}{\sigma_{ij}}\,.$$

The kinematic integrand (1.1.8) therefore depends on the polarisation vectors ϵ_i, the momenta k_i and the puncture locations σ_i associated with the external particles. The matrix M has co-rank two[4], so the reduced Pfaffian in (1.1.8) is well-defined. Indeed, it is easy to check that its kernel is spanned by the vectors $(1,\cdots,1,0,\cdots,0)$ and $(\sigma_1,\cdots,\sigma_n,0,\cdots,0)$ on the support of the scattering equations (1.1.3), where it is also manifestly gauge-invariant.

The tilde'd kinematic integrand in (1.1.6), relevant to describe gravity amplitudes, is obtained simply to replacing the polarisation vectors ϵ_i with tilde'd polarisation vectors, i.e., $\tilde{\mathcal{I}}_{\text{kin}} = \mathcal{I}_{\text{kin}}(\epsilon\to\tilde{\epsilon})$. This is in line with the double copy structure between Yang-Mills and gravity amplitudes. Specifically, the amplitudes resulting from $\mathcal{I}_{\text{grav}}$ correspond to NS-NS gravity, which contains the graviton, the dilaton and the B-field. By appropriately choosing traceless symmetric combinations of ϵ_i^μ and $\tilde{\epsilon}_i^\nu$ one will obtain amplitudes for the scattering of gravitons with polarisation tensors $\varepsilon_i^{\mu\nu} = \epsilon_i^\mu\tilde{\epsilon}_i^\nu$.

[3]This terminology is reminiscent of the Parke-Taylor factors in the four-dimensional spinor-helicity scheme, since writing $\lambda_i = (1,\sigma_i)$, we have that $\langle ji\rangle = \epsilon_{\alpha\beta}\lambda_j^\alpha\lambda_i^\beta = \sigma_i-\sigma_j$.

[4]For this reason, the Pfaffian of M is zero, and so one must use the reduced Pfaffian

Throughout this work we will be mainly concerned with the theories presented here; that is, Yang-Mills and gravity. However there exist a variety of theories for which CHY integrands have been found, such as those in [41, 42]. These are based off double-copy relations between the amplitudes of theories, which is now known to be part of a more general 'web of theories' [63–65]. These include (but of course are not limited to) Einstein Yang-Mills (EYM), Yang-Mills scalar (YMS), (Dirac-)Born-Infeld ((D)BI), and the non-linear sigma model (NLSM). An example of a theory whose amplitudes we can find with the ingredients above is the biadjoint scalar theory. If one takes the Yang-Mills integrand (1.1.6) and replaces the kinematic half-integrand with *another* colour-integrand (potentially corresponding to a different gauge group $\tilde{G}$), one obtains scattering amplitudes for a theory of scalars which transform in the adjoint representation of both gauge groups, possessing a cubic self-interaction. The action for this theory is, in D-dimensions,

$$S_{\text{bi-adj}} = \int d^D x \, \frac{1}{2} \, \partial_\mu \phi^{aa'} \, \partial^\mu \phi^{aa'} + \frac{\lambda}{3!} f^{abc} f^{a'b'c'} \phi^{aa'} \phi^{bb'} \phi^{cc'} \,, \tag{1.1.10}$$

where λ is the coupling constant, and f^{abc} ($f^{a'b'c'}$) are the structure constants for the gauge group G ($\tilde{G}$). In the case of G and $\tilde{G}$ being SU(N) and SU($\tilde{N}$) respectively, the amplitudes of this theory are the result of the CHY integral (1.1.1) with CHY integrand

$$\mathcal{I}_{\text{bi-adj}} = \mathcal{I}_{\text{SU}(N)} \, \mathcal{I}_{\text{SU}(\tilde{N})} \,. \tag{1.1.11}$$

This theory plays a fundamental role in understanding how the double-copy works at the level of classical solutions also [4, 5, 66–70].

1.2 SL$(2, \mathbb{C})$ weights and field theory amplitudes

In the last section we introduced the integrands for Yang-Mills and gravity, how they exhibit a double copy structure, and how this allows one to construct similar integrands for a variety of other theories. The integrands will depend on the data relevant to describe the tree-level S-matrix of a particular theory, as well as the locations σ_i of the marked points on the Riemann sphere. Indeed, any massless theory can be represented in the form (1.1.1) for some CHY integrand. However, it is worth mentioning that not *any* integrand will give expressions that make sense in the integral (1.1.1). In fact, the integrands that can produce a valid expression are constrained by the SL$(2, \mathbb{C})$ symmetry. To be concrete, the SL$(2, \mathbb{C})$ transformations act on the coordinates σ as

$$\sigma \to \frac{A\sigma + B}{C\sigma + D} \,, \qquad\qquad AD - BC = 1. \tag{1.2.1}$$

with $A, B, C, D \in \mathbb{C}$. It is straightforward to show that

$$\frac{1}{\sigma_{ij}} := \frac{1}{\sigma_i - \sigma_j} \qquad \to \qquad \frac{(C\sigma_i + D)(C\sigma_j + D)}{\sigma_{ij}} \,, \tag{1.2.2}$$

and that

$$d\sigma_i \qquad \to \qquad \frac{d\sigma_i}{(C\sigma_i + D)^2} \,. \tag{1.2.3}$$

As a result, the objects in the CHY measure transform as

$$d^n\sigma \to \left[\prod_{i=1}^{n} (C\sigma_i + D)^{-2} \right] d^n\sigma \,, \qquad \prod_i{}' \, \bar{\delta}(\mathcal{E}_i) \to \left[\prod_{i=1}^{n} (C\sigma_i + D)^{-2} \right] \prod_i{}' \, \bar{\delta}(\mathcal{E}_i) \,, \tag{1.2.4}$$

The latter holding from momentum conservation and the nullity of the external momenta. Therefore the CHY measure transforms uniformly under SL(2, ℂ),

$$d\mu_n \quad \to \quad \left[\prod_{i=1}^{n}(C\sigma_i + D)^{-4}\right] d\mu_n \,, \tag{1.2.5}$$

and is said to have SL(2, ℂ) *weight* −4 in all of the particles. The reason this is important is that for the CHY integral to be well-defined, it must have vanishing SL(2, ℂ) weight. This implies that the CHY integrand must have SL(2, ℂ) weight +4 to compensate the measure,

$$\mathcal{I}_n \quad \to \quad \left[\prod_{i=1}^{n}(C\sigma_i + D)^{+4}\right] \mathcal{I}_n \,. \tag{1.2.6}$$

Valid CHY integrands are therefore constrained. This provides a non-trivial consistency check when considering different integrands, or proposals for quantum corrections. It is not difficult to see that the colour and kinematic half-integrands going into (1.1.6) each have SL(2, ℂ) weight +2, and so in pairs form valid CHY integrands. This is a prerequisite for any physical amplitude represented in terms of an integration over the moduli space of punctured Riemann spheres.

As mentioned in section 1.1, it may seem peculiar from the perspective from field theory that scattering amplitudes can be expressed in this way; that is, (1.1.1). Indeed, were the scattering equations not present, it would resemble an amplitude for the scattering of massless strings. Of course, this resemblance turns out not to be a coincidence, as we will discuss in later chapters. For now we simply note that moduli space integrals are typically a very stringy feature in the context of scattering amplitudes.

The integrations to be performed in (1.1.1) however are localised by the delta functions enforcing the scattering equations in the measure (1.1.2). Indeed, by using the definition of $\bar{\delta}(\cdots)$ and using Stokes' theorem one can recast (1.1.1) as a set of contour integrals around the poles determined by $\{\mathcal{E}_i = 0\}$. The amplitude (1.1.1) is then written more succinctly as

$$\mathcal{A}_n^{(0)} = \int d\mu_n \, \mathcal{I}_n = \sum_{\text{sol}^{\text{n}}\text{s}\,\{\sigma_i\}} \frac{\mathcal{I}_n}{\mathcal{J}_n} \tag{1.2.7}$$

where the sum is over the $(n-3)!$ solutions to the scattering equations. The factor $\mathcal{J}_n$ is a Jacobian factor coming from the set of delta functions, and can be written as

$$\mathcal{J}_n = \frac{\det[\,\partial_{\sigma_i}\mathcal{E}_j\,]^{r's't'}_{r's't'}}{\sigma_{rs}\sigma_{st}\sigma_{tr}\sigma_{r's'}\sigma_{s't'}\sigma_{t'r'}} \,. \tag{1.2.8}$$

The notation on the determinant signifies the same thing as for the reduced Pfaffian; namely that one removes the rows and columns r', s' and t' before evaluating the determinant. This occurs because we do not impose the scattering equations associated to the labels r', s' and t' from (1.1.5) so they should be absent in the resulting Jacobian. The denominator factors are precisely those arising from fixing the SL(2, ℂ) symmetry and the definition of the primed product (1.1.5) above.

Therefore, to obtain the n-point amplitude one need only solve the scattering equations. This is precisely their purpose in this set-up, and in this way it is clear that they remove

the apparent 'stringyness' in the form of the CHY amplitudes (1.2.7). From their structure (1.1.3), clearly solutions to the scattering equations will be rational functions of the kinematic invariants $k_i \cdot k_j$, and therefore the resulting tree-level amplitudes will be rational functions of the kinematic data. In this formalism it is also clear that the tree-level amplitudes for Yang-Mills (gravity) exhibit other ideal properties, such as gauge-invariance and linearisation of the polarisation vectors (tensors) respectively, which can be seen directly from the Pfaffian structure.

As mentioned though, solving the scattering equations is in general not an easy task. They will however be central to the entirety of this thesis: we will use them to obtain n-point formulae in a variety of theories, particularly at loop-level. Whilst we do this, we would like to emphasise one thing: *we will never need to solve the scattering equations.*

That this is possible is quite a remarkable feat, and is the result of developments that have gone into understanding how to use the scattering equations. Of these many great developments, there will be two that will be fundamental in our endeavour, which we will review in the next two sections.

1.3 The Pfaffian expansion

One of the main ingredients going into the CHY integrand for Yang-Mills and gravity is the reduced Pfaffian. This is also a feature that is reminiscent of string theory, arising in the correlation functions for worldsheet fermions. We will see this explicitly in a later chapter, but for now we wish to connect this more strongly with field theory, particularly in a way that is more recognisable with the colour-kinematics duality. In this respect it turns out that on the support of the scattering equations the reduced Pfaffian can be written in a form more akin to the colour integrand,

$$\mathcal{I}_{\text{kin}} = \text{Pf}'(M) \overset{\mathcal{E}_i=0}{=} \sum_{\rho\in S_{n-2}} \frac{N(1,\rho(2),\cdots,\rho(n-1),n)}{\sigma_{1\rho(2)}\sigma_{\rho(2)\rho(3)}\cdots\sigma_{\rho(n-1)\,n}\sigma_{n1}}\,. \tag{1.3.1}$$

The numerators N above depend only on the kinematics through the ordering in the permutation, and so all of the dependence on the marked points σ_i is now in the Parke-Taylor factors of the denominators. In (1.3.1) the first and last elements, which are fixed, is a choice; here we have chosen them to be 1 and n. They correspond to the rows and columns one decides to remove in the reduced Pfaffian (1.1.8), and so the amplitude is invariant under this choice. The significance of this representation of the kinematic half-integrand is two-fold. Firstly the data going into the reduced Pfaffian $\{\epsilon_i, k_i, \sigma_i\}$ becomes de-emulsified into the kinematic numerators with data $\{\epsilon_i, k_i\}$ and the Parke-Taylor factors with data $\{\sigma_i\}$. Secondly, it will allow us to more closely connect the CHY amplitudes with field theory. In particular, it will be seen in the upcoming sections that the numerators N are in fact BCJ numerators. This section is dedicated to giving an overview of the algorithm to straightforwardly calculate the numerators N to arbitrary multiplicity.

This section follows quite closely the work of [52,71], where the expansion was presented[5] and an algorithm for calculating the numerators given explicitly for the cases of tree level

[5]Such an expansion was previously sought after in [39]. Indeed, such an expression was given, but it correctly stated that there the result was 'tautological' since it required pre-determined knowledge of the colour-ordered amplitudes. Nevertheless, it did show that such an expansion does exist.

and one-loop respectively. Equation (1.3.1) relies on expanding the Pfaffian recursively and fixing its coefficients using gauge invariance; the interested reader is referred to the original works of [52, 72] where this was first done explicitly.

Since the numerators in (1.3.1) depend on the *ordering* of the specific permutation, there are three notions we have to introduce in order to present the algorithm. These are

- A *reference ordering* (RO), which is an aribitrary ordering of the particle labels,
- A *colour ordering* (CO), which will be the ordering inside the corresponding numerator,
- A *split ordering* (SO), which heuristically encodes the difference between the two orderings above.

For clarity it will be useful to introduce notation which symbolises whether a given label i is to the left of another label j in any particular ordering, since this is quite important in the algorithm. To this end, we introduce this notation in the table below.

Relation	'Particle i is the left of particle j in the':
$i \dashv j$	Reference ordering RO
$i \lhd j$	Colour ordering CO
$i \prec j$	Split ordering SO

Since the reference ordering is arbitrary, we could choose it to be the canonical ordering $\mathrm{RO} = (12\cdots n)$ for example. Whichever choice one makes, it must be the same for *all* numerators calculated; the amplitude will be invariant under this choice, but different ROs will lead to different numerators. When calculating any one numerator in the permutation sum (1.3.1), that permutation dictates the colour ordering. Given a reference ordering, each colour ordering will define a set of split orderings. For any colour-ordering, to obtain these split orderings, one needs to do the following.

Consider the set of all particle labels *apart* from 1 and n (our choice of rows/columns removed in the reduced Pfaffian). Then decompose this set into colour-ordered subsets I and their complement $\bar{I}$. For $\bar{I}$, construct all (disjoint) decompositions into R subsets $\alpha^{(r)}$ which satisfy the following criteria,

(i) The union of all subsets reproduce $\bar{I}$, $\cup_{r=1}^{R}\alpha^{(r)} = \bar{I}$.

(ii) Each subset $\alpha^{(r)}$ respects the colour ordering,

$$\alpha_i^{(r)} \lhd \alpha_j^{(r)}\,, \quad \forall\, i<j.$$

(iii) The last element of the subset $\alpha^{(r)}$ is the left-most in the reference ordering with respect to the others in $\alpha^{(r)}$,

$$\alpha_{n_r}^{(r)} \dashv \alpha_i^{(r)}\,, \quad \forall\, i.$$

(iv) The last elements of all R subsets respect the reference ordering,

$$\alpha_{n_1}^{(r)} \dashv \cdots \dashv \alpha_{n_R}\,.$$

For each decomposition $\bar{I} = \cup_{r=1}^{R}\alpha^{(r)}$ that satisfy these criteria, the split ordering is defined as

$$\mathrm{SO} = (1\, I\, \alpha^{(1)}\cdots\alpha^{(R)}\, n)\,. \tag{1.3.2}$$

Once one has obtained all the split orderings for a given colour-ordering, the numerator for that colour ordering is given by

$$N_{\rm RO}({\rm CO}) = \sum_I (-1)^{n_I} W_I \left(\sum_{\rm SO} \prod_r Y\left(\alpha^{(r)}\right) \right) , \tag{1.3.3}$$

where W_I is defined as

$$W_I = \begin{cases} \epsilon_1 \cdot \epsilon_n & I = \emptyset \\ \epsilon_1 \cdot F_{i_1} \dots F_{n_I} \cdot \epsilon_n & I \neq \emptyset \end{cases} \tag{1.3.4}$$

and the objects Y are defined as

$$Y\left(\alpha^{(r)}\right) = \begin{cases} 1 & \alpha^{(r)} = \emptyset \\ \epsilon_a \cdot Z_a & \alpha^{(r)} = \{a\} \\ \epsilon_{a_{n_r}} \cdot F_{a_{n_r-1}} \dots F_{a_2} \cdot \epsilon_{a_1} & \alpha^{(r)} = \{a_1, a_2, \cdots, a_{n_r}\} . \end{cases} \tag{1.3.5}$$

In the above equations, $F_i^{\mu\nu} := \epsilon_i^\mu k_i^\nu - \epsilon_i^\nu k_i^\mu$, and Z_a is defined to be the sum of all momenta to the left of particle a in the colour ordering *and* the split ordering,

$$Z_a = \sum_{i \lhd a \text{ and } i \prec a} k_i \, . \tag{1.3.6}$$

Simple example: $N(1324)$. To see how this works in practice we will go over one of the simplest examples, which is to calculate the numerator $N(1324)$ at four points. We choose the reference ordering to be RO = (1234), and for this numerator we have CO = (1324). As part of the algorithm we have to decompose $\{3,2\}$ into subsets I and their complement. We will denote by Split($\bar{I}$) the set of subsets $\{\alpha^{(r)}\}$ of $\bar{I}$ that are consistent with the criteria described above. Let us first consider I being the empty set,

$$\begin{aligned} I = \emptyset \quad &\Rightarrow \quad \bar{I} = \{3,2\} \\ &\text{Split}(\bar{I}) = \{\{2\},\{3\}\} \cup \{\{3,2\}\} \\ &\Rightarrow \text{SO} = (1234), (1324) \, . \end{aligned}$$

In this case both subsets of $\{3,2\}$ satisfy the criteria above. Single-element subsets such as $\{\{2\},\{3\}\}$ will always satisfy the criteria by virtue of only being composed of single elements; they will always be in the RO from criterion (iv). The second subset $\{\{3,2\}\}$ appears by virtue of criterion (ii) and (iii) and arises precisely because the RO and the CO are different; this is one way in which the SO encodes the difference between the two. The contribution from $I = \emptyset$ to the numerator is therefore, from (1.3.3),

$$I = \emptyset : \qquad (\epsilon_1 \cdot \epsilon_4) \left[(\epsilon_2 \cdot k_1)(\epsilon_3 \cdot k_1) + (\epsilon_2 \cdot F_3 \cdot k_1) \right] . \tag{1.3.7}$$

The two terms come from the sum over SO, and $W_{I=\emptyset} = \epsilon_1 \cdot \epsilon_n$ is the overall factor. Suppose now we consider the decomposition $I = \{3\}$. Then $\bar{I} = \{2\}$ so trivially $\alpha^{(r)} = \text{Split}(\{2\}) = \{2\}$ and one can read off the SO straightforwardly from (1.3.2), SO = (1324). Its contribution to the numerator is read off from (1.3.3) and the factors above as

$$I = \{3\} : \qquad -(\epsilon_1 \cdot F_3 \cdot \epsilon_4)(\epsilon_2 \cdot (k_1 + k_3)) \, . \tag{1.3.8}$$

There is only one term in the sum over SO; the first factor comes from $W_{I=\{3\}}$ and the minus sign is due to the factor $(-1)^{n_I}$. Notice that the last factor is $\epsilon_2 \cdot Z_2$ with $Z_2 = k_1 + k_3$ since labels 1 and 3 are to the left of 2 in both the SO and the CO (here SO = CO = (1324)). The decomposition $I = \{2\}$ works similarly; one reads off straightforwardly SO = (1234) and its contribution to the numerator is then given by

$$I = \{2\}: \qquad -(\epsilon \cdot F_2 \cdot \epsilon_4)(\epsilon_3 \cdot k_1). \tag{1.3.9}$$

In this case the second factor is $\epsilon_3 \cdot Z_3$, but only the label for particle 1 is to the left of 3 in both CO = (1324) and SO = (1234). Finally, one has $I = \{3, 2\}$ and therefore $\bar{I} = \emptyset$. In this case the contribution to the numerator solely comes from the W_I factor,

$$I = \{3, 2\}: \qquad +(\epsilon_1 \cdot F_3 \cdot F_2 \cdot \epsilon_4)\,. \tag{1.3.10}$$

Therefore the numerator is given in total by

$$\begin{aligned} N(1324) = {} & +(\epsilon_1 \cdot \epsilon_4)[(\epsilon_2 \cdot k_1)(\epsilon_3 \cdot k_1) + (\epsilon_2 \cdot F_3 \cdot k_1)] - (\epsilon_1 \cdot F_2 \cdot \epsilon_4)(\epsilon_3 \cdot k_1) \\ & -(\epsilon_1 \cdot F_3 \cdot \epsilon_4)(\epsilon_2 \cdot (k_1 + k_3)) + (\epsilon_1 \cdot F_3 \cdot F_2 \cdot \epsilon_4)\,. \end{aligned} \tag{1.3.11}$$

This directly matches the calculation of [72] for the same numerator, up to a convention-dependent minus sign. Notice that each term is linear in the polarisation vectors for the external particles, as follows from the reduced Pfaffian. We stress that this numerator corresponds to the reference ordering RO = (1234). This reference ordering should also be used in calculating the other numerator $N(1234)$, which would be simpler because one can see by repeating the process above that there will be a unique decomposition for any $\bar{I}$ satisfying the criteria above, consisting of only single-element subsets. This is a general statement for whenever RO = CO.

This algorithm can be used to calculate the numerators in the decomposition of the kinematic integrand (1.3.1) at arbitrary multiplicity. We will see in later chapters that the same algorithm can be used to calculate numerators at loop-level. The fundamental ideas to be taken away from this section are that (*i*) the kinematic integrand can be put into an expansion of the form (1.3.1), and that (*ii*) there exists an algorithm to calculate the numerators explicitly in said expansion. This will allow one to explicitly calculate the numerators appearing in n-point expressions for amplitudes at tree- and loop-level throughout this thesis.

1.4 The trivalent graph expansion

In the last section we discussed how the kinematic half-integrand can take the form as a sum over permutations of Parke-Taylor factors with kinematic numerators,

$$\mathcal{I}_{\text{kin}} \overset{\varepsilon_i=0}{=} \sum_{\rho \in S_{n-2}} \frac{N(1, \rho(2), \cdots, \rho(n-1), n)}{\sigma_{1\rho(2)}\sigma_{\rho(2)\rho(3)} \cdots \sigma_{\rho(n-1)\,n}\sigma_{n1}}\,, \tag{1.4.1}$$

and reviewed an algorithm to calculate the numerators N to arbitrary multiplicity. It turns out that the colour half-integrand can also be written in a similar form by utilising a Del Duca-Dixon-Maltoni (DDM) colour-basis [73],

$$\mathcal{I}_{\text{SU}(N)} = \sum_{\gamma \in S_{n-2}} \frac{c(1, \gamma(2), \cdots, \gamma(n-1), n)}{\sigma_{1\gamma(2)}\sigma_{\gamma(2)\gamma(3)} \cdots \sigma_{\gamma(n-1)\,n}\sigma_{n1}}\,, \tag{1.4.2}$$

where the *colour factors* $c(1,\gamma(2),\cdots,\gamma(n-1),n)$ are given in terms of the structure constants of the the theory,

$$c(1,\gamma(2),\cdots,\gamma(n-1),n) = f^{a_1 a_{\gamma(2)} b_1} f^{b_1 a_{\gamma(3)} b_2} \cdots f^{b_{n-3} a_{\gamma(n-1)} a_n} \,. \tag{1.4.3}$$

This basis will be fundamental and used throughout this thesis, since we will be utilising the colour-kinematics duality for which this colour basis is well-suited. Like the kinematic half-integrand, the expansion of the colour half-integrand (1.4.2) will straightforwardly be applicable at loop-level, in line with the DDM loop-level colour decomposition [73].

With the decompositions (1.4.1) and (1.4.2), the dependence of the CHY integrand on the marked points is now exhibited in terms of Parke-Taylor factors. For example, substituting (1.4.1) and (1.4.2) into the Yang-Mills amplitude gives

$$\mathcal{A}^{(0)}_{\text{YM}} = \sum_{\rho,\gamma\in S_{n-2}} \int_{\mathfrak{M}_{0,n}} d\mu_n \, \frac{N(1,\rho(2),\cdots,\rho(n-1),n)}{\sigma_{1\rho(2)}\sigma_{\rho(2)\rho(3)}\cdots\sigma_{\rho(n-1)\,n}\sigma_{n1}} \times \frac{c(1,\gamma(2),\cdots,\gamma(n-1),n)}{\sigma_{1\gamma(2)}\sigma_{\gamma(2)\gamma(3)}\cdots\sigma_{\gamma(n-1)\,n}\sigma_{n1}} \tag{1.4.4}$$

and similarly for gravity we have

$$\mathcal{A}^{(0)}_{\text{grav}} = \sum_{\rho,\tilde{\rho}\in S_{n-2}} \int_{\mathfrak{M}_{0,n}} d\mu_n \, \frac{N(1,\rho(2),\cdots,\rho(n-1),n)}{\sigma_{1\rho(2)}\sigma_{\rho(2)\rho(3)}\cdots\sigma_{\rho(n-1)\,n}\sigma_{n1}} \times \frac{\tilde{N}(1,\tilde{\rho}(2),\cdots,\tilde{\rho}(n-1),n)}{\sigma_{1\tilde{\rho}(2)}\sigma_{\tilde{\rho}(2)\tilde{\rho}(3)}\cdots\sigma_{\tilde{\rho}(n-1)\,n}\sigma_{n1}} \tag{1.4.5}$$

where $\tilde{N} = N(\epsilon\to\tilde{\epsilon})$, following from the definition of $\tilde{\mathcal{I}}_{\text{kin}}$. Since the dependence on the marked points entirely lies in the Parke-Taylor factors, the moduli space integrals require knowledge of how to perform e.g.

$$\int_{\mathfrak{M}_{0,n}} d\mu_n \, \frac{1}{\sigma_{1\rho(2)}\sigma_{\rho(2)\rho(3)}\cdots\sigma_{\rho(n-1)\,n}\sigma_{n1}} \times \frac{1}{\sigma_{1\gamma(2)}\sigma_{\gamma(2)\gamma(3)}\cdots\sigma_{\gamma(n-1)\,n}\sigma_{n1}} \,. \tag{1.4.6}$$

These happen to be the *double-partial amplitudes* $m(1,\rho,n|1,\gamma,n)$ of the biadjoint scalar theory, discussed in section 1.1. Amazingly, there exists a diagrammatic method of obtaining the result of these double-partial amplitudes, and hence the moduli space integrals (1.4.6) for any multiplicity, first shown and detailed in [39]. The result is expressed in terms of a set of propagators corresponding to trivalent diagrams, with coefficients ±1. In this section, we will summarise this simple and beautiful method. Although we will do it in a very informal way, we believe it is sufficient, and point the interested reader to more specific details in the original reference.

Following the notation of [39], let us denote by $m^{(0)}(\alpha|\beta)$ the double-partial amplitude for Parke-Taylor factors in the ordering α, β,

$$m^{(0)}(\alpha|\beta) = \int_{\mathfrak{M}_{0,n}} d\mu_n \, \frac{1}{\sigma_{\alpha(1)\alpha(2)}\cdots\sigma_{\alpha(n)\,\alpha(1)}} \times \frac{1}{\sigma_{\beta(1)\beta(2)}\cdots\sigma_{\beta(n)\,\beta(1)}} \,. \tag{1.4.7}$$

It will be convenient to introduce terminology for when particle labels are consecutive in the α or β ordering, and we shall say that they are α-consecutive and β-consecutive respectively. Here we intend this to operate forwards and backwards, so for example given $\alpha = (12345)$ and $\beta = (14325)$, the particle sets (15) and (234) are considered to be both α,β-consecutive. On the other hand, for $\alpha = (12345)$ and $\beta = (13524)$, there are no particle set which are both α,β-consecutive.

With this the integral (1.4.7) can be calculated diagrammatically by doing the following.

(i) First check how many (disjoint) sets are α, β-consecutive. If there are less than two sets, then $m^{(0)}(\alpha|\beta) = 0$.

(ii) Provided one has two or more such sets, draw a disk and place nodes on the edge for the particle labels according to the α ordering.

(iii) Now draw lines connecting the nodes according to the β ordering.

(iv) For any set of consecutive nodes corresponding to particle labels that are both α, β-consecutive, the lines connecting them will be closest to the edge and not intersect any others. For each such set, bring the nodes therein close together.

(v) The lines inside the disk now define a set of polygons which meet each other at intersection points, or *internal nodes*. Each polygon defines a *sub-amplitude*; if the polygon has m vertices, its sub-amplitude is equal to sum of propagator sets of all m-point ordered trivalent diagrams with external points given by the vertices.

(vi) Multiply all the sub-amplitudes together, along with propagators connecting them via internal nodes. This is the result of $m^{(0)}(\alpha|\beta)$ up to a determinable sign.

Note that if the 'external polygons' formed in step (iii) already have one only one internal node, there is no need to bring the external points close together, and one can proceed straight to step (v). The overall sign is very important, since it will carry through to determine the Jacobi relations between numerators and colour factors for example in Yang-Mills and gravity. There is another set of rules to determine the overall sign, which apply to the same graphs drawn in the above steps. Firstly, draw arrows on the lines made in step (iii) above according to the β ordering; each polygon now has a relative ordering with respect to the α ordering on the edge of the disk. Then the rules are as follows:

- Each polygon with an even number of vertices contributes a minus sign.
- Each polygon with an odd number of vertices contributes a plus sign if its orientation is the same as the disk (α ordering), and a minus sign if its orientation is opposite to the disk.
- Each internal node contributes a minus sign.

The product of these signs determines the overall sign of $m^{(0)}(\alpha|\beta)$. We will give two examples of how this works, one for five-points and on for eight-points. Let us first look at the example $m^{(0)}(12345|14325)$, displayed in figure 1.1. Note that since sets (234) and (15) are consecutive in both orderings, we will have a non-zero answer by step (i). Step (ii) and (iii) then gives us decomposition into two polygons; since they both have only a single internal node, there is no need to bring the external points together according to step (iv). The polygon with external nodes (234) has four vertices, and so contributes a subamplitude whose set of ordered trivalent diagrams have propagators $\frac{1}{s_{23}} + \frac{1}{s_{34}}$. The set (15) gives a three-point subamplitude, and so contributes 1, since there are no propagators present in a three-point amplitude. The internal point connecting these polygons however correspond to a propagator $\frac{1}{s_{234}} = \frac{1}{s_{15}}$ connecting the subamplitudes, so the amplitude up to a sign is

$$m^{(0)}(12345|14325) = \left(\frac{1}{s_{23}} + \frac{1}{s_{34}}\right)\frac{1}{s_{15}}\,. \tag{1.4.8}$$

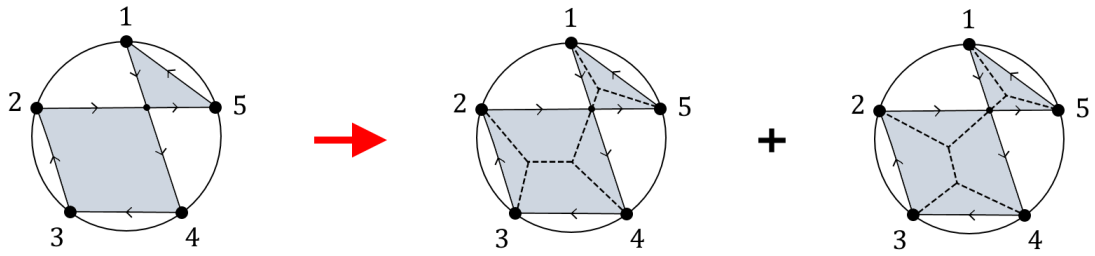

Figure 1.1: An example of the diagrammatic calculation of $m^{(0)}(12345|14325)$. The first diagram corresponds to steps (i) - (iii). Each of the two polygons formed should be considered as contributing a subamplitude; in this case there is only one internal point so we can draw inside the polygons the resulting trivalent diagrams.

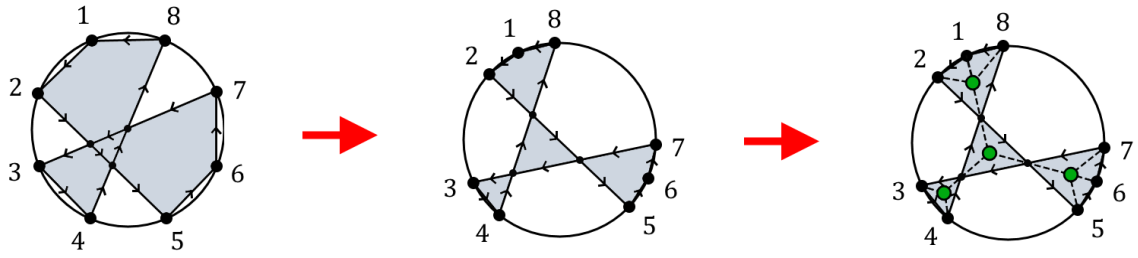

Figure 1.2: Another example at eight-points for $m^{(0)}(12345678|12567348)$. In this case, there is more than one internal point so we bring together connected adjadjacent labels according to step (iv), which occurs in the second diagram. The green blobs in the third diagram represent the sum of all trivalent diagrams involving the lines connected to it, in a similar manner to the two diagrams on the right of figure 1.1.

To determine the overall sign we use the rules above. The (234) polygon contributes a minus sign because it has an even number of vertices, and the (15) polygon contributes a plus sign because it has the same orientation as the disk. Finally, the single internal point contributes a minus sign, leading to an overall sign $(-1)^2 = +1$, making (1.4.8) already the correct answer.

Another example is given in figure 1.2 and corresponds to $m^{(0)}(12345678|12567348)$. Amazingly the higher addition of points does not contribute much to the complexity of solving the problem, which makes this method very efficient. In this case, the polygons formed though step (iii) have more than one internal point, so by step (iv) we bring the nodes in sets of consecutive external points closer together to obtain a polygon decomposition with only single internal nodes; this is shown graphically in going form the first to the second diagrams in figure 1.2. The same reasoning above is then applied to each of the polygons, of which there are now four. Note that there is now an 'internal polygon' which serves the connect the external ones, and so contributes a set of propagators $1/(s_{128}s_{567}s_{34})$ (one for each internal node). Following the rules above, we get that this double partial amplitude, up to a sign, is given by

$$m^{(0)}(12345678|12567348) = \left(\frac{1}{s_{12}} + \frac{1}{s_{18}}\right)\left(\frac{1}{s_{56}} + \frac{1}{s_{67}}\right)\frac{1}{s_{128}s_{567}s_{34}}\,. \tag{1.4.9}$$

The sign counting works as before; the (812) polygon gives a (-1) by virtue of having an

even number of points, whilst the (34), (567), and internal polygon give $+1$, -1 and -1 respectively due to their orientation with respect to the disk (see figure 1.2). Finally, the three internal points contribute -1 each, giving a total of $(-1)^6 = +1$; therefore (1.4.9) is indeed the correct result.

Notice that if α and β are the same, $\alpha = \beta$, then a single n-point polygon is formed, where $n = \text{Length}(\alpha)$. In this case the result is simply the sum over all propagator sets for all n-point tree-level trivalent diagrams respecting the α ordering (possibly with a sign depending on whether n is even or odd according to the sign rules above). Any result for $\alpha \neq \beta$ simply contributes a subset of these terms according to which sets of particles respect the α and β ordering. For example, at five-points one has that

$$m^{(0)}(12345|12345) = \frac{1}{s_{12}s_{34}} + \frac{1}{s_{23}s_{45}} + \frac{1}{s_{34}s_{51}} + \frac{1}{s_{45}s_{12}} + \frac{1}{s_{51}s_{23}}\,, \tag{1.4.10}$$

and our five-point example above (1.4.8) corresponds to the last and third terms in (1.4.10) respectively.

Therefore, the double-partial amplitudes act as a generator of the set of scalar propagators for amplitudes expressible in terms of trivalent diagrams. In particular it will generate the set of propagators required for the Yang-Mills and gravity amplitudes in (1.4.4) and (1.4.5), with the relative signs that will be important to express the colour-kinematics duality. We will see this explicitly in the next section, but for now let us note that this is not a surprise. Indeed, the double-partial amplitudes can be related to the (inverse) KLT matrix, which is used in describing the KLT relations between Yang-Mills and gravity amplitudes [8, 74–78]. The precise connection can be found in [39], exploiting again certain properties of the scattering equations called KLT orthogonality [37].

We should mention that similar integration rules exist for more general CHY integrands; that is, those which are not explicitly in a double Parke-Taylor basis as we have considered in this section. They are an interesting study in themselves and incorporate methods from graph-theory, also making a great connection with Feynman diagrams. Examples of these can be found at tree-level in [40, 72, 79–82] and at one-loop in [83–85].

1.5 From CHY to BCJ

Let us recap on what we have seen so far. In section 1.1 the CHY integrands for Yang-Mills and gravity were presented in (1.1.6), being expressed in terms of colour and kinematic half-integrands. In section 1.3 we discussed how the kinematic half-integrand could be expressed, on the support of the scattering equations, as a permutation sum of numerators with Parke-Taylor factors and presented the algorithm to compute these numerators to arbitrary multiplicity [52]. Then in section 1.4 we saw that the colour half-integrand could also be expressed in a similar permutation sum, so that the dependence of the integrands (1.1.6) on the marked points is only in terms of Parke-Taylor factors. In the previous section we presented the diagrammatic method of [39] to calculate the moduli space integrals in this case.

With these methods in hand, from CHY one can now straightforwardly obtain tree-level field theory amplitudes for Yang-Mills and gravity for any number of particles in any number of dimensions *without* solving the scattering equations, only using their special properties. In this section we will see precisely what this results in.

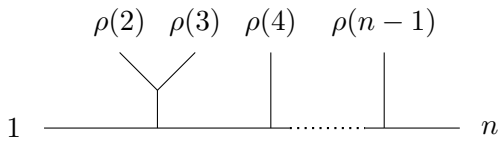

Figure 1.3: An example a of tree-level diagram. Any such diagram can be drawn this way with 1 and n being the endpoints of the diagram.

Let us go back to (1.4.4) and (1.4.5), which we now recognise as

$$\mathcal{A}^{(0)}_{n,\mathrm{YM}} = \sum_{\rho,\gamma\in S_{n-2}} N(1,\rho,n)\; m^{(0)}(1,\rho,n|1,\gamma,n)\; c(1,\gamma,n) \tag{1.5.1}$$

$$\mathcal{A}^{(0)}_{n,\mathrm{grav}} = \sum_{\rho,\tilde{\rho}\in S_{n-2}} N(1,\rho,n)\; m^{(0)}(1,\rho,n|1,\gamma,n)\; \tilde{N}(1,\tilde{\rho},n)\,. \tag{1.5.2}$$

The previous sections were dedicated to obtaining this representation and presenting ways in which they may be calculated. In particular, we know that each of the double-partial amplitudes $m^{(0)}(\cdots|\cdots)$ correspond to a set of propagators. If one performs this sum and plugs in the values for these double partial amplitudes, then the amplitudes above can be expressed as

$$\mathcal{A}^{(0)}_{n,\mathrm{YM}} = (-1)^{n+1}\sum_{\mathrm{a}\in\Gamma_n}\frac{N_\mathrm{a}\,c_\mathrm{a}}{D_\mathrm{a}}\,, \qquad \mathcal{A}^{(0)}_{n,\mathrm{grav}} = (-1)^{n+1}\sum_{\mathrm{a}\in\Gamma_n}\frac{N_\mathrm{a}\,\tilde{N}_\mathrm{a}}{D_\mathrm{a}}\,, \tag{1.5.3}$$

where Γ_n represents the set of n-point trivalent diagrams, and D_a represents the set of propagators for each $\mathrm{a}\in\Gamma_n$. The numerators N_a and colour factors c_a are the corresponding numerators and colour factors associated with each diagram. Any such diagram can be drawn as in 1.3, with particles 1 and n on the 'end-points'. To see the significance of this, note that certain numerators and colour factors satisfy Jacobi relations by virtue of the relative signs coming from the *moduli space integrations*. We will see this in an explicit example momentarily, but for now let us point out one important detail. The numerators and colour factors that one calculates in e.g. (1.4.1) and (1.4.2) correspond to diagrams that can be drawn as 'half-ladders', such as the one in figure 1.4. Numerators and colour factors for diagrams that cannot be drawn directly as a half-ladder, such as the one in figure 1.3 which contains an external tree are precisely obtained through those corresponding to the half-ladders via Jacobi relations. These appear pairwise for relevant diagrams, so that the

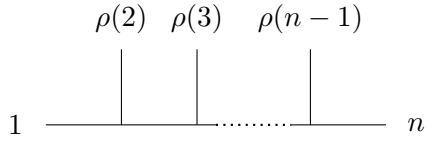

Figure 1.4: A half-ladder diagram at tree-level, with end-points 1 and n. They are the 'master diagrams' whose numerators are defined to be 'master numerators'. Numerators for any tree-level diagram which is not directly a half-ladder, such as the one in figure 1.3 are determined from these by Jacobi relations.

colour-kinematics duality is manifest, i.e.

$$c_{\rm a} + c_{\rm b} + c_{\rm c} = 0 \qquad \Leftrightarrow \qquad N_{\rm a} + N_{\rm b} + N_{\rm c} = 0\,. \tag{1.5.4}$$

The representation of the amplitudes (1.5.3) coming from CHY in this way precisely give the amplitudes in a BCJ representation. The numerators $N_{\rm a}$ are therefore BCJ numerators, and those for the half-ladder diagrams are *master BCJ numerators* since they determine the numerators for all other diagrams. We stress again however that the numerators are *not* constructed to be BCJ numerators; that they are is simply a consequence of the moduli space integrations being localised on solutions to the scattering equations.

Let us consider an example at four-points to see how this works out explicitly. We will consider Yang-Mills theory, but since there is a clear structural similarity with gravity this example extends straightforwardly thereof. Starting with (1.5.1), there will be four terms coming from the sum over permutations, $|S_2|^2 = 4$. Explicitly these terms are, from (1.5.1),

$$\begin{aligned}\mathcal{A}^{(0)}_{\rm YM} = &+ N(1,2,3,4)\; m^{(0)}(1,2,3,4|1,2,3,4)\; c(1,2,3,4)\\ &+ N(1,3,2,4)\; m^{(0)}(1,3,2,4|1,2,3,4)\; c(1,2,3,4)\\ &+ N(1,2,3,4)\; m^{(0)}(1,2,3,4|1,3,2,4)\; c(1,3,2,4)\\ &+ N(1,3,2,4)\; m^{(0)}(1,3,2,4|1,3,2,4)\; c(1,3,2,4)\,.\end{aligned} \tag{1.5.5}$$

Noting that, using the method described in the last chapter, one can easily find

$$\begin{aligned} m^{(0)}(1,2,3,4|1,2,3,4) &= -\frac{1}{s_{12}} - \frac{1}{s_{14}}\,, & m^{(0)}(1,2,3,4|1,3,2,4) &= \frac{1}{s_{14}}\,,\\ m^{(0)}(1,3,2,4|1,3,2,4) &= -\frac{1}{s_{13}} - \frac{1}{s_{14}}\,, & m^{(0)}(1,3,2,4|1,2,3,4) &= \frac{1}{s_{14}}\,,\end{aligned} \tag{1.5.6}$$

and therefore (1.5.5) is expressed as

$$\begin{aligned}\mathcal{A}^{(0)}_{\rm YM} = &- c(1,2,3,4)\left[\frac{N(1,2,3,4)}{s_{12}} + \frac{N(1,2,3,4) - N(1,3,2,4)}{s_{14}}\right]\\ &- c(1,3,2,4)\left[\frac{N(1,3,2,4)}{s_{13}} + \frac{N(1,3,2,4) - N(1,2,3,4)}{s_{14}}\right].\end{aligned} \tag{1.5.7}$$

Let us rename $N(1,2,3,4) \equiv n_s$, $N(1,3,2,4) \equiv n_u$, $c(1,2,3,4) \equiv c_s$, $c(1,3,2,4) \equiv c_u$, $s_{12} \equiv s$, $s_{14} \equiv t$ and $s_{13} \equiv u$. Then (1.5.7) is written as

$$\begin{aligned}\mathcal{A}^{(0)}_{\rm YM} &= -\frac{c_s n_s}{s} - \frac{c_s(n_s - n_u)}{t} - \frac{c_u n_u}{u} - \frac{c_u(n_u - n_s)}{t}\\ &= -\frac{c_s n_s}{s} - \frac{(c_s - c_u)(n_s - n_u)}{t} - \frac{c_u n_u}{u}\,.\end{aligned} \tag{1.5.8}$$

Indeed, now defining $c_t := c_s - c_u$ and $n_t := n_s - n_u$, we see that this is the recognisable BCJ form of the four-point amplitude for Yang-Mills,

$$\mathcal{A}^{(0)}_{\rm YM} = -\frac{c_s n_s}{s} - \frac{c_t n_t}{t} - \frac{c_u n_u}{u}\,. \tag{1.5.9}$$

The definition of the colour and numerator factors c_t and n_t can be seen diagrammatically in figure 1.5 below.

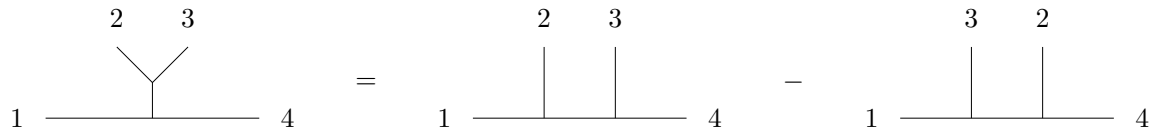

Figure 1.5: An example of a Jacobi relation between numerators and colour factors for certain diagrams. This rule can be applied continuously on any diagram to obtain the relationship between its numerator/colour factor and those of the master diagrams.

Clearly, if we were working with gravity instead, then we would have had $c(\cdots) \to \tilde{N}(\cdots)$ from the beginning, and would have obtained through the same manipulations

$$\mathcal{A}^{(0)}_{\text{grav}} = -\frac{n_s \tilde{n}_s}{s} - \frac{n_t \tilde{n}_t}{t} - \frac{n_u \tilde{n}_u}{u}\,. \tag{1.5.10}$$

This example exhibits a point we mentioned earlier; that the numerators and colour factors for certain diagrams (here the t-channel diagram) are related to others by Jacobi relations *not* because they were designed that way, but simply as a consequence of the relative signs in the moduli space integrations. Therefore, if the CHY half-integrands for *any* theory can be written in a Parke-Taylor decomposition, then their numerators will obey kinematic Jacobi relations. This provides another way of obtaining numerators for theories which exhibit the colour-kinematics duality, provided one has a corresponding CHY representation.

This section provides a clear connection between the CHY expressions and the BCJ expressions of tree-level amplitudes. There is still the question however of whether there exists a more intuitive formalism from which the CHY expressions, and therefore the scattering equations, naturally arise. Unsurprisingly, there does exist such a formalism, which not only achieves these tasks, but also suggest natural extensions to loop-level, which we will discuss in the next chapter.

Chapter 2

The ambitwistor string

Not long after the discovery of the CHY formalism, Mason and Skinner discovered a worldsheet theory whose correlation functions gave the amplitudes depicted by CHY for Yang-Mills and gravity [43]. They proposed a string theory whose target space was not Minkowski spacetime, but rather ambitwistor space, subsequently called the ambitwistor string. Ambitwistor space is the space of complexified null geodesics in spacetime. It of course has deep connections with twistor space [86–88], and in fact in four-dimensions it is related to twistor space and its dual [89] (hence the name).

Whilst it shares many features with string theory in its formulation, it has many crucial distinguishing features. Firstly, there is no notion of α', and indeed one should think of the ambitwistor string having $\alpha' = 0$. This has the consequence that the spectrum of the string consists of massless states (as opposed to the tower of massive states in string theory), and that the amplitudes directly correspond to field theory amplitudes. The latter should be compared with ordinary string theory, in which such amplitudes arise in the field theory limit $\alpha' \to 0$. Secondly, whilst there is some notion of worldsheet supersymmetry in the models we will be considering, the theory is not formulated on a super-Riemann surface, in contrast to superstring theory. On top of that, requiring the theory properly be placed in ambitwistor space introduces another gauge symmetry, which turns out to be the crucial feature in describing field theory amplitudes. These previous two points are indeed connected. Given the differences mentioned, the ambitwistor string should be thought of as a *worldsheet model*; that is, a model for field theory amplitudes formulated on a worldsheet.

In this section we introduce the ambitwistor string and how, after quantisation, it gives rise to the CHY formulae from the last section. Particular focus will be on how the scattering equations arise, since this will be important for following chapters. We will then review how the ambitwistor string gives rise to one-loop amplitudes in field theory, as a consequence of considering the theory on a genus-one Riemann surface. This is natural from the point of string theory, but there will be new features appearing in the ambitwistor string. These key features will be present in further chapters, when we consider higher-genus expressions, corresponding to field theory amplitudes at higher loops.

2.1 The type II ambitwistor string action

The model we will be utilising, and that which is the best understood, will be the type II ambitwistor string, first discussed in [43]. This is reminiscent of the type II theory in the superstring, though there will be crucial differences as we will see. Prior to gauge-fixing,

the action for this theory is written as

$$S = \frac{1}{2\pi}\int_\Sigma P_\mu \bar\partial X^\mu + \frac{1}{2}\Psi_\mu \bar\partial \Psi^\mu + \frac{1}{2}\tilde\Psi_\mu \bar\partial \tilde\Psi^\mu - e\left(P_\mu \partial X^\mu + \frac{1}{2}\Psi_\mu \partial \Psi^\mu + \frac{1}{2}\tilde\Psi_\mu \partial \tilde\Psi^\mu\right) - \tilde e\,\frac{P^2}{2} - \chi P_\mu \Psi^\mu - \tilde\chi P_\mu \tilde\Psi^\mu\,. \tag{2.1.1}$$

In contrast to ordinary (closed) string theory, all fields in the action are *chiral*; that is to say they should all be considered left-movers, as opposed to having left- and right-movers. The fields (P, X) describe a map into bosonic ambitwistor space. Specifically, for a spacetime M the field X is a map from the string worldsheet to spacetime, $X : \Sigma \to M$, whilst P is a holomorphic (1,0)-form which takes values in the cotangent bundle T^*M, $P \in \Omega^{1,0}(\Sigma, T^*M)$. As fields in a two-dimensional conformal field theory (CFT), this means they have conformal weight (0,0) and (1,0) respectively. The anticommuting fields Ψ_μ, $\tilde\Psi_\mu$ correspond to fermions on the worldsheet, which take values in[1] $\Pi\Omega^0(\Sigma, K_\Sigma^{1/2} \otimes TM)$, where K_Σ is the canonical bundle on Σ, and therefore these fields have conformal weight $(\frac{1}{2}, 0)$. The field e acts as a Lagrange multiplier setting the worldsheet energy-momentum tensor to zero, which is common in string theory. Similarly, the field $\tilde e$ acts as a Lagrange multiplier enforcing that $P^2 = 0$ on the worldsheet. This constraint, along with its corresponding symmetry, properly places the theory in ambitwistor space, as we will discuss momentarily. Finally, the fields χ and $\tilde\chi$ are Lagrange multipliers setting $P\cdot\Psi = P\cdot\tilde\Psi = 0$, which are related to supersymmetric extensions of the previous constraint.

Before we discuss the symmetries of the action, let us briefly comment on why the action (2.1.1) makes sense. The operator $\bar\partial$ is defined as $\bar\partial = d\bar z\,\partial_{\bar z}$, and given that P is a (1,0)-form on Σ, the kinetic term $P\cdot\bar\partial X$ provides an appropriate measure for integrating over the worldsheet; that is, it is a top-top form. Similarly, ∂ is defined as $dz\,\partial_z$ such that the energy-momentum tensor in (2.1.1) is a quadratic differential on Σ. As P^2 is also a quadratic differential, the fields e and $\tilde e$ must be (0,1)-forms with values in the tangent bundle on the worldsheet, $e, \tilde e \in \Omega^{0,1}(\Sigma, T_\Sigma)$; in other words, they are Beltrami differentials[2]. Finally, to have the correct Grassmann properties and integration measure on Σ, it must be that $\chi, \tilde\chi \in \Pi\Omega^{0,1}(\Sigma, T_\Sigma^{1/2})$.

The action (2.1.1) has three main symmetries. The first, which is common from string theory, is the set of holomorphic worldsheet reparametrisations, generated by the energy-momentum tensor. Under a diffeomorphism parametrised by a smooth worldsheet vector field v, the bosonic fields transform as

$$\begin{aligned} \delta_v X^\mu &= v\partial X^\mu\,, & \delta_v P_\mu &= \partial(vP_\mu)\,,\\ \delta_v e &= \bar\partial e + v\partial e - e\partial v\,, & \delta_v \tilde e &= \bar\partial \tilde e + v\partial \tilde e - \tilde e\partial v\,, \end{aligned} \tag{2.1.2a}$$

and the fermionic fields transform as

$$\begin{aligned} \delta_v \Psi^\mu &= v\partial\Psi^\mu + \frac{1}{2}\Psi^\mu\partial v\,, & \delta_v \tilde\Psi^\mu &= v\partial\tilde\Psi^\mu + \frac{1}{2}\tilde\Psi^\mu\partial v\,,\\ \delta_v \chi &= v\partial\chi - \frac{1}{2}\chi\partial v\,, & \delta_v \tilde\chi &= v\partial\tilde\chi - \frac{1}{2}\tilde\chi\partial v\,. \end{aligned} \tag{2.1.2b}$$

[1] Π is often called the 'parity-reversing functor', and for our purposes simply states that the fields are anti-commuting.

[2] Beltrami differentials $\mu = \mu^{\bar z}_z d\bar z \otimes \partial_z$ parametrise the complex structure of Riemann surfaces. Nice reviews of these objects in the context of string theory can be found for example in [90, 91]. Notice that the kinetic terms and the energy-momentum tensor arise from a single term with the differential operator $\bar\partial + e\partial$.

The action (2.1.1) also contains another symmetry associated with the field $\tilde{e}$ that affect the bosonic fields, which can be called the ambitwistor gauge symmetry,

$$\delta_\alpha X^\mu = \alpha\, \eta^{\mu\nu} P_\nu\,, \qquad \delta_\alpha P_\mu = 0\,, \qquad \delta_\alpha e = 0\,, \qquad \delta_\alpha \tilde{e} = \bar{\partial}\alpha + e\partial\alpha - \alpha\partial e\,. \tag{2.1.3}$$

Combined with the constraint that $P^2 = 0$, the first of these transformations instructs us that we should not consider as different two points X^μ and X'^μ that differ by a translation along a null direction P_μ. Therefore, this symmetry is associated with the theory being placed in the space of complex null geodesics, i.e. ambitwistor space, hence why it is called the ambitwistor gauge symmetry.

Finally, the presence of the fermions gives the action (2.1.1) an $\mathcal{N} = 2$ supersymmetric extension of the ambitwistor gauge symmetry. For one set of these transformations parametrised by a Grassmann odd ϵ (associated to Ψ^μ), the bosonic fields transform according to

$$\delta_\epsilon X^\mu = \epsilon\Psi^\mu\,, \qquad \delta_\epsilon P_\mu = 0\,, \qquad \delta_\epsilon e = 0\,, \qquad \delta_\epsilon \tilde{e} = 2\epsilon\chi \tag{2.1.4a}$$

and the fermionic fields transform according to

$$\delta_\epsilon \Psi^\mu = \epsilon\, \eta^{\mu\nu} P_\nu\,, \qquad \delta_\epsilon \tilde{\Psi}^\mu = 0\,, \qquad \delta_\epsilon \chi = \bar{\partial}\epsilon + e\partial\epsilon - \frac{1}{2}\epsilon\partial e\,, \qquad \delta_\epsilon \tilde{\chi} = 0\,. \tag{2.1.4b}$$

The other set have similar transformations parametrised by $\tilde{\epsilon}$ (associated with $\tilde{\Psi}^\mu$). These transformations point out another crucial difference with respect to string theory. Namely, they are associated with the ambitwistor gauge transformations, generated by P^2, as opposed to the worldsheet diffeomorphisms generated by the energy-momentum tensor. Indeed, this can be seen by noticing that the supersymmetry transformations square not to the diffeomorphisms generated by the energy-momentum tensor, but to the ambitwistor gauge transformations generated by P^2. Consequently, one does not have worldsheet super-diffeomorphisms in the ambitwistor string, and therefore the theory is *not* formulated on a super-Riemann surface.

It should be mentioned that the bosonic part of the action (2.1.1) can be derived straightforwardly either from a chiral complexification of the worldline action for a massless particle, or from a chiral $\alpha' \to 0$ limit of Polyakov action in the bosonic string. This was noticed in [43], and indeed there it can also be seen that the full type II action similarly results from the chirally complexified worldline action by including fermions[3]. The ambitwistor string underpins the scattering amplitudes of CHY, and the action (2.1.1) results in the corresponding formulae for NS-NS gravity. Naturally one may then consider different ambitwistor string actions which give rise to amplitudes in different theories, and a large number have been found for the known CHY formulae [92]. The bosonic part of the action (2.1.1) forms the backbone for all of these theories[4].

2.2 Quantisation

In order to be able to calculate scattering amplitudes, one needs to be able to quantise the theory and find the physical vertex operators. In this section we will focus on the former,

[3] However, a chiral $\alpha' \to 0$ limit which results in the *full* action (2.1.1) has not yet been found. One of the difficulties behind this is that fermions in the type II superstring have opposite chirality, whereas here they have the same chirality.

[4] Though on its own, it forms an unrecognisable theory of gravity. It was believed that it would violate diffeomorphism invariance at one-loop, which motivated the use of including fermions [93]. Reference [94] suggests that the bosonic action could be seen as a double-copy of the $(DF)^2$ theory of [95].

which will in turn aid us in completing the latter for the theory we will be considering. Using BRST quantisation, much of the gauge-fixing procedure is similar to ordinary string theory. Therefore, we will be focusing on the crucial differences in comparison with the ambitwistor string, as well as any other results that will be of significant use to us in the next section where we calculate the vertex operators and subsequently the tree-level scattering amplitudes in the type II ambitwistor string. Both of these manifest in the form of picture-changing operators (PCOs). Since we will ultimately be considering n-point correlation functions, we will approach the gauge-fixing procedure with the knowledge that we will be working on a worldsheet with punctures.

As usual we introduce ghost systems associated with the gauge symmetries, discussed in the last section, we need to fix in the path integral. Like in ordinary string theory this gives us a bc system for the worldsheet diffeomorphisms and a $\beta\gamma$, $\tilde{\beta}\tilde{\gamma}$ system for the supersymmetries associated with Ψ, $\tilde{\Psi}$ respectively. For the ambitwistor gauge symmetry, being a bosonic symmetry, we also introduce a $\tilde{b}\tilde{c}$ system. We note since all fields in the ambitwistor string are chiral, so too are the ghosts, and that

$$b, \tilde{b} \in \Pi\Omega^0(\Sigma, K_\Sigma^2)\,, \qquad c, \tilde{c} \in \Pi\Omega^0(\Sigma, T_\Sigma)\,, \tag{2.2.1a}$$

$$\beta, \tilde{\beta} \in \Omega^0(\Sigma, K_\Sigma^{3/2})\,, \qquad \gamma, \tilde{\gamma} \in \Omega^0(\Sigma, T_\Sigma^{1/2})\,. \tag{2.2.1b}$$

Therefore the fields $b, \tilde{b}$ have conformal weight $(2, 0)$, $c, \tilde{c}$ have conformal weight $(-1, 0)$, $\beta, \tilde{\beta}$ have conformal weight $(\frac{3}{2}, 0)$ and $\gamma, \tilde{\gamma}$ have conformal weight $(-\frac{1}{2}, 0)$.

Worldsheet diffeomorphisms are gauge-fixed as in string theory; namely by setting $e = 0$ and integrating over the moduli space of the punctured Riemann sphere. Notice that when we set $e = 0$, from (2.1.3), (2.1.4b) the fields $\tilde{e}$, χ and $\tilde{\chi}$ transform with respect to their corresponding symmetries according to

$$\delta_\alpha \tilde{e} = \bar{\partial}\tilde{e}\,, \qquad \delta_\epsilon \chi = \bar{\partial}\chi\,, \qquad \delta_{\tilde{\epsilon}}\tilde{\chi} = \bar{\partial}\tilde{\chi}\,. \tag{2.2.2}$$

Since the gauge transformations are required to vanish at the locations of the punctures, the fields can then only vary according to a fixed Dolbeault cohomology class[5]. As $\tilde{e} \in \Omega^{0,1}(\Sigma, T_\Sigma)$, its relevant cohomology class is given by $H^{0,1}(\Sigma, T_\Sigma(-z_1 \cdots - z_n))$ which has dimension $3g + n - 3$. Likewise, since $\chi, \tilde{\chi} \in \Pi\Omega^{0,1}(\Sigma, T_\Sigma^{1/2})$ its relevant cohomology class is given by $H^{0,1}(\Sigma, T_\Sigma^{1/2}(-z_1 \cdots - z_n))$ which has dimension $2g + n - 2$. These cohomology classes are finite-dimensional and so can be expanded in a basis, which is chosen to be $\{\mu_r\}$ with $r = 1, \cdots 3g + n - 3$ and $\{\chi_\alpha\}$ with $\alpha = 1, \cdots, 2g + n - 2$.

As is usual in a quantisation procedure, we add a gauge-fixing term to the action, here in the form of [51, 97]

$$S_{\text{GF}} = \int_\Sigma \{Q, \tilde{b}\, F(\tilde{e}) + \beta\, G(\chi) + \tilde{\beta}\, \tilde{G}(\tilde{\chi})\} \tag{2.2.3}$$

where F, G, $\tilde{G}$ are gauge-fixing functions. Because we are working on a punctured Riemann surface (in the presence of vertex operators) we cannot straightforwardly use these functions to set the Lagrange multipliers to zero due to the transformations (2.2.2). From the considerations above we can at most set them to be elements of their respective cohomology

[5] As $\bar{\partial}^2 = 0$, there is naturally a cohomology determined by the Dolbeault operator $\bar{\partial}$, consisting of forms ϕ which are $\bar{\partial}$-closed, $\bar{\partial}\phi = 0$, but not $\bar{\partial}$-exact, $\phi \neq \bar{\partial}\tilde{\phi}$; see e.g. [96]

classes

$$F(\tilde{e}) = \tilde{e} - \sum_{r=1}^{3g+n-3} s_r \mu_r \,, \quad G(\chi) = \chi - \sum_{\alpha=1}^{2g+n-2} \zeta_\alpha \chi_\alpha \,, \quad \tilde{G}(\tilde{\chi}) = \tilde{\chi} - \sum_{\alpha=1}^{2g+n-2} \tilde{\zeta}_\alpha \chi_\alpha \,, \tag{2.2.4}$$

where s_r, ζ_α and $\tilde{\zeta}_\alpha$ are simply coefficients of the bases $\{\mu_r\}$ and $\{\chi_\alpha\}$. Doing this introduces (finite-dimensional) integrals over these coefficients along with $q_r = Q \circ s_r$, $\rho_\alpha = Q \circ \zeta_\alpha$, $\tilde{\rho}_\alpha = Q \circ \tilde{\zeta}_\alpha$ as well as (functional) integrals over the Nakanishi-Lautrup fields $H = Q \circ \tilde{b}$, $B = Q \circ \beta$ and $\tilde{B} = Q \circ \tilde{\beta}$. The functional integral over $\tilde{e}$ can then be performed explicitly which sets $H = P^2/2$. Following this, the integrals over the coefficients s_r and q_r then lead to PCOs in the path integral of the form [50]

$$\prod_{r=1}^{3g+n-3} \bar{\delta}\left(\int_\Sigma \mu_r P^2\right)\left(\int_\Sigma \mu_r \tilde{b}\right) . \tag{2.2.5}$$

At genus-zero we can choose the basis μ_r such that, when integrated against a quadratic differential over the worldsheet, it picks up the residue at a puncture location y_r. The role of the second factor in (2.2.5) is then similar to ordinary string theory. If we treat all vertex operators as fixed, then each one comes with a factor $c\tilde{c}$, however the residues of $b\tilde{b}$ at the marked points soak up these factors on account of $b_{-1}\tilde{b}_{-1}c\tilde{c} = 1$, which leaves the form of the vertex operators that are subsequently integrated over the worldsheet [90]. The first factor (2.2.5) is a characteristic feature of ambitwistor strings, which will inevitably fix the moduli space integrations onto the solutions of the scattering equations.

Likewise, the basis $\{\chi_\alpha\}$ can be chosen to pick up the value of a function at locations $\{x_\alpha\}$. Much of the remaining part of the procedure then proceeds as in traditional string theory; namely for those parameters related to $\chi, \tilde{\chi}$, similar integrations to those described above lead to the insertion of PCOs in the path integral of the form

$$\prod_{\alpha=1}^{2g+n-2} \left(\delta(\beta)\delta(\tilde{\beta})\, P\cdot\Psi\, P\cdot\tilde{\Psi}\right)(x_\alpha) \,. \tag{2.2.6}$$

These also play their respective role as in string theory, as we shall see below.

After this procedure, the gauge-fixed action becomes free with the inclusion of the ghost fields,

$$S = \frac{1}{2\pi}\int_\Sigma P_\mu \bar{\partial} X^\mu + \frac{1}{2}\Psi_\mu \bar{\partial}\Psi^\mu + \frac{1}{2}\tilde{\Psi}_\mu \bar{\partial}\tilde{\Psi}^\mu + b\bar{\partial}c + \tilde{b}\bar{\partial}\tilde{c} + \beta\bar{\partial}\gamma + \tilde{\beta}\bar{\partial}\tilde{\gamma} \,. \tag{2.2.7}$$

To complete the procedure, we would like to discuss the critical dimension, which is directly related to the condition that the BRST charge is nilpotent[6], $Q^2 = \{Q, Q\} = 0$. In string theory this is commonly assured by having the total central charge of the system vanish. The gauge-fixed (P, X) system consists of such fields, whose central charge $c_{X,P}$ is calculated in the usual way to be the $\mathcal{O}(\sigma^{-4})$ term in the energy-momentum tensor self-OPE. From (2.1.1) one reads off the energy-momentum tensor for this system to be $T_{X,P} = P_\mu \partial X^\mu$, whose self-OPE is easily calculated to be

$$[P_\mu \partial X^\mu](\sigma)[P_\mu \partial X^\mu](\sigma') \sim \frac{2D}{(\sigma-\sigma')^4} + \frac{[2P_\mu \partial X^\mu](\sigma')}{(\sigma-\sigma')^2} + \frac{[\partial(P_\mu \partial X^\mu)](\sigma')}{(\sigma-\sigma')}$$

[6] This is a necessary but not sufficient condition that that the theory is consistent in the quantum regime. For example, it is also required that the loop integration is well-defined; we will come back to this in a later section.

wherein one sees that $c_{X,P} = 2D$, with D the spacetime dimension. The central terms for all the other fields are known since they are simply free CFTs in two-dimensions upon gauge-fixing. For example, the two free fermion systems are known [90] to give a contribution $c_{\Psi,\tilde{\Psi}} = 2(D/2) = D$, and two copies of the b, c, β,γ system (or equivalently the B,C system [98]) with $\lambda = 2$ gives [99] a contribution $2c_{B,C} = 2(-15) = -30$. The condition that the total central charge vanish for the theory reads

$$c_{X,P} + c_{\Psi,\tilde{\Psi}} + c_{B,C} = 0 = 2D + D - 30 = 3(D - 10),$$

i.e. that the critical dimension is $D = 10$. This is again analogous to the RNS superstring, though as previously pointed out, all fields in this theory are chiral and we have $\alpha' = 0$, restricting us to massless modes of the string. This makes the ambitwistor string model fundamentally different to the CHY formalism, since there one can construct these amplitudes in any dimension, whereas here these are only physical in $D = 10$. On the Riemann sphere however is no obstruction in dimensionally reducing the formulae to produce amplitudes in lower-dimensions, whereas on higher-genus surfaces the requirement that $D = 10$ will be necessary for modular invariance, as we will discuss in later chapters. In the next section we will introduce the vertex operators required to obtain the NS-NS gravity amplitudes of CHY, as well as the conditions under which they are physical.

2.3 Vertex operators and the scattering equations

The method of obtaining amplitudes in string theory derive from the Polyakov path integral [100, 101]. At any *genus* g, this formalism instructs us to integrate over all worldsheet configurations in the presence of string insertions. Through the state-operator correspondence, the string states are accounted for by the insertion of vertex operators; the conditions under which these are physical is determined by their behaviour under the BRST transformations. Specifically, vertex operators correspond to physical states if they belong to the BRST cohomology. In this section we will present the vertex operators relevant to us and see how the scattering equations arise explicitly.

Let us now see the effect of the PCOs (2.2.5), (2.2.6) we obtained in the last section. Since we are primarily concerned with obtaining the scattering amplitudes for NS-NS gravity, we will use the vertex operators corresponding the NS-NS states[7]. Given the similarities with the RNS string, we can assume the unintegrated vertex operators take a similar form therein,

$$U_i(\sigma) = \delta(\gamma)\delta(\tilde{\gamma})\, \epsilon_i \cdot \Psi\, \tilde{\epsilon}_i \cdot \tilde{\Psi}\, e^{ik_i \cdot X(\sigma)}\,, \tag{2.3.1}$$

where k_i is the momentum of the i'th state. Note that this vertex operator has vanishing conformal weight as required. Each polarisation vector is associated with an NS state, and their outer product constitutes the polarisation tensor characterising the graviton, dilaton, and B-field in NS-NS gravity.

For an n-particle amplitude on the sphere ($g = 0$) let us assume the presence of n fixed vertex operators of the form (2.3.1). Being fixed, each of these will be accompanied by a $c\tilde{c}$ factor. Bosonisation of the superconformal ghosts $\gamma, \tilde{\gamma}$ give the vertex operators (2.3.1) being in the -1 picture. From (2.2.6) we have $n + 2g - 2$ PCOs which act on (2.3.1) through

[7] A more complete discussion involving Ramond states can be found in [50], where examples are also calculated explicitly.

the OPE

$$\begin{aligned}&\left[\delta(\beta)\delta(\tilde{\beta})\, P\cdot\Psi\, P\cdot\tilde{\Psi}\right](x)\ \left[\delta(\gamma)\delta(\tilde{\gamma})\,\epsilon_i\cdot\Psi\,\tilde{\epsilon}_i\cdot\tilde{\Psi}\, e^{ik_i\cdot X}\right](\sigma)\\ &\sim\left[(\epsilon_i\cdot P+\epsilon_i\cdot\Psi\, k_i\cdot\Psi)(\tilde{\epsilon}_i\cdot P+\tilde{\epsilon}_i\cdot\tilde{\Psi}\, k_i\cdot\tilde{\Psi})\, e^{ik_i\cdot X}\right](\sigma)\,,\end{aligned}\tag{2.3.2}$$

giving the vertex operators in the 0 picture, denoted $V_i(\sigma)$,

$$V_i(\sigma)=(\epsilon_i\cdot P+\epsilon_i\cdot\Psi\, k_i\cdot\Psi)(\tilde{\epsilon}_i\cdot P+\tilde{\epsilon}\cdot\tilde{\Psi}\, k_i\cdot\tilde{\Psi})\, e^{ik_i\cdot X(\sigma)}\,.\tag{2.3.3}$$

On the sphere there will be $n-2$ of these; this is in line with the fact that there must be two factors of $\delta(\gamma)\delta(\tilde{\gamma})$ for the two zero-modes of $\gamma,\tilde{\gamma}$ on the sphere [99]. One may check that the vertex operators (2.3.1) and (2.3.3) are BRST-closed under the conditions that $k_i^2=0$ and $\epsilon_i\cdot k_i=\tilde{\epsilon}_i\cdot k_i=0$, for which they are physical. They are also BRST-exact for $\epsilon_i\sim k_i$, $\tilde{\epsilon}\sim k_i$, in which the state is pure gauge.

We then have the PCOs given by (2.2.5). As mentioned in the last section, for each vertex operator V_i it acts on, the factors[8] $\int_\Sigma\hat{\mu}\, b\int_\Sigma\mu\,\tilde{b}$ remove the corresponding factors of $c\tilde{c}$ and replace them with $d\sigma_i^2$, following from the (holomorphic) form degrees. On the sphere there will be $n-3$ of these; this is in line with the fact that there must be three factors of $c\tilde{c}$ for the three zero-modes associated with the residual $\mathrm{SL}(2,\mathbb{C})$ symmetry [90]. Each of these however will also be accompanied by a factor $\bar{\delta}\left(\int_\Sigma\mu P^2\right)$. As mentioned in the last section, on the sphere we choose μ such that this extracts the residue of P^2 at the marked point σ_i, and therefore the integrated vertex operators take the form[9]

$$\mathcal{V}_i=\int_\Sigma\bar{\delta}(\mathrm{Res}_{\sigma_i}P^2)\, V_i(\sigma_i)\,.\tag{2.3.4}$$

But what is this residue? Let us look more closely at what occurs in the path integral. Each vertex operator from (2.3.1) and (2.3.3) contains the factor $e^{ik_i\cdot X(\sigma_i)}$, which in the path integral can be brought into the action (2.2.7) on the support of delta functions. The relevant part of the action then becomes

$$\frac{1}{2\pi}\int_\Sigma P\cdot\bar{\partial}X+2\pi i\, d\sigma\sum_{i=1}^n k_i\cdot X(\sigma)\,\bar{\delta}(\sigma-\sigma_i)\,.\tag{2.3.5}$$

By integrating by parts we can evaluate the X path integral straightforwardly. As in string theory the integration over the zero-modes of X produces a momentum-conserving delta-function, whilst the integration over the non-zero modes fix P to its classical value,

$$\bar{\partial}P_\mu(\sigma)=2\pi i\, d\sigma\sum_{i=1}^n k_{i\mu}\,\bar{\delta}(\sigma-\sigma_i)\,.\tag{2.3.6}$$

Using the fact that $2\pi i\,\bar{\delta}(\sigma-\sigma_i)=\bar{\partial}(1/(\sigma-\sigma_i))$, this has the following solution at genus-zero:

$$P_\mu(\sigma)=d\sigma\sum_{i=1}^n\frac{k_{i\mu}}{\sigma-\sigma_i}\,.\tag{2.3.7}$$

[8] The first of these arises as in the usual string, and $\hat{\mu}$ is the Beltrami differential associated directly with fixing the worldsheet diffeomorphisms.

[9] To make sense of this, we take the residue of a quadratic differential to be a one-form on Σ, so that when its form degree is taken out of the delta function it essentially cancels one of the $d\sigma_i$ coming from $V_i(\sigma_i)$, which is itself a quadratic differential from (2.3.3). Recall that the delta function itself is defined to be a distribution-valued $(0,1)$-form on Σ, so overall the correct measure is obtained in order to integrate over Σ.

On the sphere the field P is frozen to this value by the (X, P) path integral, so one may calculate the residue of P^2 directly from (2.3.7). Using momentum conservation and the fact that the k_j are null, this results precisely in the scattering equation for the i'th particle:

$$\text{Res}_{\sigma_i} P^2 = k_i \cdot P(\sigma_i) = d\sigma_i \sum_{j \neq i} \frac{k_i \cdot k_j}{\sigma_i - \sigma_j} \equiv d\sigma_i \, \mathcal{E}_i \, . \tag{2.3.8}$$

This is how the scattering equations arise in the ambitwistor string. In total, gauge-fixing the symmetry which enforces the target space to be ambitwistor space produces PCO insertions into the correlation functions which enforce the scattering equations. Therefore, they naturally arise from the fact that the string is in ambitwistor space, the space of complex null geodesics. The integrated vertex operators (2.3.4) are henceforth given by

$$\mathcal{V}_i = \int_\Sigma \bar{\delta}(k_i \cdot P(\sigma_i)) \, V_i(\sigma_i) \, , \tag{2.3.9}$$

with $V_i(\sigma_i)$ given as in (2.3.3). On the sphere there will be $n-3$ of these; this is in line with the fact that only $n-3$ of the scattering equations need to be enforced, due to its properties under $\text{SL}(2, \mathbb{C})$ as discussed in section 1.2.

Note that from (2.3.9), each moduli space integral $d\sigma_i$ is coupled to a scattering equation $\bar{\delta}(\mathcal{E}_i)$ to be enforced. All moduli space integrals are therefore fixed by the solutions to the scattering equations. The results of the correlation functions are thus more akin to field theory, where there is no notion of a worldsheet. The ambitwistor string is therefore a worldsheet model of quantum field theory.

2.4 From the ambitwistor string to CHY

In the last section we calculated the vertex operators for the NS-NS states in the ambitwistor string, taking into account the PCOs from the gauge-fixing procedure of section 2.2. We will now compute the n-point correlation function using these vertex operators, and in turn obtain the n-point NS-NS gravity amplitude.

From the considerations in the last section, this correlation function will take the form

$$\mathcal{A}^{(0)}_{\text{NS-NS}} = \left\langle c_r \tilde{c}_r U_r \, c_s \tilde{c}_s U_s \, c_t \tilde{c}_t V_t \prod_{i \neq r,s,t} \int_\Sigma \bar{\delta}(k_i \cdot P(\sigma_i)) V_i(\sigma_i) \right\rangle \, , \tag{2.4.1}$$

where we have chosen the PCOs (2.2.5) to act on all but three vertex operators labelled by r, s, t and the PCOs (2.2.6) to act on all but two vertex operators r, s. This is in line with the zero-mode counting of the $c, \tilde{c}$ and $\gamma, \tilde{\gamma}$ ghosts, as mentioned in the last section. The vertex operators U_i and V_i take the forms (2.3.1) and (2.3.3) respectively. In the last section we discussed how the X, P path integral is performed, so we have yet to perform the path integral for $\Psi, \tilde{\Psi}$ and the ghost fields. The latter is well-studied [90, 98, 99], so for now we will focus on the former. Note that in the action (2.2.7) the fermion fields are decoupled and symmetric under interchanges, so their path integrals will yield identical contributions in form. Let us then study in detail the Ψ path integral, which is analogous to

$$\int \mathcal{D}\Psi \, e^{-\frac{1}{2\pi} \int_\Sigma \Psi_\mu \bar{\partial} \Psi^\mu} \prod_{i=1}^{n} (\epsilon_i \cdot P(\sigma_i) + \epsilon_i \cdot \Psi(\sigma_i) \, k_i \cdot \Psi(\sigma_i)) \tag{2.4.2}$$

containing n picture-0 vertex operators (2.3.3). Of course, our path integral actually has $n-2$ of these, ($n-3$ which are integrated, and 1 from $c_t\tilde{c}_t V_t$) but we will deal with this later. To give an idea of how this is evaluated, one of the terms appearing in the product expansion of (2.4.2) will be

$$\int \mathcal{D}\Psi \; e^{-\frac{1}{2\pi}\int_\Sigma \Psi_\mu \bar{\partial}\Psi^\mu} \prod_{i=1}^{n} \epsilon_i \cdot \Psi(\sigma_i)\, k_i \cdot \Psi(\sigma_i)\,, \tag{2.4.3}$$

which is the term in (2.4.2) with maximal degree in Ψ. By considering all possible Wick contractions or otherwise, (2.4.3) can be seen to be equivalent to the Pfaffian of the $2n \times 2n$ matrix M',

$$M' = \begin{pmatrix} A & -C'^T \\ C' & B \end{pmatrix} \tag{2.4.4}$$

with block entries

$$A_{ij} = \frac{k_i \cdot k_j}{\sigma_{ij}} \sqrt{d\sigma_i d\sigma_j}\,, \qquad B_{ij} = \frac{\epsilon_i \cdot \epsilon_j}{\sigma_{ij}} \sqrt{d\sigma_i d\sigma_j}\,, \qquad C'_{ij} = \frac{\epsilon_i \cdot k_j}{\sigma_{ij}} \sqrt{d\sigma_i d\sigma_j}$$

for $i \neq j$ and $A_{ii} = B_{ii} = C'_{ii} = 0$. Here we have accounted for the form degrees by including them inside the matrix entries. On the other hand, the term in (2.4.2) with minimal degree in Ψ is

$$\int \mathcal{D}\Psi \; e^{-\frac{1}{2\pi}\int_\Sigma \Psi_\mu \bar{\partial}\Psi^\mu} \prod_{i=1}^{n} \epsilon_i \cdot P(\sigma_i)\,. \tag{2.4.5}$$

The field P has been fixed by the X path integral to be (2.3.7), so these terms appear as

$$\epsilon_i \cdot P(\sigma_i) = \sum_{j \neq i} \frac{\epsilon_i \cdot k_j}{\sigma_{ij}}\, d\sigma_i\,.$$

If one considers a square matrix M'' defined by

$$M'' = \begin{pmatrix} 0 & -C''^{\mathrm{T}} \\ C'' & 0 \end{pmatrix}$$

with 0 being the $n \times n$ empty matrix, and the block matrices C'' defined as

$$C''_{ii} = -\epsilon_i \cdot P(\sigma_i) = -\sum_{j \neq i} \frac{\epsilon_i \cdot k_j}{\sigma_{ij}} d\sigma_i\,, \qquad C''_{ij} = 0 \qquad \text{for } \; i \neq j$$

then the expression (2.4.5) can also be expressed as a Pfaffian, here of the matrix M''. Returning to (2.4.2), note that being an ordered product of these terms, we can write it as an expansion into all possible ordered subsets of the elements in the product

$$\int \mathcal{D}\Psi \; e^{-\frac{1}{2\pi}\int_\Sigma \Psi_\mu \bar{\partial}\Psi^\mu} \sum_{\substack{\mathfrak{b} \in \text{ordered} \\ \text{subset}}} \prod_{i \in \mathfrak{b}} \epsilon_i \cdot P(\sigma_i) \prod_{j \in \mathfrak{b}^c} \epsilon_j \cdot \Psi(\sigma_j)\, k_j \cdot \Psi(\sigma_j) \tag{2.4.6}$$

where $\mathfrak{b}^c$ denotes the complement of $\mathfrak{b}$. Given the examples above, the correlation function (2.4.6) can henceforth be written in terms of sums over products of Pfaffians

$$\sum_{\substack{\mathfrak{b} \in \text{ordered} \\ \text{subset}}} \mathrm{sgn}(\mathfrak{b}, \mathfrak{b}^c) \mathrm{Pf}\,(M''^{\{i\}}_{\{i\}}) \mathrm{Pf}\,(M'^{\{j\}}_{\{j\}})\,; \qquad i \in \mathfrak{b},\; j \in \mathfrak{b}^c.$$

Here the matrix $M''^{\{i\}}_{\{i\}}$ is simply the matrix M'' with the rows and columns of the subset $\mathfrak{b}$ removed; $M'^{\{j\}}_{\{j\}}$ is defined similarly, only with the rows and columns of $\mathfrak{b}^c$ removed. The $\text{sgn}(\mathfrak{b},\mathfrak{b}^c)$ factor has been added to cancel the minus signs that arise from the Pfaffians[10]. The Ψ path integral is performed in producing the Pfaffian of M'. To simplify this, we note the identity [50]

$$\text{Pf}\,(X+Y)=\sum_{\substack{\mathfrak{b}\in\text{ordered}\\ \text{subset}}}\text{sgn}(\mathfrak{b},\mathfrak{b}^c)\text{Pf}\,(X^{\{i\}}_{\{i\}})\text{Pf}\,(Y^{\{j\}}_{\{j\}})\,;\qquad i\in\mathfrak{b},\ j\in\mathfrak{b}^c$$

which gives the fermion path integral (2.4.2) as

$$\int\mathcal{D}\Psi_1\ e^{-\frac{1}{2\pi}\int_\Sigma\Psi_\mu\bar\partial\Psi^\mu}\prod_{i=1}^n(\epsilon_i\cdot P(\sigma_i)+\epsilon_i\cdot\Psi(\sigma_i)\,k_i\cdot\Psi(\sigma_i))=\text{Pf}\,(M'+M'')=:\text{Pf}\,(M).$$

The matrix M is defined to be the sum of M' and M'' and is precisely the matrix (1.1.9) present in the CHY expressions for Yang-Mills and gravity. As mentioned above the path integral over the other fermionic field $\tilde\Psi$ will yield an identical contribution, only with tilde'd polarisation vectors.

This is not however what we have in our correlation function; we do not have n picture-0 vertex operator insertions, but only $n-2$ of them. The others come from treating the U insertions as if they were V insertions, though they differ by a factor involving $k_i\cdot\Psi(\sigma_i)$ and an additional $\epsilon_i\cdot P(\sigma_i)$ factor. To give the correct contributions accounting for the U insertions, we only need to get rid of the rows and columns which contain these differing factors. Since, from (2.4.1), the U insertions are associated with the particles labelled by r and s, the correct Pfaffian structure is obtained by removing these rows and columns, $\text{Pf}\,(M)\to\text{Pf}\,(M^{rs}_{rs})$.

Evaluating the $\beta\gamma$ path integral gives a factor $\sqrt{d\sigma_r d\sigma_s}/\sigma_{rs}$ from the $\delta(\gamma)\delta(\gamma)$ contraction at locations σ_r,σ_s, which we combine with the Pfaffian above to form the reduced Pfaffian:

$$\frac{\sqrt{d\sigma_r d\sigma_s}}{\sigma_{rs}}\,\text{Pf}\,(M^{rs}_{rs})\cong\text{Pf}'(M)\,.\tag{2.4.7}$$

The form degree is here included in the reduced Pfaffian so that it has the appropriate form degree for all particles. From the CHY perspective the (unreduced) Pfaffian of M vanishes due to being co-rank 2; in the ambitwistor string this Pfaffian actually vanishes to second order as a consequence of the worldsheet supersymmetry (2.1.4a), (2.1.4b) at $e=0$ [43]. Likewise, the permutation symmetry of the reduced Pfaffian, is simply a consequence of our freedom in applying the PCOs.

Finally, what remains is the path integrals for the bc and $\tilde b\tilde c$ ghost systems. The integration over the $c\tilde c$ factors in (2.4.2) is well-known[11] at genus-zero, and both result in a factor $\sigma_{rs}\sigma_{st}\sigma_{tr}/d\sigma_r d\sigma_s d\sigma_t$. Respecting the notation of [43] we write one of these factors as $1/\text{vol}\,\text{SL}(2,\mathbb{C})$ and combine the other with the delta-functions in (2.3.9) to give

$$\frac{\sigma_{rs}\sigma_{st}\sigma_{tr}}{d\sigma_r d\sigma_s d\sigma_t}\prod_{i\neq r,s,t}\bar\delta(k_i\cdot P(\sigma_i))=\frac{\sigma_{rs}\sigma_{st}\sigma_{tr}}{d^n\sigma}\prod_{i\neq r,s,t}\bar\delta(\mathcal{E}_i)=:\prod_i{}'\,\bar\delta(\mathcal{E}_i)\tag{2.4.8}$$

[10] Expanding the product in (2.4.2) produces only positive signs so explicit minus signs are undesirable

[11] See e.g. [90].

pulling out the form degree in the delta functions.

Altogether, we have that the n-point NS-NS gravity amplitude is given by

$$\mathcal{A}^{(0)}_{\text{NS-NS}} = \int_\Sigma \frac{1}{\text{vol SL}(2,\mathbb{C})} \prod_i{}' \bar{\delta}(\mathcal{E}_i)\, \text{Pf}'(M)\, \text{Pf}'(\tilde{M})\,, \tag{2.4.9}$$

with ten-dimensional momentum conservation implicit from the X zero-mode path integral, and $\tilde{M} = M(\epsilon \to \tilde{\epsilon})$ following from the $\tilde{\Psi}$ path integral. This is precisely equal to the CHY form of NS-NS gravity amplitudes from section 1.1. Indeed, pulling out the form degrees from the Pfaffians and the primed product, we obtain an overall $d^n\sigma$ which combines with the $1/\text{vol SL}(2,\mathbb{C})$ and $\prod_i' \bar{\delta}(\mathcal{E}_i)$ factors to form the CHY measure $d\mu_n$,

$$\mathcal{A}^{(0)}_{\text{NS-NS}} = \int_{\mathfrak{M}_{0,n}} d\mu_n\, \text{Pf}'(M)\, \text{Pf}'(\tilde{M})\,, \tag{2.4.10}$$

where now the reduced Pfaffians and CHY measure are defined exactly as in section 1.1. With the $d^n\sigma$ and vol $\text{SL}(2,\mathbb{C})$ factors explicit we understand the integration to be over the moduli space $\mathfrak{M}_{0,n}$. The type II model of the ambitwistor string therefore leads directly to the CHY formulae of NS-NS gravity.

What is also transparent in the derivation is that the 'CHY integrand' follows from the Ψ, $\tilde{\Psi}$ path integral, and the 'CHY measure' follows from the X, P and ghost path integrals and PCOs from the gauge-fixing procedure. In other words, it is specifically the type II model with matter fields Ψ, $\tilde{\Psi}$ which produces the formulae for gravity. Naturally one may consider ambitwistor string models with *different* matter fields, whose correlation functions give rise to CHY formulae for *different* theories.

In its inception [43] it was proposed that one could obtain Yang-Mills amplitudes by considering another model which contained the fermionic system Ψ along with a current algebra $j^a(\sigma) \in K_\Sigma \times \mathfrak{g}$, with $\mathfrak{g}$ an arbitrary affine Lie algebra and $a = 1, \cdots, \dim \mathfrak{g}$. These current algebras would have the OPE

$$j^a(\sigma)\, j^b(\sigma') \sim \frac{k\delta^{ab}}{(\sigma-\sigma')^2} + \frac{i f^{abc} T^c}{(\sigma-\sigma')} + \cdots \tag{2.4.11}$$

where the T^a are the generators (bases) of the gauge group (Lie algebra), and f^{abc} are the corresponding structure constants with $[T^a, T^b] = f^{abc}T^c$. The factor k denotes the level of the affine Lie algebra and δ^{ab} is the respective Killing form. The inclusion of such a current algebra produces correlation functions whose single-trace contribution correspond to the tree-level amplitudes of Yang-Mills theory. This means however that one must discard multi-trace contributions by hand if one were to consider it a model thereof.

Reference [92] attempted to remedy this by considering instead a 'comb system', whose correlation functions would yield Parke-Taylor factors with strings of structure constants as numerators, which is precisely used in the representation of the colour half-integrands (1.4.2). This system uses worldsheet spinors which take values in $\mathfrak{g}$,

$$S_{\text{CS}} = \int_\Sigma \tilde{\rho} \cdot \bar{\partial}\rho + q \cdot \bar{\partial} y + \chi\rho \cdot \left(\frac{1}{2}[\rho, \tilde{\rho}] + [q, y]\right) \tag{2.4.12}$$

where $\rho, \tilde{\rho} \in \Pi\Omega^0(\Sigma, K_\Sigma^{1/2} \times \mathfrak{g})$ are fermionic, $q, y \in \Omega^0(\Sigma, K_\Sigma^{1/2} \times \mathfrak{g})$ are bosonic, and $\cdot$ represents the Killing form. This system can be incorporated to obtain amplitudes e.g. in

EYM, but turns out to be anomalous [92]. This motivated a 'reduced' Yang-Mills system which provides the correct Yang-Mills amplitudes, but is also anomalous[12]. This reference therefore also provides ambitwistor string models for the (Dirac-)Born-Infeld ((D)BI) theory, Einstein-Maxwell (EM), the Galileon, the non-linear sigma model (NLSM), Einstein-Maxwell scalar (EMS), Einstein Yang-Mills scalar (EYMS), generalised Yang-Mills scalar and the biadjoint scalar. This followed and expanded on previous work in [102] which had already obtained the ambitwistor string model for the Galileon and BI theories.

2.5 The ambitwistor string at genus-one: the scattering equations and worldsheet degeneration

It was not long after the discovery of the ambitwistor string, which completely described the tree-level CHY amplitudes, that a one-loop extension was found. Since the tree-level description followed from the ambitwistor string at genus-zero, it was then natural to suggest that one-loop formulae could be obtained by studying the ambitwistor string at genus-one, on the torus. This was performed explicitly by Adamo, Casali and Skinner (ACS) in [50], where the genus-one analogue of the scattering equations was found and explicit formulae for the scattering amplitudes on the torus were presented. This was further studied by the authors of [103, 104], who provided a new interpretation of the results of ACS which we will use throughout the thesis. Here we will briefly summarise the main points of these references that will be relevant for the following chapters.

To be somewhat pedagogical let us look again at what occurs in the correlation function at genus one, following the gauge-fixing procedure. From the discussion of section 2.2, there are n PCOs from gauge-fixing each of the symmetries discussed therein, of which we will focus on those arising from the ambitwistor gauge-transformation (2.2.5). These will act in a similar way to the genus-zero case, except here one only needs to use $n-1$ of them to set the residues of P^2 equal to zero. This is because the torus has translation invariance, which is analogous to the $\mathrm{SL}(2,\mathbb{C})$ invariance on the sphere, so that one of the marked points should be fixed. As a result, setting $n-1$ of the residues at the marked points to zero ensures that all n residues of the quadratic differential P^2 vanish. Unlike the genus-zero case however, doing this does *not* ensure that $P^2 = 0$ globally on the worldsheet. To see this, let us recall that P is fixed by the X, P path integral via (2.3.6),

$$\bar{\partial} P_\mu(z) = 2\pi i \, dz \sum_{i=1}^{n} k_{i\mu} \, \bar{\delta}(z - z_i) \, . \tag{2.5.1}$$

Equation (2.3.7) gave the solution to this at genus-zero, but at genus-one the solution can be written as [97]

$$P_\mu(z) = 2\pi i \ell_\mu \, \omega(z) + \sum_{i=1}^{n} k_{i\mu} \, \omega_{i,*}(z) \, . \tag{2.5.2}$$

Let us briefly talk about the new elements appearing here. Firstly, on a genus-g Riemann surface there exist g holomorphic Abelian differentials[13] ω_I, $I = 1, \cdots, g$, which can constitute the zero-modes of a $(1,0)$-form on the genus-g surface. Consequently, at genus-one

[12] The comb-system, whilst appropriate to describe EYM amplitudes, has two types of gluons and thus is not appropriate on its own to describe Yang-Mills amplitudes. The interested reader is referred to the original reference [92] for more details.

[13] This is a standard result of the Riemann-Roch theorem.

the solution for P should contain a single zero-mode, thought of as a constant of integration. The first term of (2.5.2) is this zero-mode, where $\omega(z)$ is an *Abelian differential of the first kind* defined in appendix A, forming a basis for this zero-mode and ℓ_μ is simply the coefficient of this basis. The object $\omega_{i,*}(z)$ is an *Abelian differential of the third kind*, also defined in appendix A, and produces a simple pole with residue ± 1 as $z \approx z_i$ and as $z \approx z_*$ respectively, here with z_* being an arbitrary point. Whilst (2.5.2) appears differently to the form of $P_\mu(z)$ appearing in e.g. [50] and [103], it can be shown that it is equivalent to both, up to redefinitions of ℓ_μ and momentum conservation. In fact, if one extended (2.5.2) to have g such zero-mode terms, it would be the solution for genus-g [51].

Returning to the previous discussion, since there were no zero-modes at genus-zero P^2 only contained simple poles, and so setting the residues to zero ensured that P^2 vanished on the worldsheet. On the torus, the presence of zero modes in P means that setting the residues at the poles to zero (via $n-1$ PCOs) only makes P^2 holomorphic on the worldsheet. As was first noticed in [50], the role of the final PCO is to set this holomorphic piece to zero by setting $P^2(z_0) = 0$ at an arbitrary point z_0,

$$\bar{\delta}\left(\int_\Sigma \mu\, P^2\right)\left(\int_\Sigma \mu\, \tilde{b}\right) = \bar{\delta}(P^2(z_0))\, \tilde{b}(z_0)\,. \tag{2.5.3}$$

With this insertion into the path integral, P^2 vanishes on the worldsheet. As at genus-zero the scattering equations arise from this constraint and therefore, the genus-one scattering equations are equivalent to

$$\begin{aligned} \text{Res}_{z_i} P^2 = k_i \cdot P(z_i) = 0 \qquad\qquad & i = 2, \cdots, n \\ P^2(z_0) = 0 & \end{aligned} \tag{2.5.4}$$

where we have fixed one of the coordinates (here z_1) using the translation invariance on the torus. It is important to mention that on the genus-one surface, the field P (and therefore the genus-one scattering equations (2.5.4)) depends on the modular parameter[14] τ. Consequently, it is (they are) expressed in terms of functions naturally adapted to higher-genus Riemann surfaces, involving e.g. Jacobi theta functions. These objects are highly non-trivial, which makes solving the scattering equations (2.5.4) non-viable. Luckily, the constraint $P^2(z_0) = 0$ in (2.5.4) plays a signature role in the ambitwistor string which alleviates this issue.

To see how this is, let us consider a general genus-one amplitude that arises from the ambitwistor string correlator. To be heuristic, we will write the n-point expression as

$$\mathcal{A}_n^{(1)} = -\int d^D\ell\, d\tau\, \mathfrak{I}(z;\tau)\, \bar{\delta}(P^2(z_0;\tau)) \prod_{i=2}^{n} \bar{\delta}(k_i \cdot P(z_i))\,. \tag{2.5.5}$$

In the above expression, the integration is over the fundamental domain of the genus-one surface (see figure 2.1), as well as the $n-1$ marked points not fixed by translation invariance.

[14] In the path integral one has sum over all possible worldsheet geometries. Any compact genus-zero Riemann surface is equivalent to the Riemann sphere $\mathbb{CP}^1$ by diffeomorphism and Weyl transformations. Heuristically, on higher genus surfaces these transformations are not sufficient to completely fix the 'shape' of the Riemann surface in the same way, and the *intrinsic moduli* parametrise the shapes of the surface modulo these transformations. In this sense the integration over the modular parameters completes the sum over worldsheet geometries. At genus-one there is one modular parameter τ, and for genus $g \geq 2$ there are in general $3g-3$ modular parameters.

The object $\mathfrak{I}(z;\tau)$ denotes the rest of the string integrand, involving e.g. the correlation function of the fields. From this we have also pulled out the integration over the zero-modes of P into a D-dimensional[15] finite integral, $d^D\ell$. Importantly, the delta function setting $P^2(z_0)$ to zero should be treated as a global form, so that for our purposes it should be thought of as $\bar\delta(\cdots) = d\bar\tau\,\partial_{\bar\tau}(1/\cdots)$. In this respect, (2.5.5) is equivalent to

$$\mathcal{A}_n^{(1)} = -\int d^D\ell\; d\tau\wedge d\bar\tau\;\mathfrak{I}(z;\tau)\;\frac{\partial}{\partial\bar\tau}\left(\frac{1}{P^2(z_0;\tau)}\right)\prod_{i=2}^n\bar\delta(k_i\cdot P(z_i))\,. \tag{2.5.6}$$

Let us change variables here to $q = e^{2\pi i\tau}$, wherein (2.5.6) becomes

$$\mathcal{A}_n^{(1)} = -\int d^D\ell\;\frac{dq\wedge d\bar q}{2\pi i\,q}\;\mathfrak{I}(z;q)\;\frac{\partial}{\partial\bar q}\left(\frac{1}{P^2(z_0;q)}\right)\prod_{i=2}^n\bar\delta(k_i\cdot P(z_i))\,. \tag{2.5.7}$$

What we can do now exhibits a signature feature of the ambitwistor string at higher genus. If the object $\mathfrak{I}(z,q)$ is holomorphic[16] in q, then when we perform an integration by parts the derivative now moves to the factor $1/2\pi iq$, which by Stokes' theorem results in a contour integral around $q=0$, localising the amplitude to this value. This can be seen graphically in figure 2.1, equivalently as a *global residue theorem* [103] which brings the integration over the fundamental domain to a contour integral over the boundary. By modular invariance all pieces except that at $q=0$ ($\tau = i\infty$) cancel each other, leaving the amplitude localised on the boundary $q=0$.

It is well-known that this boundary corresponds to the infinite 'pinching' of one of the cycles of the torus, leading to a configuration which is equivalent to a sphere with two nodes corresponding to points which have been identified. This is called the *nodal sphere*. To be more precise, the global residue theorem localises the amplitude onto the maximal non-separating boundary divisor of the genus-one surface $\mathfrak{D}_{n,1}^{\rm max}\cong\mathfrak{M}_{0,n+2}$. The role of the final scattering equation is therefore two-fold; firstly, it localises the modular parameter onto $\tau = i\infty$, equivalently $q=0$, such that the torus degenerates into a nodal sphere. Under this the amplitude (2.5.7) then becomes

$$\mathcal{A}_n^{(1)} = \int_{\mathfrak{M}_{0,n+2}} d^D\ell\;\frac{1}{P^2(\sigma_0;0)}\,\hat{\mathcal{I}}(\sigma)\;\prod_{i=2}^n\bar\delta(k_i\cdot P(\sigma_i))\,, \tag{2.5.8}$$

where we change variables from z to σ in going to the nodal sphere with moduli space $\mathfrak{M}_{0,n+2}$, and the integrands now become functions of coordinates on the Riemann sphere $\hat{\mathcal{I}}(\sigma)$. Secondly it provides an overarching factor necessary for the one-loop integrands: It can be shown [50, 103], that in the degeneration limit, one has $P^2(\sigma_0;0) = \ell^2\,\omega_{+-}^2(\sigma_0)$, so that the final formula for the one-loop amplitude becomes

$$\mathcal{A}_n^{(1)} \to \int_{\mathfrak{M}_{0,n+2}}\frac{d^D\ell}{\ell^2}\,\hat{\mathcal{I}}(\sigma)\;\prod_{i=2}^n\bar\delta(k_i\cdot P(\sigma_i))\,. \tag{2.5.9}$$

[15] In order to connect properly with field theory, it should be understood that we integrate over a middle-dimensional cycle of $\mathbb{C}^D$ such that ℓ_μ is real. In principle, given a well-defined integrand $\mathfrak{I}(z;\tau)$, the dimension D is determined by modular invariance. For the type II model first described in [50] which we will discuss in the next section, modular invariance requires $D=10$. We elaborate on modular invariance more generally in section 5.1.2.

[16] This is true for the type II theory discussed in [50] which we will elaborate on in the next section. In general, it is crucial that the integrand has this property in order to perform the global residue theorem cleanly.

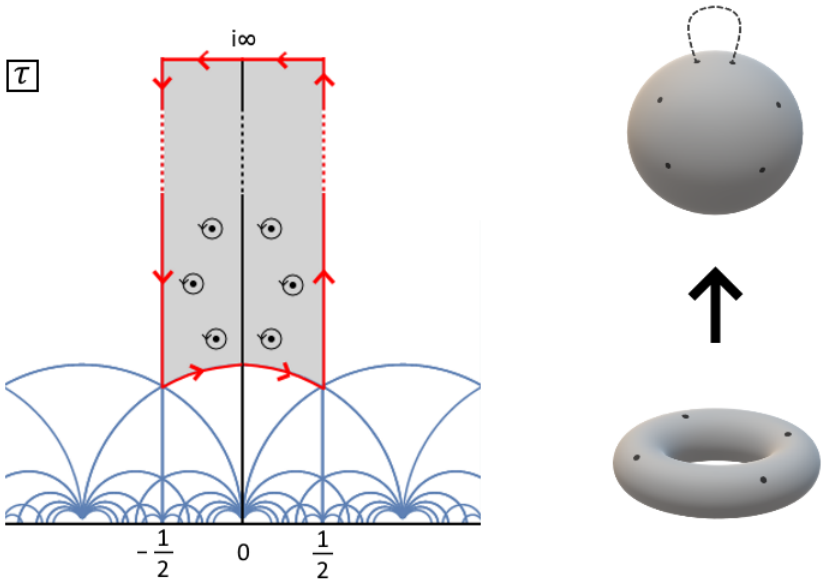

Figure 2.1: The effect of enforcing the 'modular' scattering equation at genus-one. The integration over the fundamental domain of τ (the grey region in the left diagram above) becomes a contour integral over the boundary from Stokes' theorem. By modular invariance, only the contour at $\tau \to i\infty$ survives, where the torus degenerates onto a Riemann sphere with two nodal points.

These features of the 'modular scattering equations' on the higher-genus surface persevere at higher-genus, as shown for example at two-loops in [51, 105].

The two nodes that result from the degeneration should be thought of as two extra states with back-to-back momenta, preserving momentum conservation. In performing the degeneration, the two nodes, which we will call σ_+ and σ_- become fixed. For example, the coordinate transformation in [104], given by $\sigma = e^{2\pi i(z-\tau/2)}$, maps in the limit $\tau \to i\infty$ the fundamental domain for z to the Riemann sphere with the points $\sigma_+ = 0$ and $\sigma_- = \infty$ identified. This leads to an expression on the sphere with 3 fixed punctures and $n-1 = (n+2)-3$ punctures that are integrated over. One should think of these fixed points as being fixed by the $\mathrm{SL}(2,\mathbb{C})$ invariance of the nodal sphere. With this $\mathrm{SL}(2,\mathbb{C})$ symmetry restored (so that $\sigma_1, \sigma_+, \sigma_-$ are no longer fixed), the field $P(\sigma)$ from (2.5.2) on the sphere takes the form

$$P_\mu(\sigma) = \ell_\mu\, \omega_{+-}(\sigma) + \sum_{i=1}^{n} k_{i\mu}\, \omega_{i,*}(\sigma)\,, \tag{2.5.10}$$

where in the degeneration limit the Abelian differentials become

$$2\pi i\, \omega \rightsquigarrow \omega_{+-}(\sigma) = \frac{(\sigma_+ - \sigma_-)}{(\sigma-\sigma_+)(\sigma-\sigma_-)}\, d\sigma\,, \quad \omega_{i,j} \rightsquigarrow \omega_{i,j}(\sigma) = \frac{(\sigma_i - \sigma_j)}{(\sigma-\sigma_i)(\sigma-\sigma_j)}\, d\sigma\,. \tag{2.5.11}$$

Substituting (2.5.11) into (2.5.10) makes concrete that the field P is now defined as at tree-level with two extra states having back-to-back momenta ℓ_μ,

$$P_\mu(\sigma) = \ell_\mu \left(\frac{1}{\sigma-\sigma_+} - \frac{1}{\sigma-\sigma_-} \right) d\sigma + \sum_{i=1}^{n} \frac{k_{i\mu}}{\sigma-\sigma_i} d\sigma\,, \tag{2.5.12}$$

wherein the dependence on the arbitrary point σ_* drops out by momentum conservation. Unlike the tree-level case however, P^2 now has double poles in the nodal points, since the momentum ℓ_μ is generically off-shell[17]. The tree-level scattering equations were defined as the residues of a meromorphic quadratic differential (there simply P^2), and one can do the same here by defining a similar object

$$\mathfrak{P}_1(\sigma) = P^2(\sigma) - \ell^2\omega_{+-}^2(\sigma) \tag{2.5.13}$$

which has only simple poles. The residues at the marked points (including the nodes) of this object define the *one-loop scattering equations*:

$$\mathcal{E}_A^{(1)} = \text{Res}_{\sigma_A}\mathfrak{P}_1(\sigma) \tag{2.5.14}$$

where the label A runs over the external labels and the nodal labels, $A \in \{1, \cdots, n, +, -\}$. These are dubbed the *off-shell* scattering equations [104], and are aligned with the $(n+2)$-point tree-level scattering equations with 2 massive states in the forward-limit [84]. Specifically, the one-loop scattering equations take the form

$$\begin{aligned}\mathcal{E}_i^{(1)} &= \frac{k_i\cdot\ell}{\sigma_i-\sigma_+} - \frac{k_i\cdot\ell}{\sigma_i-\sigma_-} + \sum_{j\neq i}\frac{k_i\cdot k_j}{\sigma_i-\sigma_j}\,,\\ \mathcal{E}_\pm^{(1)} &= \pm\sum_{i=1}^n \frac{\ell\cdot k_i}{\sigma_\pm-\sigma_i}\,.\end{aligned} \tag{2.5.15}$$

Note that the one-loop scattering equations follow from but are not the same as the genus-one scattering equations (2.5.4). The latter are defined on the genus-one surface and are seemingly impracticable to solve, whilst the former are defined on the nodal sphere and can in principle be solved[18].

Although these are called off-shell scattering equations, they bare a remarkable resemblance to the tree-level scattering equations with an on-shell back-to-back momentum. We will exploit this in chapter 4 when we speak about non-supersymmetric amplitudes at two-loops. Of course, this resemblance disintegrates when one considers the solutions to these equations, first studied in [84]. There they found that there are two types of solutions that contribute to the amplitude:

$$\begin{aligned}(n-1)!-2(n-2)! \qquad & \textit{regular} \text{ solutions},\\ (n-2)! \qquad & \textit{singular} \text{ solutions}.\end{aligned}$$

The *regular* solutions correspond to solutions where the nodal points are distinct, $\sigma_+ \neq \sigma_-$, whilst the *singular* solutions correspond to solutions in which the nodal points coincide, $\sigma_+ = \sigma_-$. These do not add up to $(n-1)!$, the number of solutions to the $(n+2)$-point tree-level scattering equations[19]. For the supersymmetric theories to be discussed in the next section, the resulting worldsheet formulae vanish on the singular solutions [104], so only the regular solutions are required. For more generic theories (without supersymmetry) however, the singular solutions will generically contribute and should be included.

[17] Recall that at tree-level, there were no double poles due to all k_i being null.

[18] In fact, four-point solutions to these equations can be found in [104].

[19] From the perspective of [84], where these were derived using a massive forward-limit, the remaining $(n-2)!$ do not survive the forward limit, and so do not contribute to the amplitude.

One reason for this follows from the analysis of [106], where it was shown that with the one-loop scattering equations, integrands can admit discriminant-type poles which are unphysical, even when considering the regular solutions. This happens because, even though the regular solutions are characterised by having $\sigma_{+-} \neq 0$, there may be special kinematic configurations in which the solutions for $\sigma_\pm$ become degenerate. Notice from (2.5.15) that when $\sigma_+ = \sigma_-$, the $\mathcal{E}_i$ simply become the tree-level scattering equations, and $\mathcal{E}_\pm$ take the same functional form. The former implies that the solutions for the $\{\sigma_i\}$ are those of the tree-level scattering equations, and the latter implies that solutions for $\sigma_\pm$ then become degenerate. It is possible to see what this unphysical pole looks like. Writing $N_\pm$ as the numerator of $\mathcal{E}_\pm$, which is a polynomial in the $\{\sigma_i, \sigma_\pm\}$, the solutions for $\sigma_\pm$ become degenerate when the discriminant of the polynomial $N_\pm$ becomes 0. The unphysical kinematic poles therefore take the form

$$\Delta = \prod_{\{\sigma_i\} \text{ tree sols}} \text{Disc}\, N_\pm \,. \tag{2.5.16}$$

These unphysical kinematic poles can typically arise when considering the regular solutions. For maximally supersymmetric theories however, they can be localised on the singular solutions which do not contribute to the amplitude, and therefore do not occur. For non-supersymmetric theories however, this is not generally the case, and so omitting singular solutions will lead to these unphysical poles.

To summarise, the n-point genus-one amplitudes in the ambitwistor string can be formulated on a nodal sphere with $n+2$ marked points, making the one-loop calculation analogous to that at tree-level, now with one-loop scattering equations. Like there, these scattering equations again fix the moduli space integrals, leaving only the $d^D\ell$ integration to be performed. Thus, the momentum ℓ can be recognised as the *loop momentum*, and the result of the moduli space integrations, localised on the one-loop scattering equations, recognised as the *loop integrand*.

2.6 The genus-one ambitwistor string: integrands

In the last section we discussed certain aspects of the ambitwistor string at genus-one resulting from the quantisation procedure. In particular, we saw that whilst string amplitudes involves an integration over the intrinsic modular parameter τ at genus-one, enforcing $P^2 = 0$ on the worldsheet necessitated the inclusion of a PCO enforcing a 'modular scattering equation'. This scattering equation localises the modular integration to the maximal non-separating boundary divisor $\mathfrak{D}^{\text{max}}_{1,n}$ where the torus degenerates to the nodal sphere, $\mathfrak{D}^{\text{max}}_{1,n} \equiv \mathfrak{M}_{0,n+2}$. The result is an n-amplitude expressed on the sphere with two extra punctures σ_+, σ_- associated with the nodes, essentially corresponding to states with back-to-back momenta identified as the loop-momentum.

We stress that this degeneration relies crucially on the integrand $\mathcal{I}(z;q)$ having no poles in $q = e^{2\pi i\tau}$. Otherwise, the residue theorem would pick up different poles and the amplitude would not be fully localised on the nodal sphere. In an attempt to give an overview of the global residue theorem we did not specify the integrand $\mathcal{I}(z;q)$; in this section we elaborate on this object a little more.

At genus-zero there was one natural worldsheet theory to consider in obtaining gravity amplitudes, which was the type II theory. To date, only this model is well-known in the

context of the genus-one ambitwistor string. This model was studied in detail at genus-one by ACS in [50], wherein the correlators were calculated in detail for all (even and odd) spin structures. We will mainly be focused here on the even spin structures, since this will be most relevant for us. From [50, 104] this contribution is given by

$$\begin{aligned}\mathfrak{I}(z;\tau) &= \frac{1}{4}\sum_{\alpha,\beta=2,3,4}(-1)^{\alpha+\beta}\mathcal{Z}_{\alpha;\beta}(\tau)\mathrm{Pf}\,(M_\alpha)\,\mathrm{Pf}\,(M_\beta)\\ &= \left(\frac{1}{2}\sum_{\alpha=2,3,4}(-1)^{\alpha}\mathcal{Z}_{\alpha}(\tau)\,\mathrm{Pf}\,(M_\alpha)\right)\left(\frac{1}{2}\sum_{\beta=2,3,4}(-1)^{\beta}\mathcal{Z}_{\beta}(\tau)\,\mathrm{Pf}\,(\tilde{M}_\beta)\right)\,.\end{aligned} \tag{2.6.1}$$

This sum arises as part of the GSO projection invoking a sum over spin structures, which is natural step in the RNS formalism and is required for modular invariance of the amplitude. There are $2^{g-1}(2^g+1)=3$ even spin structures at genus one (labelled here for even characteristics $\alpha,\beta=2,3,4$) and $2^{g-1}(2^g-1)=1$ odd spin structure; the factor of $1/4$ arises from the sum over the total $2^{2g}=4$ spin structures. The $\mathcal{Z}_\alpha(\tau)$ are chiral partition functions which arise from worldsheet CFT correlators on the torus. Again, via Wick contractions the fermionic path integral produces Pfaffians M_α ($\tilde{M}_\beta$) of matrices which are genus-one extensions of the CHY matrices and depend on the spin structure through *Szegö kernels*, as well as the polarisations ϵ_i ($\tilde{\epsilon}_i$) and momenta k_i of the external states. At genus-zero, the Szegö kernels reduce to σ_{ij}^{-1}, resulting in the tree-level CHY matrix. The precise form of the matrices M_α and the Szegö kernels at genus-one can be found in [50, 104]. Of more interest to us is that the integrand $\mathfrak{I}(z;\tau)$ from (2.6.1) again splits into two chiral half-integrands, $\mathfrak{I}(z;\tau)=\mathfrak{I}_{1/2}(z;\tau)\,\tilde{\mathfrak{I}}_{1/2}(z;\tau)$, which by performing the sum explicitly in (2.6.1) are given by

$$\mathfrak{I}_{1/2}(z;\tau)=\frac{1}{2}\left(\mathcal{Z}_2(\tau)\mathrm{Pf}\,(M_2)-\mathcal{Z}_3(\tau)\mathrm{Pf}\,(M_3)+\mathcal{Z}_4(\tau)\mathrm{Pf}\,(M_4)\right) \tag{2.6.2}$$

with $\tilde{\mathfrak{I}}_{1/2}(z;\tau)$ related to $\mathfrak{I}_{1/2}(z;\tau)$ by $\epsilon_i\to\tilde{\epsilon}_i$ as usual. From the discussion in the previous section we are interested in the limit $\tau\to i\infty$ of these expressions, corresponding to the degeneration limit. Reference [104] studied these limits in detail using coordinates $\sigma=e^{2\pi i(z-\tau/2)}$ better suited to the sphere in the degeneration limit. There it was calculated that the half integrands (2.6.2) simplify in the limit $\tau\to i\infty$, or $q=0$, to

$$\hat{\mathcal{I}}^{(1)}_{\text{susy-kin}}=\mathrm{Pf}\,(M_3)|_{q^{1/2}}+8(\mathrm{Pf}\,(M_3)|_{q^0}-\mathrm{Pf}\,(M_2)|_{q^0})\,, \tag{2.6.3}$$

where e.g. $(\cdots)|_{q^0}$ corresponds to the $\mathcal{O}(q^0)$ term in the Taylor expansion of $(\cdots)$ around $q=0$. These integrands are well-defined on the nodal sphere and the superscript '(1)' and subscript 'susy-kin' denote that it corresponds to the one-loop integrand for the kinematic piece of a supersymmetric theory. For example, from the above discussion the one-loop integrand of type II supergravity is then given by

$$\hat{\mathcal{I}}^{(1)}_{\text{sugra}}=\hat{\mathcal{I}}^{(1)}_{\text{susy-kin}}\,\hat{\tilde{\mathcal{I}}}^{(1)}_{\text{susy-kin}} \tag{2.6.4}$$

and depends on the polarisation vectors $\epsilon_i,\tilde{\epsilon}_i$, the momenta k_i and the nodal sphere coordinates σ_i of the external particles[20].

[20] Recall that, as mentioned above, the nodal points σ_+, σ_- are fixed to the points $0,\infty$ with the coordinate transformation used.

What about super-Yang-Mills amplitudes? There is no well-defined ambitwistor string model that produces these amplitudes at one-loop naturally, but lessons from genus-zero (or tree-level CHY) suggest that they may be obtained by utilising the double-copy. Indeed, this double-copy structure between integrands can already be seen in (2.6.4). This motivated a proposal given in [103] for the integrand of super Yang-Mills on the nodal sphere by replacing one of the kinematic integrands with a one-loop analogue of the Parke-Taylor factor,

$$\hat{\mathcal{I}}^{(1)}_{\rm PT} = \sum_{i=1}^{n} \frac{\sigma_{+-}}{\sigma_{+i}\sigma_{i\,i+1}\cdots\sigma_{i+n\,-}} \tag{2.6.5}$$

under the identification $i \sim i+n$. The single-trace contribution to the one-loop amplitude for super Yang-Mills theory can then be expressed through the integrand

$$\hat{\mathcal{I}}^{(1)}_{\rm SYM} = \hat{\mathcal{I}}^{(1)}_{\text{susy-kin}}\,\hat{\mathcal{I}}^{(1)}_{\rm PT} \tag{2.6.6}$$

in line with the double-copy interpretation between the (worldsheet) integrands of these theories. In a manifestly $\mathrm{SL}(2,\mathbb{C})$ covariant form, the one-loop (colour-ordered) amplitudes for (super Yang-Mills) supergravity may be written as

$$\mathcal{A}^{(1)}_{\rm SYM}(1\cdots n) = \int \frac{d^D\ell}{\ell^2}\frac{d^{n+2}\sigma}{\text{vol }\mathrm{SL}(2,\mathbb{C})}\,{\prod_A}'\,\bar{\delta}(\mathcal{E}^{(1)}_A)\,\mathcal{I}^{(1)}_{\rm SYM}\,, \tag{2.6.7}$$

$$\mathcal{A}^{(1)}_{\rm sugra} = \int \frac{d^D\ell}{\ell^2}\frac{d^{n+2}\sigma}{\text{vol }\mathrm{SL}(2,\mathbb{C})}\,{\prod_A}'\,\bar{\delta}(\mathcal{E}^{(1)}_A)\,\mathcal{I}^{(1)}_{\rm sugra}\,, \tag{2.6.8}$$

where $\mathcal{E}^{(1)}_A$ are the one-loop scattering equations of (2.5.15). In this form the notion of the genus-one ambitwistor string being a one-loop extensions of CHY becomes explicit. Note that these integrands are related to those[21] of (2.6.4) and (2.6.6) by

$$\mathcal{I}^{(1)}_{\rm sugra} = \frac{1}{\sigma^4_{+-}}\hat{\mathcal{I}}^{(1)}_{\rm sugra} \qquad\qquad \mathcal{I}^{(1)}_{\rm SYM} = \frac{1}{\sigma^4_{+-}}\hat{\mathcal{I}}^{(1)}_{\rm SYM} \tag{2.6.9}$$

so that they have the have the same $\mathrm{SL}(2,\mathbb{C})$ weight in all $\sigma_A \in \{\sigma_i, \sigma_+, \sigma_-\}$.

The kinematic half-integrand (2.6.3) forms the backbone for the supersymmetric theories of gravity and Yang-Mills. It follows from the GSO projection in the type II theory and is defined in ten-dimensions, the critical dimension of the type II string. On the torus, these are both required for modular invariance of the amplitude. On the nodal sphere, there is no notion of modular invariance and therefore (i) the different terms in the GSO projection can be isolated, corresponding to NS or R states flowing through the loop, and (ii) there is no restriction in dimensionally reducing to $D < 10$. The first point can be seen explicitly from (2.6.3); noting that [51] $\mathcal{Z}_1$, $\mathcal{Z}_2$ correspond to the R sector and $\mathcal{Z}_3$, $\mathcal{Z}_4$ correspond to the NS sector, one can write the kinematic integrand as

$$\mathcal{I}_{\text{susy-kin}} = \mathcal{I}_{\rm NS} + \mathcal{I}_{\rm R}\,, \tag{2.6.10}$$

with

$$\mathcal{I}_{\rm NS} = \mathrm{Pf}\,(M_3)|_{q^{1/2}} + 8\mathrm{Pf}\,(M_3)|_{q^0}\,, \qquad\qquad \mathcal{I}_{\rm R} = -8\mathrm{Pf}\,(M_2)|_{q^0}\,. \tag{2.6.11}$$

[21] We should point out another difference, where in this form the Szegö kernels have a slightly different expansion in q due to σ_+, σ_- no longer being explicitly fixed; see [104].

Being able to extract these at the integrand level on the Riemann sphere is another feature of ambitwistor strings[22]. In its current standing, (2.6.11) correspond to the chiral integrands for a vector and a Majorana-Weyl fermion in $D = 10$. The second point above can then be addressed by considering the dimensional reduction of these integrands to obtain amplitudes in lower dimensions. In this respect the analysis of [107] can be used to identify which parts correspond to additional states (scalars and fermions) from dimensional reduction. This was performed in [104], where it was found that upon dimensional reduction to D-dimensions, the individual parts of the chiral half-integrand corresponding to vectors, scalars and fermions amount to

$$\mathcal{I}_{\text{vector}} = \text{Pf}\,(M_3)|_{q^{1/2}} + (D-2)\,\text{Pf}\,(M_3)|_{q^0} \tag{2.6.12a}$$

$$\mathcal{I}_{\text{fermion}} = -c_D\,\text{Pf}\,(M_2)|_{q^0} \tag{2.6.12b}$$

$$\mathcal{I}_{\text{scalar}} = \text{Pf}\,(M_3)|_{q^0}\,. \tag{2.6.12c}$$

The constant c_D is related to the number of fermions that result from the dimensional reduction. From the 10-dimensional Majorana-Weyl spinor one can obtain an 8-dimensional Weyl spinor, four 6-dimensional Weyl-simplectic spinors, or four 4-dimensional Majorana spinors. Therefore given $c_{10} = 8$ comparing (2.6.11) and (2.6.12a), one can read off that $c_8 = c_{10}/1 = 8$, and $c_6 = c_4 = c_{10}/4 = 2$.

This decomposition under dimensional reduction allows one to obtain a variety of integrands corresponding to different states running in the loop in various dimensions. For example, the D-dimensional integrand for NS-NS gravity is given simply by $\mathcal{I}^{(1),D}_{\text{NS-NS}} = \mathcal{I}_{\text{vector}}\tilde{\mathcal{I}}_{\text{vector}}$, and in $D = 4$ one can then obtain the pure-gravity integrand by subtracting the contribution from the two scalar states[23] of the dilaton and the B-field from the tensor product

$$\mathcal{I}^{(1),D=4}_{\text{pure-grav}} = (\text{Pf}\,(M_3)|_{q^{1/2}} + 2\text{Pf}\,(M_3)|_{q^0})^2 - 2(\text{Pf}\,(M_3)|_{q^0})^2\,. \tag{2.6.13}$$

Likewise, one obtains integrands for single-trace contributions to pure Yang-Mills in four-dimensions by simply multiplying the vector integrand with the one-loop analogue of the Parke-Taylor factor,

$$\mathcal{I}^{(1),D=4}_{\text{pure-YM}} = (\text{Pf}\,(M_3)|_{q^{1/2}} + 2\text{Pf}\,(M_3)|_{q^0})\,\mathcal{I}^{(1)}_{\text{PT}}\,. \tag{2.6.14}$$

Clearly the NS contribution $\mathcal{I}^{(1)}_{\text{NS}}$, or its $D < 10$ equivalent $\mathcal{I}_{\text{vector}}$, forms the backbone of chiral integrands for these theories without supersymmetry, and therefore plays a similar role to the kinematic half-integrand of CHY at tree-level (1.1.8). Structurally they seem quite different though; whilst $\mathcal{I}_{\text{vector}}$ is a sum of full Pfaffians of different matrices, its tree-level counterpart (1.1.8) is a *reduced* Pfaffian of a single matrix. In fact, it can be shown that on the support of the one-loop scattering equations (2.5.15), the former can also be written as a reduced Pfaffian,

$$\mathcal{I}_{\text{vector}} = \text{Pf}\,(M_3)|_{q^{1/2}} + (D-2)\,\text{Pf}\,(M_3)|_{q^0} \overset{\mathcal{E}^{(1)}_A=0}{=} \sum_r \text{Pf}'(M_{\text{NS}})\,. \tag{2.6.15}$$

[22] Although one ought to be careful about this at higher-genus, since there could be contributions cancelling out in the GSO projection on the higher-genus surface. This will be very important when we discuss the genus-two case in 4.

[23] In four-dimensions the B-field has $(D-3)(D-2)/2 = 1$ component corresponding to a scalar state, called the 'axion'.

This was shown and proved in [104], where the matrix $M_{\rm NS}$ can be found explicitly. Here we will simply describe its structure. Imagine the CHY matrix M in (1.1.9) with dimension $2(n+2)\times 2(n+2)$, the two extra states associated with $\{\ell,\epsilon_+^r,\sigma_+\}$ and $\{-\ell,\epsilon_-^r,\sigma_-\}$, $r=1,\cdots,D-2$ characterising the relevant polarisation state. The matrix $M_{\rm NS}$ is simply this matrix with $A_{+-}=0$; the sum over polarisation states results in a completeness relation giving a physical state projector

$$\sum_r \epsilon_+^r\epsilon_-^r = \Delta_{\mu\nu} := \eta_{\mu\nu} - \frac{q_\mu\ell_\nu + q_\nu\ell_\mu}{\ell\cdot q}\,. \tag{2.6.16}$$

The factor $(D-2)$ then arises for example from the element $B_{+-}\sim \epsilon_+^r\,\epsilon_-^r$. We will study this in more detail in chapter 4 when we go on to study the two-loop extension. For now we simply point out that the one-loop kinematic half-integrand is in fact analogous to its tree-level counterpart. The reduced Pfaffian in (2.6.15) is defined via

$$\mathrm{Pf}'(M_{\rm NS}) = \frac{1}{\sigma_{+-}}\mathrm{Pf}\left((M_{\rm NS})^{+-}_{+-}\right)\,, \tag{2.6.17}$$

where the matrix $(M_{\rm NS})^{+-}_{+-}$ is defined as at tree-level, here with the rows and columns with respect to the nodal states $\{\ell,\epsilon_+^r,\sigma_+\},\{-\ell,\epsilon_-^r,\sigma_-\}$ removed.

The reduced Pfaffian (2.6.17) can be used in worldsheet formulae for non-supersymmetric Yang-Mills and gravity, and we will be expanding on this in chapter 4. We remind the reader here that if performing the moduli space integrals explicitly, all solutions to the scattering equations (including the singular type) should in principle be included for generic theories. As the singular solutions have $\sigma_+=\sigma_-$, note that by fixing both σ_+ and σ_- using the $\mathrm{SL}(2,\mathbb{C})$ symmetry the singular solutions will be lost. However, the argument presented in [106] indicates that any potential unphysical discriminant-type poles that result from this actually integrate to zero.

2.7 Worldsheet factorisation and loop-propagators

The scattering equations are not only important in being able to obtain an amplitude (or loop integrand), but also in determining what it will look like. This becomes increasingly important at higher loops, as we shall discuss. From the discussion of section 1.4, the moduli space integrals, which are localised on the solutions to the scattering equations, essentially provide the relevant propagator structure for the relevant amplitude. This is exactly true in the case the worldsheet half-integrands are expressed in a Parke-Taylor decomposition, as seen there. The tree-level scattering equations (1.1.3) are designed for tree-level scattering amplitudes of massless states. There also exist 'massive scattering equations' [108,109] which are designed to provide the correct propagator structure for massive amplitudes [110–113].

It is clear in this sense that the one-loop scattering equations (2.5.15) will provide the loop propagators for the corresponding loop-integrand. However, the form of the resulting one-loop integrand is quite different to that coming from a traditional calculation using Feynman diagrams. This section is dedicated to discussing how precisely the scattering equations are related to the kinematic propagators resulting from the moduli space integral, and consequently what the one-loop integrands arising from (2.5.15) look like.

Both of these can be understood through factorisation. In field theory, when a partial sum of momenta goes on-shell, the amplitude factorises into the product of two amplitudes

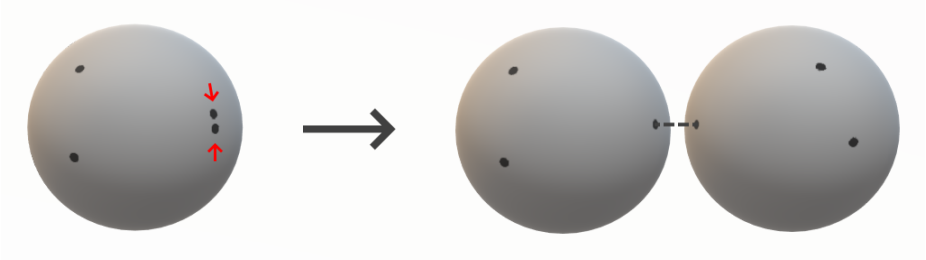

Figure 2.2: As a subset of marked points coalesce, the worldsheet factorises on the support of the scattering equations into two. The coalescence point becomes a 'common point' on both worldsheets, which are identified, and can be thought of as an on-shell state crossing a cut.

multiplied by an intermediate propagator corresponding to the partial sum. In the worldsheet model, the scattering equations relate these kinematic configurations with boundaries of the moduli space, where the corresponding marked points begin to coalesce. In other words, for a proper non-empty subset S of the particle labels, let

$$\sigma_i = \sigma_0 + \epsilon x_i + \mathcal{O}(\epsilon^2) \qquad\qquad \forall\, i \in S\,. \tag{2.7.1}$$

for a point σ_0 not coincident with any of the other marked points, and ϵ parametrising the coalescence. It follows from (2.7.1) that

$$\begin{aligned} &\text{for} \quad i \in S,\ j \in S \qquad \frac{1}{\sigma_i - \sigma_j} = \frac{1}{\epsilon}\,\frac{1}{x_i - x_j} + \mathcal{O}(\epsilon) \\ &\text{for} \quad i \notin S,\ j \in S \qquad \frac{1}{\sigma_i - \sigma_j} = \frac{1}{\sigma_i - \sigma_0} + \mathcal{O}(\epsilon)\,. \end{aligned} \tag{2.7.2}$$

By studying the tree-level scattering equations using this parametrisation, one will find that they imply the relation

$$\epsilon \to 0 \qquad \Longrightarrow \qquad k_S^2 = \left(\sum_{i\in S} k_i\right)^2 \to 0\,. \tag{2.7.3}$$

One can also derive that consequently the worldsheet measure behaves as

$$d\mu \to \epsilon^{2(|S|-1)}\,\frac{1}{\epsilon}\,\bar{\delta}(k_S^2 + \epsilon\mathcal{F})\,d\epsilon\,d\mu_S\,d\mu_{\bar{S}}\,, \tag{2.7.4}$$

and therefore factorises. At tree-level, to have the right pole structure for a realisable factorisation channel, the theory-specific integrand must scale as $\epsilon^{2(|S|-1)}$, i.e.

$$\mathcal{I} \to \epsilon^{-2(|S|-1)}\,\mathcal{I}\,. \tag{2.7.5}$$

An integrand which does not exhibit this scaling for the subset S cannot produce a kinematic pole k_S^2. If the integrand is expressed in terms of a (double) Parke-Taylor basis, i.e. those constructed using (1.4.1), (1.4.2) it is very easy to see how this is the case using (2.7.2). Detailed derivations of this procedure can be found explicitly in the literature, both at tree [38, 114, 115] and loop [1, 50, 104] level. Intuitively one can understand the factorisation at the level of the worldsheet. As the subset S of points coalesce, the Riemann surface

degenerates into two, Σ_S and $\Sigma_{\bar{S}}$, which are connected by a common point. The surface Σ_S has $|S|+1$ marked points, corresponding to those in S and the common point; $\Sigma_{\bar{S}}$ likewise has $|\bar{S}|+1$ marked points. This is shown graphically in figure 2.2. Each worldsheet itself corresponds to an amplitude from the worldsheet perspective, and so the connection to field theory is clear[24].

This is to say that the scattering equations encode all of the kinematic poles that can arise from the moduli space integrals; that is, it solely determines the propagators arising in a local field theory.

This however implies something peculiar at one-loop. On the Riemann sphere we have $n+2$ marked points, including σ_+ and σ_- corresponding to the nodal points and being associated with the loop momentum. Suppose we have a subset S of marked points coalescing, in which $\sigma_+ \in S$ but $\sigma_- \notin S$. From the discussion above, the relevant kinematic pole will correspond to an internal propagator involving the loop momentum and a sum of the external momenta in S. Traditionally these (inverse) propagators have the form $(\ell+K)^2$, where $K=\sum_{i\in S} k_i$, but the one-loop scattering equations (2.5.15) imply the actual kinematic pole corresponds to

$$\frac{1}{2\ell\cdot K+K^2} \neq \frac{1}{(\ell+K)^2}\,, \tag{2.7.6}$$

that is, the loop propagators are *linear* in the loop momentum, instead of quadratic. This is another novel feature of ambitwistor string models at loop-level. However, this makes sense from the form of the one-loop scattering equations (2.5.15); their solutions can only be rational functions of the kinematic invariants they possess, and since they do not possess ℓ^2 explicitly, it can never appear in the solutions. In fact, the only place ℓ^2 appears in the integrand is in the overarching $1/\ell^2$ e.g. in (2.6.8) that comes from the scattering equation used in the global residue theorem; all other loop propagators will be linear in the loop momentum. For example, a typical four-point box diagram that results at one-loop from the scattering equation formalism will have the form

$$\frac{N(\ell)}{\ell^2\,(2\ell\cdot k_1)\,(2\ell\cdot(k_1+k_2)+(k_1+k_2)^2)\,(-2\ell\cdot k_4)} \tag{2.7.7}$$

where $N(\ell)$ is a generic numerator which may depend on ℓ as well as other (kinematic, colour, etc.) data specific to the theory under consideration. The representation of the loop integrand coming from this worldsheet model, a natural extension of CHY, is therefore quite different from the traditional (Feynman) representation. The latter however can be related to the former by applying *partial fraction identities*

$$\prod_{i=1}^{n}\frac{1}{D_i}=\sum_{i=1}^{n}\frac{1}{D_i\prod_{j\neq i}(D_j-D_i)} \tag{2.7.8}$$

and shifting the loop-momentum for each term in the sum on the RHS above, so that each term has the same over-arching $1/\ell^2$ prefactor as occurs in the worldsheet models. This relation was first shown in [103], which alternatively can be seen from the point of view of a residue theorem in [116], which formulated the *$\mathcal{Q}$-cut representation* of field theory

[24] Factorisation provides a way of proving the validity of worldsheet formulae. The worldsheet formulae for Yang-Mills and gravity (with and without supersymmetry) in the previous section was proved using this method in [104].

loop integrands, a representation designed to have these 'linear-type' propagators[25]. The simplest example of this procedure can be seen for a massive bubble:

$$\frac{1}{\ell^2(\ell+K)^2} = \frac{1}{\ell^2(2\ell\cdot K+K^2)} + \frac{1}{(\ell+K)^2(-2\ell\cdot K-K^2)} \tag{2.7.9}$$

$$\cong \frac{1}{\ell^2(2\ell\cdot K+K^2)} + \frac{1}{\ell^2(-2\ell\cdot K+K^2)}\,. \tag{2.7.10}$$

In the first line we have applied the identity (2.7.8), and in the second line we have shifted $\ell \to \ell - K$ in the last term to obtain the factor $1/\ell^2$; the symbol $\cong$ is then meant as equality under integration.

Unfortunately, it is not generically possible to do the converse operation, that is to take the loop integrand coming from the nodal sphere formulae, containing linear propagators, and perform (2.7.8) *backwards*, relating it directly to a standard Feynman representation. This is because the numerators (2.7.7) are typically not in a form which allow this; the loop-momenta have to be shifted for each term but the numerators for these terms are not typically related this way. However there *are* ways to obtain quadratic propagators from one-loop worldsheet formulae, as we demonstrate in the next chapter.

[25] Reference [116] also describes a method of performing the loop *integration* with these types of propagators and gives examples for low numbers of points at one-loop. This however can become quite involved at higher points. Luckily, a representation of the loop integrand with linear-type propagators will match its counterpart with quadratic propagators on a set of (maximal) unitarity cuts, since their cut-conditions will be the same. This will be seen at two-loops in section 4.3.4. We note that generically the integrands of the one-loop worldsheet formulae and the $\mathcal{Q}$-cut representation match up only to terms that integrate to zero.

Chapter 3

One-loop BCFW and scattering equations for quadratic propagators

In the previous chapter we discussed worldsheet formulae for one-loop corrections, how they arise from the genus-one ambitwistor string, and their unorthodox representation. Though being a natural extension of the successful CHY formalism to the one-loop regime, in practice the differences from a more traditional representation make it more difficult in obtaining the *amplitude*; that is performing the loop *integration*. Like their tree-level counterparts however, the one-loop formulae are incredibly compact. Therefore, a natural question to ask is whether there is a way to obtain worldsheet formulae which results in a one-loop integrand more akin to the Feynman representation, i.e. with quadratic propagators. There have been attempts to do this by using "double-forward-limit" scattering equations [117–119], but the corresponding worldsheet formulae do not provide the correct multiplicities of diagrams to properly connect with more conventional results [1].

In this chapter we will provide a method to aid in attaining this goal. This will be inspired by a novel form of Britto-Cachazo-Feng-Witten (BCFW) recursion for one-loop integrands, which we will develop and demonstrate in examples with and without supersymmetry. First developed at tree-level in [120–123], the BCFW recursion provided a way of (as the name suggests) recursively calculating tree-level scattering amplitudes to any multiplicity, thus making the entire tree-level S-matrix obtainable from simple low-point results. At tree-level the BCFW recursion and the scattering equation formalism are well-connected, both exploiting the use of 'on-shell methods' to calculate scattering amplitudes more efficiently. In fact, worldsheet formulae have been proved via the BCFW recursion [108, 114, 124]. Moreover, the connection between these two formalisms has inspired new geometric ways of interpreting scattering amplitudes, such as the amplituhedron [125] and the associahedron [126]. Whilst the extension of BCFW to one-loop have been formulated using momentum-twistors and other approaches [127–132], there have been formulations in momentum-space [133–137]. Our formulation will implicitly be equivalent to the latter approaches, though it will have different features which make e.g. the cancellation of spurious poles more transparent.

After this development we will go on to provide 'modified' one-loop scattering equations which, following the discussion in the previous section, will result in kinematic poles corresponding to quadratic loop propagators. Though inspired by our version of BCFW recursion, it will not exhibit spurious poles in the same way. The use of these new scattering equations will necessitate new descriptions of the integrands in the worldsheet formulae,

which we will discuss how to attain, and give examples in several cases. By construction, both of these formulations are best adapted to planar theories, but in either case we will discuss their application to non-planar theories.

3.1 BCFW at one-loop: planar recursion

Let us consider a generic representation for the one-loop amplitude seen from the perspective of Feynman diagrams. Prior to integration, an n-point amplitude will have the generic form

$$\mathcal{A}_n^{(1)} = \int d^D\ell \, \mathfrak{I}_n^{(1)} \tag{3.1.1}$$

where $\mathfrak{I}_n^{(1)}$ will be the n-point one-loop integrand of the theory under consideration. Let us decompose the loop momentum into

$$\ell = \ell_0 + \alpha q \tag{3.1.2}$$

where ℓ_0 and q are null. Reminiscent of what happens at tree-level, the vector q will be associated to the BCFW shift. Under this decomposition, the measure in (3.1.1) becomes

$$d^D\ell = d^D\ell_0 \, \delta(\ell_0^2) \, d\alpha \, 2\ell_0 \cdot q \, . \tag{3.1.3}$$

We will choose the loop momentum to reside between particles 1 and n in the planar case. This is of course a free choice, which will in turn dictate the form of the BCFW-type shifts to be performed. In this case, we will now consider the following BCFW-type shifts:

$$\begin{aligned} &\hat{k}_1 = k_1 + zq, && \hat{k}_n = k_n - zq, \\ &\hat{\alpha} = \alpha - z \qquad \Rightarrow && \hat{\ell} = \ell_0 + (\alpha - z)q = \ell - zq. \end{aligned} \tag{3.1.4}$$

We choose q satisfying $q \cdot k_1 = q \cdot k_n = 0$ so that k_1 and k_n are still null under the shift. Upon applying the shifts (3.1.4) the integrand becomes a rational function in the complex parameter z; the original amplitude (3.1.1) is of course equal to the residue at $z = 0$,

$$\mathcal{A}_n^{(1)} = \int d^D\ell \oint_{z=0} \frac{dz}{2\pi i} \frac{\mathfrak{I}_n^{(1)}(z)}{z}. \tag{3.1.5}$$

The integrand $\mathfrak{I}_n^{(1)}(z)$ will also exhibit poles in z, which will either be at finite locations z_I or potentially at $z = \infty$. Due to the structure of local integrands, the former can only come from the propagators in the various diagrams, of which there are three types:

(i) **Propagators of the form $1/\ell^2$:**

Under the shift (3.1.4), $\ell^2 \to \hat{\ell}^2$ and thus one encounters a potential pole from $\hat{\ell}^2 = 0$. Since $\hat{\ell} = \ell_0 + (\alpha - z)q$ with ℓ_0 null, this pole occurs for $z = \alpha$, and can be made explicit by writing

$$\frac{1}{\hat{\ell}^2} = \frac{1}{(\ell_0 + (\alpha - z)q)^2} = \frac{\alpha}{\alpha - z} \frac{1}{2\alpha \, \ell_0 \cdot q} = \frac{\alpha}{\alpha - z} \frac{1}{\ell^2} \, . \tag{3.1.6}$$

Expressing $\mathfrak{I}_n^{(1)}(z) = \frac{1}{\ell^2} \mathscr{I}_n^{(1)}(z)$, the integrand of (3.1.5) will have the following residue at this pole:

$$\oint_{z=\alpha} \frac{dz}{2\pi i} \frac{1}{\hat{\ell}^2} \frac{\mathscr{I}_n^{(1)}(z)}{z} = \oint_{z=\alpha} \frac{dz}{2\pi i} \frac{\alpha}{\alpha - z} \frac{1}{\ell^2} \frac{\mathscr{I}_n^{(1)}(z)}{z} = -\frac{1}{\ell^2} \mathscr{I}_n^{(1)}(\alpha). \tag{3.1.7}$$

Notice that $\ell = \ell_0$ inside of $\mathscr{I}_n^{(1)}(\alpha)$ and is therefore on-shell, corresponding to a single cut interpreted as the forward limit of an $n+2$-particle tree-amplitude,

$$\mathscr{I}_n^{(1)}(\alpha) = \sum_{\text{states}_0} \mathcal{A}_{n+2}^{(0)}(\ell_0, k_1 + \alpha q, k_2, \cdots, k_{n-1}, k_n - \alpha q, -\ell_0) =: \sum_{\text{states}_0} \mathcal{A}_{n+2}^{(0)}(\alpha) \tag{3.1.8}$$

wherein one sums over the states flowing through the cut.

(*ii*) **Propagators of the form** $1/(\ell + k_1 + \cdots + k_i)^2$:

These are the generic internal propagators of the diagrams which involve the loop momentum aside from the type considered above. They can all be chosen to have this form since we insisted on the loop momentum residing between particles 1 and n. The benefit of this is that the shift in ℓ cancels the shift in k_1, so propagators of this type do not have any dependence on z, and thus exhibit no poles.

(*iii*) **Propagators of the form** $1/(k_i + \cdots + k_j)^2$:

These are the propagators coming from massive corners of diagrams and external trees thereof and will contain a subset I of the external particles. Since only particles 1 and n are shifted, it is clear these propagators can exhibit a pole only when $1 \in I$ and $n \notin I$ *or* $1 \notin I$ and $n \in I$. When this happens, we have a pole at z_I with

$$\hat{K}_I^2 = K_I^2 + 2 z_I \, K_I \cdot q = 0 \qquad \Rightarrow \qquad z_I = -\frac{K_I^2}{2 K_I \cdot q}\,, \tag{3.1.9}$$

where $K_I = \sum_{i \in I} k_i$. These correspond to tree-level factorisations in the integrand and mirror closely the BCFW story at tree-level. In light of this it is easy to see that the integrand will factorise accordingly and have the following residue at these locations:

$$\oint_{z=z_I} \frac{dz}{2\pi i} \frac{\mathfrak{I}_n^{(1)}(z)}{z} = -\sum_{\text{states}_I} \mathcal{A}_{n_I+1}^{(0)}(z_I) \frac{1}{K_I^2} \mathfrak{I}_{n-n_I+1}^{(1)}(z_I). \tag{3.1.10}$$

Note that the loop momentum in each contribution of this type has the form $\check{\ell} = \ell_0 + (\alpha - z_I) q$.

Now that we understand the pole structure of the integrand as a rational function of z, we can deform the contour of integration to (3.1.5) and relate it to all the other residues discussed above, as in the BCFW procedure at tree-level. Doing so gives a recursion formula for the planar one-loop integrand:

$$\mathfrak{I}_n^{(1)} = \sum_{\text{states}_0} \int \frac{d^D \ell}{\ell^2} \mathcal{A}_{n+2}^{(0)}(\alpha) + \sum_{\text{states}_I} A_{n_I+1}^{(0)}(z_I) \frac{1}{K_I^2} \mathfrak{I}_{n-n_I+1}^{(1)}(z_I) + \mathcal{B}_n. \tag{3.1.11}$$

The first term above corresponds to a forward-limit due to the pole at $z = \alpha$ coming from the propagators of type (i) above. The second term corresponds to potential tree-level factorisations from poles at $z = z_I$, arising from propagators of type (iii) above. The final term, denoted $\mathcal{B}_n$, corresponds to potential residues of the n-point integrand at $z = \infty$,

$$\mathcal{B}_n = -\oint_{z=\infty} \frac{dz}{2\pi i} \frac{\mathfrak{I}_n^{(1)}(z)}{z}\,, \tag{3.1.12}$$

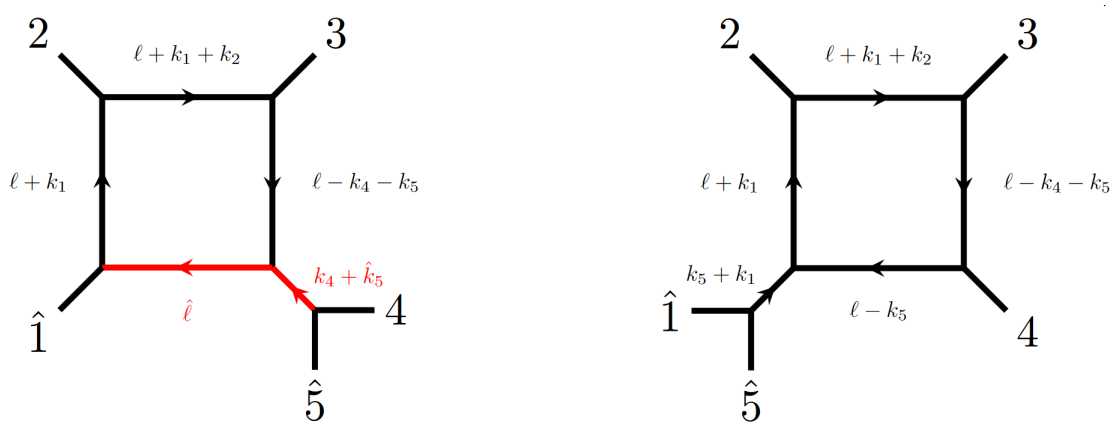

Figure 3.1: Examples of diagrams that do and do not exhibit poles in z. The diagram on the left has two sources of potential poles, highlighted by the propagators in red; these correspond to a forward-limit term (from the pole at $\hat{\ell}^2 = 0$) and a tree-type factorisation term (from $(k_4 + \hat{k}_5)^2 = 0$). In the diagram on the right however, there are no sources of sources of potential poles, because the states with shifted external momenta are on the same vertex, which also implies that there is no explicit ℓ^2 factor from our convention. This diagram is therefore invisible to the recursion. In the case of the MHV sector of $\mathcal{N} = 4$ super Yang-Mills, diagrams such as those on the right vanish completely, which is compatible with the fact that $X_{5,1} = 0$ due to the MHV nature of the kinematics, as we will see in section 3.2.3.

i.e., boundary terms. We will discuss the fate of these boundary terms for the theories to be considered later.

For now let us note that in the forward-limit term, since one has $\hat{k}_1 = k_1 + \alpha q$, $\hat{k}_n = k_n - \alpha q$, diagrams with one of the shifted particles (but not both) in an external tree may pick up spurious poles in α, coming from e.g. $(\hat{k}_1 + k_2)^2 = (k_1 + k_2)^2 + 2\alpha q \cdot k_2$. Whilst these do typically arise, we will demonstrate in examples below that the role of the tree-type factorisation terms will be precisely to (a) cancel this spurious pole, and (b) provide missing pieces in the integrand from the forward-limit term alone. This occurs very straightforwardly in low-point examples precisely because of the shifts applied also to the loop momentum, which is a distinguishing feature from previous formulations such as [137].

3.1.1 Loop placement, choices of shift, and diagrams

As is well-known, a generic Feynman-diagram-type representation of a field theory loop integrand is not uniquely defined. This is highlighted in the freedom one has in their assignment of the internal loop propagators, such as the location of $1/\ell^2$. As mentioned above however, any assignment for the planar loop integrand determines a set of shifts to perform for the recursion. In the above, and for the preceding discussions, we choose the loop momentum to lie between particles 1 and n for an n-point planar integrand. If one were instead to choose the loop-momentum to lie between particles i and $i+1$, then the set of shifts (3.1.4) would take the same form, except with i and $i+1$ taking the role of 1 and n respectively. The types of poles encountered would be determined by similar reasoning to the discussion above, and one would obtain the same form of the recursion (3.1.11).

Even for planar theories, however, there seems at first glance to be a possible issue with this convention. For a generic planar integrand, one cannot assign the loop-momentum to be in the same position for all diagrams. An example of this is in figure 3.1, where in the second diagram the two shifted particles (in our case, 1 and n) appear on a massive corner. Adhering to our convention that ℓ should lie between these particles means that there cannot be any $1/\ell^2$ propagator, so this diagram cannot exhibit a pole that produces a forward-limit term. Moreover, since the shifts in momenta k_1 and k_n cancel each other, they also cannot contain a pole which contributes to tree-level factorisations. Unless they contribute to a pole at infinity, that is, to the boundary term (3.1.12), they seem to be blind to the recursion.

In the examples to be presented below, we will consider theories admitting a representation in which these types of diagrams either do not appear, and/or have sufficient fall-off behaviour for large z. In the latter case, they cannot then exhibit a pole in z of any kind, and thus will not appear in the recursion. Despite this however, it will be seen that the correct expressions are indeed obtained.

3.2 BCFW recursion for $\mathcal{N}=4$ super Yang-Mills: MHV

Planar $\mathcal{N}=4$ super Yang-Mills is an ideal place to study new methodologies, in this context due to the vast simplicity of their scattering amplitudes. This simplicity owes to the many symmetries it possesses: on top of conformal and maximal supersymmetry in four-dimensions, it also encodes 'hidden' symmetries such as dual-conformal symmetry [138–143] and more generally an infinite-dimensional 'Yangian' symmetry [144–147]. A BCFW recursion for the loop integrand of this theory has been studied extensively, even to all orders in the loop expansion for the planar sector [129], and using on-shell diagrams [130]. The latter can in fact be compared directly with our form of the BCFW integrand recursion [1].

In this section we will consider the recursion (3.1.11) for the MHV integrands of $\mathcal{N}=4$ super Yang-Mills, giving explicit examples of the recursion up to six-points.

3.2.1 MHV recursion

Here we will refine the formula (3.1.11) for the case of MHV integrands in maximally supersymmetric Yang-Mills theory. The resulting formula will be simpler and coincide with a known form of the integrand recursion [129].

The precise form of the integrands will not be important in this endeavour. As mentioned above we choose the loop momentum to lie between particles 1 and n and can satisfy the conditions $q^2 = q\cdot k_1 = q\cdot k_2 = 0$ in four-dimensions by setting $q = \lambda_1\tilde{\lambda}_n$ with λ_1, $\tilde{\lambda}_n$ being Weyl spinors in the spinor-helicity scheme. We would like to note here that whilst the external kinematics are in four-dimensions, we will generically consider a D-dimensional loop-momentum which, in the forward-limit term, is only massless in D-dimensions. Recall that the recursion formula (3.1.11) consists of three types of terms. For $\mathcal{N}=4$ super Yang-Mills the forward-limit term can be expressed as

$$\frac{1}{\ell^2}\sum_{\text{states}_0}\mathcal{A}^{(0)}_{n+2}(\alpha) = \frac{1}{\ell^2}\int d^4\eta_0\,\mathcal{A}^{(0)}_{\text{NMHV}}(\ell_0,\hat{k}_1,k_2,\cdots,k_{n-1},\hat{k}_n,-\ell_0)\,, \tag{3.2.1}$$

where the sum over states is conveniently performed via an integration over the Grassmann parameters $\eta_0 =: \eta_{\ell_0} = \eta_{-\ell_0}$ parametrising the on-shell states crossing the single-cut. The

tree-level superamplitude must consequently be NMHV to ensure the integral has the correct Grassmann degree. Since the above arises as the residue at $z=\alpha$, one has the following super-shifts in accordance with the recursion:

$$\begin{aligned}\hat{k}_1 &= k_1 + \alpha q = \lambda_1(\tilde{\lambda}_1 + \alpha\tilde{\lambda}_n) \equiv \lambda_1\hat{\tilde{\lambda}}_1\,, & \hat{\eta}_1 &= \eta_1 + \alpha\eta_n\,,\\ \hat{k}_n &= k_n - \alpha q = (\lambda_n - \alpha\lambda_1)\tilde{\lambda}_n \equiv \hat{\lambda}_n\tilde{\lambda}_n\,, & \hat{\eta}_n &= \eta_n\,.\end{aligned} \tag{3.2.2}$$

The shift in η_1 is to ensure that supermomentum is still conserved, mirroring the usual super-BCFW procedure [148]. Then there is the term in the recursion corresponding to factorisations. Similarly to what occurs for MHV at tree-level, it can be shown that supersymmetric Ward identities and special three-point kinematics invoke that the sum over multi-particle channels reduce to a single term,

$$\sum_{\text{states}_I} \mathcal{A}^{(0)}_{n_I+1}(z_I)\frac{1}{K_I^2}\mathfrak{I}^{(1)}_{n-n_I+1}(z_I) = \int d^4\eta_K\, \mathcal{A}^{(0)}_{\overline{\text{MHV}}}(-K, n-1, \check{n})\frac{1}{K^2}\mathfrak{I}^{(1)}_{\text{MHV}}(\check{1},\cdots,n-2,K)\,, \tag{3.2.3}$$

where again the Grassmann integral performs the sum over states crossing the propagator. Since this corresponds to the residue at $z=z_n$ with

$$z_n = -\frac{(-K)^2}{2q\cdot(-K)} = \frac{\langle n-1\, n\rangle}{\langle n-1\, 1\rangle} \tag{3.2.4}$$

we will for the factorisation terms label shifted quantities by $\check{\kappa}$ as opposed to $\hat{\kappa}$ which we reserve for the shifts in the forward-limit term (3.2.2). The on-shell momenta flowing through the propagator is

$$\begin{aligned}K = k_{n-1} + \check{k}_n &= \lambda_{n-1}\tilde{\lambda}_{n-1} + \check{\lambda}_n\tilde{\lambda}_n\\ &= \lambda_{n-1}\tilde{\lambda}_{n-1} + \lambda_n\tilde{\lambda}_n - \frac{\langle n-1\, n\rangle}{\langle n-1\, 1\rangle}\lambda_1\tilde{\lambda}_n\\ &= \lambda_{n-1}\left(\tilde{\lambda}_{n-1} + \frac{\langle n\, 1\rangle}{\langle n-1\, 1\rangle}\tilde{\lambda}_n\right) \equiv \lambda_K\tilde{\lambda}_K\end{aligned} \tag{3.2.5}$$

using the Schouten identity in the third equality. The form of the three-point $\overline{\text{MHV}}$ superamplitude in (3.2.3) is well-known and takes the form

$$\mathcal{A}^{(0)}_{\overline{\text{MHV}}}(-K, n-1, \check{n}) = \frac{\delta^{(4)}([n-1\, n]\,\eta_K + [n\, K]\,\eta_{n-1} + [K\, n-1]\,\eta_n)}{[n-1\, n][n\, K][K\, n-1]}\,. \tag{3.2.6}$$

To perform the $d^4\eta_K$ integral in (3.2.3), we note that if η_K appears in $\mathfrak{I}^{(0)}_{\text{MHV}}$ then we can substitute it on the support of the delta function above, so that η_K only appears in $\mathcal{A}^{(0)}_{\overline{\text{MHV}}}$. The practical significance of this is two-fold: firstly, it allows us to perform the fermionic integration in (3.2.3) simply, and secondly it has the effect of restoring full n-point supermomentum conservation inside of $\mathfrak{I}^{(1)}_{\text{MHV}}$; this will be highlighted in the examples

below. For now, we emphasise the former point by writing (3.2.3) as

$$\int d^4\eta_K\, \mathcal{A}^{(0)}_{\rm MHV}(-K, n-1, \check{n})\frac{1}{K^2}\mathfrak{I}^{(1)}_{\rm MHV}(\check{1},\cdots,n-2,K)$$

$$= \int d^4\eta_K\, \frac{\delta^{(4)}([n-1\,n]\,\eta_K + [n\,K]\,\eta_{n-1} + [K\,n-1]\,\eta_n)}{[n-1\,n][n\,K][K\,n-1]}\frac{1}{\langle n\,n-1\rangle[n-1\,n]}\tilde{\mathfrak{I}}^{(1)}_{\rm MHV}(\check{1},\cdots,n-2,K)$$

$$= \frac{\langle n-1\,1\rangle}{\langle n-1\,n\rangle\langle n\,1\rangle}\tilde{\mathfrak{I}}^{(1)}_{\rm MHV}(\check{1},\cdots,n-2,K)\,, \tag{3.2.7}$$

where $\tilde{\mathfrak{I}}^{(1)}_{\rm MHV}$ is simply $\mathfrak{I}^{(1)}_{\rm MHV}$ with its η_K dependence substituted through the support of the delta function in (3.2.6). Its precise form can be envisaged by viewing the momentum K in (3.2.7) as a shifted version of the momenta corresponding to particle $n-1$. In other words, the factorisation term for the MHV recursion can be written as

$$\sum_{\text{states}_I}\mathcal{A}^{(0)}_{n_I+1}(z_I)\frac{1}{K_I^2}\mathfrak{I}^{(1)}_{n-n_I+1}(z_I) = \frac{\langle n-1\,1\rangle}{\langle n-1\,n\rangle\langle n\,1\rangle}\mathfrak{I}^{(1)}_{\rm MHV}(\check{1},\cdots,n-2,n\,\check{-}\,1) \tag{3.2.8}$$

where $\mathfrak{I}^{(1)}_{\rm MHV}(\check{1},\cdots,n-2,n\,\check{-}\,1)$ is the colour-ordered one-loop $(n-1)$-point integrand subject to the super-shifts

$$\begin{aligned}
&\check{\lambda}_1 = \lambda_1 && \check{\tilde{\lambda}}_1 = \tilde{\lambda}_1 + \frac{\langle n-1\,n\rangle}{\langle n-1\,1\rangle}\tilde{\lambda}_n && \check{\eta}_1 = \eta_1 + \frac{\langle n-1\,n\rangle}{\langle n-1\,1\rangle}\eta_n\\
&\check{\lambda}_{n-1} = \lambda_{n-1} && \check{\tilde{\lambda}}_{n-1} = \tilde{\lambda}_{n-1} + \frac{\langle n\,1\rangle}{\langle n-1\,1\rangle}\tilde{\lambda}_n && \check{\eta}_{n-1} = \eta_{n-1} + \frac{\langle n\,1\rangle}{\langle n-1\,1\rangle}\eta_n.
\end{aligned} \tag{3.2.9}$$

We will shortly see, once we discuss a convenient representation of the n-point integrands which we will use to demonstrate the recursion, that there are no boundary terms for the MHV sector of $\mathcal{N}=4$ super Yang-Mills. This can be proved more generally for Yang-Mills theory at one-loop as in [1]. Therefore the n-point MHV integrand recursion for $\mathcal{N}=4$ super Yang-Mills can be expressed simply as

$$\mathfrak{I}^{(1)}_{\rm MHV}(1,2,\cdots,n) = \frac{\langle n-1\,1\rangle}{\langle n-1\,n\rangle\langle n\,1\rangle}\mathfrak{I}^{(1)}_{\rm MHV}(\check{1},2,\cdots,n\,\check{-}\,1) + \frac{1}{\ell^2}\int d^4\eta_0\mathcal{A}^{(0)}_{\rm NMHV}(\ell_0,\hat{1},2,\cdots,\hat{n},-\ell_0) \tag{3.2.10}$$

The prefactor of the $(n-1)$-point integrand is often referred to as an 'inverse soft factor' in the literature. Since for MHV only one term contributes to the factorisation part of the recursion, we will throughout refer to the shifts (3.2.9) as $\vee$-shifts, and the forward limit shifts (3.2.2) as $\wedge$-shifts where necessary. We recount that the loop-momentum is in practice D-dimensional, with ℓ_0 massless in D-dimensions but possessing a non-zero mass in four-dimensions. This will essentially be necessary to obtain the correct result for theories without supersymmetry, as we shall explore later.

3.2.2 Integrand representations

Here we discuss a representation of the integrand which is most convenient in demonstrating the recursion for the MHV sector of maximally supersymmetric Yang-Mills. This representation for the n-point loop integrand was described in [149] and is derived from the field-theory limit of string theory. It directly makes use of the colour-kinematics duality and expresses

n-point MHV loop integrands in terms of trivalent diagrams with D-dimensional loop momenta. The numerators for these diagrams are therefore a valid set of one-loop MHV BCJ numerators, allowing for a natural extension to constructing MHV gravity integrands.

Reference [149] presents an algorithm for constructing the MHV loop integrand with these numerators. We will not discuss the algorithm here but simply state the results needed to demonstrate the recursion. Defining

$$\mathfrak{I}^{(1)}_{\text{MHV}}(1,2,\cdots,n;\ell) = \frac{\delta^{(8)}(Q)}{\prod_{i=2}^{n}\langle 1i\rangle^2}\,\mathcal{I}_{1,2,\cdots,n}(\ell) \tag{3.2.11}$$

where $Q=\sum_i \lambda_i\eta_i$ is the supermomentum, we have at four- and five-points

$$\mathcal{I}_{1,2,3,4}(\ell) = \frac{X_{2,4}X_{2,3}}{\ell^2(\ell+k_1)^2(\ell+k_{12})^2(\ell+k_{123})^2}, \tag{3.2.12a}$$

$$\begin{aligned}\mathcal{I}_{1,2,3,4,5}(\ell) = {}& \frac{X_{2,4}X_{2,3}X_{\ell,5}+X_{2,5}X_{2,3}X_{2+3,4}+X_{3,5}X_{\ell,2}X_{2+3,4}}{\ell^2(\ell+k_1)^2(\ell+k_{12})^2(\ell+k_{123})^2(\ell+k_{1234})^2} + \frac{X_{2,3}\ X_{2+3,4}X_{2+3,5}}{s_{23}\ell^2(\ell+k_1)^2(\ell+k_{123})^2(\ell+k_{1234})^2}\\ &+\frac{X_{3,4}\ X_{2,3+4}X_{2,5}}{s_{34}\ell^2(\ell+k_1)^2(\ell+k_{12})^2(\ell+k_{1234})^2} + \frac{X_{4,5}\ X_{2,3}X_{2,4+5}}{s_{45}\ell^2(\ell+k_1)^2(\ell+k_{12})^2(\ell+k_{123})^2}.\end{aligned} \tag{3.2.12b}$$

Here we use the notation $k_{1\cdots i}=k_1+\cdots k_i$, and

$$X_{A,B} := \langle 1|K_A K_B|1\rangle = -X_{B,A}, \qquad X_{A+B,C} = X_{A,C}+X_{B,C} \tag{3.2.13}$$

with the momenta K_A, K_B possibly off-shell. For on-shell momenta k_i, k_j this is simply

$$X_{i,j} = \langle 1i\rangle[ij]\langle j1\rangle. \tag{3.2.14}$$

One can in fact can think of these objects as rescaled spinor brackets. Consequently they satisfy the Schouten identity,

$$X_{A,B}X_{C,D}+X_{A,D}X_{B,C}+X_{A,C}X_{D,B}=0\,,$$

which underpins the colour-kinematics duality in this representation of the loop-integrand. Practically, the numerator in the first term of (3.2.12b) is a BCJ numerator for the pentagon diagram, and the numerators for all other diagrams are obtained from this one through Jacobi relations. Note that in the definitions above, particle 1 is chosen as a reference spinor λ_1. This choice is closely tied to the position of the loop-momenta in the corresponding diagrams, as one might notice in the expressions above. This representation will henceforth be very convenient from the point of view of the recursion, as we will now see.

3.2.3 Absence of boundary terms for MHV

As mentioned earlier, there are no boundary terms for the one-loop MHV recursion of $\mathcal{N}=4$ super Yang-Mills. We are now ready to show this, given the loop-integrand representation of the previous section. After applying the BCFW shifts (3.1.4) the integrand becomes a rational function in z. The boundary terms arise as possible residues at $z=\infty$, so we are required to study the behaviour of the integrand at large values of z.

From the point of view of keeping the recursion as simple as possible, choosing the loop momentum to lie between particles 1 and n leads to $q=\lambda_1\tilde{\lambda}_n$ being the most natural choice

of shift for the representation of the loop-integrand above. Notice in particular that λ_1 is unaffected by the shift, so that both the $\delta^{(8)}(Q)$ and $\prod_{i=2}^{n}\langle 1i\rangle^2$ of (3.2.11) are actually invariant. The more crucial ingredients $\mathcal{I}_{1,2,\cdots,n}(\ell)$ essentially consist of a sum of terms corresponding to trivalent diagrams, each with a corresponding numerator and propagator structure. Notice that $X_{1,A}=0$ by virtue of (3.2.13); this has two important consequences with respect to the recursion. On the one hand, the numerators used to construct the MHV integrands must then be invariant under the BCFW shifts, since $X_{A,q}=0$ with $q=\lambda_1\tilde{\lambda}_n$. On the other hand, the numerators for diagrams with particle 1 on a massive corner must vanish, which means (i) there are no massive 1-n corners that can contribute to the boundary term, and (ii) the number of possible spurious poles encountered in the procedure is essentially halved.

It is clear then that only the propagators are affected by the BCFW shifts (3.1.4). By construction, particle 1 is always attached directly to the loop, so all terms are suppressed for large z by the overarching $1/\hat{\ell}^2=\alpha/(\alpha-z)\times 1/\ell^2$ factor. Beyond that, all other propagators involving the loop momenta are invariant under the shift since $\hat{\ell}+\hat{k}_1+\cdots=\ell+k_1+\cdots$. Finally, propagators composed solely of Mandelstam invariants (from external trees) are only affected by the shift if they contain particle n, so any terms containing propagators of the form $1/s_{i\cdots n}$ are further suppressed for large z. Overall, one can see that each term in the MHV integrand behaves (at most) as $\mathcal{O}(z^{-1})$ for large z, so that there cannot be a residue at $z=\infty$ from (3.1.12). These statements apply quite generally to arbitrary multiplicity, thus proving the absence of boundary terms in the MHV integrands.

3.3 Examples for $\mathcal{N}=4$ super Yang-Mills: MHV

We will go on now to demonstrate explicitly how the recursion works in obtaining higher-point integrands for the MHV sector of $\mathcal{N}=4$ super Yang-Mills. An important point that will be highlighted in these examples is the cancellation of spurious poles amongst different terms in the recursion. To see how this occurs it suffices to consider some low-point examples.

3.3.1 $n=4$

At four-points, the expression (3.2.12a) matches the well-known result (up to a sign due to our conventions) since

$$\frac{\delta^{(8)}(Q)}{\prod_{i=2}^{4}\langle 1i\rangle^2}X_{2,4}X_{2,3}=-\delta^{(8)}(Q)\frac{[12][34]}{\langle 12\rangle\langle 34\rangle}. \tag{3.3.1}$$

Because the three-point amplitude vanishes, only the forward-limit term of (3.1.11) contributes:

$$\begin{aligned}\frac{1}{\ell^2}\int d^4\eta_0\,\mathcal{A}^{(0)}_{\text{NMHV}}(\ell_0,\hat{1},2,3,\hat{4},-\ell_0)&=-\delta^{(8)}(\hat{Q})\frac{[\hat{1}2][34]}{\langle 12\rangle\langle 3\hat{4}\rangle}\frac{1}{\ell^2(\ell_0+\hat{k}_1)^2(\ell_0+\hat{k}_1+k_2)^2(\ell_0-\hat{k}_4)^2}\\&=-\delta^{(8)}(Q)\frac{[12][34]}{\langle 12\rangle\langle 34\rangle}\frac{1}{\ell^2(\ell+k_1)^2(\ell+k_1+k_2)^2(\ell-k_4)^2},\end{aligned}$$

recalling that $\ell=\ell_0+\alpha q$. The supermomentum is invariant by construction of the super-shift, and the invariance of the spinor-helicity prefactor follows from its permutation symmetry via momentum conservation. The well-known four-point MHV superintegrand is therefore straightforwardly recovered from the recursion.

3.3.2 $n = 5$

The case of five-particles is the simplest example highlighting certain aspects of the integrand recursion. In particular, the tree-type factorisation term is here non-zero and plays a crucial role, as we will now see.

The forward-limit term almost completely produces the five-point integrand (3.2.12b); structurally every term is present, wherein particles 1 and 5 are shifted according to $\hat{k}_1 = k_1 + \alpha q$, $\hat{k}_5 = k_5 - \alpha q$ with $q = \lambda_1\tilde{\lambda}_5$. As mentioned in section 3.2.3, the numerators and prefactors in (3.2.11) are invariant under the BCFW shifts, and thus only the propagators are affected. Those involving the loop momentum are invariant on account of $\ell_0 + \hat{k}_1 + \cdots = \ell + k_1 + \cdots$, and propagators involving Mandelstam variables are unaffected unless they contain particle 5. Of these, only the last term in (3.2.12b) has such a propagator, which is

$$\frac{1}{s_{4\hat{5}}} = \frac{1}{\langle 4\hat{5}\rangle[54]} = \frac{1}{s_{45} - \alpha\langle 41\rangle[54]} = \frac{1}{s_{45}}\,\frac{1}{1-\alpha\frac{\langle 41\rangle}{\langle 45\rangle}}. \tag{3.3.2}$$

Here we can see the spurious pole explicitly. The factorisation term from (3.2.10) is expressed as, including the loop measure,

$$\frac{\langle 41\rangle}{\langle 45\rangle\langle 51\rangle}\int d^D\check{\ell}\;\mathfrak{I}^{(1)}_{\rm MHV}(\check{1},2,3,\check{4}) = \frac{\langle 41\rangle}{\langle 45\rangle\langle 51\rangle}\int\frac{d^D\check{\ell}}{\check{\ell}^2}\,\frac{\delta^{(8)}(Q)}{\prod_{i=1}^4\langle 1i\rangle^2}\,\frac{X_{2,3}X_{2,\check{4}}}{(\check{\ell}+k_{\check{1}})^2(\check{\ell}+k_{\check{1}2})^2(\check{\ell}+k_{\check{1}23})^2}. \tag{3.3.3}$$

Here we are using the $\vee$-shifts of (3.2.9), which in this case take the form

$$\begin{aligned}
&\check{\lambda}_1 = \lambda_1 && \check{\tilde{\lambda}}_1 = \tilde{\lambda}_1 + \frac{\langle 45\rangle}{\langle 41\rangle}\tilde{\lambda}_4 && \check{\eta}_1 = \eta_1 + \frac{\langle 45\rangle}{\langle 41\rangle}\eta_5\\
&\check{\lambda}_4 = \lambda_4 && \check{\tilde{\lambda}}_4 = \tilde{\lambda}_4 + \frac{\langle 51\rangle}{\langle 41\rangle}\tilde{\lambda}_5 && \check{\eta}_4 = \eta_4 + \frac{\langle 51\rangle}{\langle 41\rangle}\eta_5.
\end{aligned} \tag{3.3.4}$$

Notice that the numerators in (3.3.3) are affected by the $\vee$-shift, whilst the prefactors are invariant since the λ_i's are actually unaffected by the $\vee$-shift. The shift in the numerator has the effect that

$$X_{2,\check{4}} = \langle 12\rangle[2\check{4}]\langle 41\rangle = \langle 12\rangle[24]\langle 41\rangle + \langle 12\rangle[25]\langle 51\rangle = X_{2,4+5} \tag{3.3.5}$$

and we also have

$$\frac{\langle 41\rangle}{\langle 45\rangle\langle 51\rangle}\frac{1}{\prod_{i=2}^4\langle 1i\rangle^2} = \frac{\langle 41\rangle\langle 51\rangle}{\langle 45\rangle}\frac{1}{\prod_{i=2}^5\langle 1i\rangle^2} = \frac{\langle 41\rangle[45]\langle 51\rangle}{s_{45}}\frac{1}{\prod_{i=2}^5\langle 1i\rangle^2} = \frac{X_{4,5}}{s_{45}}\frac{1}{\prod_{i=2}^5\langle 1i\rangle^2}.$$

Then the factorisation term (3.3.3) can be written as

$$\frac{\langle 41\rangle}{\langle 45\rangle\langle 51\rangle}\int d^D\check{\ell}\;\mathfrak{I}^{(1)}_{\rm MHV}(\check{1},2,3,\check{4}) = \int\frac{d^D\check{\ell}}{\check{\ell}^2}\,\frac{\delta^{(8)}(Q)}{\prod_{i=2}^5\langle 1i\rangle^2}\,\frac{X_{2,3}X_{2,4+5}X_{4,5}}{s_{45}(\check{\ell}+k_{\check{1}})^2(\check{\ell}+k_{\check{1}2})^2(\check{\ell}+k_{\check{1}23})^2}. \tag{3.3.6}$$

In order to combine this with the forward-limit term, we are required to shift the integration measure to coincide with $d^D\ell$. This is a crucial part in our version of the integrand recursion. Since $z_n = \langle 45\rangle/\langle 41\rangle$ we have that

$$\check{\ell} = \ell_0 + \left(\alpha - \frac{\langle 45\rangle}{\langle 41\rangle}\right)q = \ell - \frac{\langle 45\rangle}{\langle 41\rangle}q \qquad \Rightarrow \qquad \frac{d^D\check{\ell}}{\check{\ell}^2} = \frac{d^D\ell}{\ell^2}\,\frac{\alpha}{\alpha - \frac{\langle 45\rangle}{\langle 41\rangle}}$$

and subsequently $\check{\ell}+k_{\tilde{1}}+\cdots=\ell+k_1+\cdots$. Notice that the spurious pole above is of the same type as (3.3.2). With these manipulations the factorisation term can be combined with the problematic term from the forward-limit, the last term of (3.2.12b),

$$\frac{X_{2,3}X_{2,4+5}X_{4,5}}{s_{45}\ell^2(\ell+k_1)^2(\ell+k_{12})^2(\ell+k_{123})^2}\left[\frac{1}{1-\alpha\frac{\langle 41\rangle}{\langle 45\rangle}}+\frac{\alpha}{\alpha-\frac{\langle 45\rangle}{\langle 41\rangle}}\right]=\frac{X_{2,3}X_{2,4+5}X_{4,5}}{s_{45}\ell^2(\ell+k_1)^2(\ell+k_{12})^2(\ell+k_{123})^2}.$$

The spurious poles cancel, and the correct expression is obtained. Thus, the recursion correctly produces the five-point MHV integrand.

3.3.3 $n=6$

It was quite clear for five particles how the spurious poles cancel and give the correct overall expression. The higher-point cases work analogously to this, and here we demonstrate the rise in complexity in the cancellation of spurious poles by considering the $n=6$ case. The six-point MHV integrand can be found in [149] and is there written as

$$\begin{aligned}\mathcal{I}_{1,2,3,4,5,6}(\ell)=\frac{1}{\ell^2(\ell+k_1)^2}\Bigg\{&\frac{\mathfrak{n}_{\underline{1}|2|3|4|5|6}}{(\ell+k_{12})^2(\ell+k_{123})^2(\ell+k_{1234})^2(\ell+k_{12345})^2}\\
&+\frac{\mathfrak{n}_{\underline{1}|[2,3]|4|5|6}}{s_{23}(\ell+k_{123})^2(\ell+k_{1234})^2(\ell+k_{12345})^2}+\frac{\mathfrak{n}_{\underline{1}|2|[3,4]|5|6}}{s_{34}(\ell+k_{12})^2(\ell+k_{1234})^2(\ell+k_{12345})^2}\\
&+\frac{\mathfrak{n}_{\underline{1}|2|3|[4,5]|6}}{s_{45}(\ell+k_{12})^2(\ell+k_{123})^2(\ell+k_{12345})^2}+\frac{\mathfrak{n}_{\underline{1}|2|3|4|[5,6]}}{s_{56}(\ell+k_{12})^2(\ell+k_{123})^2(\ell+k_{1234})^2}\\
&+\left(\frac{X_{2,3}X_{2+3,4}}{s_{23}}+\frac{X_{4,3}X_{4+3,2}}{s_{34}}\right)\frac{X_{2+3+4,5}X_{2+3+4,6}}{s_{234}(\ell+k_{1234})^2(\ell+k_{12345})^2}+\frac{X_{2,3}X_{4,5}\,X_{2+3,4+5}X_{2+3,6}}{s_{23}s_{45}(\ell+k_{123})^2(\ell+k_{12345})^2}\\
&+\left(\frac{X_{3,4}X_{3+4,5}}{s_{34}}+\frac{X_{5,4}X_{5+4,3}}{s_{45}}\right)\frac{X_{2,3+4+5}X_{2,6}}{s_{345}(\ell+k_{12})^2(\ell+k_{12345})^2}+\frac{X_{2,3}X_{5,6}\,X_{2+3,4}X_{2+3,5+6}}{s_{23}s_{56}(\ell+k_{123})^2(\ell+k_{1234})^2}\\
&+\left(\frac{X_{4,5}X_{4+5,6}}{s_{45}}+\frac{X_{6,5}X_{6+5,4}}{s_{56}}\right)\frac{X_{2,3}X_{2,4+5+6}}{s_{456}(\ell+k_{12})^2(\ell+k_{123})^2}+\frac{X_{3,4}X_{5,6}\,X_{2,3+4}X_{2,5+6}}{s_{34}s_{56}(\ell+k_{12})^2(\ell+k_{1234})^2}\Bigg\}\,,\end{aligned}\tag{3.3.7}$$

with

$$\begin{aligned}\mathfrak{n}_{\underline{1}|2|3|4|5|6}&=X_{2,4}X_{2,3}X_{\ell-6,5}X_{\ell,6}+X_{2,5}X_{2,3}X_{2+3,4}X_{\ell,6}+X_{2,6}X_{2,3}X_{2+3,4}X_{2+3+4,5}\\
\mathfrak{n}_{\underline{1}|[2,3]|4|5|6}&=X_{2,3}(X_{2+3,5}X_{2+3,4}X_{\ell,6}+X_{2+3,6}X_{2+3,4}X_{2+3+4,5}+X_{4,6}X_{\ell,2+3}X_{2+3+4,5})\\
\mathfrak{n}_{\underline{1}|2|[3,4]|5|6}&=X_{3,4}(X_{2,5}X_{2,3+4}X_{\ell,6}+X_{2,6}X_{2,3+4}X_{2+3+4,5}+X_{3+4,6}X_{\ell,2}X_{2+3+4,5})\\
\mathfrak{n}_{\underline{1}|2|3|[4,5]|6}&=X_{4,5}(X_{2,4+5}X_{2,3}X_{\ell,6}+X_{2,6}X_{2,3}X_{2+3,4+5}+X_{3,6}X_{\ell,2}X_{2+3,4+5})\\
\mathfrak{n}_{\underline{1}|2|3|4|[5,6]}&=X_{5,6}(X_{2,4}X_{2,3}X_{\ell,5+6}+X_{2,5+6}X_{2,3}X_{2+3,4}+X_{3,5+6}X_{\ell,2}X_{2+3,4}).\end{aligned}\tag{3.3.8}$$

As mentioned above, here we understand $\mathfrak{n}_{\underline{1}|2|3|4|5|6}$ to be the BCJ master numerator for the hexagon and all other numerators are obtainable from this via Jacobi identities. For example, one can see from the second term in (3.3.7) that $\mathfrak{n}_{\underline{1}|[2,3]|4|5|6}$ is the numerator for the pentagon with a massive 2-3 corner, which is defined to be $\mathfrak{n}_{\underline{1}|[2,3]|4|5|6}=\mathfrak{n}_{\underline{1}|2|3|4|5|6}-\mathfrak{n}_{\underline{1}|3|2|4|5|6}$. For brevity, numerators in (3.3.7) involving further higher-order Jacobi relations (such as $\mathfrak{n}_{\underline{1}|2|[3,4]|[5,6]}$ or $\mathfrak{n}_{\underline{1}|2|3|[4,[5,6]]}$) have been written explicitly since they combine with other terms to give a more compact expression.

Like the previous example, the forward limit contribution of the recursion almost completely reproduces the result (3.3.7), except all Mandelstam variables $1/s_{i\cdots 6}$ involving particle 6 produce spurious poles. From (3.3.7) and (3.3.8) these terms are

$$\frac{d^D\ell}{\ell^2}\,\frac{\delta^{(8)}(Q)}{\prod_{i=2}^6\langle 1i\rangle^2}\left[\frac{X_{5,6}(X_{2,4}X_{2,3}X_{\ell,5+6}+X_{2,5+6}X_{2,3}X_{2+3,4}+X_{3,5+6}X_{\ell,2}X_{2+3,4})}{s_{5\hat{6}}(\ell+k_1)^2(\ell+k_{12})^2(\ell+k_{123})^2(\ell+k_{1234})^2(\ell+k_{12345})^2}\right.$$
$$+\frac{X_{2,3}X_{5,6}X_{2+3,4}X_{2+3,5+6}}{s_{23}s_{5\hat{6}}(\ell+k_1)^2(\ell+k_{123})^2(\ell+k_{1234})^2}+\frac{X_{3,4}X_{5,6}X_{2,3+4}X_{2,5+6}}{s_{34}s_{5\hat{6}}(\ell+k_1)^2(\ell+k_{12})^2(\ell+k_{1234})^2} \tag{3.3.9}$$
$$\left.+\frac{X_{4,5}X_{4+5,6}X_{2,3}X_{2,4+5+6}}{s_{45}s_{45\hat{6}}(\ell+k_1)^2(\ell+k_{12})^2(\ell+k_{123})^2}+\frac{X_{6,5}X_{6+5,4}X_{2,3}X_{2,4+5+6}}{s_{5\hat{6}}s_{45\hat{6}}(\ell+k_1)^2(\ell+k_{12})^2(\ell+k_{123})^2}\right].$$

In the above we have already made use of the fact that $\hat{Q}=Q$, $X_{\ell_0,A}=X_{\ell,A}$ and $\ell_0+\hat{k}_1+\cdots=\ell+k_1+\cdots$. Notice that at this multiplicity, there are two sources of spurious poles, namely the propagators $1/s_{5\hat{6}}$ and $1/s_{45\hat{6}}$. In this representation, other sources of poles such as propagators of the form $1/s_{345\hat{6}}$ do not appear as a result of the 'no-triangle hypothesis' of $\mathcal{N}=4$ super Yang-Mills[1] [140, 150].

As in the previous example the factorisation contribution to the recursion will provide the correction that cancels these spurious poles. Using the five-point integrand (3.2.12b) and adapting the $\vee$-shifts gives this contribution to be

$$\frac{d^D\check{\ell}}{\check{\ell}^2}\,\frac{\delta^{(8)}(Q)}{\prod_{i=2}^6\langle 1i\rangle^2}\,\frac{X_{5,6}}{s_{56}}\left[\frac{X_{2,4}X_{2,3}X_{\ell,\check{5}}+X_{2,\check{5}}X_{2,3}X_{2+3,4}+X_{3,5}X_{\ell,2}X_{2+3,4}}{(\ell+k_1)^2(\ell+k_{12})^2(\ell+k_{123})^2(\ell+k_{1234})^2}\right.$$
$$+\frac{X_{2,3}X_{2+3,4}X_{2+3,\check{5}}}{s_{23}(\ell+k_1)^2(\ell+k_{123})^2(\ell+k_{1234})^2}+\frac{X_{3,4}X_{2,3+4}X_{2,\check{5}}}{s_{34}(\ell+k_1)^2(\ell+k_{12})^2(\ell+k_{1234})^2} \tag{3.3.10}$$
$$\left.+\frac{X_{4,\check{5}}X_{2,3}X_{2,4+\check{5}}}{s_{4\check{5}}(\ell+k_1)^2(\ell+k_{12})^2(\ell+k_{123})^2}\right],$$

wherein we have already made use of the fact that $\check{Q}=Q$, $X_{\check{\ell},A}=X_{\ell,A}$, $\check{\ell}+\check{k}_1+\cdots=\ell+k_1+\cdots$, as well as the relation

$$\frac{\langle 51\rangle}{\langle 56\rangle\langle 61\rangle}\,\frac{1}{\prod_{i=2}^5\langle 1i\rangle^2}=\frac{1}{\prod_{i=2}^6\langle 1i\rangle^2}\,\frac{X_{5,6}}{s_{56}}\,.$$

Note that, as demonstrated in the previous example, for any momentum K_A we have

$$X_{A,\check{5}}=\langle 1|K_A|\check{5}]\langle 51\rangle=\langle 1|K_A|5]\langle 51\rangle+\langle 1|K_A|6]\langle 61\rangle=X_{A,5+6}$$

allowing (3.3.10) to be better expressed as

$$\frac{d^D\check{\ell}}{\check{\ell}^2}\,\frac{\delta^{(8)}(Q)}{\prod_{i=2}^6\langle 1i\rangle^2}\left[\frac{X_{5,6}(X_{2,4}X_{2,3}X_{\ell,5+6}+X_{2,5+6}X_{2,3}X_{2+3,4}+X_{3,5}X_{\ell,2}X_{2+3,4})}{s_{56}(\ell+k_1)^2(\ell+k_{12})^2(\ell+k_{123})^2(\ell+k_{1234})^2}\right.$$
$$+\frac{X_{2,3}X_{5,6}X_{2+3,4}X_{2+3,5+6}}{s_{23}s_{56}(\ell+k_1)^2(\ell+k_{123})^2(\ell+k_{1234})^2}+\frac{X_{3,4}X_{5,6}X_{2,3+4}X_{2,5+6}}{s_{34}s_{56}(\ell+k_1)^2(\ell+k_{12})^2(\ell+k_{1234})^2} \tag{3.3.11}$$
$$\left.+\frac{X_{4,5+6}X_{2,3}X_{2,4+5+6}X_{5,6}}{s_{4\check{5}}s_{56}(\ell+k_1)^2(\ell+k_{12})^2(\ell+k_{123})^2}\right].$$

[1] This property implies that, using this representation of the MHV integrand, there will be $n-4$ sources of spurious poles encountered at n-points using the recursion.

As usual in this procedure we are required to shift the loop-momentum in order to sensibly combine this with the forward-limit contribution. For the six-point case we have that $z_n = \langle 56\rangle/\langle 51\rangle$, so that

$$\frac{d^D\check{\ell}}{\check{\ell}^2} = \frac{d^D\ell}{\ell^2}\frac{\alpha}{\alpha - \frac{\langle 56\rangle}{\langle 51\rangle}} \,. \tag{3.3.12}$$

By comparing the two contributions then, one can readily see that the first three terms in (3.3.11) take the precise form that corrects the first three terms in (3.3.9) in a way that mirrors the five-point case. In fact, all spurious poles arising solely from $1/s_{n-1\,\hat{n}}$ propagators are cancelled very straightforwardly this way. What is less obvious is how the last term of (3.3.11) cancels the remaining problematic terms of (3.3.9). However, it may be checked that

$$\frac{X_{4,5}X_{4+5,6}}{s_{45}s_{45\hat{6}}} + \frac{X_{5,6}X_{4,5+6}}{s_{5\hat{6}}s_{45\hat{6}}} + \frac{\alpha}{\alpha - \frac{\langle 56\rangle}{\langle 51\rangle}}\frac{X_{5,6}X_{4,5+6}}{s_{4\check{5}}s_{56}} = \frac{X_{4,5}X_{4+5,6}}{s_{45}s_{456}} + \frac{X_{5,6}X_{4,5+6}}{s_{56}s_{456}}$$

where the spurious poles are cancelled, and the correct expression is obtained for the six-point integrand.

3.4 BCFW recursion in pure Yang-Mills: all-plus

Another class of amplitudes which are relatively simple are the all-plus amplitudes of pure Yang-Mills theory. These amplitudes are described by the self-dual sector of pure Yang-Mills, and is one of the few cases in which the 'kinematic algebra' (that is, the algebra underlying the colour-kinematics duality for this theory) is known [151–153]. The all-plus one-loop integrands are related to those of the MHV sector of $\mathcal{N} = 4$ super Yang-Mills by dimension-shifting formulae [154], and the one-loop *amplitudes* are known to be purely rational functions in the kinematic invariants. Moreover, through supersymmetric Ward identities, these one-loop amplitudes can also be calculated by instead having scalars running in the loop, as opposed to gluons. These properties exhibit their simplicity, and therefore make them another ideal testing ground for new methodologies.

In this section we will see how the recursion for the integrand (3.1.11) works for the first non-trivial amplitude at four-points, here in different representations to demonstrate the versatility of the recursion. In [1] a demonstration for the five-point amplitude is also given, and it is also shown how our recursion for the *integrand* results in the known recursion for the *amplitude* [155].

3.4.1 All-plus recursion

Like MHV integrands in $\mathcal{N} = 4$ super Yang-Mills, the recursion formula can be refined for all-plus pure Yang-Mills integrands, and in fact the refined formula is almost identical to the former,

$$\mathfrak{I}^{(1)}(1^+,2^+,\cdots,n^+) = \frac{\langle n-1\,1\rangle}{\langle n-1\,n\rangle\langle n\,1\rangle}\mathfrak{I}^{(1)}(\check{1}^+,2^+,\cdots,\check{n-1}^+) + \frac{2}{\ell^2}\mathcal{A}^{(0)}(\ell_0,\hat{1}^+,2^+,\cdots,\hat{n}^+,-\ell_0). \tag{3.4.1}$$

The proof of this is very similar to that in section 3.2.1, so here we will just highlight some key differences. Firstly, as mentioned above all-plus integrands arising from the forward-limit can be calculated by having a complex scalar running in the loop. This means the

sum over states propagating through the loop in (3.1.11) reduces to a sum over the 2 states of the complex scalar, hence the factor of 2 in (3.4.1). In this term one applies the shifts (3.1.4) with $z = \alpha$:

$$\begin{aligned} \hat{k}_1 &= k_1 + \alpha q = \lambda_1(\tilde{\lambda}_1 + \alpha\tilde{\lambda}_n) \equiv \lambda_1\hat{\tilde{\lambda}}_1 \\ \hat{k}_n &= k_n - \alpha q = (\lambda_n - \alpha\lambda_1)\tilde{\lambda}_n \equiv \hat{\lambda}_n\tilde{\lambda}_n. \end{aligned} \tag{3.4.2}$$

In the factorisation terms of the recursion formula (3.1.11), only two-particle factorisation channels give a non-zero contribution, as a result of the fact that all-plus and one-minus gluon amplitudes vanish at tree-level. Since particles 1 and n must be on different channels, the resulting three-point tree amplitudes can only contain states $\{1, 2, K\}$ or $\{K, n-1, n\}$, where K is associated with the state crossing the cut. Through our choice of shift, special three-particle kinematics will enforce only the latter of these amplitudes to be non-zero. Thus, only one term contributes to the factorisation term in the recursion for the case of all-plus helicities.

This contribution is precisely the same as in the analogous case for $\mathcal{N} = 4$ super Yang-Mills, only here one specifically has gluons for external states. In that example, the supersymmetric sum over states gave a factor of $[n{-}1\, n]^4$ and established n-point supermomentum conservation in the corresponding superintegrand. Here, the three-point amplitude supplies this same $[n-1\, n]^4$ factor, and so clearly the three-point amplitude combined with the propagator gives the inverse soft factor seen in (3.4.1). Since it is the same channel that contributes in each case, the $\vee$-shifts are the same, which we recount here for completeness:

$$\begin{aligned} \check{\lambda}_1 &= \lambda_1 & \check{\tilde{\lambda}}_1 &= \tilde{\lambda}_1 + \frac{\langle n-1\, n\rangle}{\langle n-1\, 1\rangle}\tilde{\lambda}_n \\ \check{\lambda}_{n-1} &= \lambda_{n-1} & \check{\tilde{\lambda}}_{n-1} &= \tilde{\lambda}_{n-1} + \frac{\langle n\, 1\rangle}{\langle n-1\, 1\rangle}\tilde{\lambda}_n. \end{aligned} \tag{3.4.3}$$

Also similarly to the MHV sector of $\mathcal{N} = 4$ super Yang-Mills, there are no boundary terms present for the all-plus integrand recursion. This will be proved in a way similar to section 3.2.3 when we discuss certain representations of the integrand. The representation we will use also makes use of the colour-kinematics duality, but will not possess as many convenient features, making the proof of vanishing boundary terms slightly more intricate. Having concluded how (3.4.1) arises, we will now go on to discuss these representations.

3.4.2 Integrand representations

As mentioned at the beginning of this section, it is instructive to show how the recursion works with different representations of the loop-integrand. That the supersymmetric Ward identities allow one to use a complex scalar running in the loop will distinguish the two representations we will consider.

Scalars in the loop. For reference, the tree amplitudes alluded to earlier, which can be used in the forward-limit, can be expressed as

$$\mathcal{A}^{(0)}(\ell_0, 1^+, 2^+, ..., n^+, -\ell_0) = \frac{\mu^2}{\langle 12\rangle ... \langle n-1\, n\rangle} \frac{[1|\, \Pi_{i=2}^{n-1}\left(L_i^2 - k_i\, L_{i-1}\right)|n]}{\Pi_{j=1}^{n-1} L_j^2}\,, \tag{3.4.4}$$

for n gluons and two scalars. In the above we denote

$$L_i = \ell_0 + \sum_{j=1}^{i} k_j \tag{3.4.5}$$

and recall that while the external kinematics lie in four-dimensions, the loop-momentum in principle lies in D-dimensions. This means that ℓ_0 is D-dimensional, and we may refer to $\ell_0^{(4D)}$ as the four-dimensional part of ℓ_0. Since ℓ_0 is massless in D-dimensions, we have

$$\ell_0^2 = 0 = {\ell_0^{(4D)}}^2 - \mu^2 \qquad \Rightarrow \qquad {\ell_0^{(4D)}}^2 = \mu^2$$

so that ℓ_0 is massive in four-dimensions, whence μ^2 is the norm of its $(D-4)$-dimensional (spacial) part. It is also to be understood that ℓ_0 is projected down to its four-dimensional part whenever it is present inside spinor-helicity expressions; for example,

$$\ell_0|i] \equiv \ell_0^{(4D)}|i].$$

Gluons in the loop. Another way of expressing the integrand, accustomed to having gluons propagate in the loop, can be derived from the self-dual sector of pure Yang-Mills. In this theory, using the lightcone gauge offers a representation of one-loop integrands that is manifestly expressed in terms of trivalent diagrams with numerators satisfying the BCJ duality [151]. For master n-gon diagrams they can be written as[2]

$$N(1^+, \cdots, n^+) = (-1)^n \prod_{i=1}^{n} \frac{1}{\langle \eta i \rangle^2} \, X_{\ell + k_1 + \cdots + k_{i-1}, k_i} \, . \tag{3.4.6}$$

These numerators can also be shown to be equal to those in the ambitwistor string by expanding the NS-NS Pfaffian (2.6.17) into a Kleiss-Kuijf (KK) basis on the support of the scattering equations [71], using the method presented in section 1.3. The spinor $|\eta\rangle$ comes from a null reference vector that is associated with the lightcone direction in the self-dual theory. Specifically, it parametrises the lightcone gauge under the gauge condition $\eta \cdot A = 0$. In fact, these numerators are associated with the symmetry of area-preserving diffeomorphisms in the self-dual theory [151], giving an explicit example of where the kinematic algebra in the colour-kinematics duality is explicitly known.

The numerators for $(n-1)$-gon diagrams and lower are obtained from the master numerators (3.4.6) via Jacobi relations; e.g. an $(n-1)$-gon with a massive $[i,j]$ corner has numerator

$$N(\cdots, [i,j], \cdots) := N(\cdots, i, j, \cdots) - N(\cdots, j, i, \cdots) \tag{3.4.7}$$

in accordance with the colour-kinematics duality. The X variables of (3.4.6) are defined similarly as in (3.2.14), with η now taking the role of the reference spinor:

$$X_{A,B} := \langle \eta | K_A K_B | \eta \rangle = -X_{B,A} \qquad X_{A+B,C} = X_{A,C} + X_{B,C} \tag{3.4.8}$$

for any momenta K_A and K_B. Since this provides a very straightforward construction of the one-loop integrand for the all-plus sector of pure Yang-Mills, it will be quite useful for us in the next section.

[2] In [156] these come with a factor of 2 which is the same factor of 2 we have already included in equation (3.4.1) arising from the sum over states.

3.4.3 Absence of boundary terms in the all-plus recursion

As stated at the end of section 3.4.1, the boundary term in the recursion, corresponding to a possible residue at $z = \infty$, is absent for the all-plus sector of pure Yang-Mills. With the knowledge of how to construct one-loop integrands from the last section, we are now in a position to show this explicitly. We will do this using the trivalent graph expansion utilising the colour-kinematics duality, the latter representation presented in the last section with gluons running in the loop.

Though this representation is similar to that used for $\mathcal{N} = 4$ super Yang-Mills in section 3.2.2, there is a key difference which makes this slightly more involved. There one had that as a result of the reference spinor being particle 1, the numerators were invariant under the BCFW shifts and diagrams with particles 1 and n in a massive corner were absent. Here, even though the reference spinor η is arbitrary, we choose it not to coincide with any of the external particles, since from the definition of the all-plus numerators (3.4.6) this would require an unnecessarily messy limiting procedure. We will henceforth keep it arbitrary, and as a result the numerators will in general *not* be invariant under BCFW shifts; this means *a priori* diagrams with a massive 1-n corner could potentially contribute to the boundary term. We will see that, despite these differences, there is still no possibility of a residue at $z = \infty$ in the contour argument.

Let us first consider the n-gon diagrams. The numerators for these are the master numerators defined in (3.4.6). Because the combination $\hat{\ell} + \hat{k}_1 = \ell + k_1$ is invariant under the shifts, it can be seen from (3.4.6) that only the first and last X variable in any numerator is not invariant under the shift, since for large z

$$X_{\hat{\ell},\hat{k}_1} \sim z\,(-X_{q,k_1} + X_{\ell,q}) = z\,X_{\ell+k_1,q} = \mathcal{O}(z)$$

$$X_{\hat{\ell}+\hat{k}_1+\cdots+k_i,k_{i+1}} = X_{\ell+k_1+\cdots+k_{i-1},k_i} = \mathcal{O}(1)$$

$$X_{\hat{\ell}+\hat{k}_1+k_2+\cdots+k_{n-1},\hat{k}_n} = X_{\ell-k_n,\hat{k}_n} \sim -z\,X_{\ell-k_n,q} = \mathcal{O}(z)$$

whence $2 \leq i \leq n-2$ in the second line above. Thus, the combination of X variables goes at most as $\mathcal{O}(z^2)$ for large z. On the other hand, since λ_n is shifted, the factor $\langle \eta\, n\rangle^2$ in the denominator of (3.4.6) also goes as $\mathcal{O}(z^2)$, and hence overall the numerators (3.4.6) go as $\mathcal{O}(1)$ for large z.
Regarding the propagators, since we place ℓ between particles n and 1, only the $1/\ell^2$ propagators in the n-gons are affected by the shift. As discussed in section 3.2.3, these propagators go as $\mathcal{O}(z^{-1})$, and thus in total the n-gon diagrams go overall as $\mathcal{O}(z^{-1})$ for large z.

Let us now consider the p-gons with $p < n$. In contrast to the n-gons, here one will encounter different scalings in the numerators and propagators for large z whenever the shifted particles appear in a massive corner. To understand the general scaling of such diagrams it suffices to recall that the numerators and propagators follow from the Feynman rules in the self-dual theory; each vertex essentially corresponds to an X factor. If a shifted particle lies on a massive corner, each vertex between the shifted external line and the loop will give an X factor containing shifted momenta, and thus contribute an extra factor of z (since it doesn't lie directly on the loop, it cannot be cancelled by the shift in ℓ). However, each vertex that gives this extra factor will be accompanied by a tree-type propagator, which will also be shifted. Thus, the extra factors of z coming from the numerators will be cancelled by the factors of z coming from the propagators in the large z-limit. This is also true if both external particles are part of the *same* external tree, except that any

vertices or propagators involving both shifted particles will *not* contribute an extra factor of z, since the shifts between these particles cancel out. Hence, the parts of the integrand corresponding to p-gons will also scale as $\mathcal{O}(z^{-1})$, and consequently the all-plus integrand as a whole cannot give a boundary term (3.1.12).

3.5 Examples for pure Yang-Mills: all-plus

Here we will give examples of the one-loop recursion for all-plus pure Yang-Mills integrands. We will study the four-point case using both representations of the integrand discussed in 3.4.2; that is, with scalars and gluons propagating through the loop. Whilst the former will be much simpler than the latter, this serves as a demonstration of the versatility of the recursion amongst different representations of the integrand. In [1] the recursion is demonstrated with $n = 5$ external states using scalars in the loop.

3.5.1 $n = 4$, scalars in the loop

With scalars running in the loop, the recursion formula for four-points will involve the forward limit of a tree amplitude involving four gluons and two back-to-back scalars, as well as a three-point one-loop integrand multiplied by the inverse soft factor (3.4.1). It is opportune to note that the three-point one-loop all-plus integrand vanishes for on-shell momenta. This can be seen for example through dimensional analysis, or by direct computation using either of the representations above. The $n = 4$ case is therefore the first non-trivial amplitude, and only the forward-limit term contributes to the recursion. Adapting (3.4.4) to four gluons then gives

$$\mathcal{A}^{(0)}(\ell_0, \hat{1}^+, 2^+, 3^+, \hat{4}^+, -\ell_0) = \frac{\mu^2}{\langle 12\rangle\langle 23\rangle\langle 3\hat{4}\rangle} \frac{[\hat{1}|(\hat{L}_2^2 - k_2\hat{L}_1)(\hat{L}_3^2 - k_3\hat{L}_2)|4]}{\hat{L}_1^2\hat{L}_2^2\hat{L}_3^2}. \tag{3.5.1}$$

Recall that the forward limit term corresponds to the residue at $z = \alpha$, so that whilst ℓ_0 is massless, the propagators lift to the full ℓ,

$$\hat{L}_i^2 = \left(\ell_0 + \sum_{j=1}^{i} \hat{k}_j\right)^2 = \left(\ell + \sum_{j=1}^{i} k_j\right)^2 = L_i^2. \tag{3.5.2}$$

Through momentum conservation, one can find after some algebra that

$$[\hat{1}|(\hat{L}_2^2 - k_2\hat{L}_1)(\hat{L}_3^2 - k_3\hat{L}_2)|4] = -\mu^2[\hat{1}2]\langle 23\rangle[34] \tag{3.5.3}$$

(recall that ℓ_0 is massive in four-dimensions) so that (3.5.1) becomes

$$\mathcal{A}^{(0)}(\ell_0, \hat{1}, 2, 3, \hat{4}, -\ell_0) = -\frac{[\hat{1}2][34]}{\langle 12\rangle\langle 3\hat{4}\rangle} \frac{\mu^4}{L_1^2L_2^2L_3^2} \equiv -\frac{[\hat{1}2][34]}{\langle 12\rangle\langle 3\hat{4}\rangle} \frac{\mu^4}{(\ell + k_1)^2(\ell + k_1 + k_2)^2(\ell - k_4)^2}. \tag{3.5.4}$$

Finally, by noting that the spinor-helicity prefactor is permutation symmetric through momentum conservation,

$$\frac{[\hat{1}2][34]}{\langle 12\rangle\langle 3\hat{4}\rangle} = \frac{[\hat{1}4][23]}{\langle 1\hat{4}\rangle\langle 23\rangle} = \frac{[14][23]}{\langle 14\rangle\langle 23\rangle} = \frac{[12][34]}{\langle 12\rangle\langle 34\rangle}, \tag{3.5.5}$$

the four-point integrand takes the form, according to the recursion (3.4.1)

$$\mathfrak{I}^{(1)}(1^+,2^+,3^+,4^+) = -2\frac{[12][34]}{\langle 12\rangle\langle 34\rangle}\int d^D\ell\,\frac{\mu^4}{\ell^2(\ell+k_1)^2(\ell+k_1+k_2)^2(\ell-k_4)^2} \tag{3.5.6}$$

which matches the well-known result for this integrand. For clarification, note that one could write the measure as $d^D\ell = d^4\ell^{(4D)}\,d^{-2\epsilon}\mu$ and the propagators as e.g. $(\ell+K)^2 = (\ell^{(4D)}+K)^2-\mu^2$.

3.5.2 $n=4$, gluons in the loop

Here we discuss the method of obtaining the four-point all-plus integrand in pure Yang-Mills by having gluons run in the loop. As discussed in the last section, for four external states only the forward-limit term in the recursion contributes,

$$\mathcal{A}^{(1)}(1^+,2^+,3^+,4^+) = \int\frac{d\alpha}{\alpha}d^D\ell_0\,\delta(\ell_0^2)\,\mathcal{A}^{(0)}(\ell_0,\hat{1}^+,2^+,3^+,\hat{4}^+,-\ell_0),$$

where we have placed in the loop measure for clarity. In the above one performs the BCFW shifts according to $z=\alpha$,

$$\hat{k}_1 = k_1+\alpha q, \qquad\qquad \hat{k}_4 = k_4-\alpha q.$$

From the perspective of the scattering equation formalism, this corresponds to keeping σ_+, σ_- positioned between σ_1 and σ_4 in the Parke-Taylor factor dressing the colour, as we shall discuss later. Let us write the resulting tree-level amplitude of pure Yang-Mills in terms of the shifts above as[3]

$$\mathcal{A}^{(0)}(\ell_0,\hat{1}^+,2^+,3^+,\hat{4}^+,-\ell_0) = \mathcal{I}(\ell_0,\alpha)+\mathcal{I}(-\ell_0,\alpha)$$

symmetrised in ℓ_0, with

$$\mathcal{I}(\ell_0,\alpha) = \frac{-1}{\prod_i\langle\eta\hat{i}\rangle^2}\left[\mathcal{I}^{\text{box}}_{1234}+\mathcal{I}^{\text{tri}}_{[12]34}+\mathcal{I}^{\text{tri}}_{[23]41}+\mathcal{I}^{\text{tri}}_{[34]12}+\mathcal{I}^{\text{bub}}_{[12][34]}\right],$$

where $\prod_i\langle\eta\hat{i}\rangle = \langle\eta 1\rangle\langle\eta 2\rangle\langle\eta 3\rangle\langle\eta\hat{4}\rangle$. If we denote by D_i the i'th propagator such that

$$D_2 = (\ell_0+\hat{k}_1)^2, \qquad D_3 = (\ell_0+\hat{k}_1+k_2)^2, \qquad D_4 = (\ell_0-\hat{k}_4)^2,$$

then the sub-integrands above are expressed as

$$\mathcal{I}^{\text{box}}_{1234} = \frac{X_{\ell_0,\hat{1}}X_{\ell_0+\hat{1},2}X_{\ell_0-\hat{4},3}X_{\ell_0,\hat{4}}}{D_2D_3D_4} \tag{3.5.7}$$

$$\mathcal{I}^{\text{tri}}_{[12]34} = \frac{1}{(2\hat{k}_1\cdot k_2)}\frac{X_{\hat{1},2}X_{\ell_0,\hat{1}+2}X_{\ell_0-\hat{4},3}X_{\ell_0,\hat{4}}}{D_3D_4} \tag{3.5.8}$$

$$\mathcal{I}^{\text{tri}}_{[23]41} = \frac{1}{(2k_2\cdot k_3)}\frac{X_{2,3}X_{\ell_0,\hat{1}}X_{\ell_0+\hat{1},2+3}X_{\ell_0,\hat{4}}}{D_2D_4} \tag{3.5.9}$$

[3]Note that a factor of 1/2 is implicit inside of the symmetrisation, but we have cancelled it against the factor of 2 coming from the definition of the numerators; see equation (3.4.6).

$$\mathcal{I}^{\text{tri}}_{[34]12} = \frac{1}{(2k_3\cdot\hat{k}_4)}\frac{X_{3,\hat{4}}X_{\ell_0\hat{1}}X_{\ell_0+\hat{1},2}X_{\ell_0,3+\hat{4}}}{D_2D_3} \tag{3.5.10}$$

$$\mathcal{I}^{\text{bub}}_{[12][34]} = \frac{1}{(2\hat{k}_1\cdot k_2)(2k_3\cdot\hat{k}_4)}\frac{X_{\hat{1},2}X_{3,\hat{4}}X_{\ell_0,\hat{1}+2}X_{\ell_0,3+\hat{4}}}{D_3}. \tag{3.5.11}$$

This expression can be derived from the gluonic forward limit using the Feynman rules for the self-dual sector of Yang-Mills in light-cone gauge as discussed in section 3.4.2, keeping the loop momentum positioned between particles 4 and 1, and performing the BCFW shifts with $z=\alpha$. The symmetrisation in $\pm\ell_0$ used above will provide convenient cancellations. We recall that the X variables are defined as

$$X_{A,B} := \langle\eta|K_AK_B|\eta\rangle$$

for K_A and K_B possibly off-shell, and $\eta = |\eta\rangle[\eta|$ is an auxiliary null reference vector. Recall from section 3.4.2 that when ℓ_0 is inside a spinor bracket it is understood to be the four-dimensional part of ℓ_0, i.e. $\ell_0^{(4D)}$, for which $\ell_0^{(4D)\,2} = \mu^2$. Alternatively, the forward-limit-type expression above can be obtained from the D-dimensional worldsheet formulas presented in [71], specialised to four dimensions and all plus helicities.[4]

Whilst presently in a form unrecognisable to the known result, e.g. equation (3.5.6), the latter may be obtained through a series of manipulations involving the spinor anti-commutation relations.[5] As an example, for four-dimensional null momenta K_A and K_B we have

$$X_{\ell_0,A}X_{\ell_0,B} = \frac{\langle\eta A\rangle\langle\eta B\rangle}{\langle AB\rangle}\left[(2\ell_0\cdot k_A)X_{B,\ell_0} - (2\ell_0\cdot k_B)X_{A,\ell_0} + \mu^2X_{A,B}\right].$$

With these manipulations one can derive e.g.

$$X_{\ell_0,\hat{1}}X_{\ell_0+\hat{1},2} = \frac{\langle\eta 1\rangle\langle\eta 2\rangle}{\langle 12\rangle}\left[D_2\,X_{\hat{1}+2,\ell_0} - D_3\,X_{\hat{1},\ell_0} + \mu^2\,X_{\hat{1},2}\right] \tag{3.5.12}$$

$$X_{\ell_0-\hat{4},3}X_{\ell_0,\hat{4}} = \frac{\langle\eta 3\rangle\langle\eta\hat{4}\rangle}{\langle 3\hat{4}\rangle}\left[D_4\,X_{3+\hat{4},\ell_0} - D_3X_{\hat{4},\ell_0} + \mu^2\,X_{3,\hat{4}}\right], \tag{3.5.13}$$

such that the sub-integrand corresponding to the box is equivalent to

$$\begin{aligned}\mathcal{I}^{\text{box}}_{1234} = \frac{\prod_i\langle\eta\hat{i}\rangle}{\langle\hat{1}2\rangle\langle 3\hat{4}\rangle}\Bigg[&\frac{X_{\hat{1}+2,\ell_0}\,X_{3+\hat{4},\ell_0}}{D_3} - \frac{X_{\hat{1}+2,\ell_0}\,X_{\hat{4},\ell_0}}{D_4} + \mu^2\frac{X_{\hat{1}+2,\ell_0}\,X_{3,\hat{4}}}{D_3D_4}\\ &- \frac{X_{3+\hat{4},\ell_0}\,X_{\hat{1},\ell_0}}{D_2} + D_3\frac{X_{\hat{1},\ell_0}\,X_{\hat{4},\ell_0}}{D_2D_4} - \mu^2\frac{X_{\hat{1},\ell_0}\,X_{3,\hat{4}}}{D_2D_4}\\ &+ \mu^2\frac{X_{\hat{1},2}\,X_{3+\hat{4},\ell_0}}{D_2D_3} - \mu^2\frac{X_{\hat{1},2}\,X_{\hat{4},\ell_0}}{D_2D_4} + \mu^4\frac{X_{\hat{1},2}\,X_{3,\hat{4}}}{D_2D_3D_4}\Bigg].\end{aligned} \tag{3.5.14}$$

[4] Here, however, we will get quadratic propagators, instead of the linear propagators there in [71]. Firstly, we consider here only a single Parke-Taylor term in the colour factor, not the cyclic sum as there; we take the term with the loop punctures lying between the punctures for 4 and 1. Secondly, we have here ℓ_0 instead of ℓ there, but α appears in the BCFW shift of particles 1 and 4. Together, ℓ_0 and α in the BCFW shift will give quadratic propagators in the full ℓ.

[5] Similar manipulations are performed in e.g. [157].

The last term will give the correct result, since

$$\frac{1}{\prod_i\langle\eta\hat{i}\rangle^2}\frac{\prod_i\langle\eta\hat{i}\rangle}{\langle\hat{1}2\rangle\langle3\hat{4}\rangle}\mu^4\frac{X_{\hat{1},2}X_{3,\hat{4}}}{D_2D_3D_4}=\frac{[\hat{1}2][34]}{\langle12\rangle\langle3\hat{4}\rangle}\frac{\mu^4}{D_2D_3D_4}=\frac{[12][34]}{\langle12\rangle\langle34\rangle}\frac{\mu^4}{D_2D_3D_4}.$$

Similar manipulations will result in two of the triangle sub-integrands being expressible as

$$\mathcal{I}^{\text{tri}}_{[12]34}=-\frac{\prod_i\langle\eta\hat{i}\rangle}{\langle12\rangle\langle3\hat{4}\rangle}\left[\frac{X_{\hat{1}+2,\ell_0}X_{3+\hat{4},\ell_0}}{D_3}-\frac{X_{\hat{1}+2,\ell_0}X_{\hat{4},\ell_0}}{D_4}+\mu^2\frac{X_{\hat{1}+2,\ell_0}X_{3,\hat{4}}}{D_3D_4}\right] \tag{3.5.15}$$

$$\mathcal{I}^{\text{tri}}_{[34]12}=-\frac{\prod_i\langle\eta\hat{i}\rangle}{\langle12\rangle\langle3\hat{4}\rangle}\left[\frac{X_{\hat{1}+2,\ell_0}X_{3+\hat{4},\ell_0}}{D_3}-\frac{X_{\hat{1},\ell_0}X_{3+\hat{4},\ell_0}}{D_2}+\mu^2\frac{X_{\hat{1},2}X_{3+\hat{4},\ell_0}}{D_2D_3}\right]. \tag{3.5.16}$$

Notice that by combining the sub-integrands at this point, several cancellations occur. For example, the bubble terms fully cancel, and all the terms in (3.5.15) and (3.5.16) are cancelled by terms in (3.5.14). What remains is

$$\begin{aligned}\mathcal{I}(\ell_0,\alpha)=&-\frac{[12][34]}{\langle12\rangle\langle34\rangle}\frac{\mu^4}{D_2D_3D_4}-\frac{1}{\prod\langle\eta\hat{i}\rangle^2}\mathcal{I}^{\text{tri}}_{[23]41}\\&-\frac{1}{\prod_i\langle\eta\hat{i}\rangle}\frac{1}{\langle12\rangle\langle3\hat{4}\rangle}\left[D_3\frac{X_{\hat{1},\ell_0}X_{\hat{4},\ell_0}}{D_2D_4}-\mu^2\frac{X_{\hat{1},2}X_{\hat{4},\ell_0}}{D_2D_4}-\mu^2\frac{X_{\hat{1},\ell_0}X_{3,\hat{4}}}{D_2D_4}\right].\end{aligned} \tag{3.5.17}$$

Now let us symmetrise[6] in ℓ_0 and pay close inspection to the second line of (3.5.17). Keeping in mind that $D_2=(2\ell_0\cdot\hat{k}_1)$ and $D_4=-(2\ell_0\cdot\hat{k}_4)$, the terms proportional to μ^2 are anti-symmetric in ℓ_0, and so are cancelled in the symmetrisation. What remains in the second line of (3.5.17) is simply the first term and its symmetrisation, which can be written as

$$\frac{1}{\prod_i\langle\eta\hat{i}\rangle^2}\frac{D_3}{(2\hat{k}_1\cdot k_2)^2}\frac{X_{\hat{1},2}X_{3,\hat{4}}X_{\hat{1},\ell_0}X_{\hat{4},\ell_0}}{D_2D_4}+(\ell_0\to-\ell_0)=\frac{2}{\prod_i\langle\eta\hat{i}\rangle^2}\frac{X_{\hat{1},2}X_{3,\hat{4}}}{(2\hat{k}_1\cdot k_2)}\frac{X_{\hat{1},\ell_0}X_{\hat{4},\ell_0}}{D_2D_4}. \tag{3.5.18}$$

Now, let us look at the symmetrisation of the term in (3.5.17) involving $\mathcal{I}^{\text{tri}}_{[23]41}$. From (3.5.9), this results in

$$\frac{1}{\prod\langle\eta\hat{i}\rangle^2}\frac{X_{2,3}X_{\ell_0+\hat{1},2+3}}{(2k_2\cdot k_3)}\frac{X_{\hat{1},\ell_0}X_{\hat{4},\ell_0}}{D_2D_4}+(\ell_0\to-\ell_0)=\frac{-2}{\prod\langle\eta\hat{i}\rangle^2}\frac{X_{2,3}X_{\hat{1},\hat{4}}}{(2k_2\cdot k_3)}\frac{X_{\hat{1},\ell_0}X_{\hat{4},\ell_0}}{D_2D_4}. \tag{3.5.19}$$

Finally, by comparing (3.5.18) and (3.5.19) and noting that

$$\frac{X_{\hat{1},2}X_{3,\hat{4}}}{(2\hat{k}_1\cdot k_2)}-\frac{X_{2,3}X_{\hat{1},\hat{4}}}{(2k_2\cdot k_3)}=0,$$

all terms in (3.5.17) aside from the first vanish in the symmetrisation of ℓ_0, and thus one is left with

$$\mathcal{I}(\ell_0,\alpha)+\mathcal{I}(-\ell_0,\alpha)=-\frac{[12][34]}{\langle12\rangle\langle34\rangle}\frac{\mu^4}{D_2D_3D_4}+(\ell_0\to-\ell_0),$$

[6] If one does not perform this symmetrisation, then the correct result will be obtained up to terms that vanish non-trivially upon loop integration.

which, by taking $\ell = \ell_0 + \alpha q$ in the first term and $\ell = \ell_0 - \alpha q$ in the second term, and changing variables back to the full ℓ, gives the one-loop amplitude to be

$$\mathcal{A}^{(1)}(1^+,2^+,3^+,4^+) = -\frac{[12][34]}{\langle 12\rangle\langle 34\rangle}\int \frac{d^D\ell}{\ell^2}\left[\frac{\mu^4}{(\ell+k_1)^2(\ell+k_1+k_2)^2(\ell-k_4)^2}\right.$$
$$\left. + \frac{\mu^4}{(\ell-k_1)^2(\ell-k_1-k_2)^2(\ell+k_4)^2}\right] \tag{3.5.20}$$

which matches directly known results for this amplitude. This result coincides with the one computed in the last subsection, whence one symmetrises (3.5.6) in $\ell \leftrightarrow -\ell$. Note that even though the forward-limit precluded diagrams with massive 1-n corners, the symmetrisation in the loop-momenta provided the correct integrand in the final result.

3.6 BCFW recursion for non-planar Yang-Mills and Gravity

In this section we discuss extending the planar recursion to the non-planar case. This is essential in obtaining the full amplitude at one-loop for theories such as Yang-Mills, and particularly gravity which is inherently a non-planar theory. The residue theorem argument presented in section 3.1 can be applied directly to the non-planar case, but there will be more subtleties since our types of shifts are, by construction, most convenient for the planar case. This will hint at another natural procedure of obtaining a non-planar recursion. Whilst presenting its own difficulties, as we shall see, it will be more natural from the point of view of the colour-kinematics duality.

3.6.1 Single shift

It is possible to straightforwardly apply the same residue argument as in section 3.1 in the case of non-planar theories. There are two fundamental differences which affect both the forward-limit and tree-type factorisation terms that arise in the recursion. Firstly, there is no longer a notion of colour-ordering, which means that the number of terms contributing to the tree-type factorisations is now greater. Secondly, the loop momentum cannot be globally chosen to lie between particles 1 and n, so one no longer receives forward-limit contributions from just the $1/\ell^2$ propagator; this also increases the number of terms arising from the forward-limit contribution. Let us see how the latter point occurs.

Recall that we decompose the loop momentum into $\ell = \ell_0 + \alpha q$, and in our procedure shift α to $\hat{\alpha} \to \alpha - z$. Continuing to follow the procedure, suppose we also decided to shift k_1 and k_n in the same manner as (3.1.4). In a generic non-planar theory, one will encounter diagrams which contain propagators such as $1/(\ell+k_2)^2$, as well as $1/\ell^2$. Under the BCFW shifts, the latter will produce a pole at $z = \alpha$, which gives the usual forward-limit contribution we've seen in the planar case. The former however will also give a pole for when $(\hat{\ell}+k_2)^2$ goes on-shell:

$$(\hat{\ell}+k_2)^2 = 0 \qquad \Rightarrow \qquad z = \frac{(\ell+k_2)^2}{2(\ell+k_2)\cdot q}. \tag{3.6.1}$$

These are the kind of poles one encounters in [137]. It is easy to see that given the shifts above, the only loop propagators which do not produce these poles are those involving ℓ and k_1, but not k_n. The shift in α (or the shift in ℓ) is designed to cancel the shift in k_1,

but introducing k_n reintroduces the dependence on z, consequently producing another pole. This can be illustrated by considering a scalar box with ordering (2143):

$$\frac{1}{\ell^2(\ell+k_2)^2(\ell+k_{21})^2(\ell+k_{214})^2} \tag{3.6.2}$$

Upon performing the BCFW shifts, the first propagator gives the usual pole at $z=\alpha$. The second propagator will also give a pole corresponding to (3.6.1). The third propagator will *not* produce a pole, since the shift in ℓ cancels the shift in k_1. However, the last propagator can be written as $1/(\ell-k_3)^2$, and thus will exhibit a pole similar to (3.6.1), except with $k_2 \to -k_3$. All in all, the scalar box above would give three forward-limit contributions. The situation is worsened in examples where the scalar box has an ordering such that particle 4 appears before particle 1 (e.g., diagrams with ordering (4213)), since all loop propagators will give forward-limit contributions.

We can ameliorate this issue by globally choosing the loop momentum to lie next to particle 1, which is a valid choice one can make in a non-planar theory. Then the last situation described above cannot occur, and the number of terms contributing to the forward-limit is vastly decreased. It is also more natural from the point of view of the shifts. Regardless, the residue argument results in an expression of the form

$$\mathfrak{I}_n^{(1)} = \sum_{I,\,\text{states}_I} \mathcal{A}^{(0)}_{n_I+1}(z_I)\frac{1}{K_I^2}\mathfrak{I}^{(1)}_{n-n_I+1}(z_I) \;+\; \sum_{J,\,\text{states}_J} \frac{1}{(\ell+K_J)^2}\,\mathcal{A}^{(0,\text{reg})}_{n+2}(z_{J_\ell}) + \mathcal{B}_n \tag{3.6.3}$$

where $\mathcal{A}^{(0,\text{reg})}_{n+2}(z_{J_\ell})$ corresponds to the regularised forward-limit of an $(n+2)$-point tree amplitude, evaluated at z_{J_ℓ} for which $(\hat{\ell}+\hat{K}_J)^2=0$. Naturally one might want to further reduce the number of forward-limit contributions by appropriately re-defining the loop momentum in each term in the integrand. For example, if we were considering the scalar box with ordering (1432), performing the shift not on ℓ but on $\tilde{\ell}=-(\ell+k_1)$ would result in only a single forward-limit term, as opposed to three from shifting ℓ. However, then we would not be applying a single BCFW shift, and this reasoning leads us to another procedure which we will now discuss.

3.6.2 Multiple shifts and gravity integrands

The other option is to decompose the integrand into planar sub-sectors and perform different shifts accordingly. This is quite natural from the point of Yang-Mills theory, or any theory with only adjoint states, where the notion of ordering is explicit. In the case of Yang-Mills, one can express the full colour-dressed integrand in terms of a DDM basis,

$$\mathfrak{I}_n^{(1),\text{YM}} = \sum_{\rho\in(S_n/\mathbb{Z}_n)/\mathcal{R}} c^{(1)}(\rho(1),\cdots,\rho(n))\;\mathfrak{I}_n^{(1),\text{YM}}(\rho(1),\cdots,\rho(n)) \tag{3.6.4}$$

wherein $(S_n/\mathbb{Z}_n)$ are the set of non-cyclic permutations, and $\mathcal{R}$ denotes reflections. For any ordering the one-loop colour factors in this basis are expressed purely in terms of the structure constants of the theory.

$$c^{(1)}(\rho(1),\cdots,\rho(n)) = f^{b_0 a_{\rho(1)} b_1} f^{b_1 a_{\rho(2)} b_2}\cdots f^{b_{n-1} a_{\rho(n)} b_0}. \tag{3.6.5}$$

Each partial integrand $\mathfrak{I}_n^{(1),\text{YM}}(\rho(1),\cdots,\rho(n))$ obeys the ordering ρ, so it is natural in each term to associate the loop momentum as lying between $\rho(n)$ and $\rho(1)$, just as we did for

the planar case. Then one can perform the planar BCFW shifts (3.1.4) adapted to the new ordering,

$$\begin{aligned} \hat{k}_{\rho(1)} &= k_{\rho(1)} + zq, & \hat{k}_{\rho(n)} &= k_{\rho(n)} - zq, \\ \hat{\alpha} &= \alpha - z \qquad \Rightarrow & \hat{\ell} &= \ell_0 + (\alpha - z)q = \ell - zq. \end{aligned} \tag{3.6.6}$$

One can minimise the number of shifts required by choosing the loop momentum to lie globally before particle 1, as mentioned in the last section. Then one would perform the above shifts on k_1 and $k_{\rho(i-1)}$ where $\rho(i) = 1$, i.e. $\rho(i-1)$ is the particle before particle 1 in the ordering. One then requires only to perform $n-1$ distinct BCFW shifts to capture the full integrand.

For generic theories one can attempt to decompose the integrand into parts with fixed ordering along the lines of the above. This is quite natural for theories obtainable through the double copy provided one has the relevant set of BCJ numerators. For example, in the DDM basis of (3.6.4) gravity amplitudes integrands can be obtained via

$$\mathfrak{I}_n^{(1),\text{grav}} = \sum_{\rho \in (S_n/\mathbb{Z}_n)/\mathcal{R}} \tilde{N}^{(1)}(\rho(1), \cdots, \rho(n))\, \mathfrak{I}_n^{(1),\text{YM}}(\rho(1), \cdots, \rho(n)) \tag{3.6.7}$$

where $\tilde{N}^{(1)}(\rho(1), \cdots, \rho(n))$ are the n-gon BCJ numerators for Yang-Mills at one-loop with the prescribed colour-ordering. In the case of $\mathcal{N} = 4$ super Yang-Mills, this procedure would give a recursion for $\mathcal{N} = 8$ supergravity, where the partial amplitudes and BCJ numerators of section 3.2.2 may be used. Importantly, consistent factorisations of gravity are guaranteed by the double copy, since in a unitarity cut for example the independent sum over states in $\tilde{N}^{(1)}$ and $\mathfrak{I}_n^{(1),\text{YM}}$ is equivalent to the gravity sum over states.

To clarify, the formula (3.6.7) for gravity amplitudes relies on the existence of BCJ numerators at one-loop. These are numerators in the loop-level conjecture of BCJ [12], for loop-integrands involving quadratic propagators. It is known that there are obstacles in constructing these numerators beyond the MHV sector mentioned above, even at one-loop [158,159]. In representations of the loop integrand using linear propagators, e.g. coming from the ambitwistor string, BCJ numerators are readily available since they are derived from a type of forward-limit of the tree-level case. However, this is not the representation we are currently discussing.

This methodology seems to suggest that the non-planar recursion follows straightforwardly from the planar case. There is however a subtlety that arises from performing different shifts for planar-like sub-sectors of the integrand. Namely, the BCFW factorisation in the non-planar case is not straightforwardly aligned with the planar BCFW factorisation. Recall that tree-type factorisation terms cancel the spurious poles coming from the corresponding forward-limit term. In the non-planar case, it is required that these spurious poles are cancelled before one obtains the correct factorisation. Let us demonstrate this by returning to the five-point example in $\mathcal{N} = 4$ super Yang-Mills. Consider the following two terms in the colour-dressed integrand of (3.6.4):

$$c(1,2,3,4,5)\, \mathfrak{I}^{(1),\text{YM}}(1,2,3,4,5) + c(1,2,3,5,4)\, \mathfrak{I}^{(1),\text{YM}}(1,2,3,5,4) \subset \mathfrak{I}_5^{(1),\text{YM}} \tag{3.6.8}$$

with the colour factors corresponding to pentagons with the relevant ordering. From our discussion above, we would perform shifts on k_1 and k_5 in the first term and shifts on k_1 and k_4 in the second term. The first term is essentially the example we considered in section

3.3.2, so it is known that a spurious pole arises in the box with a massive 45 corner. Calling the numerator for this term $N^{\text{box}}_{123[4,5]}$, these terms appear from the above as

$$\begin{aligned} &c(1,2,3,4,5)\int \frac{d^D\ell}{\ell^2}\frac{N^{\text{box}}_{123[4,5]}}{(\ell+k_1)^2(\ell+k_{12})^2(\ell+k_{123})^2 s_{45}} \\ &+ c(1,2,3,5,4)\int \frac{d^D\ell}{\ell^2}\frac{N^{\text{box}}_{123[5,4]}}{(\ell+k_1)^2(\ell+k_{12})^2(\ell+k_{123})^2 s_{45}}. \end{aligned} \tag{3.6.9}$$

Since $N^{\text{box}}_{123[5,4]} = -N^{\text{box}}_{123[4,5]}$ by construction, these terms traditionally combine into a single term

$$c(1,2,3,[4,5])\int \frac{d^D\ell}{\ell^2}\frac{N^{\text{box}}_{123[4,5]}}{(\ell+k_1)^2(\ell+k_{12})^2(\ell+k_{123})^2 s_{45}} \tag{3.6.10}$$

where $c(1,2,3,[4,5]) := c(1,2,3,4,5) - c(1,2,3,5,4)$ is formally recognised as the colour factor for the box with a massive 45 corner. Now suppose we had performed the separate shifts mentioned above in accordance with the recursion. Both terms in (3.6.9) would give a spurious pole from the $1/s_{45}$ propagator,

$$\begin{aligned} &c(1,2,3,4,5)\int \frac{d^D\ell}{\ell^2}\frac{\alpha}{\alpha-\frac{\langle 45\rangle}{\langle 41\rangle}}\frac{N^{\text{box}}_{123[4,5]}}{(\ell+k_1)^2(\ell+k_{12})^2(\ell+k_{123})^2 s_{45}} \\ &+ c(1,2,3,5,4)\int \frac{d^D\ell'}{\ell'^2}\frac{\alpha'}{\alpha'-\frac{\langle 54\rangle}{\langle 51\rangle}}\frac{N^{\text{box}}_{123[5,4]}}{(\ell'+k_1)^2(\ell'+k_{12})^2(\ell'+k_{123})^2 s_{45}}. \end{aligned} \tag{3.6.11}$$

which comes from having $q = \lambda_1\tilde{\lambda}_5$ and $q' = \lambda_1\tilde{\lambda}_4$ respectively. We put primes on α and ℓ on the second term as a reminder that they come from applying different shifts. Unlike in (3.6.10), it is generically impossible to combine these two terms at this stage. This would require

$$\ell = \ell', \qquad \frac{\alpha}{\alpha-\frac{\langle 45\rangle}{\langle 41\rangle}} = \frac{\alpha'}{\alpha'-\frac{\langle 54\rangle}{\langle 51\rangle}} \qquad \Leftrightarrow \qquad \alpha' = -\frac{\langle 41\rangle}{\langle 51\rangle}\alpha. \tag{3.6.12}$$

From the first condition we would have that

$$\ell_0 + \alpha q = \ell_0' + \alpha' q' \qquad \Rightarrow \qquad \ell_0' = \ell_0 + \alpha q - \alpha' q'$$

and thus the null condition on ℓ_0' implies

$$\alpha\,\ell_0\cdot q = \alpha'\ell_0\cdot q' \qquad \Rightarrow \qquad \alpha' = \frac{\ell_0\cdot q}{\ell_0\cdot q'}\,\alpha. \tag{3.6.13}$$

Comparing (3.6.12) with (3.6.13), it is clear that the two terms can only be combined when

$$\frac{\ell_0\cdot q}{\ell_0\cdot q'} = -\frac{\langle 41\rangle}{\langle 51\rangle},$$

however this is not true for generic ℓ_0. Essentially, the fact that performing multiple shifts will produce generically incompatible spurious poles disallows the BCFW factorisation from being straightforwardly realised in the non-planar case. Clearly, the spurious poles would have to be cancelled term by term before they can be meaningfully combined into the correct expression.

Nevertheless, this extension of the recursion to the non-planar case seems more natural in terms of the colour-kinematics duality, and will be more appropriate to extend also the worldsheet formulae giving quadratic propagators, which we will now discuss.

3.7 Worldsheet formulas for quadratic propagators

As discussed at the end of the previous chapter, worldsheet formulae for one-loop integrands result in an unorthodox representation of the integrand, which contain 'linear-type' propagators as opposed to the quadratic propagators one obtains in a typical field theory calculation. This is a result of the form of the one-loop scattering equations (2.5.15), which do not explicitly contain ℓ^2. However the scattering equations are very malleable; different forms can be considered so long as certain crucial properties, such as Möbius invariance of the amplitude, are retained. Examples of this can be seen at tree-level, with the 'massive' scattering equations giving rise to the correct propagators for theories with massive states [108–113].

The linear propagators are not the only difference with typical field theory however. To get an idea of these differences, let us have a look at the result for the scalar n-gon integrand with ordering $(12\cdots n)$ that arises from worldsheet formulae:

$$\frac{1}{\ell^2}\cdot\frac{1}{(2\ell\cdot k_1)(2\ell\cdot(k_1+k_2)+(k_1+k_2)^2)\cdots(-2\ell\cdot k_n)}+\text{cyc}(12\cdots n). \tag{3.7.1}$$

The factor $1/\ell^2$ plays a passive role in the worldsheet formalism, a remnant of the fact that they give forward-limit-type integrand representations. Indeed, this can be seen by noticing that the linear propagators appear seemingly related to Feynman-type propagators by treating ℓ as a null object[7]. The cyclic factors arise from the structure of worldsheet integrands for one-loop and are a novel feature of this formalism. Clearly, there are two things distinguishing (3.7.1) from the result obtainable from Feynman diagrams:

(1) The propagators are 'linear' in the loop momentum, contrasting traditional Feynman propagators, which appear quadratically, e.g. as $(\ell+K)^2$.

(2) The $\text{cyc}(12\cdots n)$ factor gives rise to n distinct terms in the integrand, contrasting the one term obtained for a single n-gon diagram in the Feynman representation.

The origins of these issues motivate a strategy to straightforwardly obtain quadratic propagators in worldsheet formulae without overcounting, thereby allowing them to coincide with traditional integrand representations. Let us recall that the propagator structure from performing worldsheet integrals is fully determined from the form of the scattering equations. This follows straightforwardly from the fact that the scattering equations relate kinematic poles to the boundaries of the moduli space, as discussed in section 2.7. Indeed, this is what allows the worldsheet formulae to inherently give field theory results. This means the propagators in (3.7.1) are determined a priori from the structure of the one-loop scattering equations,

$$\mathcal{E}_i:=\ell\cdot k_i\,\frac{\sigma_{+-}}{\sigma_{i+}\sigma_{i-}}+\sum_{j\neq i}\frac{k_i\cdot k_j}{\sigma_{ij}},\qquad\qquad \mathcal{E}_\pm:=\pm\sum_j\frac{\ell\cdot k_j}{\sigma_{\pm j}}. \tag{3.7.2}$$

The other issue, regarding the cyclic factors, arises from the fact that the worldsheet integrands typically involve a sum over Parke-Taylor denominators with different cyclic ordering.

[7] Although these can be derived from the standard Feynman representation by use of the partial fraction identity discussed in section 2.7 and utilised in [116], where the notion of 'Q-cuts' were introduced. Unfortunately, the converse in not generically true, which is the main motivation for this work.

For example, in the n-gon example, one of the worldsheet half-integrands have the form

$$\mathcal{I}^{(1)}_{1/2} = \sum_{\rho\in \mathrm{cyc}(12\cdots n)} \frac{1}{(+\rho_1\,\rho_2\cdots\rho_n-)}$$

where $(+\rho_1\,\rho_2\cdots\rho_n-) = \sigma_{+\rho_1}\sigma_{\rho_1\rho_2}\cdots\sigma_{\rho_n-}\sigma_{-+}$ as usual. The cyclic sum over Parke-Taylor factors in the half-integrand essentially gives rise to the cyclic sum in (3.7.1). Considering these points, it is clear what could be done to obtain, in our example, the more traditional form of the n-gon integrand:

(1) Modify the scattering equations, such that the propagators appearing are quadratic in the loop-momenta, as opposed to linear,

(2) Include only a single Parke-Taylor factor in the worldsheet integrand, such that only a single ordering appears with respect to the loop propagators.

The two modifications above are not mutually exclusive, and a choice of how one is modified will indicate how the other should be. We will now discuss these modifications in more detail.

3.7.1 Scattering equations for quadratic propagators

Let us continue considering our example in (3.7.1). Diagrammatically, the cyclic sum exemplifies how the loop-momentum is treated democratically in the scattering equation formalism. This can also be seen in the homogeneity of $\ell\cdot k_i$ in the scattering equations (3.7.2). A Feynman-type representation would consist of only a single term for this integrand, where the $1/\ell^2$ propagator corresponds to a fixed position in the loop. Suppose then we had a single term where the loop is positioned between particles n and 1 (in a sense, having already completed step (2) above), which essentially corresponds to the first term of (3.7.1). Since each propagator contains the term $2\ell\cdot k_1$ (or, using momentum conservation[8], $-2\ell\cdot k_n$), it is clear we can obtain quadratic propagators via the substitutions

$$2\ell\cdot k_1 \mapsto (\ell+k_1)^2, \qquad\qquad 2\ell\cdot k_n \mapsto -(\ell-k_n)^2.$$

Since as mentioned above the poles of the loop integrand are determined by the form of the scattering equations, this motivates us to propose new ℓ^2-*deformed scattering equations*:

$$\mathcal{E}_i^{\ell^2\text{-def}} = \mathcal{E}_i\Big|_{\substack{2\ell\cdot k_1\,\mapsto\,+(\ell+k_1)^2\\ 2\ell\cdot k_n\,\mapsto\,-(\ell-k_n)^2}}. \tag{3.7.3}$$

To spell this out in more detail, the scattering equations for all external labels not including particles 1 and n, are completely unchanged, $\mathcal{E}^{\ell^2\text{-def}}_{i\neq 1,n} = \mathcal{E}_{i\neq 1,n}$, whilst the scattering equations for particles 1 and n become

$$\mathcal{E}_1^{\ell^2\text{-def}} = +(\ell+k_1)^2\frac{\sigma_{+-}}{\sigma_{1+}\sigma_{1-}} + \sum_{j\neq 1}\frac{k_1\cdot k_j}{\sigma_{1j}}$$

$$\mathcal{E}_n^{\ell^2\text{-def}} = -(\ell-k_n)^2\frac{\sigma_{+-}}{\sigma_{n+}\sigma_{n-}} + \sum_{j\neq n}\frac{k_n\cdot k_j}{\sigma_{nj}}$$

[8]This single term would now be, in our n-gon example, the first term of (3.7.1). Note that the last propagator in this term is obtained using momentum conservation, $2\ell\cdot(k_1+\cdots k_{n-1})+(k_1+\cdots k_{n-1})^2 = -2\ell\cdot k_n$. Therefore, the deformations we are about to present ensure that each propagator becomes quadratic in the loop momentum.

and the scattering equations for the nodal points become

$$\mathcal{E}_+^{\ell^2\text{-def}} = +\frac{(\ell+k_1)^2}{\sigma_{+1}} - \frac{(\ell-k_n)^2}{\sigma_{+n}} + \sum_{j\neq 1,n}\frac{2\ell\cdot k_j}{\sigma_{+j}}$$

$$\mathcal{E}_-^{\ell^2\text{-def}} = -\frac{(\ell+k_1)^2}{\sigma_{-1}} + \frac{(\ell-k_n)^2}{\sigma_{-n}} - \sum_{j\neq 1,n}\frac{2\ell\cdot k_j}{\sigma_{-j}}.$$

Note that these deformations will preserve Möbius invariance since it is still true that

$$\sum_i \sigma_i^m \mathcal{E}_i^{\ell^2\text{-def}} = 0, \qquad\qquad m = 0,1,2$$

as a result of momentum conservation. This means that the ℓ^2-deformed scattering equations are appropriate for a CHY-type measure, so one may define

$$d\mu_n^{\ell^2\text{-def}} := \frac{d^{n+2}\sigma}{\text{vol SL}(2,\mathbb{C})}\prod_{i=1}^{n+2}{}' \,\bar{\delta}\left(\mathcal{E}_i^{\ell^2\text{-def}}\right) \tag{3.7.4}$$

in complete analogy with the usual CHY measure involving linear propagators. This will be the necessary measure to use in the worldsheet formulae to be presented that give rise to traditional Feynman-type representations of loop-integrands.

Like the tree- and one-loop construction of worldsheet models, the scattering equations can be described more succinctly as the vanishing of a quadratic differential on the nodal sphere. For the usual one-loop scattering equations this was described in section 2.5, where the quadratic differential appears as $\mathfrak{P}_1 = P^2(\sigma) - \ell^2\omega_{+-}^2$. For the ℓ^2-deformed scattering equations it can be recognised that this quadratic differential has the form $\mathfrak{P}_1^{\ell^2\text{-def}} = P^2(\sigma) - \ell^2\omega_{+-}^2 + \ell^2\omega_{+-}\omega_{1n}$ where

$$P^\mu(\sigma) = \left(\frac{\ell^\mu}{\sigma-\sigma_+} - \frac{\ell^\mu}{\sigma-\sigma_-} + \sum_{i=1}^n \frac{k_i^\mu}{\sigma-\sigma_i}\right)d\sigma, \qquad \omega_{ab}(\sigma) = \frac{\sigma_a-\sigma_b}{(\sigma-\sigma_a)(\sigma-\sigma_b)}\,d\sigma.$$

As usual, imposing that this quadratic differential vanishes on the sphere is achieved by setting the residues at its poles equal to zero, which here gives rise to the ℓ^2-deformed scattering equations:

$$\mathcal{E}_i^{\ell^2\text{-def}} = \text{Res}_{\sigma_i}\,\mathfrak{P}_1^{\ell^2\text{-def}} = \text{Res}_{\sigma_i}(P^2(\sigma) - \ell^2\omega_{+-}^2 + \ell^2\omega_{+-}\omega_{1n}). \tag{3.7.5}$$

Let us make some comments on the possibility of deriving these from a first-principles argument. Writing (3.7.5) this way seems to indicate the possibility of deriving this form of the scattering equations directly from the torus via a residue theorem. Indeed, the difference between $\mathfrak{P}_1$ and $\mathfrak{P}_1^{\ell^2\text{-def}}$, namely the term $\ell^2\omega_{+-}\omega_{1n}$, is precisely proportional to the 'modular' scattering equation at genus one, which acts to localise the modular parameter onto $\tau \to i\infty$ where the torus degenerates to the nodal sphere. In the type II ambitwistor string, as seen in section 2.5, this scattering equation is recognised as $\mathcal{E}_\tau := P^2(z_0) = 0$ for z_0 an arbitrary point. On the torus, different scattering equations related via $\mathcal{E}_i \simeq \mathcal{E}_i + \alpha_i\mathcal{E}_\tau$ are equivalent on the support of the modular scattering equation. In this case the ℓ^2-deformed scattering equations could then arise by taking $\alpha_1 = -\alpha_n = 1$ and all other $\alpha_i = 0$ such that

$$\mathcal{E}_1^{\ell^2\text{-def}} = \mathcal{E}_1 + \ell^2\frac{\sigma_{+-}}{\sigma_{1+}\sigma_{1-}}, \qquad\qquad \mathcal{E}_n^{\ell^2\text{-def}} = \mathcal{E}_n - \ell^2\frac{\sigma_{+-}}{\sigma_{n+}\sigma_{n-}}$$

with all others unchanged. However, on the nodal sphere the above equivalence is no longer manifest, since $\mathcal{E}_\tau \sim \ell^2 \neq 0$, and different choices of scattering equations can lead to very different representations of the loop integrand. These contribute to making a first-principles derivation of our formulae from the torus non-trivial. In this endeavour one ought to verify the details of the argument above and check that on the support of the scattering equations $\mathcal{E}_i + \alpha_i \mathcal{E}_\tau$, the genus-one integrand still only has a pole at $\tau = i\infty$. Once this is done it would be interesting to investigate the space of these deformations in more detail, but this has not hitherto been done.

It should also be noticed that this particular modification of the scattering equations is only well-adapted to planar theories. Indeed, this discussion was motivated by investigating the scalar n-gon expression of (3.7.1) in a particular (planar) ordering. On the other hand, the only theory to date which has had a rigorous derivation at genus-one from the ambitwistor string has been type II supergravity [50], which is naturally non-planar. One might expect then that a derivation from the torus would require not just one set of deformed scattering equations, but sets of distinct deformations, taking into account other planar-like orderings that can occur. This follows the same reasoning as section 3.6.2, and it should be that the resulting expressions on the nodal sphere would reproduce the expressions therein. We will go on to discuss the non-planar case in section 3.7.5.

3.7.2 Worldsheet integrands for quadratic propagators

As mentioned above section 3.7.1, we will also be required to modify the integrands appearing in the worldsheet formulae to ensure that the relevant Feynman representation of the loop integrand is obtained. In preceding discussions, we have noted that the structure of worldsheet formulas is such that in the resulting expressions, the loop-momentum is treated democratically. In our n-gon example (3.7.1) this was seen explicitly in the cyclic sum over the ordering we were considering. This cyclic sum arises from the cyclic sum in the worldsheet half integrand, so it is easy to single out a specific term to reproduce the desired expression. While for generic theories this can be fairly non-trivial, it is quite natural for theories which admit worldsheet integrands expressible in a Parke-Taylor basis, since the ordering of the external particles in the resulting diagram is explicit. Using the colour-kinematics duality allows this to be possible for many theories, and in fact any massless theory admitting a BCJ representation should have this property.

In this section we will give a few examples of worldsheet integrands tailored towards the ℓ^2-deformed scattering equations. The moduli-space integrations of these will result in formal expressions for the one-loop integrands containing quadratic propagators. We will do this in two cases: the n-gons, which were our initial example, and the MHV integrand for super Yang-Mills theory. The former will aid us in seeing how the latter is well described, and so will act as a toy model we go on to discuss now.

The n-gon integrands, with and without massive corners. The n-gon served as the original motivation in deducing how to alter worldsheet formulae in order to coincide with the traditional Feynman representation. We considered a specific ordering and found a set of scattering equations which gave quadratic propagators. However, in order for this to be effective, we still require only one term in the loop-integrand, as opposed to the cyclic sum, otherwise the deformed scattering would only suit their purpose for one of the terms. This is achieved for any particular ordering by keeping one term in the worldsheet integrand before

integration, so that we can propose that for the n-gon:

$$\boxed{\mathcal{I}^{(1)}_{n\text{-gon}}(12\dots n) = \frac{1}{\ell^2}\int_{\mathfrak{M}_{0,n+2}} d\mu_n^{\ell^2\text{-def}} \left(\frac{1}{\sigma_{+-}^2}\prod_{j=1}^{n}\frac{\sigma_{-+}}{\sigma_{+j}\,\sigma_{j-}}\right) \frac{1}{(+12\dots n-)}} \tag{3.7.6}$$

with $n \geq 4$. In the above we denote $(+12\cdots n-)$ as the (inverse) Parke-Taylor factor, $(+12\cdots n-) = \sigma_{+1}\sigma_{12}\cdots\sigma_{n-}\sigma_{-+}$. The measure, now containing the ℓ^2-deformed scattering equations, is defined from (3.7.4). Between the inclusion of this measure and the one Parke-Taylor above, this worldsheet formula acts to give only a single term in the loop-integrand, which has quadratic propagators. At four- and five-points for example, it can be shown either numerically or by factorisation arguments that

$$\mathcal{I}^{(1)}_{\text{box}}(1234) = \frac{1}{\ell^2(\ell+k_1)^2(\ell+k_{12})^2(\ell-k_4)^2} \tag{3.7.7a}$$

$$\mathcal{I}^{(1)}_{\text{pent}}(12345) = \frac{1}{\ell^2(\ell+k_1)^2(\ell+k_{12})^2(\ell+k_{123})^2(\ell-k_5)^2}\,. \tag{3.7.7b}$$

We note that for $n = 2, 3$, tadpole-like structures appear and so the above proposal (3.7.6) is not valid in these cases.

Another interesting example, which is less trivial, is the $(n-1)$-gon with a massive corner. A lot of work has gone into deriving worldsheet formulae which produce diagrams such as these, based on pole-power-counting [83–85]. For an $(n-1)$-gon ($n \geq 5$) with massive corner $[i\,i+1]$ ($i \neq n$), the formula should follow straightforwardly as

$$\mathcal{I}^{(1)}_{(n-1)\text{-gon}|[i\,i+1]}(12\cdots n) = \frac{1}{\ell^2}\int_{\mathfrak{M}_{0,n+2}} d\mu_n^{\ell^2\text{-def}} \left(\frac{1}{\sigma_{+-}^2}\frac{\sigma_{-+}}{\sigma_{-i}\sigma_{i\,i+1}\sigma_{i+1\,+}}\prod_{j\neq i,i+1}^{n}\frac{\sigma_{-+}}{\sigma_{+j}\,\sigma_{j-}}\right) \frac{1}{(+12\dots n-)}\,. \tag{3.7.8}$$

This formula can also be understood in terms of factorisation. In comparison to (3.7.6), the factor in the parenthesis is designed to only produce diagrams with a pole in $s_{i\,i+1}$, corresponding to when the punctures σ_i and σ_{i+1} coalesce. Indeed at five points for example one can check either numerically or via factorisation that (3.7.8) results in

$$\mathcal{I}_{\text{box}|[4,5]} = \frac{1}{s_{45}\,\ell^2(\ell+k_1)^2(\ell+k_{12})^2(\ell+k_{123})^2} \tag{3.7.9}$$

These examples will aid us in the more non-trivial examples to be considered now.

3.7.3 The MHV integrand

We can perform similar manipulations to the above to obtain the one-loop integrands of $\mathcal{N} = 4$ super Yang-Mills. Here the ordering of the particles is directly associated with the colour-ordering in the trace decomposition, where the worldsheet integrand naturally includes a factor

$$\mathcal{C}^{(1)}_{\text{cyc}}(12\cdots n) = \sum_{\gamma\in\text{cyc}(12\cdots n)} \frac{\text{tr}(T^{a_{\gamma(1)}}T^{a_{\gamma(2)}}\cdots T^{a_{\gamma(n)}})}{(+\gamma(1)\gamma(2)\cdots\gamma(n)-)}\,, \tag{3.7.10}$$

for the planar case. The subscript 'cyc' on the LHS refers to the cyclic sum on the RHS. That the MHV integrand admits such a Parke-Taylor decomposition allows us to straightforwardly

restrict only one term to the sum, according to the placement of ℓ. For ℓ between particles n and 1 this term is naturally chosen to be

$$\mathcal{C}^{(1)}(12\cdots n) = \frac{\mathrm{tr}(T^{a_1}T^{a_2}\cdots T^{a_n})}{(+\,12\cdots n\,-)} \subset \mathcal{C}^{(1)}_{\mathrm{cyc}}(12\cdots n)\,. \tag{3.7.11}$$

This allows us to propose the n-point worldsheet integrand for the MHV sector of $\mathcal{N}=4$ super Yang-Mills:

$$\boxed{\mathfrak{I}^{(1)}_{\text{SYM-MHV}}(12\ldots n) = \frac{1}{\ell^2}\int_{\mathfrak{M}_{0,n+2}} d\mu_n^{\ell^2\text{-def}}\,\mathcal{I}^{(1)}_{\text{MHV}}\,\mathcal{C}^{(1)}(12\ldots n)\,.} \tag{3.7.12}$$

In the above formula, the kinematic MHV worldsheet integrand takes the form

$$\mathcal{I}^{(1)}_{\text{MHV}} = \sum_{\rho\in S_n}\frac{N^{(1)}_\rho}{(+\,\rho(1)\,\rho(2)\cdots\rho(n)\,-)} \tag{3.7.13}$$

with

$$N^{(1)}_\rho = \delta^{(8)}(Q)\left(\prod_{i=2}^{n}\frac{1}{\langle 1i\rangle^2}\right)\mathfrak{n}^{(1)}_\rho\,. \tag{3.7.14}$$

These numerators take the same form as in the previous sections, and so share the same properties as before. Firstly, they are directly calculable to any multiplicity via the algorithm presented in [149]. Furthermore, supermomentum is manifest in this construction, and diagrams with 1-n corners vanish for the same reason as before. This is quite crucial here, since the ℓ^2-deformed scattering equations do not typically give rise to these types of diagrams and may produce unphysical poles in this factorisation channel. Another property is that they also vanish for triangles and bubbles, in line with the 'no-triangle' hypothesis for this theory. As a result, they also prevent these diagrams arising from the worldsheet formulae.

Let us now present some examples for four and five particles to demonstrate that the worldsheet formula (3.7.12) provides the correct expressions in these cases.

Four particles. This works in close analogy with the BCFW example in section 3.3.1. Firstly, notice that

$$N^{(1)}_\rho = -\delta^{(8)}(Q)\frac{[12][34]}{\langle 12\rangle\langle 34\rangle} \tag{3.7.15}$$

for all $\rho\in S_4$. This can be seen from the fact the above is permutation symmetric. Its corresponding sum of Parke-Taylor factors from (3.7.13) can be related to our previous results by noting the identity

$$\sum_{\rho\in S_n}\frac{1}{(+\,\rho(1)\,\rho(2)\cdots\rho(n)\,-)} = -\frac{1}{\sigma^2_{+-}}\prod_{i=1}^{n}\frac{\sigma_{+-}}{\sigma_{-i}\sigma i+} = (-1)^n\left(\frac{1}{\sigma^2_{+-}}\prod_{i=1}^{n}\frac{\sigma_{-+}}{\sigma_{-i}\sigma_{i+}}\right)\,. \tag{3.7.16}$$

Upon using this formula, as well as (3.7.15), the MHV worldsheet formula (3.7.13) at four points becomes

$$\mathfrak{I}^{(1)}_{\text{SYM-MHV}}(1234) = \delta^{(8)}(Q)\frac{[12][34]}{\langle 12\rangle\langle 34\rangle}\frac{1}{\ell^2}\int_{\mathfrak{M}_{0,n+2}} d\mu_n^{\ell^2\text{-def}}\left(\frac{1}{\sigma^2_{+-}}\prod_{i=1}^{4}\frac{\sigma_{-+}}{\sigma_{-i}\sigma_{i+}}\right)\frac{1}{(+\,1234\,-)}\,. \tag{3.7.17}$$

We recognise the moduli-space integral as (3.7.7a), so the above results in

$$\mathfrak{I}^{(1)}_{\text{SYM-MHV}}(1234) = \delta^{(8)}(Q)\frac{[12][34]}{\langle 12\rangle\langle 34\rangle}\frac{1}{\ell^2(\ell+k_1)^2(\ell+k_{12})^2(\ell-k_4)^2}\,, \tag{3.7.18}$$

which indeed matches the result from the known result, and that derived from the BCFW recursion in 3.3.1 up to a normalisation.

Five particles. For five particles we now expect there to be pentagons and massive boxes. Since there are no massive triangles and bubbles, and that all numerators are defined cyclically

$$\mathfrak{n}^{(1)}_{\rho(i+1)\cdots\rho(n)\,1\cdots\rho(i)} := \mathfrak{n}^{(1)}_{1\,\rho(2)\cdots\rho(n)}\,, \qquad \mathfrak{n}^{(1)}_{1\,A_2} = \mathfrak{n}^{(1)}_{1\,A_2\,A_3} = 0\,, \tag{3.7.19}$$

all of the numerators can actually be related to the pentagon numerator $\mathfrak{n}^{(1)}_{12345}$ and massive box numerators for the ordering (12345). For example, $\mathfrak{n}^{(1)}_{43512} = \mathfrak{n}^{(1)}_{12435} = \mathfrak{n}^{(1)}_{12345} - \mathfrak{n}^{(1)}_{12[34]5}$. Furthermore, boxes with massive corners [12] and [51] vanish by definition of the numerators. Collecting the terms according to the linearly independent numerators, we get

$$\mathcal{I}^{(1)}_{\text{MHV}} = N^{(1)}_{12345}\sum_{\rho\in S_5}\frac{1}{(+\rho-)} - N^{(1)}_{1[23]45}\sum_{\substack{\alpha\in S_3(145)\\ \rho\in\alpha\sqcup\{3,2\}}}\frac{1}{(+\rho-)} - N^{(1)}_{12[34]5}\sum_{\substack{\alpha\in S_3(125)\\ \rho\in\alpha\sqcup\{4,3\}}}\frac{1}{(+\rho-)} - N^{(1)}_{123[45]}\sum_{\substack{\alpha\in S_3(123)\\ \rho\in\alpha\sqcup\{5,4\}}}\frac{1}{(+\rho-)}\,,$$

where $\sqcup\!\sqcup$ denotes the shuffle product. To write this in a more recognisable way we can use the KK relations for Parke-Taylor factors,

$$\frac{1}{(+\,\alpha\,n\,\beta)} = (-1)^{|\beta|}\sum_{\rho\in\alpha\sqcup\!\sqcup\beta^T}\frac{1}{(+\,\rho\,n)} \tag{3.7.20}$$

such that for example

$$\begin{aligned}\sum_{\substack{\alpha\in S_3(123)\\ \rho\in\alpha\sqcup\{5,4\}}}\frac{1}{(+\,\rho\,-)} &= \sum_{\alpha\in S_3(123)}\frac{1}{(+\,\alpha\,-\,45)} = \frac{\sigma_{-+}}{\sigma_{-4}\sigma_{45}\sigma_{5+}}\sum_{\alpha\in S_3(123)}\frac{1}{(+\,\alpha\,-)}\\ &= -\frac{1}{\sigma^2_{+-}}\frac{\sigma_{-+}}{\sigma_{-4}\sigma_{45}\sigma_{5+}}\prod_{i\neq 4,5}\frac{\sigma_{-+}}{\sigma_{+i}\sigma_{i-}}\,.\end{aligned} \tag{3.7.21}$$

Applying this to each term in the MHV integrand results in

$$\begin{aligned}\mathcal{I}^{(1)}_{\text{MHV}} &= N^{(1)}_{12345}\sum_{\rho\in S_5}\frac{1}{(+\rho-)} + N_{1[23]45}\left(\frac{1}{\sigma^2_{+-}}\frac{\sigma_{-+}}{\sigma_{-2}\sigma_{23}\sigma_{3+}}\prod_{i\neq 2,3}\frac{\sigma_{-+}}{\sigma_{+i}\sigma_{i-}}\right)\\ &+N^{(1)}_{12[34]5}\left(\frac{1}{\sigma^2_{+-}}\frac{\sigma_{-+}}{\sigma_{-3}\sigma_{34}\sigma_{4+}}\prod_{i\neq 3,4}\frac{\sigma_{-+}}{\sigma_{+i}\sigma_{i-}}\right) + N^{(1)}_{123[45]}\left(\frac{1}{\sigma^2_{+-}}\frac{\sigma_{-+}}{\sigma_{-4}\sigma_{45}\sigma_{5+}}\prod_{i\neq 4,5}\frac{\sigma_{-+}}{\sigma_{+i}\sigma_{i-}}\right)\,.\end{aligned} \tag{3.7.22}$$

In this form we can explicitly see that each numerator is coupled with the worldsheet structure that will result in the relevant diagram after integration. Explicitly, using the results

of (3.7.6) and (3.7.8) it is easy to see that it gives the correct five-point expression,

$$\mathfrak{I}^{(1)}_{\text{SYM-MHV}}(12345) = \frac{N_{12345}}{\ell^2(\ell+k_1)^2(\ell+k_{12})^2(\ell+k_{123})^2(\ell-k_5)^2} + \frac{N_{1[23]45}}{s_{23}\,\ell^2(\ell+k_1)^2(\ell+k_{123})^2(\ell-k_5)^2} + \frac{N_{12[34]5}}{s_{34}\,\ell^2(\ell+k_1)^2(\ell+k_{12})^2(\ell-k_5)^2} + \frac{N_{123[45]}}{s_{45}\,\ell^2(\ell+k_1)^2(\ell+k_{12})^2(\ell+k_{123})^2}\,,$$

matching (3.2.12b) after using the definitions of the numerators $N^{(1)}_\rho$.

3.7.4 On constructions, proofs and extensions

Here we would like to make remarks regarding proofs of the modified worldsheet formulae, and the possibility of extending this procedure to other theories, either in different dimensions or with less supersymmetry.

Firstly, let us remind the reader that the ℓ^2-deformed scattering equations may have a natural interpretation as arising from a choice of scattering equations on the torus. This proposal however relies on the worldsheet integrand retaining a pole only on the non-separating degeneration (as well as the other scattering equations). This is essential for the global residue theorem to work as intended, and supposing this occurs the integrand will in principle take a different form after the degeneration. Moreover, the Yang-Mills formulae on the nodal sphere are actually inferred from those of type-II supergravity, by notion of the colour-kinematics duality, but this is inherently a non-planar theory, so it is expected in general that different deformations would be required to achieve the correct integrand; more on this in the next section.

This being said, one could seek a construction for the modified worldsheet formulae on the nodal sphere directly. Using the new scattering equations, one could attempt to construct the worldsheet integrands on the principle that the resulting loop expression satisfy the BCFW recursion presented in previous sections. However, this seems to be an arduous process, and it may not be easy to recognise structures on the worldsheet [1].

However, we note that the MHV integrand of (3.7.12) can been proven to arbitrary multiplicity, using our BCFW recursion formulae. We point the interested reader to [1] where this proof is rigorously presented. In the scattering equation formalism, applying the recursion at first seems peculiar, since only the pole from ℓ^2 appears manifestly in the worldsheet formulae. The only other poles in the worldsheet formulae arise when points on the Riemann surface begin to coalesce (i.e., the boundary of the moduli space), but luckily the scattering equations relate these to the kinematic poles resulting from the moduli space integration. The proof thus relies heavily on the scattering equations.

Finally, let us discuss the possibility of extending this procedure to more generic theories. In this respect there are two glaring issues, neither of which appeared for the MHV proposal.

(1) **Diagrams with massive 1-n corners.**

Generic theories will contain Feynman diagrams that do not typically result from the worldsheet formulae. This is because of our choice in the planar theory to assign the loop-momentum to lie between particles n and 1. As mentioned in section 3.7, this choice dictates the modifications required to obtain formulae with quadratic propagators, both with the choice of deforming the scattering equations, and with which Parke-Taylor factor to keep in the cyclic sum. As a result, the moduli space integrals only give trivalent diagrams which reflect this choice; with the $1/\ell^2$ factor playing a

passive role, this means diagrams with n-1 corners do not naturally arise from the worldsheet integrations. In the MHV case, the loop-integrand admitted a representation which prohibited these diagrams from appearing in the first place, due to their kinematic numerators being 0. Of course, then this will not be an issue for any theory admitting a similar representation, but this is generically not the case. We expect that a further modification will resolve this issue.

(2) **Singular solutions.**

Another cause for concern are the singular solutions to the scattering equations, occurring when $\sigma_{+-} \to 0$. On the worldsheet these correspond to tadpole-like geometries. For the supersymmetric theories derived from the type-II formula on the torus, it is known that these do not contribute [106]. This consequently extends to the MHV case, which can be obtained from the aforementioned theory via dimensional reduction; this has also been proved using the ℓ^2-deformed scattering equations in [1]. For more generic theories however, such as pure Yang-Mills or the biadjoint scalar, they do tend to contribute. In the usual one-loop formalism with linear propagators, they could be shown to be associated with scaleless integrals, which subsequently integrate to zero [106]; in this sense the singular solutions to the usual one-loop scattering equations were well-understood. However, in this formalism with quadratic propagators it is less clear what occurs, and more study is required to understand the role of the singular solutions.

3.7.5 Non-planar theories

In this section we will discuss a natural extension of the worldsheet formulae discussed in the previous sections to the non-planar case. Since only the MHV integrand has been proved [1], we will only focus on theories utilising this structure. This of course includes the relevant sector of $\mathcal{N} = 8$ supergravity, as a result of its close connection with the former through the double copy.

The idea is based on the non-planar BCFW proposal, given in section 3.6. There we gave an instinctive way of applying separate BCFW shifts to different planar-like subsectors of the non-planar integrand. This reasoning can be applied of course also to the worldsheet formulae, where the planar-like subsectors are easily extracted by isolating Parke-Taylor factors with the relevant ordering. Again, this is a legitimate thing to do if (at least) one of the half-integrands is written in a Parke-Taylor decomposition.

Let us recall the colour-ordered MHV integrand for convenience. In the notation we will present it is given by

$$\mathfrak{I}^{(1)}_{\text{SYM-MHV}}(12\dots n) = \frac{1}{\ell^2}\int_{\mathfrak{M}_{0,n+2}} d\mu_n^{\ell^2\text{-def-}\{1,n\}}\, \mathcal{I}^{(1)}_{\text{MHV}}\, \frac{1}{(+12\cdots n-)}\,. \tag{3.7.23}$$

The notation $\{1, n\}$ in the measure signifies that the deformation of the scattering equations is associated with particles 1 and n, as in (3.7.3). Precisely, the modifications given by the deformed scattering equations and choice of colour factor to isolate were based on the planar case in which the loop momentum resided between particles 1 and n. This resulted in integrands with the ordering prescribed by the colour factor, and quadratic propagators accordingly. Whilst the modification depends on the planar colour-ordered integrand under consideration, the full integrand (including non-planar contributions) can be written in terms

of its planar subsectors as in (3.6.4),

$$\mathfrak{I}^{(1)}_{\text{SYM-MHV}} = \sum_{\rho\in S_{n-1}/\mathcal{R}} c^{(1)}(1,\rho(1),\cdots,\rho(n))\,\mathfrak{I}^{(1)}_{\text{SYM-MHV}}(1,\rho(1),\cdots,\rho(n)) \tag{3.7.24}$$

where $c^{(1)}$ was defined in (3.6.5). In comparison to (3.6.4) we have decided to fix particle 1 so the sum runs over S_{n-1}, on which the reflection $\mathcal{R}$ acts. This is related to the definition of the numerators having particle 1 directly attached to the loop; as mentioned in section 3.6.2, even in the non-planar case we can always choose the loop momentum to reside before particle 1. In each term of (3.7.24), it is understood that the loop momentum is positioned between particles $\rho(n)$ and 1. This representation of the non-planar integrand allows a straightforward extension to supergravity, as in (3.6.7),

$$\mathfrak{I}^{(1)}_{\text{sugra-MHV}} = \sum_{\rho\in S_{n-1}/\mathcal{R}} \tilde{N}^{(1)}(1,\rho(1),\cdots,\rho(n))\,\mathfrak{I}^{(1)}_{\text{SYM-MHV}}(1,\rho(1),\cdots,\rho(n))\,. \tag{3.7.25}$$

The tilde'd BCJ numerators $\tilde{N}^{(1)}$ follow directly from (3.7.14). Note that the $\delta^{(8)}(\tilde{Q})$ combines with the $\delta^{(8)}(Q)$ to give the factorisation of the supermomentum conserving delta function $\delta^{(16)}(Q)$ in supergravity. Now we have expressed the non-planar integrands in terms of their planar subsectors, we can modify each term as we did in the planar case accordingly,

$$\boxed{\mathfrak{I}^{(1)}_{n,\,\text{SYM-MHV}} = \frac{1}{\ell^2}\sum_{\rho\in S_{n-1}/\mathcal{R}}\int_{\mathfrak{M}_{0,n+2}} d\mu_n^{\ell^2\text{-def-}\{1,\rho(n)\}}\,\mathcal{I}^{(1)}_{\text{MHV}}\,\frac{c^{(1)}\big(1,\rho(2),\cdots,\rho(n)\big)}{\big(+\,1\,\rho(2)\ldots\rho(n)\,-\,\big)}\,.} \tag{3.7.26}$$

for $\mathcal{N}=4$ super Yang-Mills, and

$$\boxed{\mathfrak{I}^{(1)}_{n,\,\text{sugra-MHV}} = \frac{1}{\ell^2}\sum_{\rho\in S_{n-1}/\mathcal{R}}\int_{\mathfrak{M}_{0,n+2}} d\mu_n^{\ell^2\text{-def-}\{1,\rho(n)\}}\,\mathcal{I}^{(1)}_{\text{MHV}}\,\frac{\tilde{N}^{(1)}_{\text{MHV}}\big(1,\rho(2),\cdots,\rho(n)\big)}{\big(+\,1\,\rho(2)\ldots\rho(n)\,-\,\big)}} \tag{3.7.27}$$

for $\mathcal{N}=8$ supergravity. The measure in each term now enforces different scattering equations,

$$d\mu_n^{\ell^2\text{-def-}\{i,j\}} := \frac{d^{n+2}\sigma}{\text{vol}\,\text{SL}(2,\mathbb{C})}\prod_{a=1}^{n+2}{}'\bar{\delta}\left(\mathcal{E}_a\,\middle|\,\begin{smallmatrix}2\ell\cdot k_i\mapsto+(\ell+k_i)^2\\ 2\ell\cdot k_j\mapsto-(\ell-k_j)^2\end{smallmatrix}\right)\,, \tag{3.7.28}$$

according to the ordering determined by ρ. In complete analogy with the non-planar BCFW story, the sum over $S_{n-1}/\mathcal{R}$ dictates that only $n-1$ sets of scattering equations are required to obtain the full integrand, associated to the combinations of $\{1,\rho(n)\}$. This is because the BCFW shifts and deformed scattering equations work to achieve the same goal, and are both determined by the choice of ordering. In this sense, they are in one-to-one correspondence with each other. We could have also expressed (3.7.26) and (3.7.27) as

$$\mathfrak{I}^{(1)}_{n,\text{SYM-MHV}} = \frac{1}{2\ell^2}\sum_{i=2}^{n}\int_{\mathfrak{M}_{0,n+2}} d\mu_n^{\ell^2\text{-def-}\{1,i\}}\,\mathcal{I}^{(1)}_{\text{MHV}}\sum_{\rho\in S_{n-2}}\frac{c^{(1)}(1,\rho(1),\cdots,\rho(n-1),i))}{(+1\rho(2)\cdots\rho(n-1)i-)}\,, \tag{3.7.29}$$

$$\mathfrak{I}^{(1)}_{n,\text{sugra-MHV}} = \frac{1}{2\ell^2}\sum_{i=2}^{n}\int_{\mathfrak{M}_{0,n+2}} d\mu_n^{\ell^2\text{-def-}\{1,i\}}\,\mathcal{I}^{(1)}_{\text{MHV}}\sum_{\rho\in S_{n-2}}\frac{\tilde{N}^{(1)}(1,\rho(1),\cdots,\rho(n-1),i))}{(+1\rho(2)\cdots\rho(n-1)i-)}\,, \tag{3.7.30}$$

to separate out these $n-1$ sets scattering equations. In the above, the factor of $1/2$ now accounts for the reflections.

We remark that for generic theories, the issues presented in the last section still apply. As mentioned there though, these subtleties are not present for the proposals given above for $\mathcal{N}=4$ super Yang-Mills and $\mathcal{N}=8$ supergravity. Their viability should follow directly from the proof given in [1].

To pick up on another point we also mentioned in the last section, we expect that something similar to this procedure will have to occur on the torus in order to derive expressions for supergravity from first principles, in a manner described near the end of (3.7.1). It would be interesting to see how this would work in practice.

3.8 Discussion

In this chapter we have demonstrated a new formulation of a recursion for one-loop integrands in momentum space, which differ from previous developments [137] by including shifts in the loop-momentum, which make the cancellation of spurious poles clear. Though outstanding work has given results from recursion to all loop orders using momentum-twistors [129], the integrand recursion we have presented here is valid in any number of dimensions and extend beyond the planar limit. We demonstrated the practical use of the recursion via a number of non-trivial examples. A central feature of the recursion was the forward-limit, which is also how one may interpret results coming from worldsheet formulae at loop-level. This interpretation is due to the form of the scattering equations at one-loop. We therefore went on to propose new scattering equations which give quadratic propagators, which we call the ℓ^2-deformed scattering equations. These are to be used with new worldsheet formulae that are specially adapted to these scattering equations, providing the correct number of Feynman diagrams in any one calculation. Together, these provide worldsheet formulae for one-loop integrand expressions more akin to conventional field theory, which may therefore be integrated using standard techniques. The integrand recursion as well as the new scattering equations are best suited to planar theories, but in either case we discussed how they may be applied to the non-planar case.

We would like to refer the interested reader to [1] where more details are presented. On the topic of BCFW recursion these include the connections with previous work on BCFW at one-loop: the connection to on-shell diagrams [129, 130] and momentum-twistors, and previous work on integrand recursions in momentum space [137]. Regarding the new worldsheet formulae, a rigorous proof of the MHV integrand (3.7.12) is given, as well as details comparing with the "double forward-limit" scattering equations of [117–119].

Given the vast study into these two topics, there are many avenues for further investigation. The two most common (and natural) questions arise for both formalisms for example, which are: what the extension to other theories will look like, and how to extend this to higher loops. The latter would be particularly interesting for the BCFW recursion, as it may point to an all-loop recursion in momentum space in general dimension, including for non-planar sectors. The former is of more concern for the worldsheet formulae, specifically what the integrands will look like beyond the MHV sector, for $D>4$, and for non-supersymmetric theories. The challenges in this include handling tadpole-like worldsheet geometries, associated with singular solutions, which are typically involved for generic theories. Another important topic we have already discussed in section 3.7.4 would be the origin of these scattering equations from the point of view of the genus-one worldsheet. It would be interesting

to see what happens starting from the torus, and if the formulae for $\mathcal{N} = 8$ supergravity we presented here can therefore be derived from first principles. Worldsheet formulae for other theories would have to be inferred through the double copy, since there is no known expression on the torus for e.g. super Yang-Mills. More importantly however, a derivation from the torus is likely to instruct us how to get worldsheet formulae with the above extensions (beyond the MHV sector, for $D > 4$, and for non-supersymmetric theories). Finally, it would be hopeful that these formalisms could give insights into the connection between field theory and typical string theory, as well as the more geometric interpretations involving the amplituhedron [125], the associahedron [126], and other polytope constructions [160, 161] of the S-matrix.

Chapter 4

Two-loop formulae from colour-kinematics duality and the forward-limit

One of the most fruitful developments in scattering amplitudes of recent times has been the loop-level conjecture of BCJ [12]. This powerful mechanism has allowed computations in $\mathcal{N} = 8$ supergravity to be computed up to five loops [12, 162–166], and studies of the ultraviolet behaviour of this theory [167–170] also. Solving the problem amounts to finding the BCJ numerators of the theory. At loop-level this can be quite challenging for more generic theories. As we have seen in chapter 1, at tree-level worldsheet formulae can lead directly to the BCJ representation of scattering amplitudes. At loop-level however, the difference in their representations (concerning the linear propagators) generally preclude a similar relation. Whilst the kinematic numerators of BCJ are designed for quadratic propagators, at loop-level kinematic numerators from the worldsheet theory work in conjunction with linear-type propagators. As mentioned in section 2.7, the one-loop worldsheet formulae appears similar to a forward-limit of its tree-level counterpart, reminiscent of the Feynman tree theorem [171–173]. This similarity can in fact be made concrete, allowing loop-level kinematic numerators to be directly computable from tree-level.

In this chapter we will review this idea at tree-level and one-loop and see how in each case a representation of the amplitude manifesting the colour-kinematics duality arises naturally. This will be done in the context of non-supersymmetric theories, particularly NS-NS gravity and Yang-Mills, from which one can straightforwardly obtain results for the scattering in the pure theories, i.e. with just gravitons and gluons respectively. We will then use the same idea at two-loops to obtain non-supersymmetric formulae for the two-loop integrand of these theories. The naive attempt will require a slight modification, which we will discuss and use to give a final proposal for these two-loop formulae, again exhibiting the colour-kinematics duality. Furthermore, we will study the case of supersymmetric amplitudes at two-loops following from studies of the genus-two ambitwistor string [51] and relate it to the previous results. This will in turn give an insight into the origins of the modification required for the non-supersymmetric theories from the point of view of the genus-two ambitwistor string.

4.1 Stratagem at tree-level and one-loop

Let us recall how one obtains expressions for amplitudes at tree-level and one-loop using the scattering equations. An n-point tree-level amplitude for massless particles can be written elegantly as the integral over the moduli space of an n-punctured sphere,

$$\mathcal{A}_n^{(0)} = \int_{\mathfrak{M}_{0,n}} d\mu_n^{(0)}\, \mathcal{I}^{(0)} \qquad\qquad d\mu_n^{(0)} := \frac{d^n\sigma}{\text{vol SL}(2,\mathbb{C})} \prod_{i=1}^{n}{}' \bar{\delta}(\mathcal{E}_i^{(0)}) \tag{4.1.1}$$

The CHY framework naturally exemplifies the colour-kinematics duality between double copy theories through their CHY integrand $\mathcal{I}^{(0)}$. The relevant ones we will be considering here are Yang-Mills and gravity, whose tree-level CHY integrands can be factored accordingly,

$$\mathcal{I}_{\text{YM}}^{(0)} = \mathcal{I}_{\text{kin}}^{(0)}\, \mathcal{I}_{\text{SU}(N)}^{(0)} \qquad\qquad \mathcal{I}_{\text{grav}}^{(0)} = \mathcal{I}_{\text{kin}}^{(0)}\, \tilde{\mathcal{I}}_{\text{kin}}^{(0)}. \tag{4.1.2}$$

As explained in section 1.4, the ingredients to these are traditionally expressed as

$$\mathcal{I}_{\text{kin}}^{(0)} = \text{Pf}'(M) = \frac{(-1)^{ij}}{\sigma_{ij}} \text{Pf}(M_{ij}^{ij})\,, \quad \mathcal{I}_{\text{SU}(N)}^{(0)} = \sum_{\rho\in S_n/\mathbb{Z}_n} \frac{\text{Tr}(T^{a_{\rho(1)}} T^{a_{\rho(2)}} \cdots T^{a_{\rho(n)}})}{\sigma_{\rho(1)\rho(2)}\sigma_{\rho(2)\rho(3)}\cdots\sigma_{\rho(n)\rho(1)}} \tag{4.1.3}$$

where M_{ij}^{ij} is the tree-level matrix defined in (1.1.8) with the rows and columns $1 \leq i < j \leq n$ removed, and the T^{a_i} is the SU(N) generator associated with the colour degrees of freedom for the i'th particle. The tree-level scattering equations, which we repeat here for convenience,

$$\mathcal{E}_i = \sum_{j\neq i} \frac{k_i\cdot k_j}{\sigma_{ij}} = 0, \tag{4.1.4}$$

allow us to translate the CHY integrand (4.1.1) directly into the BCJ representation of these theories. In fact, many techniques developed in this formalism, has shown this to be possible without actually solving the scattering equations [39,52,71,72,79,80]. For example, it is known that the 'kinematic half-integrand' $\mathcal{I}_{\text{kin}}^{(0)}$ can be expressed on the support of the scattering equations as [52,71]

$$\mathcal{I}_{\text{kin}}^{(0)} = \text{Pf}'(M) \overset{\mathcal{E}_i^{(0)}=0}{=} \sum_{\rho\in S_{n-2}} \frac{N^{(0)}(1,\rho(2),\cdots,\rho(n-1),n)}{\sigma_{1\rho(2)}\sigma_{\rho(2)\rho(3)}\cdots\sigma_{\rho(n-1)n}\sigma_{n1}} \tag{4.1.5}$$

where the numerators $N^{(0)}$ can be calculated explicitly through an algorithm derived in [52] and presented in section 1.3. They do not depend on the marked points σ_i and are simply polynomials in the kinematic data $\{\epsilon_i, k_i\}$; the half-integrand is thus expressed in terms of a KK basis. In the above, the particles 1 and n have been chosen to be fixed, but this choice is arbitrary[1]. The colour factor $\mathcal{I}_{\text{SU}(N)}^{(0)}$ can also be written in a similar manner, by expressing it in a Del Duca-Dixon-Maltoni (DDM) basis [73],

$$\mathcal{I}_{\text{SU}(N)}^{(0)} = \sum_{\rho\in S_{n-2}} \frac{c^{(0)}(1,\rho(2),\cdots,\rho(n-1),n)}{\sigma_{1\rho(2)}\sigma_{\rho(2)\rho(3)}\cdots\sigma_{\rho(n-1)n}\sigma_{n1}}. \tag{4.1.6}$$

[1]Recall that this choice is related to the rows and columns i and j one decides to remove in the reduced Pfaffian.

where we here also have the freedom to fix two particles, which we choose again to be 1 and n. Writing the colour factor this way is most natural from the point of view of the BCJ double copy, where they are written in terms of the structure constants of the theory,

$$c^{(0)}(1,\rho(2),\cdots,\rho(n-1),n) = f^{a_1 a_{\rho(2)} b_1} f^{b_1 a_{\rho(3)} b_2} \cdots f^{b_{n-2} a_{\rho(n-1)} a_n}. \tag{4.1.7}$$

Both the numerators (4.1.5) and colour factors (4.1.6) can be associated with half-ladder diagrams which are determined by the specific ordering ρ, see figure 1.4. The endpoints of the half-ladders correspond in our case to the choice of fixing particle 1 and n in (4.1.5) and (4.1.6), though we recount that this choice is arbitrary.

After substituting (4.1.5) and (4.1.6) into the CHY expression for the tree-level amplitude (4.1.1), all dependence on the marked points resides in the Parke-Taylor factors, and one can use the integration rules of [39] to evaluate the moduli space integrals without having to solve the scattering equations directly. The result of the integration will give a set of propagators with coefficient ± 1, which will be such that each term corresponds to a trivalent graph whose colour factor and kinematic numerator is, by construction, obtainable from those of the master diagrams. For Yang-Mills the result can then be stated as[2]

$$\mathcal{A}^{(0)}_{\text{YM}} = \sum_{a\in\Gamma_n} \frac{N_a^{(0)} c_a^{(0)}}{D_a} \tag{4.1.8}$$

With Γ_n being the set of all trivalent diagrams and D_a are the set of (inverse) propagators specific for each diagram. Thus, the tree-level BCJ representation of Yang-Mills scattering amplitudes follows directly from the scattering equation formalism. Importantly, the methodology above works at any multiplicity and does not require solving the scattering equations explicitly, which is known to be quite a difficult task.

In the case of gravity, one simply uses (instead of the SU(N) integrand of (4.1.6)) another another copy of the kinematic integrand $\tilde{\mathcal{I}}^{(0)}_{\text{kin}}$ from (4.1.5). Using the same techniques described above simply yields

$$\mathcal{A}^{(0)}_{\text{grav}} = \sum_{a\in\Gamma_n} \frac{N_a^{(0)} \tilde{N}_a^{(0)}}{D_a}, \tag{4.1.9}$$

where $\tilde{N}_a^{(0)} = N_a^{(0)}(\epsilon \to \tilde{\epsilon})$. The product of polarisations ϵ and $\tilde{\epsilon}$ are meant to be seen as the factorisation of polarisation tensors $\epsilon_{\mu\nu} = \epsilon_\mu \tilde{\epsilon}_\nu$ corresponding to the massless states of NS-NS gravity; that is, the graviton, the dilaton and the B-field. From previous discussions the scattering of gravitons is obtained by considering appropriate combinations of polarisation vectors for each state such that their product forms a symmetric traceless tensor.

4.1.1 One-loop: integrands

The known extension of the CHY formalism applies to computing the loop-integrand for a theory. As mentioned in section 2.5 it is based on the ambitwistor string first considered at genus-one in [50] and refined in [103, 104]. Naturally, it follows directly from utilising the genus-one scattering equations, formally defined on the torus. The fundamental difference with respect to tree-level (or genus-0) is the presence of one 'modular' scattering equation

[2] We change conventions here slightly by not including the factor $(-1)^{n+1}$ in the expressions. In practice of course this isn't significant since the amplitude is only defined up to a phase.

which, through a residue argument, serves to localise the integration over the modular parameter τ to $\tau = i\infty$. In this region the torus degenerates to a nodal sphere, where the two extra 'nodes' are punctures associated to states with back-to-back momenta $\pm\ell_\mu$. This momentum ℓ_μ arises as the zero-mode of the meromorphic one-form $P_\mu(\sigma)$ at genus-one and is consequently integrated over in the amplitude, allowing us to recognise it formally as the loop-momentum. This residue argument reduces the moduli space from $\mathfrak{M}_{1,n}$ to its maximal non-separating boundary divisor $\mathfrak{D}_{1,n}^{\text{max}} \cong \mathfrak{M}_{0,n+2}$ and the resulting formulae are obtained on the $(n+2)$-punctured Riemann sphere, similar to the tree-level case.

In this manner, one-loop amplitudes for Yang-Mills can be written in a CHY form as

$$\mathcal{A}^{(1)}_{\text{YM}} = \int \frac{d^D\ell}{\ell^2} \int_{\mathfrak{M}_{0,n+2}} d\mu^{(1)}_{n+2}\, \mathcal{I}^{(1)}_{\text{kin}}\, \mathcal{I}^{(1)}_{\text{SU}(N)}, \tag{4.1.10}$$

and gravity amplitudes as

$$\mathcal{A}^{(1)}_{\text{grav}} = \int \frac{d^D\ell}{\ell^2} \int_{\mathfrak{M}_{0,n+2}} d\mu^{(1)}_{n+2}\, \mathcal{I}^{(1)}_{\text{kin}}\, \tilde{\mathcal{I}}^{(1)}_{\text{kin}}. \tag{4.1.11}$$

The CHY integrals in the loop integrands are related to $n+2$ punctures, each associated with an on-shell momentum state. Of these, n correspond to the external insertions $\{\sigma_i, k_i\}$, and two are associated with the loop insertions $\{\sigma_\pm, \pm\ell\}$. The notion of computing n-point one loop-integrands by considering $(n+2)$-tree amplitudes with the two extra states having back-to-back momenta is reminiscent of the forward-limit of field theory. It is not surprising then that one can construct the various ingredients of the integrands above by considering a null version of the loop momentum L such that

$$L^2 = 0, \qquad L\cdot k_i = \ell\cdot k_i, \qquad L\cdot\epsilon_i = \ell\cdot\epsilon_i. \tag{4.1.12}$$

One can interpret L is effectively being a higher-dimensional extension of ℓ, in which it is null only in higher-dimensions. By using L in the integrand, the analogue with the $(n+2)$-point tree amplitude becomes exact. Indeed, such constructions of one-loop integrands in the CHY framework was already considered in [84] after the successes of the one-loop ambitwistor string [104].

The universal measure appearing in (4.1.10) and (4.1.11) can then be defined as

$$d\mu^{(1)}_{n+2} \equiv \frac{d^{n+2}\sigma}{\text{vol SL}(2,\mathbb{C})} \prod_a{}' \bar{\delta}(\mathcal{E}^{(1)}_a) \tag{4.1.13}$$

where $a = \{i, \pm\}$ and $\mathcal{E}^{(1)}_i$ are the one-loop scattering equations

$$\mathcal{E}^{(1)}_i = \frac{\ell\cdot k_i}{\sigma_{+i}} - \frac{\ell\cdot k_i}{\sigma_{-i}} + \sum_{j\neq i}\frac{k_i\cdot k_j}{\sigma_{ij}}, \qquad \mathcal{E}^{(1)}_\pm = \pm\sum_i \frac{\ell\cdot k_i}{\sigma_{\pm i}}. \tag{4.1.14}$$

That these do not depend on ℓ^2 reinforces the idea of utilising the use of a null L and interpreting these equations as arising from a forward-limit. In fact, the authors of [84] arrived at the above expressions by considering the forward-limit of the massive scattering equations. Their study also derives the nature of the singular solutions associated with the one-loop scattering equations, which we discussed in section 2.5.

The CHY half-integrands of (4.1.10) and (4.1.11) can also can be described from the interpretation of a forward-limit. The colour factors at one-loop take the same form as at

tree-level except we identify the gauge indices a_+ and a_- associated with the two extra insertions,

$$\mathcal{I}^{(1)}_{\mathrm{SU}(N)}(\{a_i,\sigma_i\},\{\sigma_\pm\}) = \delta^{a_+a_-}\,\mathcal{I}^{(0)}_{\mathrm{SU}(N)}(\{a_i,\sigma_i\},\{a_\pm,\sigma_\pm\}). \tag{4.1.15}$$

Similarly for the kinematic half-integrand we can consider the $(n+2)$-point tree expression, using the null momentum L, and sum over the polarisation states of the extra insertions,

$$\mathcal{I}^{(1)}_{\mathrm{kin}}(\{\epsilon_i,k_i,\sigma_i\},\{\pm\ell,\sigma_\pm\}) = \sum_r \mathcal{I}^{(0)}_{\mathrm{kin}}(\{\epsilon_i,k_i,\sigma_i\},\{\epsilon^r_\pm,\pm L,\sigma_\pm\}). \tag{4.1.16}$$

Since we are directly using the tree-level expressions, this kinematic integrand will be relevant for the scattering of non-supersymmetric states; we will go on to discuss supersymmetry in section 4.3. The sum over polarisation states in (4.1.16) can be performed by substituting an appropriate physical state projector,

$$\sum_r \epsilon^r_{+\,\mu}\epsilon^r_{-\,\nu} = \eta_{\mu\nu} - \frac{L_\mu q_\nu + L_\nu q_\mu}{L\cdot q} =: \Delta_{\mu\nu}, \tag{4.1.17}$$

for a null reference vector q_μ. Note that although L as mentioned above can be interpreted as a higher-dimensional analogue of the D-dimensional ℓ, the completeness relation above still projects down to a $(D-2)$-dimensional subspace, as can be seen from the fact that $\Delta^\mu_\mu = D-2$. The kinematic integrand (4.1.3) can then be written at one-loop by virtue of (4.1.16) as

$$\mathcal{I}^{(1)}_{\mathrm{kin}} = \sum_r \mathrm{Pf}'(M) = \Delta_{\mu\nu}\mathrm{Pf}'(M^{\mu\nu}) \tag{4.1.18}$$

where $M^{\mu\nu}$ is now a $2(n+2)\times 2(n+2)$ CHY Pfaffian matrix with the polarisation states $\epsilon^r_{+\,\mu}$ and $\epsilon^r_{-\,\nu}$ removed. At one-loop, the loop-integrand is gauge invariant and independent of the choice of q if one considers only the regular solutions to the scattering equations, whilst for generic theories only the *amplitude* is gauge-invariant if one also considers the singular solutions [104]. In hindsight then we can anticipate the independence of the amplitude on q, allowing us to use an effective substitution rule when applying the state-projector (4.1.17),

$$V^\mu\Delta_{\mu\nu}W^\nu \;\rightsquigarrow\; V\cdot W\,, \qquad\qquad V,W\in\{k_i,\epsilon_i\}$$

and we have from (4.1.17) that $\Delta_{\mu\nu}L^\nu = 0$. The latter condition essentially follows by construction of the state-projector, as is expected for an on-shell L.

As discussed, the one-loop integrand for gravity (4.1.11) will involve two of the kinematic factors (4.1.18), one with tilde'd polarisation states and one untilde'd polarisation. In this case one applies the state projector (4.1.17) for each copy separately in each

$$\sum_{r,r'} \epsilon^r_{+\,\mu}\epsilon^r_{-\,\nu}\tilde{\epsilon}^{r'}_{+\,\bar\mu}\tilde{\epsilon}^{r'}_{+\,\bar\nu} \equiv \Delta_{\mu\nu}\Delta_{\bar\mu\bar\nu}. \tag{4.1.19}$$

This is quite natural to do from the point of view of the BCJ double copy. Recall that, as we mentioned in the tree-level case, in general the gravity states scattered when utilising the BCJ double copy correspond to the states of NS-NS gravity, where the graviton is coupled with the dilaton and the B-field. By using appropriate combinations of the state-projector (4.1.19) one can choose which states propagate through the loop. For example, in the pure Einstein case (just gravitons) one would use

$$\Delta^{\text{pure-grav}}_{\mu\nu\bar\mu\bar\nu} = \frac{1}{2}(\Delta_{\mu\nu}\Delta_{\bar\mu\bar\nu} + \Delta_{\mu\bar\nu}\Delta_{\bar\mu\nu}) - \frac{1}{D-2}\Delta_{\mu\bar\mu}\Delta_{\nu\bar\nu}, \tag{4.1.20}$$

where the index symmetrisation in the first term eliminates the (antisymmetric) B-field, and the second term will eliminate the dilaton. These can be derived from (4.1.19) by taking the appropriate combinations of the polarisation vectors for the desired states.

4.1.2 One-loop: trivalent diagrams and colour-kinematics duality

Let us now see how the colour-kinematics duality becomes manifest in this set up after performing the CHY integrals. Since the matrix M in (4.1.18) and the scattering equations mirror the tree-level cases when utilising using the null L, we can as before write the kinematic factors as

$$\mathcal{I}^{(1)}_{\text{kin}} \overset{\mathcal{E}^{(1)}_i=0}{=} \sum_{\rho\in S_n} \frac{N^{(1)}(+,\rho(1),\cdots,\rho(n),-)}{\sigma_{+\rho(1)}\sigma_{\rho(1)\rho(2)}\cdots\sigma_{\rho(n)-}\sigma_{-+}} \tag{4.1.21}$$

where the one-loop numerators follow from (4.1.18) and (4.1.16) to be

$$N^{(1)}(\cdots) = \sum_r N^{(0)}(\cdots)\,. \tag{4.1.22}$$

Similarly from (4.1.15) we have that

$$\mathcal{I}^{(1)}_{\text{SU}(N)} = \sum_{\rho\in S_n} \frac{c^{(1)}(+,\rho(1),\cdots,\rho(n),-)}{\sigma_{+\rho(1)}\sigma_{\rho(1)\rho(2)}\cdots\sigma_{\rho(n)-}\sigma_{-+}} \tag{4.1.23}$$

where the one-loop colour factors are now

$$c^{(1)}(\cdots) = \delta^{a_+a_-}\, c^{(0)}(\cdots)\,. \tag{4.1.24}$$

In this way all dependence on the marked points resides in the Parke-Taylor factors, and the moduli space integrations of can be performed using the integration rules of [39] to give a set of propagators for trivalent diagrams, such that the one-loop amplitude for Yang-Mills (4.1.10) and gravity (4.1.11) are expressed as

$$\mathcal{A}^{(1)}_{\text{YM}} = \int \frac{d^D\ell}{\ell^2} \sum_{\text{a}\in\Gamma^{(1)}_{n+2}} \frac{N^{(1)}_{\text{a}} c^{(1)}_{\text{a}}}{D_{\text{a}}}\,, \qquad \mathcal{A}^{(1)}_{\text{grav}} = \int \frac{d^D\ell}{\ell^2} \sum_{\text{a}\in\Gamma^{(1)}_{n+2}} \frac{N^{(1)}_{\text{a}} \tilde{N}^{(1)}_{\text{a}}}{D_{\text{a}}}\,. \tag{4.1.25}$$

The moduli space integrations will provide the propagators with an appropriate sign such that the numerators and colour factors share the same Jacobi identities between certain graphs,

$$c^{(1)}_{\text{a}} + c^{(1)}_{\text{b}} + c^{(1)}_{\text{c}} = 0 \qquad \Rightarrow \qquad N^{(1)}_{\text{a}} + N^{(1)}_{\text{b}} + N^{(1)}_{\text{c}} = 0. \tag{4.1.26}$$

The resulting trivalent diagrams can then be expressed in terms of tree diagrams with the legs $+$ and $-$, associated to the loop, on the endpoints. Diagrams which form 'half-ladders', such as those in figure 4.1 are considered the master diagrams, and their corresponding numerators are considered the master numerators. As at tree-level, the numerators and colour factors for trivalent diagrams which do not directly form half-ladders with endpoints $+$, $-$ are obtained from those of the master diagrams by successive Jacobi identities (4.1.26). An

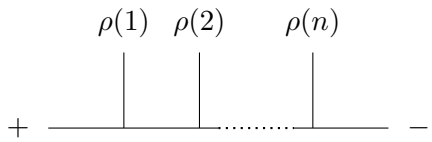

Figure 4.1: The set of one-loop master diagrams are half-ladders, with end-points + and − in our setting associated with the loops.

example of this is given in figure 1.5.

Let us make a few comments and clarifications regarding the interpretation of the one-loop amplitudes in (4.1.25). At first sight they appear to mirror the original conjectured expressions of the BCJ representation of loop amplitudes [12]. Whilst aesthetically true, it is important to note that (4.1.25) is very much different than the original proposal of BCJ.

Firstly, the set $\Gamma^{(1)}_{n+2}$ represents the set of trivalent *tree-level* diagrams, which is interpreted as a loop diagram only after the legs + and − at the endpoints are glued together, making the forward-limit implicit. The superscript on $\Gamma^{(1)}_{n+2}$ is to indicate that we do not include diagrams which, when glued together, form external bubbles and tadpoles. This exclusion actually follows from the result of the moduli space integrals at one-loop, where it can be seen that these diagrams either cancel amongst themselves or integrate to zero in dimensional regularisation [106]. Furthermore, the (inverse) loop propagators appearing inside the $D_{\rm a}$ are *linear* in the loop-momentum, as opposed to those which are *quadratic* in the BCJ conjecture. This can be seen to result from using the null loop-momentum L as part of the forward-limit. An example of this is displayed in figure 4.1, where the relevant set of propagators $1/D_{\rm a}$ has the form

$$\frac{1}{D_{\rm a}} = \frac{1}{\prod_{j=1}^{n-1}(L+K_j)^2} = \frac{1}{\prod_{j=1}^{n-1} 2\ell\cdot K_j + K_j^2}\,, \qquad \text{where} \quad K_j = \sum_{i=1}^{j} k_{\rho(i)}\,.$$

This unorthodox representation of the loop integrand is, as we have seen, a novel feature of utilising the scattering equation formalism in its usual setting.

Secondly, we recount that the kinematic numerators in (4.1.25) follow directly from those at tree-level via the forward-limit procedure. This allows them to be calculated using the same procedure as in [71], which solely relies on the properties of the Pfaffian, gauge invariance, and the scattering equations. Therefore, the master numerators in this formalism can be calculated explicitly to any multiplicity and are valid in any dimension. In contrast, the numerators appearing in the BCJ loop-level conjecture are not in general related to those at tree-level, and much work has gone on to find such a set of numerators. To date, however, it has only been in some cases that a set of BCJ one-loop numerators have been constructed [149, 156, 174–176], though the recent works of [177, 178] has shown to be quite promising.

4.2 Two-loop application

Two-loop extensions of the worldsheet formulae in the scattering equation formalism are naturally provided by studying the ambitwistor string at genus-two. This was rigorously done in [51], where n-point formulae for supergravity were derived from first principles. Also

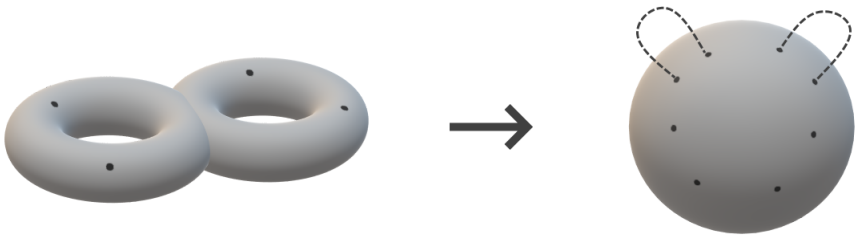

Figure 4.2: The degeneration of the genus-two surface to the bi-nodal sphere.

there, explicit four-point formulae for Yang-Mills and supergravity were extracted, consistent with previous work on the two-loop superstring [179] and the pure-spinor formulation of the ambitwistor string [180].

Here we will straightforwardly apply the strategy presented in the previous section to two-loops, using formulae on a *bi-nodal sphere*. This will be analogous to the one-loop case, but there are additional subtleties that begin at two-loops which make the formalism have different features. Here we will highlight some of these features on the bi-nodal sphere, with some intuition from the genus-two surface, which we will expand upon in the next section.

4.2.1 The two-loop scattering equations

Much like at genus-one, a number of the scattering equations at genus-two localise the integration over the modular parameters, such that the genus-two surface degenerates onto its maximal non-separating boundary divisor, the bi-nodal Riemann sphere[3]. This is done by successively applying residue theorems that effectively pinch the A-cycles on the surface, thereby degenerating it to the nodal sphere; see figure 4.2.

At any genus the (X, P) path integral in the ambitwistor string requires us to solve

$$\bar{\partial} P_\mu(z) = 2\pi i \sum_{i=1}^{n} k_{i\mu}\, \bar{\delta}(z - z_i)\, dz \tag{4.2.1}$$

in the presence of n vertex operators. The zero-mode integration for X as usual provides an overall momentum-conserving delta function. On the support of this, (4.2.1) can be re-written as

$$\bar{\partial} P_\mu(z) = 2\pi i \sum_{i=1}^{n} k_{i\mu}\, [\bar{\delta}(z - z_i) - \bar{\delta}(z - z_*)]\, dz \tag{4.2.2}$$

where z_* is an arbitrary reference point. Noting that $2\pi i \bar{\delta}(z) = \partial(1/z)$, the general solution to this equation can be written as

$$P_\mu(z) = 2\pi i\, \ell^I_\mu\, \omega_I + \sum_{i=1}^{n} k_{i\mu}\, \omega_{i,*}(z). \tag{4.2.3}$$

[3] There is a caveat here. A generic basis of the scattering equations will *not* fully localise the type II amplitude onto the bi-nodal sphere, and contributions from nodal-tori can in general appear. However, it is possible to choose a basis such that the amplitude *is* fully localised on the bi-nodal sphere, as demonstrated in [51].

Here the ω_I are normalised Abelian differentials of the *first* kind, whose integrals around B-cycles determine the period matrix. The $\omega_{i,j}$ are Abelian differentials of the *third* kind[4], which has residues ± 1 as $z \approx z_i, z_j$ respectively. At genus-g there exist g constant holomorphic Abelian differentials[5], given by the ω_I, and so the first term on the RHS of (4.2.3) are to be thought of as the constants of integration. In other words, they parametrise the zero-modes of P.

In the gauge-fixing procedure at genus-two, much like genus-zero and genus-one, enforcing $P^2 = 0$ requires setting its residues at the punctures z_i to zero, $\text{Res}_{z_i} = 0$. This ensures that P^2 is free of simple poles, and essentially provides the scattering equations related to the marked points. On the support of these P^2 can only be a holomorphic quadratic differential, and so setting $P^2 = 0$ requires

$$P^2 = u^{IJ}\omega_I\,\omega_J = 0 \tag{4.2.4}$$

where the u^{IJ} are simply coefficients for the basis of holomorphic quadratic differentials given by $\omega_I\,\omega_J$. The genus-two scattering equations are thus encoded by

$$\begin{aligned} \text{Res}_{z_i} P^2 &= 0\,, & i &= 1, 2, \cdots, n \\ u^{IJ} &= 0\,, & I, J &= 1, 2\,. \end{aligned} \tag{4.2.5}$$

Given that the u^{IJ} are symmetric, these $n + g(g+1)/2 = n + 3$ scattering equations are sufficient to fully localise[6] the genus-two moduli space of dimension $3g + n - 3 = n + 3$. Of these, two will be used in the residue theorem to degenerate the amplitude to the bi-nodal sphere, corresponding to the pinching of two A-cycles or combinations thereof. Heuristically, the pinching of an A-cycle degenerates a genus g surface to a surface of genus $g - 1$ with two extra nodes, so a genus-two surface with n punctures can be degenerated to a bi-nodal Riemann sphere with $n + 4$ punctures via the residue theorem. Thus, the remaining $n + 1 = (n + 4) - 3$ scattering equations are associated to the $n + 4$ punctures modulo the $\text{SL}(2, \mathbb{C})$ transformations of the Riemann sphere.

More specifically, the scattering equations can always be be associated to the residues of a meromorphic quadratic differential. From (4.2.3) and (4.2.4) one notices that $u^{11} = \ell_1^2$ and $u^{22} = \ell_2^2$, where in an abuse of notation we have set $\ell^I = \ell_1, \ell_2$ for $I = 1, 2$ respectively. Such an object at genus-two could therefore be

$$\tilde{\mathfrak{P}}_2 = P^2 - \ell_1^2\,\omega_1^2 - \ell_2^2\,\omega_2^2\,. \tag{4.2.6}$$

Whilst the above quadratic differential indeed only has simple poles, for two-loops (and higher) one is also free to consider

$$\mathfrak{P}_2 = P^2 - \ell_1^2\,\omega_1^2 - \ell_2^2\,\omega_2^2 + u\,\omega_1\,\omega_2 \tag{4.2.7}$$

wherein u is a linear combination of the u^{IJ} of (4.2.5). Having u be a linear combination of the u^{IJ} essentially amounts to choosing a different basis for the scattering equations; indeed, this procedure is necessary at two-loops to ensure the amplitude fully localises on

[4] These objects are standard in the study of higher-genus Riemann surfaces, and their precise definitions can be found in e.g. [51]; for completeness we also give them in appendix A

[5] This follows from the Riemann-Roch theorem, see e.g. [181].

[6] We should point out here that only for genus $g = 2, 3$ do the number of scattering equations match the dimension of the moduli space this way; we also make a comment about this in section 5.1

the bi-nodal sphere [51]. It turns out that a convenient choice at two-loops is to take $u = \alpha(u^{11} + u^{22}) = \alpha(\ell_1^2 + \ell_2^2)$, where $\alpha = \pm 1$ [105]. The choice $\alpha = \pm 1$ is required in order for correct factorisations of the amplitude, and is associated with the loop-momenta ℓ_1 and ℓ_2 being parallel ($\alpha = +1$) or anti-parallel ($\alpha = -1$) in the corresponding two-loop diagrams, as we shall see.

On the nodal sphere the Abelian differentials of the first and third kind become

$$2\pi i\,\omega_I \rightsquigarrow \omega_{I^+I^-}(\sigma) = \frac{(\sigma_{I^+} - \sigma_{I^-})}{(\sigma - \sigma_{I^+})(\sigma - \sigma_{I^-})}\,d\sigma\,, \quad \omega_{i,j} \rightsquigarrow \omega_{i,j}(\sigma) = \frac{(\sigma_i - \sigma_j)}{(\sigma - \sigma_i)(\sigma - \sigma_j)}\,d\sigma\,, \tag{4.2.8}$$

denoting σ as the coordinates on the Riemann sphere. The scattering equations then follow from the residues of the quadratic differential

$$\mathfrak{P}_2(\sigma) = P^2(\sigma) - \ell_1^2\,\omega_{1^+1^-}^2(\sigma) - \ell_2^2\,\omega_{2^+2^-}^2(\sigma) + \alpha(\ell_1^2 + \ell_2^2)\,\omega_{1^+1^-}(\sigma)\,\omega_{2^+2^-}(\sigma) \tag{4.2.9}$$

at the $n+4$ marked points σ_A. The meromorphic differential $P(\sigma)$ in the above formula on the sphere is now

$$P^\mu(\sigma) = \ell_1^\mu\,\omega_{1^+1^-}(\sigma) + \ell_2^\mu\,\omega_{2^+2^-}(\sigma) + \sum_{i=1}^{n} \frac{k_i^\mu}{\sigma - \sigma_i}\,d\sigma \tag{4.2.10}$$

where the dependence on the arbitrary point drops out by momentum conservation. Explicitly the scattering equations are given by

$$\begin{aligned}
\mathcal{E}_i^{(2,\alpha)} &= k_i \cdot \ell_1\;\omega_{1^+1^-}(\sigma_i) + k_i \cdot \ell_2\;\omega_{2^+2^-}(\sigma_i) + \sum_{j\neq i} \frac{k_i \cdot k_j}{\sigma_i - \sigma_j}\,,\\
\pm\mathcal{E}_{1^\pm}^{(2,\alpha)} &= \frac{\alpha}{2}(\ell_1 + \alpha\ell_2)^2\;\omega_{2^+2^-}(\sigma_{1^\pm}) + \sum_i \frac{\ell_1 \cdot k_i}{\sigma_{1^\pm} - \sigma_i}\,,\\
\pm\mathcal{E}_{2^\pm}^{(2,\alpha)} &= \frac{\alpha}{2}(\ell_1 + \alpha\ell_2)^2\;\omega_{1^+1^-}(\sigma_{2^\pm}) + \sum_i \frac{\ell_2 \cdot k_i}{\sigma_{2^\pm} - \sigma_i}\,.
\end{aligned} \tag{4.2.11}$$

Analogously to the one-loop case, discussed in the last section, these equations can be written more clearly by considering null versions of the loop-momenta L_I with $I = 1, 2$, such that

$$\begin{aligned}
&L_I^2 = 0\,, \qquad L_I \cdot k_i \mapsto \ell_I \cdot k_i\,, \qquad L_I \cdot \epsilon_i \mapsto \ell_I \cdot \epsilon_i\,,\\
&L_1 \cdot L_2 \mapsto \frac{\alpha}{2}(\ell_1 + \alpha\ell_2)^2\,.
\end{aligned} \tag{4.2.12}$$

In this way the two-loop scattering equations can be written as $(n+4)$-point tree-level ones, where the $n+4$ null momenta are $\{k_i, +L_1, -L_1, +L_2, -L_2\}$. The resulting loop-integrands will thus have the interpretation as arising from a double-forward-limit of an $n+4$ particle tree amplitude. Whilst this feature will be crucial in understanding how the colour-kinematics duality emerges at two-loops, it will turn out not to be as straightforward for theories without supersymmetry.

Let us make two comments regarding the use of the two-loop scattering equations (4.2.11). Firstly, this formalism will of course share many features with the one-loop case.

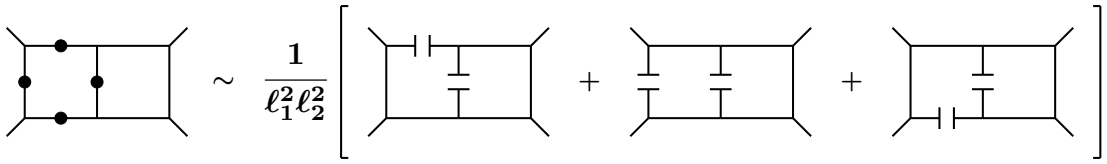

Figure 4.3: One of the ways of decomposing a planar double-box diagram in terms of tree-level diagrams with $n+4$ external legs. The dots on the left part denote three ways of placing one loop momentum (say ℓ_1), which leads to the three diagrams on the right-hand side, whereas the dot in the middle denotes the other loop momentum.

Namely, in comparison to the standard Feynman representation, the loop-integrand will be comprised of many more terms and will contain 'linear-type' loop propagators. However, each term can still be associated with a two-loop diagram, since in the double-forward-limit interpretation these are obtained by gluing the relevant legs of the $(n+4)$-particle tree amplitudes. An example of this is given in figure 4.3, which displays one way how a planar double-box diagram can be decomposed this way. The second diagram has the propagator structure

$$\frac{1}{(2\ell_1\cdot k_2)(\ell_1+\ell_2+k_2)^2(\ell_1+\ell_2+k_2+k_3)^2(\ell_1+\ell_2-k_1)^2(2\ell_1\cdot k_1)} \tag{4.2.13}$$

if we assign the loop momenta as below:

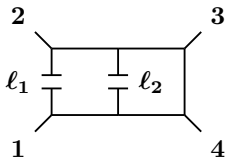

Such a representation can be obtained by performing partial-fraction identities and shifts in the loop momenta, as at one-loop. Notice that from (4.2.12), propagators that involve both ℓ_1 and ℓ_2 appear quadratically,

$$\frac{1}{(L_1+\alpha L_2+K)^2} \quad\mapsto\quad \frac{1}{(\ell_1+\alpha\ell_2+K)^2}\,, \tag{4.2.14}$$

which is a new feature appearing at two-loops with these scattering equations. It is also clear from the above that the choice $\alpha=\pm1$ correspond to parallel/anti-parallel loop-momenta respectively. The consequences of this will be discussed in the next section.

We conclude this section with comments regarding the solutions of the scattering equations (4.2.11). There are three types of solutions, two of which are considered singular. This is true for either set of scattering equations ($\alpha=+1$ or $\alpha=-1$). The nature of the solutions was studied in [105], where it was shown that there are:

- $(n+1)!-4n!+4(n-1)!+6(n-3)!$ regular solutions, with all $\sigma_{1^+},\sigma_{1^-},\sigma_{2^+},\sigma_{2^-}$ distinct,
- $2n((n-1)!-2(n-2)!)$ singular solutions in which $\sigma_{1^+}=\sigma_{1^-}$ *or* $\sigma_{2^+}=\sigma_{2^-}$, and
- $(n-2)^2(n-3)!$ singular solutions in which $\sigma_{1^+}=\sigma_{1^-}$ *and* $\sigma_{2^+}=\sigma_{2^-}$.

The total number does not add up to $(n+1)!$ because some of the solutions do not survive the double forward-limit. This is similar to what occurs at one-loop; see e.g. [84]. Also like the one-loop case, only the regular solutions contribute to amplitudes for supersymmetric theories, whilst for generic theories all solutions should in principle be included into the computation to avoid the presence of unphysical discriminant-like poles.

4.2.2 Two-loop attempt: integrands

In this section we will follow the methodology of section 4.1.1 and attempt to construct two-loop amplitudes utilising the double-forward-limit interpretation. If we are successful, we will have obtained all-multiplicity formulae for the two-loop integrands of Yang-Mills and gravity, in which the colour-kinematics duality is manifest. Moreover, we will give two prescriptions to do this which highlight novel features appearing at two-loops, whose origins follow from the ambitwistor string at genus-two.

Let us recount our position. For two-loops we have $n+4$ punctures corresponding to n external particle insertions and four nodal insertions (two per loop). We also have two sets of scattering equations $\mathcal{E}^{(2,\alpha)}$ corresponding to the choice $\alpha=+1$ or $\alpha=-1$. To treat them on the same footing, we will symmetrise over these two choices in the amplitude. A natural question to ask then is whether the two-loop amplitudes we are considering follow from the following worldsheet formula:

$$\mathcal{A}^{(2)} \stackrel{?}{=} \frac{1}{2}\int \frac{d^D\ell_1\, d^D\ell_2}{\ell_1^2\ell_2^2} \int_{\mathfrak{M}_{0,n+4}} \Big[\, d\mu_{n+4}^{(2,+)}\, \mathcal{I}^{(2,+)} + d\mu_{n+4}^{(2,-)}\, \mathcal{I}^{(2,-)} \,\Big] \tag{4.2.15}$$

with the measures defined as natural extensions of (4.1.13) for each choice of α,

$$d\mu_{n+4}^{(2,\alpha)} \equiv \frac{d^{n+4}\sigma}{\text{vol SL}(2,\mathbb{C})} \prod_a{}' \,\bar{\delta}(\mathcal{E}_a^{(2,\alpha)})\,. \tag{4.2.16}$$

Following the reasoning used for one-loop in section 4.1.1, we can construct the objects above in the spirit of the double-forward-limit. The colour part follows analogously as before; we can utilise the $(n+4)$-point tree-level expression and glue the gauge indices for the loops,

$$\mathcal{I}^{(2)}_{\text{SU}(N)}(\{a_i,\sigma_i\},\{\sigma_{I^\pm}\}) = \delta^{a_1+a_{1^-}}\delta^{a_{2^+}+a_{2^-}}\,\mathcal{I}^{(0)}_{\text{SU}(N)}(\{a_i,\sigma_i\},\{a_{I^\pm},\sigma_{I^\pm}\})\,. \tag{4.2.17}$$

The kinematic factors can be defined likewise; here we take

$$\begin{aligned}\mathcal{I}^{(2,\alpha)}_{\text{kin}}(\{\epsilon_i,k_i,\sigma_i\},\{\pm\ell_I,\sigma_{I^\pm}\}) &= \sum_{r_1,r_2} \mathcal{I}^{(0)}_{\text{kin}}(\{\epsilon_i,k_i,\sigma_i\},\{\epsilon^{r_I}_{I^\pm},\pm L_I,\sigma_\pm\}) \\ &= \sum_{r_1,r_2} \text{Pf}'(M) = \Delta_{1\,\mu_1\nu_1}\Delta_{2\,\mu_2\nu_2}\text{Pf}'(M)^{\mu_1\nu_1\mu_2\nu_2}\end{aligned} \tag{4.2.18}$$

where now we sum over states for both loops, each giving their respective physical state projector according to

$$\sum_{r_I} \epsilon^{r_I}_{I^+\,\mu}\epsilon^{r_I}_{I^-\,\nu} = \eta_{\mu\nu} - \frac{L_{I\mu}q_\nu + L_{I\nu}q_\mu}{L_I\cdot q} =: \Delta_{I\,\mu\nu}. \tag{4.2.19}$$

To clarify what we mean by (4.2.18), first note that M is defined as at tree-level as the $2(n+4)\times 2(n+4)$ matrix,

$$M = \begin{pmatrix} A & -C^T \\ C & B \end{pmatrix}. \tag{4.2.20}$$

The reduced Pfaffian is also defined as before. The object $\mathrm{Pf}'(M)^{\mu_1\nu_1\mu_2\nu_2}$ is interpreted similarly to its one-loop counterpart; explicitly one could write

$$\mathrm{Pf}'(M)_{\mu_1\nu_1\mu_2\nu_2} = \partial_{\epsilon_{1^+}^{\mu_1}} \partial_{\epsilon_{1^-}^{\nu_1}} \partial_{\epsilon_{2^+}^{\mu_2}} \partial_{\epsilon_{2^-}^{\nu_2}} \mathrm{Pf}'(M)\,. \tag{4.2.21}$$

To be more explicit, the elements for the matrix $M^{\mu_1\nu_1\mu_2\nu_2}$ are described below. For the A submatrix,

$$A_{I^+I^-} = 0 \qquad A_{1^\pm 2^+} = \pm\frac{\alpha\,(\ell_1+\alpha\,\ell_2)^2}{2\,\sigma_{1^\pm 2^+}} \qquad A_{1^\pm 2^-} = \mp\frac{\alpha\,(\ell_1+\alpha\,\ell_2)^2}{2\,\sigma_{1^\pm 2^-}}$$
$$A_{I^\pm j} = \pm\frac{\ell_I\cdot k_j}{\sigma_{I^\pm j}} \qquad A_{ij} = \frac{k_i\cdot k_j}{\sigma_{ij}}\,;$$

for the B submatrix,

$$B^{\mu_I\nu_I}_{I^+I^-} = \frac{\eta^{\mu_I\nu_I}}{\sigma_{I^+I^-}} \qquad B^{\mu_I\mu_J}_{I^+J^+} = \frac{\eta^{\mu_I\mu_J}}{\sigma_{I^+J^+}} \qquad B^{\mu_I\nu_J}_{I^+J^-} = \frac{\eta^{\mu_I\nu_J}}{\sigma_{I^+J^-}}$$
$$B^{\mu_I}_{I^+j} = \frac{\epsilon_j^{\mu_I}}{\sigma_{I^+j}} \qquad B^{\nu_I}_{I^-j} = \frac{\epsilon_j^{\nu_I}}{\sigma_{I^-j}} \qquad B_{ij} = \frac{\epsilon_i\cdot\epsilon_j}{\sigma_{ij}}\,;$$

and for the C submatrix,

$$C_{I^+I^-} = 0 \qquad C^{\mu_I}_{I^+J^\pm} = \pm\frac{L_J^{\mu_I}}{\sigma_{I^+J^\pm}} \qquad C^{\mu_I}_{I^+j} = \frac{k_j^{\mu_I}}{\sigma_{I^+j}}$$
$$C^{\nu_I}_{I^-J^\pm} = \pm\frac{L_J^{\nu_I}}{\sigma_{I^-J^\pm}} \qquad C^{\nu_I}_{I^-j} = \frac{k_j^{\nu_I}}{\sigma_{I^-j}}$$
$$C_{iI^\pm} = \pm\frac{\epsilon_i\cdot\ell_I}{\sigma_{iI^\pm}} \qquad C_{ij} = \frac{\epsilon_i\cdot k_j}{\sigma_{ij}} \qquad C_{aa} = -\sum_{b\neq a} C_{ab}\,.$$

Notice the quadratic factor appearing in the A submatrix as a result of the $L_1\cdot L_2$ contractions. It is to be understood in this way that the kinematic integrand implicitly depends on the choice of α. Importantly, it also retains many essential features as at tree-level and one-loop[7], as a result of utilising the null L_I. Furthermore, the arbitrariness of q_μ allows us to avoid its use altogether by using effective substitution rules,

$$\begin{aligned}
&\Delta_{I\mu\nu}\,V^\mu W^\nu\,,\ \Delta_{I\mu}{}^\alpha\Delta_{J\alpha\nu}\,V^\mu W^\nu \quad \rightsquigarrow \quad V\cdot W\,,\\
&\Delta_{I\mu\nu}\,L_J^\mu V^\nu\,,\ \Delta_{I\mu}{}^\alpha\Delta_{J\alpha\nu}\,L_J^\mu V^\nu \quad \rightsquigarrow \quad V\cdot(L_J-L_I)\mapsto V\cdot(\ell_J-\ell_I)\,,\\
&\Delta_{1\mu\nu}\,L_2^\mu L_2^\nu\,,\ \Delta_{2\mu\nu}\,L_1^\mu L_1^\nu\,,\ -\Delta_{1\mu}{}^\alpha\Delta_{2\alpha\nu}\,L_2^\mu L_1^\nu \quad \rightsquigarrow \quad -2\,L_1\cdot L_2\mapsto -\alpha(\ell_1+\alpha\,\ell_2)^2\,,
\end{aligned} \tag{4.2.25}$$

with $\Delta_{I\mu}{}^\mu = \Delta_{1\mu\nu}\,\Delta_2^{\mu\nu} = D-2$. The viability of these substitution rules has been explicitly checked by evaluating the kinematic object (4.2.18) numerically on the solutions to the scattering equations.

[7] These include manifest gauge-invariance, if evaluated on the regular solutions to the two-loop scattering equations.

With the colour and kinematic objects in hand, let us give a proposition for two-loop worldsheet integrand formulae of Yang-Mills and gravity in (4.2.15). We will in fact present two representations of these integrands, each associated with a certain prescription. They are based on the colour-kinematics duality but contain novel features that arise at two-loops, following the genus-two ambitwistor string. We will discuss this point momentarily, but first let us present the following two proposals.

In the first representation, the worldsheet integrands are given by

$$\mathcal{I}^{(2,\alpha)}_{\rm YM} = \xi^{(\alpha)}\, \mathcal{I}^{(2,\alpha)}_{\rm kin}\, \mathcal{I}^{(2)}_{{\rm SU}(N)} \qquad\qquad \mathcal{I}^{(2,\alpha)}_{\rm grav} = \xi^{(\alpha)}\, \mathcal{I}^{(2,\alpha)}_{\rm kin}\, \tilde{\mathcal{I}}^{(2,\alpha)}_{\rm kin} \tag{4.2.26}$$

where the $\xi^{(\alpha)}$ are cross ratios in the nodal points,

$$\xi^{(+)} = \frac{\sigma_{1^+2^-}\sigma_{2^+1^-}}{\sigma_{1^+1^-}\sigma_{2^+2^-}}\,, \qquad\qquad \xi^{(-)} = \frac{\sigma_{1^+2^+}\sigma_{2^-1^-}}{\sigma_{1^+1^-}\sigma_{2^+2^-}} \tag{4.2.27}$$

with the property that

$$\xi^{(+)} + \xi^{(-)} = 1\,. \tag{4.2.28}$$

We will call this the *cross-ratio* prescription.

In the second representation, which we denote by a 'slash', they are given by

$$\mathcal{I}^{(2,\alpha)}_{\rm YM} = \mathcal{I}^{(2,\alpha)}_{\rm kin}\, \mathcal{I}^{(2,\not{\alpha})}_{{\rm SU}(N)} \qquad\qquad \mathcal{I}^{(2,\alpha)}_{\rm grav} = \mathcal{I}^{(2,\alpha)}_{\rm kin}\, \tilde{\mathcal{I}}^{(2,\not{\alpha})}_{\rm kin}\,, \tag{4.2.29}$$

which we call the *slash* prescription. We use $\not{\alpha}$ as opposed to α to denote the following. Consider the two-loop colour object defined in (4.2.17), which follows directly from its $(n+4)$-point tree-level counterpart,

$$\begin{aligned}\mathcal{I}^{(2)}_{{\rm SU}(N)} &= \delta^{a_{1^+}a_{1^-}}\delta^{a_{2^+}a_{2^-}} \sum_{\gamma\in S_{n+2}} \frac{c^{(0)}(1^+,\gamma(1),\gamma(2),\cdots,\gamma(n+2),1^-)}{\sigma_{1^+\gamma(1)}\sigma_{\gamma(1)\gamma(2)}\cdots\sigma_{\gamma(n+2)\,1^-}\sigma_{1^-1^+}} \\ &= \delta^{a_{1^+}a_{1^-}}\delta^{a_{2^+}a_{2^-}} \sum_{\gamma\in S_{n+2}} \frac{f^{a_{1^+}a_{\gamma(1)}b_1} f^{b_1 a_{\gamma(2)} b_2}\cdots f^{b_{n-1}a_{\gamma(n+2)}a_{1^-}}}{\sigma_{1^+\gamma(1)}\sigma_{\gamma(1)\gamma(2)}\cdots\sigma_{\gamma(n+2)\,1^-}\sigma_{1^-1^+}}.\end{aligned} \tag{4.2.30}$$

in terms of the structure constants of the Lie algebra. In comparison to (4.2.30), its 'slashed' version is expressed as

$$\mathcal{I}^{(2,\not{\alpha})}_{{\rm SU}(N)} = \delta^{a_{1^+}a_{1^-}}\delta^{a_{2^+}a_{2^-}} \sum_{\gamma\in S^{(\alpha)}_{n+2}} \frac{f^{a_{1^+}a_{\gamma(1)}b_1} f^{b_1 a_{\gamma(2)} b_2}\cdots f^{b_{n-1}a_{\gamma(n+2)}a_{1^-}}}{\sigma_{1^+\gamma(1)}\sigma_{\gamma(1)\gamma(2)}\cdots\sigma_{\gamma(n+2)\,1^-}\sigma_{1^-1^+}}\,. \tag{4.2.31}$$

The distinction is that in (4.2.31) we consider a restricted set of permutations, denoted by $S^{(\alpha)}_{n+2}$, as opposed to the full set of permutations S_{n+2} in (4.2.30). The set $S^{(\alpha)}_{n+2}$ is defined according to the relative positions of the labels 2^+ and 2^- in the ordering, such that $S^{(+)}_{n+2}$ contains all permutations in which 2^+ appears before 2^-, and $S^{(-)}_{n+2}$ contains all permutations in which 2^- appears before 2^+, i.e.

$$\{\cdots, 2^{\pm}, \cdots, 2^{\mp}, \cdots\} \;\in\; S^{(\pm)}_{n+2}\,.$$

Clearly, $S^{(+)}_{n+2} \cup S^{(-)}_{n+2} = S_{n+2}$, and so

$$\mathcal{I}^{(2)}_{{\rm SU}(N)} = \mathcal{I}^{(2,+)}_{{\rm SU}(N)} + \mathcal{I}^{(2,-)}_{{\rm SU}(N)}\,. \tag{4.2.32}$$

This notion also extends to the kinematic object of (4.2.18). The reduced Pfaffian can be expanded into a KK basis on the support of the scattering equations, just as its one-loop and tree counterpart,

$$\mathcal{I}_{\text{kin}}^{(2,\alpha)} \overset{\mathcal{E}^{(2)}=0}{=} \sum_{\rho\in S_{n+2}} \frac{N^{(2)}(1^+,\rho(1),\cdots,\rho(n+2),1^-)}{\sigma_{1^+\,\rho(1)}\sigma_{\rho(1)\rho(2)}\cdots\sigma_{\rho(n+2)\,1^-}\sigma_{1^-1^+}} \tag{4.2.33}$$

where the two-loop numerators follow from those at tree-level,

$$N^{(2)}(\cdots) = \sum_{r_1,r_2} N^{(0)}(\cdots)\,. \tag{4.2.34}$$

and have no dependence on the marked points. Therefore its slashed version is naturally defined as

$$\mathcal{I}_{\text{kin}}^{(2,\not{\alpha})} \overset{\mathcal{E}^{(2)}=0}{=} \sum_{\rho\in S_{n+2}^{(\alpha)}} \frac{N^{(2)}(1^+,\rho(1),\cdots,\rho(n+2),1^-)}{\sigma_{1^+\,\rho(1)}\sigma_{\rho(1)\rho(2)}\cdots\sigma_{\rho(n+2)\,1^-}\sigma_{1^-1^+}}\,, \tag{4.2.35}$$

which determines the gravity integrand (4.2.29) in the slash prescription.

Both prescriptions have origins from the ambitwistor string at genus-two, where amplitudes for supergravity and super Yang-Mills were studied [51]. Heuristically, in going from the genus-two surface to the nodal sphere, the process of integrating the last modular parameter (after the other two were used in the residue theorem) introduced a cross-ratio into the amplitudes[8]. This cross-ratio is precisely $\xi^{(+)}$ in (4.2.27) and motivates the use of the cross-ratio in the worldsheet formula proposal of (4.2.26). The necessity of including cross-ratios in the worldsheet expressions is a novel feature that first appears at two-loops, and persists at higher-loops.

The slash prescription also arises in [51] in the context of super Yang-Mills amplitudes. There n-point worldsheet formulae were proposed for this theory on the bi-nodal sphere. Their proposal was based on the colour-kinematics duality, since a first-principles derivation was obstructed by there being no straightforward worldsheet expression on the genus-two surface. Specifically, the colour-kinematics duality was utilised in defining a two-loop colour integrand on the bi-nodal sphere, which coincides with the definition of $\mathcal{I}_{\text{SU}(N)}^{(2,+)}$ in (4.2.31). That is, the object defined there was a sum over restricted permutations. This motivates the second proposal (4.2.29) for the worldsheet integrands.

You may notice that for the theories considered there, which involved maximal supersymmetry, only one cross-ratio $\xi^{(+)}$, or one set of restricted permutations $S_{n+2}^{(+)}$ was required to adequately describe the amplitude. Moreover, for supergravity the cross-ratio and the slash prescription has the same effect. We will discuss precisely why this is when we consider supersymmetric theories in section 4.3.

For now, let us point out that for generic theories, the prescriptions only agree once we have summed over both sets of scattering equations in (4.2.15). In both cases we are splitting

[8] To be somewhat more concrete, in an attempt to trivialise the isomorphism $\mathfrak{D}_{2,n}^{\text{max}} \cong \mathfrak{M}_{0,n+4}$, where $\mathfrak{D}_{2,n}^{\text{max}}$ is the maximal non-separating boundary divisor, the domain of integration of the last complex parameter was, using modular invariance, extended to the whole complex plane on the support of a function $f(q_{12})$, where q_{12} is related to the last modular parameter. The requirement that this does not introduce a pole in the integrand on the support of the scattering equations uniquely fixes this function to be $f(q_{12}) = (1-q_{12})^{-1}$. This function, after using Fay's degeneration formula to determine q_{12} in terms of the nodal points, is precisely the cross-ratio given by $\xi^{(+)}$.

the expression into two parts, either by the use of different cross-ratios as in (4.2.26), or by considering half the permutations as in (4.2.29). Each part is to be integrated with its respective set of scattering equations, as in (4.2.15). The reason for this splitting is that the choice α in the scattering equations determines a relative orientation of the loop momenta in the resulting diagrams. This follows from the fact that the scattering equations, in general, determine the kinematic poles arising after integration over the moduli. In this case the two-loop scattering equations (4.2.11) admit loop-level propagators of the form

$$\frac{1}{(L_1 \pm L_2 + K)^2} \qquad \mapsto \qquad \frac{1}{\pm\alpha(\ell_1 + \alpha\ell_2)^2 + 2(\ell_1 \pm \ell_2)\cdot K + K^2}\,, \tag{4.2.36}$$

for K some partial sum of the external momenta. Considering the LHS propagator with a minus sign and using the $\alpha = +1$ scattering equations produces in a unphysical propagator, whose inverse has the form $-(\ell_1+\ell_2)^2+2(\ell_1-\ell_2)\cdot K+K^2$. A similar situation occurs when considering the plus sign on the LHS and using the $\alpha = -1$ scattering equations. These types of unphysical propagators, arising from the orientation of the different loop momenta, naturally start arising at two-loops.

This provides the necessity of the splitting across the two prescriptions. The cross ratios effectively eliminate poles in the worldsheet integrand that, when evaluated on the relevant scattering equations, will produce these unphysical propagators. Likewise, the slash prescription also eliminates these poles, such that no unphysical propagators occur in any of the two parts.

It is not difficult to see how they do this when our worldsheet integrands are expressed in a KK basis. Consider the loop propagators on the LHS of (4.2.36) with a minus sign. From the point of view of factorisation on the worldsheet, these arise when a subset of the marked points including σ_{1^+} and σ_{2^-} (but not the other nodal points) coalesce. However, with the cross-ratio $\xi^{(+)}$ in (4.2.27), the $\sigma_{1^+2^-}$ in the numerator effectively kills this pole, so no such propagator can occur when utilising the $\alpha = +1$ scattering equations. The slash prescription achieves the same goal. The terms with $\alpha = +1$ are paired with Parke-Taylor factors which have the relative ordering $(1^+, \cdots, 2^+, \cdots, 2^-, \cdots, 1^-)$, as the slash prescription drops the others. But such Parke-Taylor factors cannot have a pole as $\sigma_{1^+2^-} \to 0$ by construction, so the unphysical poles cannot arise. The same reasoning applies when considering the minus sign in the LHS of (4.2.36).

In total, the use of each prescription serves to kill any unphysical poles that may arise from using the two-loop scattering equations (4.2.11).

Let us conclude this section by making a comment on the versatility of this set-up. At tree-level, there exist CHY-type formulae for a variety of theories, such as those in [41,42,92]. These all have grounds in the notion of the double copy, and are in fact part of a 'web of theories' connected by this notion [63–65]. Their worldsheet formulae should also possess a natural extension to two-loops in the way presented above; that is, in the form (4.2.15). This would follow from the double-forward-limit of their respective $(n+4)$-particle expressions at tree-level. This is all that is required in the cross-ratio prescription. In the slash prescription it is required that at least one of the half-integrands are expressible in a Parke-Taylor basis, so that one can appropriately drop half the terms in this basis. An example which uses the ingredients we have already established is the biadjoint scalar theory, whose worldsheet integrand consists of two sets of the colour half-integrand (4.2.30). From the discussion in this section one can naturally formulate two-loop integrands for the biadjoint scalar using

either

$$\mathcal{I}^{(2,\alpha)}_{\text{bi-adj}} = \xi^{(\alpha)}\, \mathcal{I}^{(2)}_{\text{SU}(N)}\, \mathcal{I}^{(2)}_{\text{SU}(\tilde{N})} \tag{4.2.37}$$

in the cross-ratio prescription, or

$$\mathcal{I}^{(2,\alpha)}_{\text{bi-adj}} = \mathcal{I}^{(2)}_{\text{SU}(N)}\, \mathcal{I}^{(2,\not{\alpha})}_{\text{SU}(\tilde{N})} \tag{4.2.38}$$

in the slash prescription. Of course, it doesn't matter which of the half-integrands are slashed. These expressions are directly applicable to (4.2.15) to potentially produce a two-loop integrand for the biadjoint scalar theory. The two prescriptions in this case have been explicitly checked to be equivalent by numerically evaluating (4.2.15) on the regular solutions of the scattering equations at four-points.

4.2.3 Two-loop attempt: trivalent diagrams and colour-kinematics duality

Now we have established the appropriate worldsheet integrands for Yang-Mills and gravity via (4.2.15), we can proceed as at tree-level and one-loop to obtain expressions for their respective two-loop integrands.

Though we have exhibited the novel two-loop features, regarding the two prescriptions introduced in the last section, we do not expect them to complicate the moduli space integral. This seems quite clear from the slash prescription, where only Parke-Taylor factors are directly involved in the integration. With the cross-ratio prescription it seems less clear, but since the two prescriptions are meant to be equivalent after summing over each set of scattering equations, it seems this should also bring no complications. Thus, in principle we expect that (4.2.15) results in the following expressions for the two-loop amplitudes:

$$\mathcal{A}^{(2)}_{\text{YM}} \stackrel{?}{=} \int \frac{d^D\ell_1\, d^D\ell_2}{\ell_1^2\, \ell_2^2} \sum_{\text{a}\in\Gamma^{(2)}_{n+4}} \frac{N^{(2)}_{\text{a}} c^{(2)}_{\text{a}}}{D_{\text{a}}}\,, \quad \mathcal{A}^{(2)}_{\text{grav}} \stackrel{?}{=} \int \frac{d^D\ell_1\, d^D\ell_2}{\ell_1^2\, \ell_2^2} \sum_{\text{a}\in\Gamma^{(2)}_{n+4}} \frac{N^{(2)}_{\text{a}} \tilde{N}^{(2)}_{\text{a}}}{D_{\text{a}}}. \tag{4.2.39}$$

In the above formulae we denote $\Gamma^{(2)}_{n+4}$ by the set of all $(n+4)$-point tree-level trivalent diagrams, excluding those which form two-loop-type tadpole and external-leg bubbles upon gluing the relevant legs associated with the loops (1^+ with 1^-, and 2^+ with 2^-)[9]. The colour and numerator factors for this set of trivalent diagrams are obtained from those of the set of $(n+2)!$ master diagrams displayed in figure 4.4 through successive applications of the Jacobi identity. The kinematic numerators and colour factors associated with the master diagrams are determined by equations (4.2.33), (4.2.34) and (4.2.30).

We recall that the loop propagators that result from using the scattering equations are generically linear in the loop momentum, though from our two-loop scattering equations those that involve both loop momenta are quadratic. The loop-integrand is therefore not fully expressed in a standard Feynman representation; for example, diagrams with the form as in figure 4.4 have the following propagator structure:

[9]Note that this does not exclude diagrams where only one external leg bubble is formed when gluing the legs associated with the loops. The exclusion of two-loop-type tadpoles and external bubbles follows the reasoning of one-loop, where it was shown that these are associated to singular solutions, whose finite contributions integrate to zero. Unfortunately, with the quadratic propagators that appear at two-loops, it is more difficult to see the total set of contributions that integrate to zero.

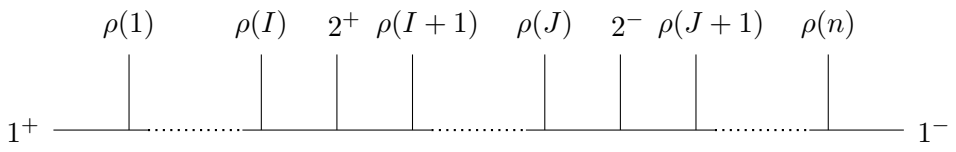

Figure 4.4: The set of two-loop master diagrams are also the set of half ladders, here with 1^+ and 1^- as the end-points.

$$\frac{1}{\left(\prod_{i=1}^{I}(L_1+K_i)^2\right)\left(\prod_{i=I}^{J}(L_1+L_2+K_i)^2\right)\left(\prod_{i=J}^{n-1}(L_1+K_i)^2\right)}$$

$$\mapsto \quad \frac{1}{\left(\prod_{i=1}^{I}2\ell_1\cdot K_i+K_i^2\right)\left(\prod_{i=I}^{J}(\ell_1+\ell_2+K_i)^2\right)\left(\prod_{i=J}^{n-1}2\ell_1\cdot K_i+K_i^2\right)}$$

where $K_i=\sum_{j=1}^{i}k_{\rho(j)}$. As a result of utilising either the cross-ratio or slash prescription, there are no unphysical propagators resulting from e.g. (4.2.36), as mentioned in the last section.

The expressions (4.2.39) manifestly exhibit the colour-kinematics duality by construction. Moreover, the numerators follow directly from tree-level, via the double forward-limit. The reader should be reminded that this contrasts the loop-level BCJ proposal, which is formulated with quadratic propagators and therefore, have the standard Feynman form of loop-integrands. Unfortunately, the details of the BCJ proposal, which has been proven [182–184] and is very well-established at tree-level, is not yet fully understood at loop-level. In the setup we are considering, the colour-kinematics duality at loop-level becomes very clear and follows directly from the tree-level structure. That being said, there are obvious glaring setbacks to this formalism, such as how to appropriately perform the loop-integration; the work initiated in [116] regarding the Q-cuts construction may help alleviate this. Nevertheless, this unorthodox representation still presents a valid representation of the loop integrand.

Unfortunately, however, it turns out that for generic theories, the proposal 4.2.39 is incorrect and requires a modification. In the following sections, we will discuss why this is, how we can obtain the correct two-loop formulae, and why we suspect that this failed.

4.2.4 Failure of the first attempt

Whilst (4.2.15) exhibits the colour-kinematics duality in the same way as at tree-level and one-loop, it turns out that it is in fact not correct for generic theories. The reason for this is because we haven't properly taken into account the relationship between the $(n+4)$-point tree-level diagrams and the two-loop diagrams with Feynman propagators they are meant to reproduce upon gluing the relevant legs.

To understand the issue, let us consider again figure 4.3. This displays one way how a double-box may be decomposed into tree-like diagrams, or equivalently how certain tree-level diagrams can be reconstituted into a double-box. There is however more than one way in which a double-box can be decomposed, as demonstrated in figure 4.5, where two other ways are shown. This means that if we simply sum over all tree-level diagrams, the same double-box will be reconstituted three times. On the other hand, diagrams with independent loops such as the 'bow-tie' in figure 4.6 can only be reconstituted in one way. Naively summing over

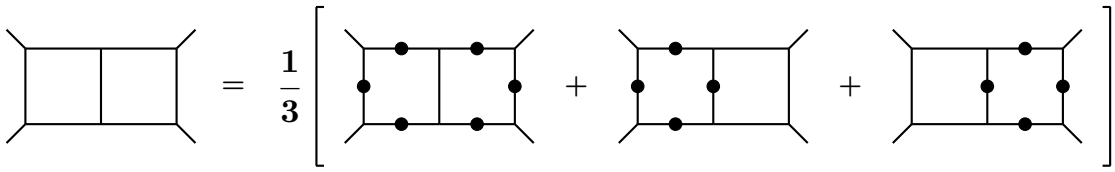

Figure 4.5: A double-box can be reconstituted three ways from the set of $(n+4)$-point tree-level diagrams. The dots signify the possible placements of loop-momenta; see figure 4.3. The first way arises from 9 tree-level diagrams, whereas the second and third each arise from 3 tree-level diagrams.

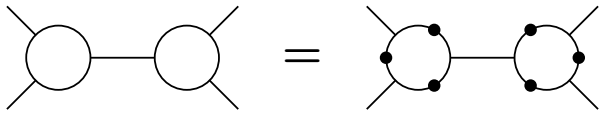

Figure 4.6: A diagram with independent loops can only be reconstituted in one way. The above arises from 9 tree-level diagrams.

Figure 4.7: The vacuum topologies at two-loops.

all tree-level diagrams then effectively results in three double-boxes for every bow-tie. The terms representing these two diagrams therefore do not have the correct multiplicities with respect to each other in order to match the corresponding number of Feynman diagrams.

Understanding these multiplicities requires understanding the symmetry factors between two-loop diagrams. A natural way to do this is to look at the two vacuum topologies at two-loops displayed in figure 4.7, where any diagram is obtained by attaching external legs or trees thereof. Of all two-loop diagrams built this way, there are only three cases that present distinct multiplicity factors:

- Case **T1a**: first topology, with any placement of labelled external legs or trees thereof distinguishing the three internal lines. A double box for example (planar or non-planar) fits into this category, such as the one in 4.3. The multiplicity is $\rho_{\text{T1a}} = 6$, with a factor of 3 coming from the considerations in figure 4.5, and a factor of 2 from being able to exchange ℓ_1 and ℓ_2.

- Case **T1b**: first topology, with all external legs and trees thereof attached to *only one* of the internal lines. This makes the other two internal lines indistinguishable, so the number of terms appearing in the loop-integrand is half that of case **T1a**. The multiplicity is therefore $\rho_{\text{T1b}} = \rho_{\text{T1a}}/2 = 3$

- Case **T2**: second topology, where figure 4.6 provides an example. Here one may only exchange $\ell_1 \leftrightarrow \ell_2$, so the multiplicity is $\rho_{\text{T2}} = 2$. Notice that at least two external lines must be attached to both disconnected loops, otherwise the resulting diagram will be a tadpole or an external-leg bubble, which we exclude in $\Gamma^{(2)}_{n+4}$.

Since the proposal (4.2.39) fails to take this multiplicity into consideration, we conclude that it must be incorrect for generic theories. It follows by extension that the worldsheet formulae (4.2.15) must also be incorrect for generic theories. For supersymmetric theories however this is not the case, and we will discuss why this is in section 4.3.2.

4.2.5 Two-loops proposal

The formulae (4.2.39) have many attractive qualities for a two-loop integrand. It is expressed in terms of trivalent diagrams with the colour-kinematics duality being manifest. Moreover, the ingredients going into the integrand follow straightforwardly from tree-level, via the double-forward-limit. Following the discussion in the last section however, it cannot be correct, since it does not produce the correct number of diagrams to be associated with amplitudes coming from a standard Feynman representation. Specifically, the types of diagrams arising do not have the correct multiplicity with respect to each other.

This however provides a simple fix. Since we know the relative multiplicities, which were calculated in the last section, we can simply modify the formula (4.2.39) to take them into account. As (4.2.39) is expressed as a sum over diagrams, we simply divide each term by the relevant multiplicity corresponding to that diagram. With this modification we propose the two-loop amplitudes to be

$$\boxed{\mathcal{A}^{(2)}_{\rm YM} = \int \frac{d^D\ell_1\, d^D\ell_2}{\ell_1^2\,\ell_2^2} \sum_{\mathrm{a}\in\Gamma^{(2)}_{n+4}} \frac{N^{(2)}_{\mathrm{a}}\, c^{(2)}_{\mathrm{a}}}{\rho_{\mathrm{a}}\, D_{\mathrm{a}}}\,, \qquad \mathcal{A}^{(2)}_{\rm grav} = \int \frac{d^D\ell_1\, d^D\ell_2}{\ell_1^2\,\ell_2^2} \sum_{\mathrm{a}\in\Gamma^{(2)}_{n+4}} \frac{N^{(2)}_{\mathrm{a}}\, \tilde{N}^{(2)}_{\mathrm{a}}}{\rho_{\mathrm{a}}\, D_{\mathrm{a}}}\,.} \tag{4.2.40}$$

with the multiplicity factor ρ_{a}, calculated in the last section, corresponding to the relevant diagram. This simple modification retains all positive qualities described above. In particular, having the colour-kinematics manifest allows a natural extension to other theories via the double copy, provided their CHY half-integrands can be expressed in a Parke-Taylor basis, as discussed at the end of section 4.2.2. The explicit n-point formulae proposed above in (4.2.40) corresponds to pure Yang-Mills and NS-NS gravity, or pure gravity in the case of using (4.1.20) for both loops.

Let us remark that whilst there was a relatively simple way of modifying (4.2.39), an analogous modification of the worldsheet expressions (4.2.15) does not seem as straightforward. Whilst (4.2.15) originally served as a motivation for obtaining the two-loop integrands, the fact that multiplicity factors had to be manually included in the resulting expression indicates potential difficulties in understanding the origin of (4.2.40) on the bi-nodal sphere. Since we have supposed the moduli space integration directly yields all tree-level trivalent diagrams, the need for relative multiplicity factors seems to imply that there there are missing contributions that account for these. We will discuss in section 4.3.3 where we believe these contributions come from.

4.3 Supersymmetric theories and the genus-two ambitwistor string

The two-loop field theory expressions presented in the previous sections were inspired by the study of the ambitwsitor string at genus-two, first initiated in [105] and [180] in the

pure-spinor formalism. After the successes at one-loop, where explicit formulae for field theory amplitudes with and without supersymmetry have been produced [50, 71, 103, 104], it is natural to expect that one can obtain similar formulae for two-loop corrections. Indeed, for the ambitwistor string there were originally discovered for supergravity at four-points in [180] using the pure-spinor formalism. Following this, Geyer and Monteiro rigorously derived n-point expressions for these formulae by considering the full n-point correlator in the limit that the genus-two surface degenerates to the bi-nodal sphere [51]. This degeneration naturally arises (as at genus-one) by performing residue theorems utilising the genus-two scattering equations[10].

In this section we will give a brief review of the formulae derived for supersymmetric theories from the genus-two ambitwistor string and see how they are related to the formalism presented in previous sections. Moreover, we will follow the examples at one-loop and extract the part of the correlator on the bi-nodal sphere corresponding to NS-NS states propagating in the loops, relevant for describing amplitudes without supersymmetry. This will allow us to make a comparison with the objects found for two-loops in the previous section, helping us better understand their origins from the genus-two worldsheet. Ultimately, these considerations will lead us to present an argument concerning why the initial proposal (4.2.15) was unsuccessful.

4.3.1 The supersymmetric amplitude on the bi-nodal sphere

Here we will review the formulae found in [51] for supersymmetric theories, from the point of view of the genus-two ambitwistor string. Being a worldsheet model, amplitudes follow from considering n-point correlators integrated over the moduli space of n-punctured Riemann surfaces. What makes these inherently field theory amplitudes is the localisation of the moduli space that results from enforcing the scattering equations, themselves arising from gauge-fixing the ambitwistor string action. On the genus-two surface, these scattering equations are given by imposing the constraints of (4.2.5). The central method of utilising these is to apply global residue theorems such that the amplitude localises onto the maximal non-separating divisor. For an adequate choice of the scattering equations, and representation of the integrand[11], the amplitude will then be given by a worldsheet expression on the bi-nodal sphere. We will not give the specific details of the global residue theorem, since at genus-two it is a very intricate procedure; we refer the reader to [51] for these details. We will instead look at the result of the type II amplitude after degenerating to the bi-nodal sphere, which takes the form [51]

$$\mathcal{A}^{(2)}_{n,\,\text{sugra}} = \int \frac{d^D\ell_1\, d^D\ell_2}{\ell_1^2\,\ell_2^2} \int_{\mathfrak{M}_{0,n+4}} d\mu^{(2,+)}_{n+4}\, \xi^{(+)}\, \mathcal{I}^{(2)}_{\text{susy-kin}}\, \tilde{\mathcal{I}}^{(2)}_{\text{susy-kin}}\,, \tag{4.3.1}$$

Notice in (4.3.1) the appearance of the cross-ratio from (4.2.27). As noted in section 4.2.2, this arises essentially from extending the integration of the last modular parameter from

[10] We remind the reader that as mentioned in footnote 3, applying residue theorems using on a generic set of scattering equations does not in general fully localise the amplitude onto the bi-nodal sphere, and one may obtain expressions e.g. on nodal tori. The requirement of obtaining an expression on former thus requires a specific choice of scattering equations. All details on this can be found in reference [51].

[11] The global residue theorem will only work as intended if the integrand only has simple poles corresponding to the maximal non-separating boundary divisor and the scattering equations. As mentioned in section 5.1 of [51], this is not true for all representations of the integrand. Recall from section 2.5 that this requirement is also present at genus-one.

the fundamental domain to the full complex plane, with the inclusion of a support function. On the bi-nodal sphere, this support function becomes the cross ratio, and the measure for the modular parameter provides the measure for the locations of the nodal points (along with a Jacobian factor). The specific cross-ratio corresponds to the choice of the scattering equations, in which $\alpha = +1$ was used[12].

Of particular interest to us are the kinematic worldsheet integrands,

$$\mathcal{I}^{(2)}_{\text{susy-kin}} = J \sum_{\delta} \mathcal{Z}^{\text{chi}}[\delta] \, \text{Pf}\left(M^{(2)}_{\delta}\right)\Big|_{q_1,q_2\to 0} \tag{4.3.2}$$

where the parameters q_1, q_2 are two-loop analogues of the degeneration parameter q at one-loop, such that the degeneration to the nodal sphere is governed by the limit $q_1 \to 0$ and $q_2 \to 0$. The sum runs over all 10 even spin structures at genus-two, commonly denoted by δ; more details on this can be found in appendix A. The factor J represents a Jacobian,

$$J = \frac{1}{\sigma_{1+2+}\sigma_{1+2-}\sigma_{1-2+}\sigma_{1-2-}} \,. \tag{4.3.3}$$

Notice there are actually two of these in the full integrand: one arises from the moduli measure becoming the measure for the nodal points, and one comes from the scattering equations in the degeneration limit. These Jacobians are important in supplying the correct $\text{SL}(2,\mathbb{C})$ weights for the nodal points.

The expression (4.3.2) should be compared with the analogous expression at one-loop, given by (2.6.1). Noting that $\mathcal{Z}^{\text{chi}}[\delta]$ and $M^{(2)}_{\delta}$ is the chiral partition function and a matrix involving Szegö kernels at genus-two, they obviously contain a similar structure, as a result of both being computed from the path integral over the fields in the ambitwistor string action. There the sum was over the 3 even spin structures at genus-one, here the sum is over the 10 even spin structures at genus-two[13].

While the sum over spin structures in (4.3.2) acts in part to retain modular invariance on the genus-two worldsheet, it provides a physical interpretation on the bi-nodal sphere. Namely, the combination of certain terms in the sum correspond to particular states propagating through the loops. For the even spin structures which we are considering, table 4.1 shows this designation.

	NS_1	R_1
NS_2	δ_1, δ_2, δ_3, δ_4	δ_7, δ_8
R_2	δ_5, δ_6	δ_9, δ_0

Table 4.1: The combinations of even spin structures corresponding to having either an Neveu-Schwarz (NS) or a Ramond (R) state propagating through the loops. NS_1 corresponds to an NS state in loop 1 (with loop momenta ℓ_1) and R_2 corresponds to a a Ramond state in loop 2 (with loop momenta ℓ_2) for example.

That is, the four terms in the sum (4.3.2) corresponding to δ_1, δ_2, δ_3 and δ_4 gives the contribution to the amplitude in which NS states propagate through both loops. We can

[12] Though of course $\alpha = -1$ could also have been used; both choices result in the localisation to the bi-nodal sphere.

[13] As a reminder, the sum over spin structures is part of the GSO projection, a feature coming from the RNS formulation of the superstring.

therefore extract each contribution from the amplitude in (4.3.2) on the bi-nodal sphere. As at one-loop doing this explicitly requires the expansions in q_1 and q_2 of the chiral partition functions,

$$\mathcal{Z}^{\text{chi}}[\delta] = \sum_{n_1,n_2\in\{0,1\}} (-1)^{2(n_1\delta_1''+n_2\delta_2'')}\, q_1^{-n_1}\, q_2^{-n_2}\, \mathcal{Z}_{\text{NS}}^{(-n_1,-n_2)} \qquad \delta\in\{\delta_1,\delta_2,\delta_3,\delta_4\} \tag{4.3.4a}$$

$$\mathcal{Z}^{\text{chi}}[\delta] = \sum_{n_1\in\{0,1\}} (-1)^{2n_1\delta_1''}\, q_1^{-n_1}\, \mathcal{Z}_{\text{R2}}^{(-n_1,0)} \qquad \delta\in\{\delta_5,\delta_6\} \tag{4.3.4b}$$

$$\mathcal{Z}^{\text{chi}}[\delta] = \sum_{n_2\in\{0,1\}} (-1)^{2n_2\delta_2''}\, q_2^{-n_2}\, \mathcal{Z}_{\text{R1}}^{(0,-n_2)} \qquad \delta\in\{\delta_7,\delta_8\} \tag{4.3.4c}$$

$$\mathcal{Z}^{\text{chi}}[\delta] = \mathcal{Z}_{\text{RR}_i}^{(0,0)} \qquad \delta\in\{\delta_0,\delta_9\},\quad i=0,9\,, \tag{4.3.4d}$$

as well as the expansions in the Szegö kernels that constitute the Pfaffians,

$$S_\delta(z,w) = \sum_{n_1,n_2\in\{0,1\}} (-1)^{2(n_1\delta_1''+n_2\delta_2'')}\, q_1^{n_1}\, q_2^{n_2}\, S_{\text{NS}}^{(n_1,n_2)}(z,w) \qquad \delta\in\{\delta_1,\delta_2,\delta_3,\delta_4\} \tag{4.3.5a}$$

$$S_\delta(z,w) = \sum_{n_1\in\{0,1\}} (-1)^{2n_1\delta_1''}\, q_1^{n_1}\, S_{\text{R2}}^{(n_1,0)}(z,w) \qquad \delta\in\{\delta_5,\delta_6\} \tag{4.3.5b}$$

$$S_\delta(z,w) = \sum_{n_2\in\{0,1\}} (-1)^{2n_2\delta_2''}\, q_2^{n_2}\, S_{\text{R1}}^{(0,n_2)}(z,w) \qquad \delta\in\{\delta_7,\delta_8\} \tag{4.3.5c}$$

$$S_\delta(z,w) = S_{\text{RR}_i}^{(0,0)}(z,w) \qquad \delta\in\{\delta_0,\delta_9\},\quad i=0,9\,. \tag{4.3.5d}$$

These expansions were calculated in [51] to order $\mathcal{O}(q_1\,q_2)$, the precise form of the chiral partition functions in (4.3.4) and Szegö kernels in (4.3.5) can also be found there; they will not be all be totally necessary for our purposes. In the above expansions, δ_1'' and δ_2'' correspond to the first and second components of δ'' in the spin structure $\delta = (\delta'|\delta'')$. The labels NS, R1, R2 and RR classify which states are propagating in the loops, shown in table 4.2.

	state propagating in	
	loop 1	loop 2
NS	NS	NS
R1	R	NS
R2	NS	R
RR	R	R

Table 4.2: Notation for the labels corresponding to which states propagate through the loops. In comparison to table 4.1, loops 1 and 2 correspond to subscripts 1 and 2; for example, NS_1 and R_2 (corresponding to spin structures δ_5, δ_6) here is denoted as R2. Again, by loop 1 we mean e.g. the loop where at least one propagator only involves ℓ_1.

With these in hand we can take a closer look at (4.3.2). Considering the two expansions (4.3.4) and (4.3.5), there are terms that arise at orders $\mathcal{O}(q_1^{-1}q_2^{-1})$, $\mathcal{O}(q_1^{-1})$ and $\mathcal{O}(q_2^{-1})$. It

is easy to show however that the coefficients of these terms vanish due to the relative phases in the sum over spin structures, and so the relevant terms are $\mathcal{O}(1)$. Collecting these terms according to tables 4.1 and 4.2, the integrand can be written as

$$\mathcal{I}^{(2)}_{\text{susy-kin}} = \mathcal{I}^{\text{NS}}_n + \mathcal{I}^{\text{R1}}_n + \mathcal{I}^{\text{R2}}_n + \mathcal{I}^{\text{RR}}_n \,, \tag{4.3.6}$$

where the subintegrands take the form

$$\mathcal{I}^{\text{NS}}_n = 4J \sum_{n_1,n_2\in\{0,1\}} \mathcal{Z}^{(-n_1,-n_2)}_{\text{NS}} \,\text{Pf}\,(M_{\text{NS}})^{(n_1,n_2)} \,, \tag{4.3.7a}$$

$$\mathcal{I}^{\text{R2}}_n = 2J \left(\mathcal{Z}^{(0,0)}_{\text{R2}} \,\text{Pf}(M_{\text{R2}})^{(0,0)} + \mathcal{Z}^{(-1,0)}_{\text{R2}} \,\text{Pf}\,(M_{\text{R2}})^{(1,0)} \right) , \tag{4.3.7b}$$

$$\mathcal{I}^{\text{R1}}_n = 2J \left(\mathcal{Z}^{(0,0)}_{\text{R1}} \,\text{Pf}\,(M_{\text{R1}})^{(0,0)} + \mathcal{Z}^{(0,-1)}_{\text{R1}} \,\text{Pf}\,(M_{\text{R1}})^{(0,1)} \right) , \tag{4.3.7c}$$

$$\mathcal{I}^{\text{RR}}_n = J\,\mathcal{Z}_{\text{RR}_9} \,\text{Pf}\,(M_{\text{RR}_0}) + J\,\mathcal{Z}_{\text{RR}_0} \,\text{Pf}\,(M_{\text{RR}_9}) \,, \tag{4.3.7d}$$

following directly from taking the $\mathcal{O}(1)$ terms from (4.3.2), after using the expansions (4.3.4) and (4.3.5). The labels on the Pfaffians correspond to the those in the Szegö kernels in (4.3.5).

It is in this way that the sum over spin structures allows one to extract contributions corresponding to different states propagating in the loops. This property allows one to potentially consider theories with and without supersymmetry, as was the case at one-loop in section 2.6. In particular, there the NS part of the integrand was used to construct the amplitudes for pure Yang-Mills and NS-NS gravity. An important point to mention however is that these contributions cannot be isolated on the Riemann surface before degeneration, since this would violate modular invariance. This causes a subtlety in the two-loop case: whilst each term may be extracted on the nodal sphere, there may have been terms which cancelled in the supersymmetric sum (4.3.6) on the genus-two surface, which would have led to contributions possibly with different degenerations. We will address the significance of this subtlety later, when we argue why the naive guess of (4.2.15) did not work.

For completeness let us present the structure of the ingredients going into the integrands (4.3.7). Following the scenario described in section 2.6 at one-loop, this will be necessary to construct the NS part of the integrand (4.3.6), which we will match to formulae presented in the previous sections. For this the precise form of the chiral partition functions and Szegö kernels of the NS sector are detailed in appendix B.

The chiral partition functions depend only on the nodal points $\sigma_{1^\pm}$, $\sigma_{2^\pm}$ and two auxiliary points x_1 and x_2, subject to the condition

$$\omega_{1^+1^-}(x_1)\,\omega_{2^+2^-}(x_2) = \omega_{1^+1^-}(x_2)\,\omega_{2^+2^-}(x_1) \,. \tag{4.3.8}$$

The auxiliary points are associated with the insertion of PCOs in the gauge-fixing procedure, and a choice of x_1 and x_2 corresponds to a choice of gauge [51].

All Pfaffians in (4.3.7) are defined from the following $(2n+2)\times(2n+2)$ matrices $M_{\rm S}$;

$$M_{\rm S} = \begin{pmatrix} A & -C^T \\ C & B \end{pmatrix}, \tag{4.3.9a}$$

$$A_{x_1x_2} = \wp(x_1,x_2)\, S_{\rm S}(x_1,x_2)\,, \quad A_{x_\beta,j} = P(x_\beta)\cdot k_j\, S_{\rm S}(x_\beta,\sigma_j)\,, \quad A_{ij} = k_i\cdot k_j\, S_{\rm S}(\sigma_i,\sigma_j)\,, \tag{4.3.9b}$$

$$C_{x_\beta,j} = P(x_\beta)\cdot \epsilon_j\, S_{\rm S}(x_\beta,\sigma_j)\,, \quad C_{ij} = \epsilon_i\cdot k_j\, S_{\rm S}(\sigma_i,\sigma_j)\,, \tag{4.3.9c}$$

$$C_{ii} = -P(\sigma_i)\cdot\epsilon_i\,, \qquad B_{ij} = \epsilon_i\cdot\epsilon_j\, S_{\rm S}(\sigma_i,\sigma_j)\,. \tag{4.3.9d}$$

for any spin structure $\mathrm{S}\in\{\mathrm{NS},\mathrm{R1},\mathrm{R2},\mathrm{RR}\}$. Whilst these matrices do explicitly depend on the auxiliary points x_1 and x_2, the full integrands $\mathcal{I}_n^{\rm S}$ are actually independent of the these. The definitions for the Szegö kernels $S_{\rm S}(\sigma_i,\sigma_j)$ for each spin structure S can be found in appendix D.1 of [51]. As the points in their argument coalesce, they produce a simple pole, i.e. they behave as $S_{\rm S}(\sigma_i,\sigma_j)\sim 1/\sigma_{ij}$ for $\sigma_i\sim\sigma_j$. This is true for any spin structure S.

The one-form $P(\sigma)$ on the bi-nodal sphere takes the same form as in (4.2.10),

$$P_\mu(\sigma) = \ell_{1\,\mu}\,\omega_{1^+1^-}(\sigma) + \ell_{2\,\mu}\,\omega_{2^+2^-}(\sigma) + \sum_i \frac{k_{i\,\mu}}{\sigma-\sigma_i}\,\mathrm{d}\sigma\,, \tag{4.3.10}$$

and the quantity $\wp(x_1,x_2)$, entering the matrices $M_{\rm S}$ through the component $A_{x_1x_2}$, is defined as

$$\wp(x_1,x_2) = -\frac{1}{2}\sum_{i,j}\frac{k_i\cdot k_j}{c_1c_2}\Big(c_1\omega_{i,*}(x_1)-c_2\omega_{i,*}(x_2)\Big)\Big(c_1\omega_{j,*}(x_1)-c_2\omega_{j,*}(x_2)\Big)\,, \tag{4.3.11}$$

for an auxiliary marked point σ_*. It can be verified that $\wp(x_1,x_2)$ is actually independent of σ_* by using the definition of the coefficients c_β for $\beta=1,2$,

$$c_\beta = \sqrt{\frac{(x_\beta-\sigma_{1^+})(x_\beta-\sigma_{1^-})(x_\beta-\sigma_{2^+})(x_\beta-\sigma_{2^-})}{\sigma_{1^+1^-}\sigma_{2^+2^-}}}\,\frac{1}{\mathrm{d}x_\beta}\,. \tag{4.3.12}$$

We are now ready to define the Pfaffian factors in the kinematic integrands $\mathcal{I}^{\rm S}$. Let us introduce indices $\mathrm{a},\mathrm{b}=1\ldots 2n{+}2$, which we use to label $\sigma_{\rm a}=(x_1,x_2,\sigma_1,\ldots,\sigma_n,\sigma_1,\ldots,\sigma_n)$ and $v_{\rm a}=(P(x_1),P(x_2),k_1,\ldots k_n,\epsilon_1,\ldots,\epsilon_n)$. For any choice of S, the Pfaffians are then be defined as[14]

$$\mathrm{Pf}\,(M_{\rm S})^{(0,0)} = \mathrm{Pf}\,\big(M_{\rm S}\big)\,, \qquad n_1=n_2=0 \tag{4.3.13a}$$

$$\mathrm{Pf}\,(M_{\rm S})^{(n_1,n_2)} = \sum_{\mathrm{a}<\mathrm{b}} S_{\rm S}^{(n_1,n_2)}(\sigma_{\rm a},\sigma_{\rm b})\, v_{\rm a}\cdot v_{\rm b}\,\mathrm{Pf}\,(M_{\rm S}{}^{ab}_{ab})\,, \qquad n_1+n_2>0\,. \tag{4.3.13b}$$

As usual the notation $\mathrm{Pf}\,(M_{\rm S}{}^{ab}_{ab})$ indicates that both the rows and columns a,b have been removed from the matrix $M_{\rm S}$.

[14] We note that in [51], a slightly different definition was presented, that was tailored towards the degeneration of the genus-two worldsheet. It can be checked that the two definitions are in fact equivalent.

4.3.2 Relation to new formulae

In this section we connect the previous discussion to that of section 4.2 and understand its features in the language therein. Firstly, we will give the explicit worldsheet formulae for the supersymmetric theories considered above, in the spirit of (4.2.15). After giving the four-particle amplitude for these supersymmetric theories, we will see how its two-loop integrand is naturally expressed in the form (4.2.39). Consequently, we will discuss why it can be represented this way, without requiring a modification with multiplicity factors, as was the case with the non-supersymmetric theories.

The worldsheet formula (4.3.1) gives the two-loop amplitudes for supergravity, based on the type II ambitwistor string at genus-two. A natural question to ask is what the corresponding worldsheet formula for super Yang-Mills theory is. Unlike the former, there is currently no known expression on the genus-two surface that allows a first-principles derivation of super Yang-Mills amplitudes. This however does not preclude a proposal for the relevant worldsheet integrand on the bi-nodal sphere, which was first proposed in [105] for four particles. Following this the corresponding expressions at n-points was then proposed in [51]. The integrands for these theories are given by

$$\mathcal{I}^{(2)}_{\text{SYM}} = \mathcal{I}^{(2)}_{\text{susy-kin}}\,\mathcal{I}^{(2,\not{})}_{\text{SU}(N)} \qquad\qquad \mathcal{I}^{(2)}_{\text{sugra}} = \xi^{(+)}\,\mathcal{I}^{(2)}_{\text{susy-kin}}\,\tilde{\mathcal{I}}^{(2)}_{\text{susy-kin}}\,, \tag{4.3.14}$$

We discussed the presence of the cross-ratio in the supergravity integrand in the previous section. Notice however that the colour factor in the super Yang-Mills integrand follows the slash prescription, where one drops half of the terms in the sum over permutations. Specifically, the supersymmetric kinematic integrand is given by (4.3.2) and the colour integrand above is defined according to (4.2.31). We remark that only kinematic integrands contain information about the degree of supersymmetry, not the colour factors.

Do the worldsheet integrands result in an expression for two-loop integrands similar to those in (4.2.39)? Due to the complicated structure of the supersymmetric kinematic half-integrand (4.3.2), this is quite difficult to see for arbitrary multiplicity. However, for four particles the sum over spin structures can be performed explicitly [51, 179], resulting in

$$\mathcal{I}^{(2,+)}_{\text{SYM},n=4} = \mathcal{K}\,\widehat{\mathcal{Y}}\,\mathcal{I}^{(2,\not{})}_{\text{SU}(N_c)}\,, \qquad\qquad \mathcal{I}^{(2,+)}_{\text{sugra},n=4} = \xi^{(+)}\,\big(\mathcal{K}\tilde{\mathcal{K}}\big)\,\widehat{\mathcal{Y}}^2\,; \tag{4.3.15}$$

that is, the kinematic integrand can be simplified at four-points to $\mathcal{I}^{(2)}_{\text{susy-kin},n=4} = \mathcal{K}\,\widehat{\mathcal{Y}}$. Here, $\mathcal{K}$ is a purely kinematic prefactor that can be extracted from the expression

$$\begin{aligned}\mathcal{K} = {}& \text{tr}\big(F_1F_2\big)\text{tr}\big(F_3F_4\big) + \text{tr}\big(F_1F_3\big)\text{tr}\big(F_2F_4\big) + \text{tr}\big(F_1F_4\big)\text{tr}\big(F_2F_3\big) \\ & - 4\,\text{tr}\big(F_1F_2F_3F_4\big) - 4\,\text{tr}\big(F_1F_3F_2F_4\big) - 4\,\text{tr}\big(F_1F_2F_4F_3\big)\,,\end{aligned} \tag{4.3.16}$$

where $F_i^{\mu\nu} = k_i^{[\mu}\epsilon_i^{\nu]}$, and $\widetilde{\mathcal{K}} = \mathcal{K}(\epsilon \to \tilde{\epsilon})$. The factor $\widehat{\mathcal{Y}}$ can be expressed as

$$\widehat{\mathcal{Y}} = J\,\mathcal{Y}\,, \qquad \mathcal{Y} = s\bar{\Delta}_{14}\bar{\Delta}_{23} - t\bar{\Delta}_{12}\bar{\Delta}_{34}\,, \tag{4.3.17}$$

where $J = (\sigma_{1^+2^+}\sigma_{1^-2^+}\sigma_{1^+2^-}\sigma_{1^-2^-})^{-1}$ is the Jacobian factor defined in (4.3.3), and the $\bar{\Delta}_{ij}$ are defined to be

$$\bar{\Delta}_{ij} = \omega_{1^+1^-}(\sigma_i)\,\omega_{2^+2^-}(\sigma_j) - \omega_{1^+1^-}(\sigma_j)\,\omega_{2^+2^-}(\sigma_i)\,. \tag{4.3.18}$$

This object actually descends, via (4.2.8), from a biholomorphic one-form on the genus-two surface, defined by $\Delta_{ij} = \epsilon^{IJ}\omega_I(z_i)\,\omega_J(z_j) = \omega_{[I}(z_i)\,\omega_{J]}(z_j)$ (up to factors of $2\pi i$). In fact,

the four-point amplitude, in the context of the ambitwistor string, was first discovered on the genus-two surface in [180], which strongly resembles the analogous result coming from the superstring found in [179].

At four-points the supersymmetric integrand admits a Parke-Taylor decomposition with kinematic numerators,

$$\mathcal{I}^{(2)}_{\text{susy-kin},n=4} = \mathcal{K}\,\widehat{\mathcal{Y}} = \sum_{\rho\in S_{4+2}} \frac{N^{(2)}(1^+,\rho(1),\cdots,\rho(6),1^+)}{\sigma_{1^+\rho(1)}\sigma_{\rho(1)\rho(2)}\cdots\sigma_{\rho(6)\,1^-}\sigma_{1^-1^+}} \tag{4.3.19}$$

with ρ resembling a permutation over the labels $\{1,2,3,4,\,2^+,2^-\}$. To describe these numerators, consider such a permutation written in the form $\rho=(A,2^\pm,B,2^\mp,C)$, where A, B and C are (possibly empty) non-overlapping subsets of the external labels, such that $A\cup B\cup C=\{1,2,3,4\}$. The numerators then take the form[15]

$$N^{(2)}(1^+,A,2^\pm,B,2^\mp,C,1^-) = -\frac{\mathcal{K}}{6}\begin{cases} s_{ij} & B=\{i,j\} \\ 0 & \text{otherwise}\end{cases}; \qquad i,j\in\{1,2,3,4\}\,. \tag{4.3.20}$$

Since the two-loop four-particle integrands (4.3.14) admit the representation (4.3.19), the worldsheet formulae give rise to expressions for the two-loop amplitudes similar to (4.2.39):

$$\mathcal{A}^{(2)}_{\text{SYM},n=4} = \int \frac{d^D\ell_1\,d^D\ell_2}{\ell_1^2\,\ell_2^2}\sum_{\mathrm{a}\in\Gamma^{(2)}_{4+4}}\frac{N^{(2)}_{\mathrm{a}}c^{(2)}_{\mathrm{a}}}{D_{\mathrm{a}}}\,,\quad \mathcal{A}^{(2)}_{\text{sugra},n=4} = \int \frac{d^D\ell_1\,d^D\ell_2}{\ell_1^2\,\ell_2^2}\sum_{\mathrm{a}\in\Gamma^{(2)}_{4+4}}\frac{N^{(2)}_{\mathrm{a}}\tilde{N}^{(2)}_{\mathrm{a}}}{D_{\mathrm{a}}}\,, \tag{4.3.21}$$

with the numerators defined as in (4.3.20), and the colour factors deriving from (4.2.31). We remark that unlike the non-supersymmetric integrand of (4.2.33), the Parke-Taylor decomposition (4.3.19) does *not* rely on the scattering equations; the equality is true for all puncture locations.

Also unlike the non-supersymmetric case in section 4.2, the formulae (4.3.21) are precisely correct: they require no modification involving multiplicity factors, such as those required in section 4.2.5. Why is this the case?

If you look at (4.3.21) with the numerators defined in (4.3.20), you will find that the only trivalent diagrams appearing correspond to double boxes (the others are set to zero by the numerators), such as those in figure 4.5. That only double-boxes appear is a well-known property of the two-loop supersymmetric integrands. These diagrams however correspond exactly to the type **T1a** diagrams from section 4.2.4. There is then no issue with relative multiplicity factors between diagrams, since only one type appear. The multiplicity factor becomes an overall normalisation for the integrand; in fact, the factor of 1/6 in (4.3.20) is precisely related to the multiplicity factor $\rho_{\text{T1a}}=6$ for these diagrams[16]. One could have pulled this factor out of the numerators, so that ρ_{a} is explicitly included in the formulae (4.3.21), matching the 'modified' form of (4.2.40), and it would still be correct.

[15] In practice, the specific numerators can be found by appropriately taking residues of $\mathcal{K}\hat{\mathcal{Y}}$ as certain combinations of σ_{ij} variables go to zero. From the RHS of (4.3.19), it can be seen that doing so will isolate each numerator if all such variables in a particular permutation is considered.

[16] This factor is also required to match with the typical normalisation of the two-loop four-particle amplitudes.

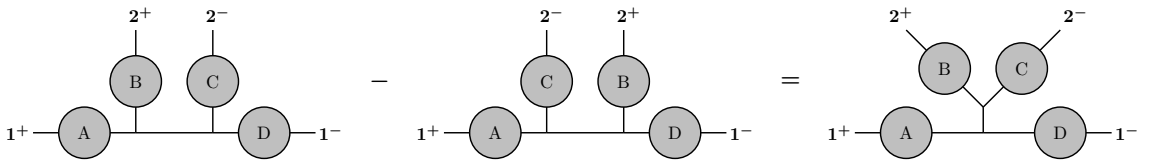

Figure 4.8: One class of Jacobi relations between trivalent diagrams at two loops. The 'blobs' (A, B, C, D) are trivalent trees where we suppress the n external legs. On the left-hand side, the diagrams contain a single quadratic propagator each, of the type $1/(\ell_1+\ell_2+K)^2$ in the first case and $1/(\ell_1-\ell_2+K)^2$ in the second case. On the right-hand side, the diagram has independent loops, and therefore possesses no propagator involving both loop momenta.

There is a further consequence of this fact which highlights another (seemingly) different aspect of the supersymmetric worldsheet integrands, in comparison to those of (4.2.15). Consider figure 4.8, where an application of the Jacobi identity is presented. In light of (4.3.19), the diagrams on the left correspond to terms in the sum with 2^+ before 2^-, whereas the diagram in the middle correspond to terms with 2^- before 2^+. The diagram on the right, once one glues the legs, becomes a diagram with disconnected loops (type **T2** from section 4.2.4), which do not appear in the supersymmetric theories. This means that the terms in the supersymmetric integrand corresponding to 2^+ before 2^- are actually the same as those corresponding to 2^- before 2^+. Recall from section 4.2.2 that the cross-ratio $\xi^{(+)}$ prevents poles where σ_{1^+} and σ_{2^-} (but no other nodal points) coalesce. This explains why only one cross-ratio (or one application of the 'slash' prescription) is required for the supersymmetric worldsheet integrands (4.3.14). Including both cross-ratios with a factor of $1/2$ would still give the integrands in (4.3.14), since the two terms would be equal.

This also seems to imply that the cross-ratio in the supergravity integrand (4.3.14), being composed of a single term, must have the same effect as the slash prescription, i.e. that

$$\xi^{(+)}\,\mathcal{I}^{(2)}_{\text{susy-kin}} = \mathcal{I}^{(2,\not{+})}_{\text{susy-kin}}\,. \tag{4.3.22}$$

At four-points, where the Parke-Taylor decomposition is known, this can be proven explicitly. Let us return to (4.3.19), and write it in the form

$$\mathcal{I}^{(2)}_{\text{susy-kin},n=4} = \sum_{\gamma\in S_4} \frac{N^{(2)}(1^+,\cdots,2^\pm,\cdots,2^\mp,\cdots,1^+)}{(1^+\cdots 2^\pm\cdots 2^\mp\cdots 1^-)} \tag{4.3.23}$$

where $\cdots$ corresponds to possible external particle labels, and $(1^+\cdots 2^\pm\cdots 2^\mp\cdots 1^-)$ represents the (inverse) Parke-Taylor factor for the relevant ordering. In the above, the $2^\pm$ and $2^\mp$ indicate that all terms are included in the sum (with both 2^+ before 2^- and 2^- before 2^+). One may check that for arbitrary values of the marked points,

$$\sum_{\gamma\in S_4} \frac{N^{(2)}(1^+,\cdots,2^+,\cdots,2^-,\cdots,1^+)}{(1^+\cdots 2^+\cdots 2^-\cdots 1^-)} = \frac{\sigma_{1^+2^-}\sigma_{1^-2^+}}{\sigma_{1^+2^+}\sigma_{1^-2^-}} \sum_{\gamma\in S_4} \frac{N^{(2)}(1^+,\cdots,2^-,\cdots,2^+,\cdots,1^+)}{(1^+\cdots 2^-\cdots 2^+\cdots 1^-)}\,.$$

If we denote the sum on the left as S^+ and the sum on the right as S^-, then this is simply

$$S^+ = \frac{\sigma_{1^+2^-}\sigma_{1^-2^+}}{\sigma_{1^+2^+}\sigma_{1^-2^-}}\,S^-\,. \tag{4.3.24}$$

Writing the explicit form of the cross ratio $\xi^{(+)}$ from (4.2.27), the claim (4.3.22) becomes quite clear, since

$$\begin{aligned}\frac{\sigma_{1^+2^-}\sigma_{1^-2^+}}{\sigma_{1^+1^-}\sigma_{2^+2^-}}\mathcal{I}^{(2)}_{\text{susy-kin},n=4} &= \frac{\sigma_{1^+2^-}\sigma_{1^-2^+}}{\sigma_{1^+1^-}\sigma_{2^+2^-}}(S^+ + S^-)\\ &= \frac{\sigma_{1^+2^-}\sigma_{1^-2^+}}{\sigma_{1^+1^-}\sigma_{2^+2^-}}\left(1+\frac{\sigma_{1^+2^+}\sigma_{1^-2^-}}{\sigma_{1^+2^-}\sigma_{1^-2^+}}\right)S^+\\ &= \left(\xi^{(+)}+\xi^{(-)}\right)S^+ = S^+ \equiv \mathcal{I}^{(2,\not{+})}_{\text{susy-kin},n=4}\end{aligned} \tag{4.3.25}$$

where we have used (4.3.24) and the fact that $\xi^{(+)}+\xi^{(-)}=1$ from (4.2.28). Thus, the cross-ratio has the same effect as the slash prescription in the same of supergravity. In constructing higher-point expressions, this would place a strong requirement on the kinematic numerators.

4.3.3 The NS sector, degenerations and multiplicities

In the last section we alluded to the idea that the sum over spin structures allows us to extract the NS contribution on the nodal sphere, and that this can potentially give results for theories with less supersymmetry. As mentioned there, this is a successful treatment at one-loop, as shown in [71], where formulae for pure Yang-Mills and NS-NS gravity were constructed. In this section we discuss this treatment at two-loops and relate the NS contribution to the formulae presented in section 4.2.2. This will lead us to an argument as to why the proposal (4.2.39) required corrections, and how this could be understood from the point of view of the worldsheet degeneration.

The NS contribution to the supersymmetric integrand on the sphere was calculated in (4.3.7). If the methodology at one-loop follows straightforwardly to two-loops, then we would expect the kinematic integrand of section 4.2.2 to be precisely equal to this contribution,

$$\mathcal{I}^{(2,+)}_{\text{kin}} \stackrel{?}{=} \mathcal{I}^{(2)}_{\mathbb{A},\text{kin}} := \mathcal{I}^{\text{NS}}_n = 4J \sum_{n_1,n_2\in\{0,1\}} \mathcal{Z}^{(-n_1,-n_2)}_{\text{NS}}\,\text{Pf}\,(M_{\text{NS}})^{(n_1,n_2)}\,, \tag{4.3.26}$$

where we put the subscript $\mathbb{A}$ to denote that this kinematic integrand is coming from the ambitwistor string. For completeness, the details of the partition functions and Szegö kernels going into the Pffafians on the RHS on (4.3.26) have been included in appendix B.

Aesthetically these integrands have a very different form. $\mathcal{I}^{(2)}_{\mathbb{A},\text{kin}}$ contains the Pfaffian of a $(2n+2)\times(2n+2)$ matrix with partition functions as coefficients. The integrand is invariant under the choice of two auxiliary points x_1 and x_2, required to describe both the Pfaffians and the partition functions, and the matrix M_{NS} depends linearly on the loop momenta, i.e. only contains entries of the form $\ell_I\cdot V$. On the other hand, from (4.2.18), $\mathcal{I}^{(2,+)}_{\text{kin}}$ contains the *reduced* Pfaffian of a $(2n+4)\times(2n+4)$ matrix, summed over the polarisation states associated to the loop-momenta. On the support of the scattering equations it is invariant under the choice of a reference vector q_μ, required for the sum over states, and the matrix M depends *quadratically* on the loop-momenta i.e. it contains entries (specifically $A_{1^\pm 2^\pm}$) proportional to $\frac{1}{2}(\ell_1+\ell_2)^2$. The former follows straightforwardly from the degeneration of the genus-two expressions, and the latter is constructed from the double-forward-limit of the tree-level expressions.

However the one-loop scenario, albeit much less intricate, has shown that certain differences in the integrands do not preclude a relationship between them. In light of this we

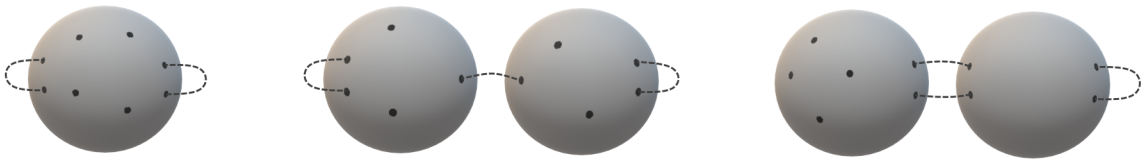

Figure 4.9: Types of worldsheet degeneration at genus-two.

have checked in the case of four-particles that the two proposals do agree on the scattering equations $\mathcal{E}_A^{(+)}$,

$$\boxed{\mathcal{I}^{(2)}_{\mathbb{A},\text{kin}} \overset{(+)}{=} \mathcal{I}^{(2,+)}_{\text{kin}}}\,. \tag{4.3.27}$$

We remark that this check is very non-trivial, considering the structural differences discussed above. As a result, we expect this result to hold to any number of external particles. Equation (4.3.27) demonstrates that the NS contribution can be thought of as arising from a double-forward-limit. We expect that this interpretation extends also to the other contributions (R1, R2 and RR), which would imply that $\mathcal{I}^{(2)}_{\text{susy-kin}}$ can also arise from a double-forward limit. Indeed, the four-point formulae in (4.3.21) also support this observation.

This however brings cause to confusion. If the supersymmetric integrand arises from a double-forward-limit, and if its NS sector which matches the non-supersymmetric integrand also does too, why was the initial proposal (4.2.39) incorrect? Why did we have to manually include multiplicities to obtain the correct two-loop amplitude for the non-supersymmetric theories?

We argue that this is due to the failure of the direct residue argument of figure 4.2 from the genus-two surface to the bi-nodal sphere in the absence of supersymmetry. Specifically, since one cannot isolate the terms (4.3.6) on the genus-two surface, the residue argument is not expected to hold for each term individually. In particular, there may have been other terms which cancelled in the supersymmetric sum (4.3.6). In the applying the global residue theorem, these extra terms may not descend directly to the bi-nodal sphere, but may result in contributions from different degenerations altogether. To give an idea of why these are relevant to the discussion of multiplicities, consider figure 4.9 which displays the other types of degeneration. Our formulation is based on the bi-nodal sphere, which corresponds to the left diagram. The terms cancelling in the supersymmetric sum however upon applying the global residue theorem can give contributions on worldsheets displayed by the center and right diagrams. The crucial feature to notice is that these lead to two-loop diagrams of type **T2** and **T1b** respectively, precisely those which required distinct multiplicity factors with respect to the full expression coming from the bi-nodal sphere. We therefore postulate that these extra contributions account for the multiplicities required in the non-supersymmetric case. We note that in principle they could be calculated directly via the 'gluing operator' of [97].

To conclude this section, let us make a comment on theories with less-than-maximal supersymmetry. That worldsheet integrands present a double-copy structure allows one to construct them for theories with varying degrees of supersymmetry, in line with the BCJ double copy [10]. Therefore, we can also present a two-loop worldsheet formula for half-maximal supergravity by utilising the kinematic factors we've discussed with and without

supersymmetry. In the spirit of (4.3.7), this corresponds to

$$\mathcal{I}^{(2,+)}_{\text{half-sugra}} = \xi^{(+)}\,\mathcal{I}^{(2)}_{\text{susy-kin}}\,\tilde{\mathcal{I}}^{(2)}_{\text{kin}}\,. \tag{4.3.28}$$

4.3.4 Checks on maximal unitarity cuts

We will here check the formulae discussed in section 4.2, describing two-loop n-point integrands for pure Yang-Mills and gravity in any dimension. A natural way of comparing the integrands of field theory is to analyse them on a set of unitarity cuts, where we place the internal loop propagators on-shell. If we take a set of maximal cuts (with *all* loop propagators on-shell), then one only need compare the numerators for the corresponding diagrams in each integrand on the cut solutions. We will do this for pure Yang-Mills at four-points, in the case of all-plus external helicities. This was found originally in [185] and is given by

$$\mathcal{A}^{(2)}_4(1^+,2^+,3^+,4^+) = \frac{g^6}{4}\sum_{S_4}\left[C^{\rm P}_{1234}A^{\rm P}_{1234} + C^{\rm NP}_{12;34}A^{\rm NP}_{12;34}\right]\,, \tag{4.3.29}$$

where $A^{\rm P}_{1234}$ and $A^{\rm NP}_{12;34}$ are the planar and non-planar colour-ordered Yang-Mills integrands respectively,

$$\begin{aligned} A^{\rm P}_{1234} = i\mathcal{T}\Big\{ & sI^{\rm P}_4\left[(D_s-2)(\lambda_1^2\lambda_2^2+\lambda_1^2\lambda_{12}^2+\lambda_{12}^2\lambda_2^2)+16((\lambda_1\cdot\lambda_2)^2-\lambda_1^2\lambda_2^2)\right](s,t) \\ & + 4(D_s-2)I^{\text{bow-tie}}_4\left[(\lambda_1^2+\lambda_2^2)(\lambda_1\cdot\lambda_2)\right](s) \\ & + \frac{(D_s-2)^2}{s}I^{\text{bow-tie}}_4\left[\lambda_1^2\lambda_2^2((\ell_1+\ell_2)^2+s)\right](s,t)\Big\}\,, \end{aligned} \tag{4.3.30}$$

$$A^{\rm NP}_{12;34} = i\mathcal{T}sI^{\rm NP}_4\left[(D_s-2)(\lambda_1^2\lambda_2^2+\lambda_1^2\lambda_{12}^2+\lambda_{12}^2\lambda_2^2)+16((\lambda_1\cdot\lambda_2)^2-\lambda_1^2\lambda_2^2)\right](s,t)\,. \tag{4.3.31}$$

In the above formulae, $I^{\rm P}_4[R]$ and $I^{\rm NP}_4[R]$ represent a planar and non-planar double-box respectively with numerator R, and $I^{\text{bow-tie}}_4$ signifies a 'box-tie' diagram (without the connecting propagator) such as that displayed in figure 4.6. The prefactor $\mathcal{T}$ depends only on the external kinematics, which are four-dimensional, and is written in spinor-helicity notation as

$$\mathcal{T} = \frac{[12][34]}{\langle 12\rangle\langle 34\rangle}\,. \tag{4.3.32}$$

Note however that the loop-momenta ℓ_I are treated in general as being D-dimensional, and that its $(D-4)$-dimensional part is λ_I. In the above $\lambda_{12} = \lambda_1 + \lambda_2$, and D_s refers to the number of intermediate gluon states. These factors of (D_s-2) arise in our formalism from certain contractions of the state projectors; see below equation (4.2.25).

The result above is in the standard Feynman representation, so we remark that it appears very different to what results from our formulae, which contains many more terms and linear-type propagators. However, for any choice of maximal cuts, only one of our terms will contribute, and the cut conditions will be the same since they will both require $\ell_1^2 = \ell_2^2 = 0$. On these two cut conditions, the linear and quadratic propagators are the same, so all other cut conditions will also match. Therefore, it is not necessary to bring the two expressions for the integrand into the same representation to make a comparison, which is possible by applying partial fraction identities and shifts in the loop momentum to (4.3.29).

We will consider two cases each for the planar and non-planar double-box. Since we are only considering these types of diagrams, we can ignore the multiplicity factors from our

approach. These examples will also highlight how the numerators for these diagrams are explicitly calculated from their tree-level counterparts through the double forward-limit.

For the double planar-boxes we will consider the examples displayed in figures 4.10 and 4.11. The first example is displayed in figure 4.10 below. The 'cuts' on the diagram on the

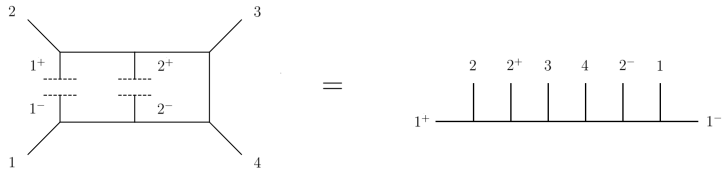

Figure 4.10: One contribution to a double-planar box, resulting from the choice of loop momenta displayed. The two-loop diagram on the left is obtained from the corresponding tree-level diagram on the right, which happens to be a master diagram.

left correspond to the placement of the loop momenta, with the + on the internal labels designating the direction of flow. In this example the tree-level diagram it is obtained from is a master diagram, displayed on the right, whose numerator is thus a (single) master numerator. In our formalism this corresponds to the following term in the integrand:

$$\frac{N^{(2)}(1^+,\,2,\,2^+,\,3,\,4,\,2^-,\,1,\,1^-)}{\ell_1^2\,\ell_2^2\,(2\ell_1\cdot k_2)\,(\ell_1+\ell_2+k_2)^2\,(\ell_1+\ell_2+k_{23})^2\,(\ell_1+\ell_2-k_1)^2\,(-2\ell_1\cdot k_1)}\,, \tag{4.3.33}$$

where we have used the shorthand notation $k_{ij}=k_i+k_j$. We recount that these numerators are constructed algorithmically from (4+4)-point tree-level numerators and depend respectively only on the ordering therein. We then match the numerator to the corresponding numerator of (4.3.29) which takes the form

$$\big[(D_s-2)(\lambda_1^2\lambda_2^2+\lambda_1^2\lambda_{12}^2+\lambda_{12}^2\lambda_2^2)+16((\lambda_1\cdot\lambda_2)^2-\lambda_1^2\lambda_2^2)\big] \tag{4.3.34}$$

on the solutions to the cut constraints

$$\ell_1^2=\ell_2^2=(\ell_1+k_1)^2=(\ell_1+\ell_2+k_2)^2=(\ell_1+\ell_2+k_{23})^2=(\ell_1+\ell_2-k_1)^2=(\ell_1-k_1)^2=0\,. \tag{4.3.35}$$

We can confirm that they indeed match on the cut solutions above, up to an overall normalisation factor.

Another example for the planar double box is displayed in figure 4.11 below.
The term in the integrand of our proposal that contributes to this is

$$\frac{N^{(2)}(1^+,\,2,\,[3,\,2^+],\,[2^-,\,4],\,1,\,1^-)}{\ell_1^2\,\ell_2^2\,(2\ell_1\cdot k_2)\,(2\ell_2\cdot k_3)\,(\ell_1+\ell_2+k_{23})^2\,(-2\ell_1\cdot k_1)\,(-2\ell_2\cdot k_2)} \tag{4.3.36}$$

where we have written a shorthand for the application of the Jacobi identity

$$N^{(2)}(\cdots,[i,j],\cdots):=N^{(2)}(\cdots,i,j,\cdots)-N^{(2)}(\cdots,j,i,\cdots) \tag{4.3.37}$$

to the numerators, shown diagrammatically in figure 4.11. Specifically, the kinematic numerator is given by

$$\begin{aligned}N^{(2)}(1^+,2,[3,2^+],[2^-,4],1,1^-)=&+N^{(2)}(1^+,2,3,2^+,2^-,4,1,1^-)-N^{(2)}(1^+,2,2^+,3,2^-,4,1,1^-)\\&-N^{(2)}(1^+,2,3,2^+,4,2^-,1,1^-)+N^{(2)}(1^+,2,2^+,3,4,2^-,1,1^-)\,.\end{aligned}$$

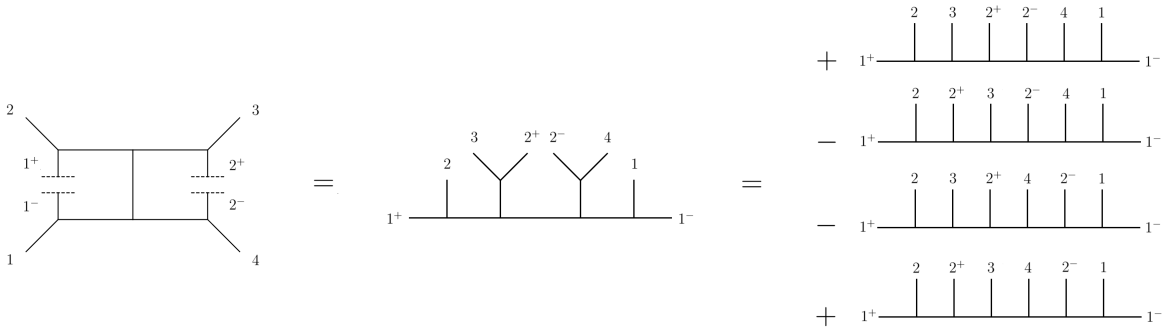

Figure 4.11: Another contribution to the double-planar box, corresponding to a different placement of the loop momenta. The two-loop diagram arises from the double forward-limit of the tree-diagram in the centre. To obtain the kinematic numerator for this diagram in terms of the (half-ladder) master numerators, the Jacobi identity must be employed twice.

The numerator is evaluated on the cut conditions here given by

$$\ell_1^2 = \ell_2^2 = (\ell_1 + k_2)^2 = (\ell_2 + k_3)^2 = (\ell_1 + \ell_2 + k_{23})^2 = (\ell_1 - k_1)^2 = (\ell_2 - k_2)^2 = 0\,. \quad (4.3.38)$$

We also confirm in this case that the numerators match.

For the non-planar double-boxes we consider the examples given in figures 4.12 and 4.13. The diagrams with their respective numerators are constructed similarly to the planar cases

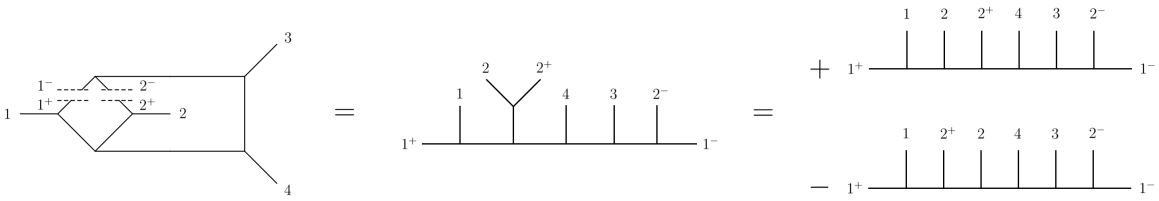

Figure 4.12: Contribution to a non-planar double-box, and the corresponding relation of its numerator to those of the master diagrams.

considered above. The non-planar double box in figure 4.12 corresponds to the following term in our two-loop integrand:

$$\frac{N^{(2)}(1^+, 1, [2, 2^+], 4, 3, 2^-, 1^-)}{\ell_1^2\,\ell_2^2\,(2\ell_1 \cdot k_1)\,(2\ell_2 \cdot k_2)\,(\ell_1 + \ell_2 + k_{12})^2\,(\ell_1 + \ell_2 - k_3)^2\,(\ell_1 + \ell_2)^2} \quad (4.3.39)$$

whose numerator we evaluate on the maximal cut solutions to

$$\ell_1^2 = \ell_2^2 = (\ell_1 + k_1)^2 = (\ell_2 + k_2)^2 = (\ell_1 + \ell_2 + k_{12})^2 = (\ell_1 + \ell_2 - k_3)^2 = (\ell_1 + \ell_2)^2 = 0. \quad (4.3.40)$$

Likewise, the example of figure 4.13 corresponds to the following term in our integrand,

$$\frac{N^{(2)}(1^+, [3, 2^+], 2, [2^-, 4], 1, 1^-)}{\ell_1^2\,\ell_2^2\,(2\ell_2 \cdot k_3)\,(-2\ell_1 \cdot k_1)\,(\ell_1 + \ell_2 + k_3)^2\,(\ell_1 + \ell_2 + k_{23})^2\,(-2\ell_2 \cdot k_4)} \quad (4.3.41)$$

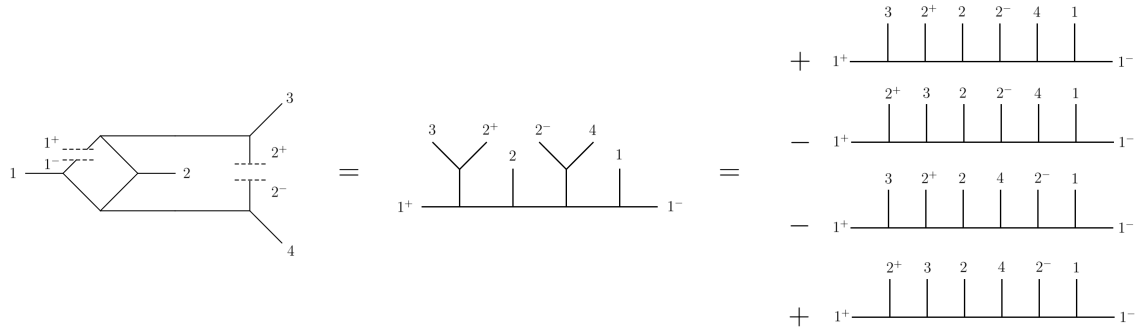

Figure 4.13: Another contribution to a non-planar double-box.

whose numerator we evaluate on the cut solutions given by

$$\ell_1^2 = \ell_2^2 = (\ell_2+k_3)^2 = (\ell_1-k_1)^2 = (\ell_1+\ell_2+k_3)^2 = (\ell_1+\ell_2+k_{23})^2 = (\ell_2-k_4)^2 = 0. \quad (4.3.42)$$

For these cases also we confirm that the numerators of (4.3.39) and (4.3.41) on their respective cut conditions (4.3.40) and (4.3.42) match the relevant numerator of (4.3.29), given by

$$(D_s-2)(\lambda_1^2\lambda_2^2+\lambda_1^2\lambda_{12}^2+\lambda_{12}^2\lambda_2^2)+16((\lambda_1\cdot\lambda_2)^2-\lambda_1^2\lambda_2^2)\,. \quad (4.3.43)$$

4.4 Discussion

This chapter studied a natural way of extending worldsheet formulae, already quite successful at tree-level and one-loop, to two-loops. We reviewed how the one-loop formulae can be seen in terms of a forward-limit, manifesting the colour-kinematics duality. In this formalism, though the loop-integrand admits an unorthodox representation (involving linear-type propagators) the kinematic numerators are computable to any order from tree-level results, detailed in section 1.3. We then applied this straightforwardly to two-loops and explained the novel features that start appearing at this order, inspiring two different representations of the proposed worldsheet formulae. This however was insufficient for the non-supersymmetric theories and we detailed the required modifications, allowing us to propose n-point formulae for the two-loop integrand of pure Yang-Mills and pure (derivable from NS-NS) gravity which also manifested the colour-kinematics duality in the same way. We then rephrased the supersymmetric results of [51] in this language, which provided insights allowing us to speculate on the origin of the modification required for generic theories, based on the genus-two ambitwistor string. Finally, we checked our formulae for pure Yang-Mills against known results at two-loops [185] using (maximal) unitarity cuts.

We remind the reader of some of the points mentioned throughout that are relevant to further research. Firstly, due to the versatility of the double copy, we believe our formulae can in principle be extended to any theory connected with a worldsheet description. We gave an example of this in (4.2.38) for the biadjoint scalar theory; its two-loop integrand can be inferred from the discussion in this chapter. Secondly, it would be fruitful to see if our conjecture regarding the origins of the modification were true. As mentioned in section 4.3.3, the use of a gluing operator [97] would be of great use in this endeavour. Thirdly, and more generally, a more detailed study of the two-loop scattering equations and their singular solutions would further the understanding of their role for theories with less supersymmetry.

It would be interesting to investigate an extension to three (and higher) loops, in the context of a *triple-forward-limit*. Unfortunately, at present this investigation would not be backed by the ambitwistor string, which has only currently been developed up to two-loops [51, 105]. Though the forward-limit interpretation seems natural, the absence of a study with the ambitwistor string would make any potential subtleties difficult to identify. Of course, we expect these to be minimised for supersymmetric theories, which we will explore in the next chapter. Furthermore, it is clear that our representation of the two-loop integrands is currently such that direct integration would be too difficult; this is due to the propagator structures and the number of terms appearing, both of which are vastly different from traditional representations. However, since these representations will agree on a set of unitarity cuts, this formalism provides a way of obtaining two-loop integrands using this method. Otherwise, one would have to find a way of making our representation more like the Feynman representation, and this would require a two-loop extension of the ℓ^2-deformed scattering equations presented in the previous chapter[17]. The discussion of section 3.8 is therefore relevant in this respect too.

[17] Although this would clearly be more intricate, since the scattering equations we use here already employ propagators involving both loop momenta to be quadratic.

Chapter 5

Superstring amplitudes from the scattering equations

A lot of worldsheet formulae at one and two loops are based on the genus one [50] and genus two [51] ambitwistor string. At this genus, the results from the ambitwistor string we have considered in this thesis have been based on the RNS formalism[1]. Therefore, many of the field theory results we have encountered in this thesis partially owe themselves to the superstring. In this sense the ambitwistor string acts as a strong connection between superstring theory and quantum field theory. On its own, field theory amplitudes can be obtained from the superstring via the field theory limit, but of course the converse is not true since there is no notion of α' in field theory. However, implicitly the field theory results contain some information from the massless spectrum of the superstring, since the field theory limit corresponds to the scattering of these states. It is therefore conceivable that one can use massless scattering in field theory to say something about the massless spectrum of the superstring. Of course, at first glance this seems incredibly difficult, since the mathematical objects used in the superstring can be much more complicated than those of field theory.

In this chapter we will argue that the ambitwistor string allows one to be capable of doing this. In light of this we will explain the relation between expressions for scattering of massless states in the superstring and their ambitwistor string counterpart, before describing more precisely how the ambitwistor string formulae are themselves related to worldsheet formulae for field theory. Amongst these relationships, modular invariance plays a fundamental role, so we dedicate section 5.1.2 to expand on the notion of modular weights and modular invariance and how they will be relevant for us. In section 5.2 we then discuss the strategy we will use to go from field theory expressions to worldsheet formulae, to ambitwistor string formulae, and finally to superstring formulae, thus reproducing the superstring amplitude purely from the results of field theory. This relies heavily on the field theory result admitting a BCJ representation for reasons that will become clear. We will demonstrate how the strategy works at two-loops, and then apply this strategy at three-loops, using known results from field theory, resulting in a proposal for the four-point scattering of massless states in the superstring at genus three.

[1]Though other formulations have been made, including the pure-spinor version [186] and the Green-Schwarz formulation [187].

5.1 Aspects of string amplitudes and their relation to field theory

The use of the scattering equations in worldsheet models precisely points out what makes string amplitudes intrinsically stringy. Namely, in superstring theory the integration over the moduli space is fairly non-trivial, and in order to actually get to this stage one has to formally understand the structure of the moduli space. This was achieved at genus-two in a series of papers [179, 188–192] by D'Hoker and Phong, where a rigorous study of the superstring amplitudes was performed. The procedure involves starting on a super-Riemann surface and integrating out the supermoduli to project onto the 'bosonic moduli space'. This space is the one more related to the discussion of this thesis, where we focus on ambitwistor strings which are naturally formulated on a bosonic Riemann surface. For the type II theories, at least up to genus-two [189], one can write the superstring integrand on the bosonic moduli space in a 'chiral way', exploiting the fact that the states of the theory come from left-movers and right-movers. This chiral splitting [193] allows the definition of the 'chiral integrand', and since the ambitwistor string is naturally a chiral theory the ambitwistor string integrand naturally coincides with the chiral integrand on a genus-g surface[2]. Indeed, this is what follows from the study of the genus-two ambitwistor string [51].

There are some issues with dealing with superstring amplitudes at higher-genus however. As mentioned above, defining the superstring amplitudes requires an understanding of the intrinsic moduli space, in order to adequately define the string measure. At any genus $g > 1$, the space of intrinsic moduli is $(3g-3)$-dimensional, and for genus $g = 2, 3$ this dimension coincides with the number of independent components of the period matrix $g(g+1)/2$. This allows the genus $g = 2, 3$ superstring measure to be directly related to the elements of the period matrix. For genus $g \geq 4$ however there must be restrictions if the measure is to be related to the period matrix, and so the measure is not currently fully understood; this is related to the well-known Schottky problem[3]. Furthermore, for genus $g \geq 5$ there is also known to be an issue with projecting the supermoduli space down to the reduced (bosonic) moduli space [195]. Of course, at genus $g = 3$ neither these fundamental issues themselves act as obstructions in achieving results therein, and this chapter is based on work that attempts to aid this endeavour.

How can we do this? The field-theory limit of superstring amplitudes is associated with $\alpha' \to 0$, or the string length going to zero. The amplitudes then pick up results from the massless spectrum of the superstring and are associated with supergravity field theory loop integrands in the case of the type II superstring. On the other hand, the scattering equation formalism arises from the ambitwistor string, which has no notion of α', and thus directly gives the field theory loop integrands of supergravity in the case of the type II ambitwistor string. Assuming then that the superstring integrands can be expressed using chiral integrands, one expects that the results from the ambitwistor string can be directly related to part of the superstring. More specifically, the amplitudes resulting from the ambitwistor string should be directly related to the scattering of massless states in the superstring. The beginning of this assumption is phrased as follows: up to three-loops, the

[2] More on this and chiral splitting in the ambitwistor string can be found in [194].
[3] We note that there exist parametrisations which avoid this issue, such as the Schottky parametrisation.

superstring amplitude for four massless states can be expressed as

$$\frac{\mathcal{A}^{(g)}_{\mathbb{S}}}{\mathcal{R}^4} = \int_{\mathfrak{M}_{g,4}} \Big| \prod_{I\leq J} d\Omega_{IJ} \Big|^2 \int d\ell \; |\mathcal{Y}^{(g)}_{\mathbb{S}}|^2 \prod_{i<j} |E(z_i,z_j)|^{\frac{\alpha' s_{ij}}{2}} \times \Big| \exp \frac{\alpha'}{2} \big(i\pi\, \Omega_{IJ}\, \ell^I \cdot \ell^J + 2\pi i \sum_j \ell^I \cdot k_j \int_{z_0}^{z_j} \omega_I \big) \Big|^2 . \tag{5.1.1}$$

In the above, the moduli space integral is over the genus-g fundamental domain parametrised by the period matrix Ω_{IJ}, and four marked points corresponding to insertions z_i of states with momenta k_i. The object $E(z_i,z_j)$ is the prime form, defined in appendix A, and we abbreviate the 'loop-measure' as $d\ell = \prod_I d^{10}\ell_I$. In fact, the part of (5.1.1) involving the prime form and the exponential together constitute the chiral $\times$ anti-chiral Koba-Nielson factors at loop-level. The prefactor $\mathcal{R}^4$ is purely kinematic and is related to the tree-level supergravity amplitude [196], which is proportional to $\mathcal{R}^4/(s_{12}s_{13}s_{14})$. Aside from this prefactor, we make no distinction between type IIA and type IIB superstrings, which differ by the choice of GSO projection, since the odd spin structures do not contribute at four points up to three-loops[4]. The object $\mathcal{Y}^{(g)}_{\mathbb{S}}$ will therefore be the primary object of interest to us. To understand why let us compare with what is expected from the genus-g ambitwistor string,

$$\frac{\mathcal{A}^{(g)}_{\mathbb{A}}}{\mathcal{R}^4} = \int d\ell \int_{\mathfrak{M}_{g,4}} \prod_{I\leq J} d\Omega_{IJ} \; (\mathcal{Y}^{(g)}_{\mathbb{A}})^2 \prod_{i=1}^{4} \bar{\delta}(\mathcal{E}_i) \prod_{I\leq J} \bar{\delta}(u_{IJ}) \,, \tag{5.1.2}$$

which provides the field theory integrands for type II supergravity. The delta functions above enforce the genus-g scattering equations, which serve to localise the intrinsic moduli integration onto the maximal non-separating boundary divisor. Of course, the loop integration is divergent in ten-dimensions, so (5.1.2) is to be understood as a formal definition of the loop integrand, which can undergo dimensional reduction on the nodal sphere[5]. As noted in section 4.3.2, the object $\mathcal{Y}^{(g)}_{\mathbb{A}}$ actually coincides with that of the superstring up to $g=2$,

$$\mathcal{Y}^{(g)}_{\mathbb{S}} = \mathcal{Y}^{(g)}_{\mathbb{A}} \,. \tag{5.1.3}$$

This means on our working assumption we can obtain the superstring chiral integrand through the knowledge of what is expected from the ambitwistor string. Since the ambitwistor string integrand corresponds to supergravity field theory integrands, we can then deduce the former through the knowledge of the field theory result. This leads to a very unexpected series of deductions,

$$\text{Field theory} \quad \mapsto \quad \text{Ambitwistor string} \quad \mapsto \quad \text{Superstring} \tag{5.1.4}$$

[4] As mentioned in section 2.6, the fermions Ψ^μ, $\tilde{\Psi}^\nu$ in the odd spin structures have zero-modes, and the integration over these zero-modes each produce a ten-dimensional Levi-Civita symbol. Prior to loop integration these must be contracted into the kinematic data $\{k_i, \epsilon_i\,(\tilde{\epsilon}_i), \ell_i\}$, with ϵ ($\tilde{\epsilon}$) associated with the Levi-Civita tensor resulting from the zero-modes of Ψ^μ_0 ($\tilde{\Psi}^\nu_0$) respectively. However, the kinematic prefactor can be written as $\mathcal{R}^4 = \mathcal{F}^4(\epsilon)\mathcal{F}^4(\tilde{\epsilon})$, where e.g. $\mathcal{F}^4(\epsilon)$ comes from the open superstring and involves products $\epsilon_i \cdot \epsilon_j$, which cannot arise through contraction with the Levi-Civita tensor. Moreover, *after* loop integration the contraction between Levi-Civita tensors will at most produce $\epsilon_i \cdot \tilde{\epsilon}_j$ contractions, but this is inconsistent with the factorisation of $\mathcal{R}^4$ above. These observations are consistent with those found in [197, 198].

[5] One cannot dimensionally reduce on the genus-g surface as $D=10$ is required for modular invariance. On the nodal sphere however, there is no such restriction and one can freely dimensionally reduce to $D<10$.

and indeed we will show how this is possible at two-loops. This is rather confounding, given that typically this is done (in a sense) in the opposite fashion. With this however, we will be able to propose an expression for the chiral integrand at three-loops.

In order to do this, we first need to understand some details about how the ambitwistor string amplitudes are related to those of field theory, which we will now discuss.

5.1.1 Aspects of ambitwistor string degenerations

The scattering equations in (5.1.2) localise the amplitude onto the maximal non-separating boundary divisor, and so the resulting worldsheet formulae are naturally expressed on a g-nodal sphere,

$$\frac{\mathcal{A}^{(g)}_{\mathbb{A}}}{\mathcal{R}^4} = \int \frac{d\ell}{\prod_I (\ell^I)^2} \int_{\mathcal{M}_{0,4+2g}} c^{(g)} \big(\mathcal{J}^{(g)} \mathcal{Y}^{(g)}\big)^2 \prod_{A=1}^{4+2g} \bar{\delta}(\mathcal{E}_A) \ . \tag{5.1.5}$$

where $\mathcal{Y}^{(g)}$ to defined as $\mathcal{Y}^{(g)}_{\mathbb{A}}$ in the limit of the non-separating degeneration, and $c^{(g)}$ is a cross-ratio appearing therein. Here we point out a few details in this process, which may be recognised from previous chapters. The purpose for this is for us to better understand how the ambitwistor string formulae result in worldsheet formulae for the corresponding field theory, so that these details can be properly considered when we go the other way.

Firstly, recall that the modular scattering equations $u^{IJ} = 0$ ensure that the holomorphic part of the quadratic differential P^2 vanishes on the Riemann surface,

$$P^2 = u^{IJ}\, \omega_I\, \omega_J = 0 \tag{5.1.6}$$

on the support of the other scattering equations $\mathcal{E}_i = 0$ (which alone ensure P^2 has no simple poles). The product of Abelian differentials of the first kind $\omega_I\, \omega_J$ act as a basis of holomorphic quadratic differentials. Since the u^{IJ} are symmetric, this gives $g(g+1)/2$ scattering equations, coincident with the number of intrinsic moduli integrations in the measure $\prod_{I\leq J} d\Omega_{IJ}$ for $g = 2, 3$. To study the degeneration limit, it is more convenient to use the parameters

$$q_{IJ} = e^{2\pi i\, \Omega_{IJ}} \qquad \Rightarrow \qquad d\Omega_{IJ} = \frac{1}{2\pi i} \frac{dq_{IJ}}{q_{IJ}} \tag{5.1.7}$$

for $I \neq J$ and analogously for $q_{II} = e^{i\pi \Omega_{II}}$. Formally speaking, the maximal non-separating degeneration occurs in the limit where the variables involving the diagonal components of the period matrix go to zero, $q_{II} \to 0$. In this limit the Abelian differentials of the first kind acquire simple poles at their respective nodal points via Fay's degeneration formula [199],

$$\omega_I(\sigma) \quad \mapsto \quad \omega_{I^+I^-}(\sigma) = \frac{(\sigma_{I^+} - \sigma_{I^-})}{(\sigma - \sigma_{I^+})(\sigma - \sigma_{I^-})} \frac{d\sigma}{2\pi i} \, . \tag{5.1.8}$$

The off-diagonal components of the period matrix then become

$$\Omega_{IJ} := \oint_{B_J} \omega_I = \int_{\sigma_{J^-}}^{\sigma_{J^+}} \frac{(\sigma_{I^+} - \sigma_{I^-})}{(\sigma - \sigma_{I^+})(\sigma - \sigma_{I^-})} \frac{d\sigma}{2\pi i} = \frac{1}{2\pi i} \ln \frac{\sigma_{I^+J^+} \sigma_{I^-J^-}}{\sigma_{I^+J^-} \sigma_{I^-J^+}} \, .$$

The parameters q_{IJ} for $I \neq J$ consequently become cross-ratios in the nodal points as a result of (5.1.7),

$$q_{IJ} = \frac{\sigma_{I^+J^+} \sigma_{I^-J^-}}{\sigma_{I^+J^-} \sigma_{I^-J^+}} \, . \tag{5.1.9}$$

This leads to a change of variables in the measure for the remaining modular parameters, with an associated Jacobian

$$\prod_{I<J} \frac{dq_{IJ}}{q_{IJ}} = \frac{\mathcal{J}^{(g)}}{\text{vol SL}(2,\mathbb{C})}\,, \qquad \mathcal{J}^{(g)} = J^{(g)} \prod_{I^\pm} d\sigma_{I^\pm}\,. \tag{5.1.10}$$

Let us now look at what happens with the scattering equations. In practice, one might enforce not the u^{IJ} alone to vanish but linear combinations thereof,

$$\prod_{I<J} \bar{\delta}(u^{IJ}) \quad \to \quad \prod_{I<J} \bar{\delta}(\tilde{u}^{IJ})\,, \tag{5.1.11}$$

where now the $\tilde{u}^{IJ}$ are linear combinations of the u^{IJ}. There is a number of reasons why one might choose to do this. Firstly, not all scattering equations will lead to the nodal sphere, and in the global residue theorem one may get contributions from e.g. nodal tori. To get an expression solely on the nodal sphere, a linear combination of scattering equations must usually be considered. An example of this can be seen at two-loops [51] where on the genus-two surface one enforces

$$\bar{\delta}(\tilde{u}^{11})\,\bar{\delta}(\tilde{u}^{22})\,\bar{\delta}(\tilde{u}^{12}) := \bar{\delta}(u^{11})\,\bar{\delta}(u^{22})\,\bar{\delta}(u^{11}+u^{22}+u^{12})\,. \tag{5.1.12}$$

The first two scattering equations are used in the global residue theorem, and the last one ensures that contributions on nodal tori vanish. Secondly, different choices will lead to different loop propagators from the resulting worldsheet formulae. This is clear since ultimately the kinematic pole structure is determined by the scattering equations on the nodal sphere. Thus, to obtain the desired loop propagators one may appropriately choose which scattering equations to enforce.

After the degeneration, the role of the remaining delta functions is to produce the scattering equations for the nodal points. To see this explicitly one writes them as

$$\mathcal{E}_{I^\pm} = \sum_J \tilde{u}^{IJ}\,\omega_{J^+J^-}(\sigma_{I^\pm})\,, \tag{5.1.13}$$

from which one can derive

$$\prod_{I<J} \bar{\delta}\left(\tilde{u}^{IJ}\right) = \mathcal{J}^{(g)} \prod_{I^\pm} \bar{\delta}\left(\mathcal{E}_{I^\pm}\right) \tag{5.1.14}$$

with an appropriate Jacobian factor $\mathcal{J}^{(g)}$. For genus $g = 2, 3$ this Jacobian is the same as that coming from the measure, leading to the factor $(\mathcal{J}^{(g)})^2$ appearing in (5.1.5). These Jacobians are important since they provide the correct $\text{SL}(2,\mathbb{C})$ weight to the nodal points.

Finally let us mention how the cross ratios typically arise, and what their purpose is in the worldsheet formulae. Notice that in (5.1.9), for some I, J were one to use the $\text{SL}(2,\mathbb{C})$ symmetry to fix $\sigma_{J^+} = 0$, $\sigma_{I^-} = 1$, $\sigma_{J^-} = \infty$ then the modular parameter q_{IJ} becomes equal to one of the nodes, $q_{IJ} = \sigma_{I^+}$. The integration of σ_{I^+} is unconstrained and over the full $\mathbb{CP}^1$, however the integration region for q_{IJ} is over the fundamental domain and thus *is* constrained. Using modular invariance there is a way to extend the integration region of q_{IJ} to the whole complex plane on the support of a weight function $f(q_{IJ})$; at two-loops this is seen in [51]. The weight functions are functions of the q_{IJ} and have to satisfy some constraints which can be used to determine them, such as $f(q_{IJ}) + f(q_{IJ}^{-1}) = 1$, and that they cannot introduce new poles into the integrand. After substituting the expressions (5.1.9) into the support functions, they become precisely the cross-ratios appearing in (5.1.5).

They play an important role on the nodal sphere in disallowing unphysical poles to arise from the moduli space integrations. We already saw this in section 4.2.2 for two-loops, when we spoke about the 'cross-ratio prescription'. Their effect can also be seen when considering worldsheet factorisations, and what propagators these allow from the scattering equations. In fact, the set of cross-ratios required can also be postulated for a given set of scattering equations based on the principle that only physical propagators should arise.

5.1.2 Modular invariance and modular weights

In order for any string-like amplitude on a Riemann surface of non-zero genus to be valid, it is a necessity that it is modular invariant. Modular invariance plays a key role in determining correct expressions for string integrands, much like how Möbius invariance plays a key role in what is an allowed CHY integrand. To be slightly more precise, whilst the latter dictates that any valid integrand on the Riemann sphere must have the correct $\mathrm{SL}(2,\mathbb{C})$ weight, the former dictates that any valid expression on higher-genus Riemann surfaces must have the correct modular weight. In this section we will discuss modular weights for the various objects appearing on the higher-genus surface, which will strongly constrain what can and cannot be uplifted to the higher-genus surface from the Riemann sphere.

At genus $g > 0$, a Riemann surface has a discrete set of symmetries, determined by the group $\mathrm{Sp}(2g,\mathbb{Z})$, the *modular group*. On the torus ($g = 1$) this is the group $\mathrm{Sp}(2,\mathbb{Z})$, generated by translations and inversions. More generally, the group $\mathrm{Sp}(2g,\mathbb{Z})$ consists of the set of matrices which preserve the symplectic form,

$$\begin{pmatrix} a & b \\ c & d \end{pmatrix} \begin{pmatrix} 0 & \mathbb{1} \\ -\mathbb{1} & 0 \end{pmatrix} \begin{pmatrix} a & b \\ c & d \end{pmatrix}^T = \begin{pmatrix} 0 & \mathbb{1} \\ -\mathbb{1} & 0 \end{pmatrix}, \qquad M = \begin{pmatrix} a & b \\ c & d \end{pmatrix} \in \mathrm{Sp}(2g,\mathbb{Z}) \tag{5.1.15}$$

where a, b, c, d are themselves $g \times g$ matrices, and $\mathbb{1}$ is the $g \times g$ unit matrix. They act on the homology basis of cycles A_I, B_I as

$$\begin{pmatrix} B'_I \\ A'_I \end{pmatrix} = \begin{pmatrix} a & b \\ c & d \end{pmatrix} \begin{pmatrix} B_I \\ A_I \end{pmatrix}, \tag{5.1.16}$$

from which one can derive that the Abelian differentials of the first kind transform as

$$\omega' = (c\Omega + d)^{-1}\,\omega \tag{5.1.17}$$

where Ω is the period matrix. This follows by assuming they transform linearly under $\mathrm{Sp}(2g,\mathbb{Z})$ and that $\oint_{A_I}\omega_J = \delta_{IJ}$ is preserved. Since they are used to define the period matrix, one can subsequently show that the period matrix must transform as

$$\Omega' = (a\Omega + b)(c\Omega + d)^{-1} \tag{5.1.18}$$

from $\oint_{B_I}\omega_J = \Omega_{IJ}$. Now in the ambitwistor string the field P_μ descends straightforwardly to the nodal sphere, so it must be invariant under modular transformations. Since on the genus-g surface it contains zero-modes of the form $\ell^I_\mu\,\omega_I$, then these must also be modular invariant. Consequently, the loop-momentum ℓ^I_μ must transform to compensate for the transformation in (5.1.17),

$$\ell'_\mu = (c\Omega + d)\,\ell_\mu\,. \tag{5.1.19}$$

With the transformation properties (5.1.18) and (5.1.19) we can see how the ambitwistor string measure transforms under modular transformations,

$$\prod_{I\leq J} d\Omega_{IJ} \quad \to \quad \det(c\Omega+d)^{-(g+1)} \prod_{I\leq J} d\Omega_{IJ}\,, \tag{5.1.20}$$

$$d\ell = \prod_{I} d^{10}\ell^I \quad \to \quad \det(c\Omega+d)^{10} \prod_{I} d^{10}\ell^I\,. \tag{5.1.21}$$

From this we say that they have *modular weight* $-(g+1)$ and 10 respectively. As for the scattering equations, those related to the external punctures come from the residue of P^2, which is modular invariant from the considerations above (5.1.19); therefore, they have modular weight 0. The scattering equations enforced by the factors $\bar{\delta}(u^{IJ})$ however must carry non-zero modular weight because if P^2 is modular invariant then $\tilde{u}^{IJ}$ must have the correct weight to compensate the weight of $\omega_I\,\omega_J$. Therefore u^{IJ} must have modular weight 2, which means that $\bar{\delta}(u^{IJ})$ has weight -2, and therefore

$$\prod_{I\leq J} \bar{\delta}(u^{IJ}) \quad \to \quad \det(c\Omega+d)^{-(g+1)} \prod_{I\leq J} \bar{\delta}(u^{IJ})\,. \tag{5.1.22}$$

To sum up what we have so far, the amplitude (5.1.2) looks like

$$\int \underbrace{\prod_{I} d^{10}\ell^I}_{+10} \int_{\mathfrak{M}_{g,4}} \underbrace{\prod_{I\leq J} d\Omega_{IJ}}_{-(g+1)} \underbrace{\left(\mathcal{Y}^{(g)}_{\mathbb{A}}\right)^2}_{+2\kappa} \underbrace{\prod_{i=1}^{4} \bar{\delta}(\mathcal{E}_i)}_{+0} \underbrace{\prod_{I\leq J} \bar{\delta}(u^{IJ})}_{-(g+1)}\,, \tag{5.1.23}$$

where the numbers in blue above display the corresponding modular weights, and we have denoted the modular weight of the unknown object $\mathcal{Y}^{(g)}_{\mathbb{A}}$ as κ. For the integrand to be modular invariant (weight 0), we therefore require

$$\kappa = g-4\,, \tag{5.1.24}$$

in other words $\mathcal{Y}^{(g)}_{\mathbb{A}}$ must transform as

$$\mathcal{Y}^{(g)}_{\mathbb{A}} \quad \to \quad \det(c\Omega+d)^{g-4}\,\mathcal{Y}^{(g)}_{\mathbb{A}} \tag{5.1.25}$$

under $\mathrm{Sp}(2g,\mathbb{Z})$. Though we have considered $(\mathcal{Y}^{(g)}_{\mathbb{A}})^2$ to form the integrand at four points, we have made no mention of this in the current argument, and therefore it is valid for any any expression which can be written this way.

Since the integrands on the nodal sphere must in principle be upgradable to the higher-genus surface, having the correct modular weight plays a key role in determining what these integrands can be composed of. This is coupled with the restrictions on the nodal sphere, in the sense that the integrand (a) must have the correct $\mathrm{SL}(2,\mathbb{C})$ weights in all the marked points, and it must also (b) have the correct modular weight in order to be upgraded to the higher-genus surface. These place strong restrictions on what the objects $\mathcal{Y}^{(g)}_{\mathbb{A}} = \mathcal{Y}^{(g)}_{\mathbb{S}}$ must be, and in the next section we will discuss a strategy to determine them.

5.2 The stratagem

Given that the ambitwistor string integrand gives the field theory amplitudes of supergravity, we can use the latter to try and deduce the former. Provided this is true, and that we can find a natural way to write this on the genus-g surface, there is a crucial feature that will allow us to relate it to the superstring. We will discuss this detail momentarily, but first let us present the general strategy. The procedure goes as follows:

(1) Take a supergravity loop-integrand, written in a BCJ double copy representation,

(2) Translate it into a formula for the ambitwistor string on the nodal sphere in the form of a moduli space integral; i.e. obtain $\mathcal{Y}^{(g)}$,

(3) Uplift the formula to the genus-g surface to be one conjecturally valid for the superstring; i.e. obtain $\mathcal{Y}^{(g)}_{\mathbb{A}} \to \mathcal{Y}^{(g)}_{\mathbb{S}}$.

Step (1) of course relies on the existence of such a representation of the loop-integrand, which is currently known up to five-loops [165]. Whilst initially inspired by the string theory story at tree-level, continuous work is going on to understand more deeply the connection at loop level [149, 200–205]. Step (2) utilises the connection with the scattering equation formalism, where the supergravity field theory integrands are obtainable from the ambitwistor string. In this respect, results from the latter have been obtained up to two-loops [51, 105, 180]. This relies on the ability to express the integrands in a basis which is reminiscent of the BCJ representation after loop integration, i.e.

$$(2\pi i)^4 \mathcal{J}^{(g)} \mathcal{Y}^{(g)} = \sum_{\rho \in S_{2+2g}} \frac{N^{(g)}(1^+, \rho, 1^-)}{(1^+ \, \rho \, 1^-)} \tag{5.2.1}$$

where as usual $(1^+ \, \rho \, 1^-)$ is defined to be the Parke-Taylor factor with the relevant ordering[6], as in 3.7.6. This decomposition has been central to this thesis, and here there is no exception. Once this is done, step (2) is achieved. Step (3) plays on the similarities of the chiral integrands of type II supergravity between the ambitwistor string and the RNS superstring. It relies crucially on two features.

The first, as described in the last section, is that the LHS of (5.2.1) is written in terms of objects that make sense and have the correct modular weight on the higher-genus surface. This is necessary for $\mathcal{Y}^{(g)}$ to be well-defined therein, and thus allows a sensible transition between $\mathcal{Y}^{(g)}$ and $\mathcal{Y}^{(g)}_{\mathbb{A}}$.

The second is that the expansion (5.2.1) *does not rely on the scattering equations*. In the superstring, there is no notion of the scattering equations, so relating the RHS of (5.2.1) to $\mathcal{Y}^{(g)}_{\mathbb{S}}$ may seem somewhat illegitimate if in principle it requires the scattering equations to do so. We have seen that in some cases expansions similar to (5.2.1) are only valid on the support of the scattering equations, however recall from section 4.3.2 that this isn't always the case. Namely, for four-points up to two-loops it is known that such an expansion turns out to follow algebraically for worldsheet models of maximally supersymmetric field theories. This property allows the $\mathcal{Y}^{(g)}_{\mathbb{A}}$ obtained from $\mathcal{Y}^{(g)}$ to be sensibly related to $\mathcal{Y}^{(g)}_{\mathbb{S}}$.

[6] We remind the reader that whilst 1^+ and 1^- has been chosen to lie at the endpoints, the sum is independent of this choice.

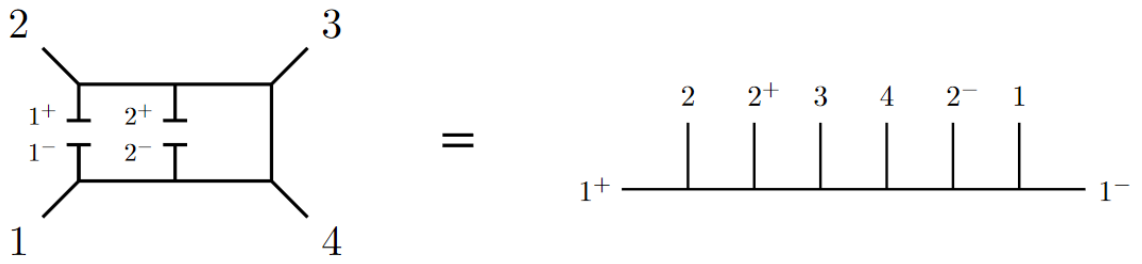

Figure 5.1: An example of a two-loop diagram whose numerator corresponds to a master numerator.

5.2.1 Two-loop example

Let us demonstrate the strategy at two-loops. For context, following the discussion of 5.1.1, the measure for the intrinsic moduli consists of the three independent components of the period matrix. These are related to the parameters q_{11}, q_{22} and q_{12} through the relation (5.1.7), and the nodal sphere limit is associated with $q_{11}, q_{22} \to 0$. In this limit the remaining parameter becomes a cross-ratio in the nodal points through (5.1.9),

$$q_{12} = \frac{\sigma_{1^+2^+}\sigma_{1^-2^-}}{\sigma_{1^+2^-}\sigma_{1^-2^+}}\,. \tag{5.2.2}$$

From this one can deduce the Jacobian factors coming from the change of variables and from the scattering equations. The cross-ratio follows from the argument given in section 5.1.1 and well-detailed in [51]. These quantities are

$$\mathcal{J}^{(2)} = \frac{d\sigma_{1^+}\, d\sigma_{1^-}\, d\sigma_{2^+}\, d\sigma_{2^-}}{\sigma_{1^+2^+}\sigma_{1^+2^-}\sigma_{1^-2^+}\sigma_{1^-2^-}}\,, \qquad c^{(2)} = \frac{1}{1-q_{12}} = \frac{\sigma_{1^+2^-}\sigma_{1^-2^+}}{\sigma_{1^+1^-}\sigma_{2^+2^-}}\,. \tag{5.2.3}$$

Again, for genus-two the Jacobian coming from the measure and the scattering equations turn out to be the same. We have already encountered the BCJ numerators for supergravity at two-loops in section 4.3.2; here we write them as

$$N^{(2)}(1^+, \rho_1, 2^\pm, \rho_2, 2^\mp, \rho_3, 1^-) = \begin{cases} s_{ij} & \rho_2 = \{i,j\} \\ 0 & \text{otherwise}\,. \end{cases} \tag{5.2.4}$$

The difference between the above and (4.3.20) is related to the factor $\mathcal{R}^4$ being pulled out of the expression in (5.1.5). These numerators as usual are related to half-ladder diagrams as in figure 5.1, and as such are considered BCJ master numerators associated with BCJ master diagrams. All other numerators are obtained from these by appropriate applications of the Jacobi identity. The identification of these numerators completes step (1).

Using the numerators (5.2.4) and the Jacobian (5.2.3), the expansion (5.2.1) follows from taking $\mathcal{Y}^{(2)}$ to be

$$\mathcal{Y}^{(2)} = \frac{1}{3}\big((s_{14}-s_{13})\Delta^{(2)}_{12}\Delta^{(2)}_{34} + \text{cyc}(234)\big) \tag{5.2.5}$$

where the objects $\Delta^{(2)}_{ij}$ are defined to be

$$\Delta^{(2)}_{ij} = \omega_{1^+1^-}(\sigma_i)\omega_{2^+2^-}(\sigma_j) - \omega_{1^+1^-}(\sigma_j)\omega_{2^+2^-}(\sigma_i)\,. \tag{5.2.6}$$

This completes step (2). As mentioned in section 4.3.2, these have a natural extension to a higher-genus expression, given in general by

$$\Delta^{(g)}_{i_1\cdots i_g} = \epsilon^{I_1\cdots I_g}\,\omega_{I_1}(\sigma_{i_1})\cdots\omega_{I_g}(\sigma_{i_g})\,. \tag{5.2.7}$$

Recall that the Abelian differentials of the first kind $\omega_I(\sigma)$ in the degeneration limit becomes $\omega_{I^+I^-}(\sigma)$ through Fay's degeneration formula [199]; this is how one gets to (5.2.6) from (5.2.7).

Since (5.2.5) is expressed in terms of objects that uplift naturally to genus-two (that is, $\Delta^{(2)}_{ij}$), we need only check that it has the right modular properties to be valid in an expression for the integrand therein. From (5.1.17), under modular transformations the objects (5.2.7) become

$$\begin{aligned}\Delta^{(g)}_{i_1\cdots i_g} &\to \epsilon^{I_1\cdots I_g}\,(c\Omega+d)^{-1}_{I_1J_1}\cdots(c\Omega+d)^{-1}_{I_gJ_g}\omega_{J_1}(\sigma_{i_1})\cdots\omega_{J_g}(\sigma_{i_g})\\ &= \det(c\Omega+d)^{-1}\;\epsilon^{J_1\cdots J_g}\,\omega_{J_1}(\sigma_{i_1})\cdots\omega_{J_g}(\sigma_{i_g})\\ &= \det(c\Omega+d)^{-1}\;\Delta^{(g)}_{i_1\cdots i_g}\,,\end{aligned} \tag{5.2.8}$$

i.e. they have modular weight -1. Then (5.2.5) must have modular weight -2, which is consistent with (5.1.25). Therefore, (5.2.5) has the correct modular properties to be upgraded to the genus-two surface, and this completes step (3).

Put into perspective, $\mathcal{Y}^{(2)}_{\mathbb{A}}$ is obtained as (5.2.5) using the definition (5.2.7) for $g=2$. We remark that the expansion of (5.2.5) into (5.2.1) does *not* rely on the scattering equations, and is true for any set of locations for the marked points, i.e. it is an algebraic equality. One thus concludes that $\mathcal{Y}^{(2)}_{\mathbb{A}}$ is a valid candidate for the superstring integrand $\mathcal{Y}^{(2)}_{\mathbb{S}}$ at genus-two. This turns out to be precisely correct, and matches the results of [179] for four massless states in the RNS formalism. Therefore, the strategy presented in the last section proves to be successful at genus-two.

Let us make one comment regarding this demonstration. The expression for $\mathcal{Y}^{(2)}$ on the nodal sphere was derived explicitly in [51] by simplifying the sum over spin structures in the amplitude for four massless states in the genus-two ambitwistor string. $\mathcal{Y}^{(2)}_{\mathbb{A}}$ consequently matches the previously obtained result on the genus-two surface [180]. However, given the numerators (5.2.4) within the expansion (5.2.1), the expression (5.2.5) could have been deduced *a priori* by considering various ansatzes based on having the correct $\mathrm{SL}(2,\mathbb{C})$ and modular weights, as well as permutation symmetry. In this respect, objects such as $\Delta_{12}\Delta_{34}$ seem quite natural, since they have the correct weight in the external punctures[7], as well as the correct modular weight on the genus-two surface. Therefore, such an ansatz could have been proposed naturally, where one could then readily solve for the correct coefficients, thereby obtaining (5.2.5). Therefore, the genus-two superstring expression for four massless states could have been proposed from field theory alone using this strategy.

There are then two logical questions one might ask: how precisely one obtains the numerators in (5.2.1), and can this be applied to three-loops. We will answer both of these questions in the upcoming sections.

[7]Recall that the $\mathrm{SL}(2,\mathbb{C})$ weights for the nodal points are supplied by the Jacobian factors.

5.3 Three-loop application

To date, four-point superstring results have only been obtained up to two-loops; in the RNS formalism this was achieved in a series of works [179, 188–192] by D'Hoker and Phong, with more complete results found by Berkovits [206] using the pure-spinor formalism. At genus three, some results have been obtained using the pure-spinor string in [197], and also studied by the authors of [207]. However there has not been a proposal for the three-loop amplitude for four massless states directly from the superstring. In fact, many results from field theory have been obtained directly from the superstring, such as the first one-loop amplitude in super Yang-Mills theory [208]. This work is an attempt to return the favour by giving such a proposal for the result potentially obtainable from the superstring at genus-three, based on the knowledge of field theory at three-loops.

Here we will show how to write the BCJ representation of the loop-integrand in the form (5.2.1), and use the strategy presented in section 5.2 to give a proposal for the three-loop superstring integrand based on modular invariance. The proposal will be consistent with a few results previously conjectured for the genus-three superstring.

5.3.1 Determining the KK expansion

In the last section we alluded to the idea that the genus-two superstring expression could have been proposed solely based on the results of field theory at two-loops. There is one question that might seem unanswered in this respect, and that is how precisely one obtains the expansion (5.2.1) from the field theory expression for the loop-integrand. For completeness, we will present in this section how this is exactly done, by constructing the expansion at three-loops. This procedure is required in going from step (1) to step (2) in our strategy.

At three-loops, step (1) requires a BCJ representation of the supergravity integrand. Such a representation is given in [12] for four-points[8]. There it gives the set of trivalent diagrams required for the three-loop integrand (figure 2 of that reference) with their corresponding BCJ numerators (table 1 of that reference). In figure 5.2 we have recreated the required set of trivalent diagrams for convenience.

The numerators in the expansion (5.2.1) correspond to the numerators of half-ladder diagrams, as seen in figure 5.1 for two-loops. For any assigned locations of the loop momenta, each of the diagrams in figure 5.2 can be 'cut' at these locations to produce a tree-like trivalent diagram with $4 + 6$ legs (two for each loop). Our numerators are then constructed as follows:

(i) Take the set of relevant trivalent loop diagrams in the BCJ representation;

(ii) Consider all possible placements of the loop momenta and 'cut' the diagrams at these places;

(iii) Collect the diagrams, with the associated placements of the loop momenta, which when 'cut' at these places produce a half ladder diagram;

(iv) Read off the BCJ numerator for those diagrams with their relevant loop assignments; this will be the numerator for the ordering prescribed by the ordering of the corresponding half-ladder.

[8] These results are for $\mathcal{N} = 8$ supergravity, but we will assume it oxidates naturally to ten-dimensions, and that the former results from dimensional reduction.

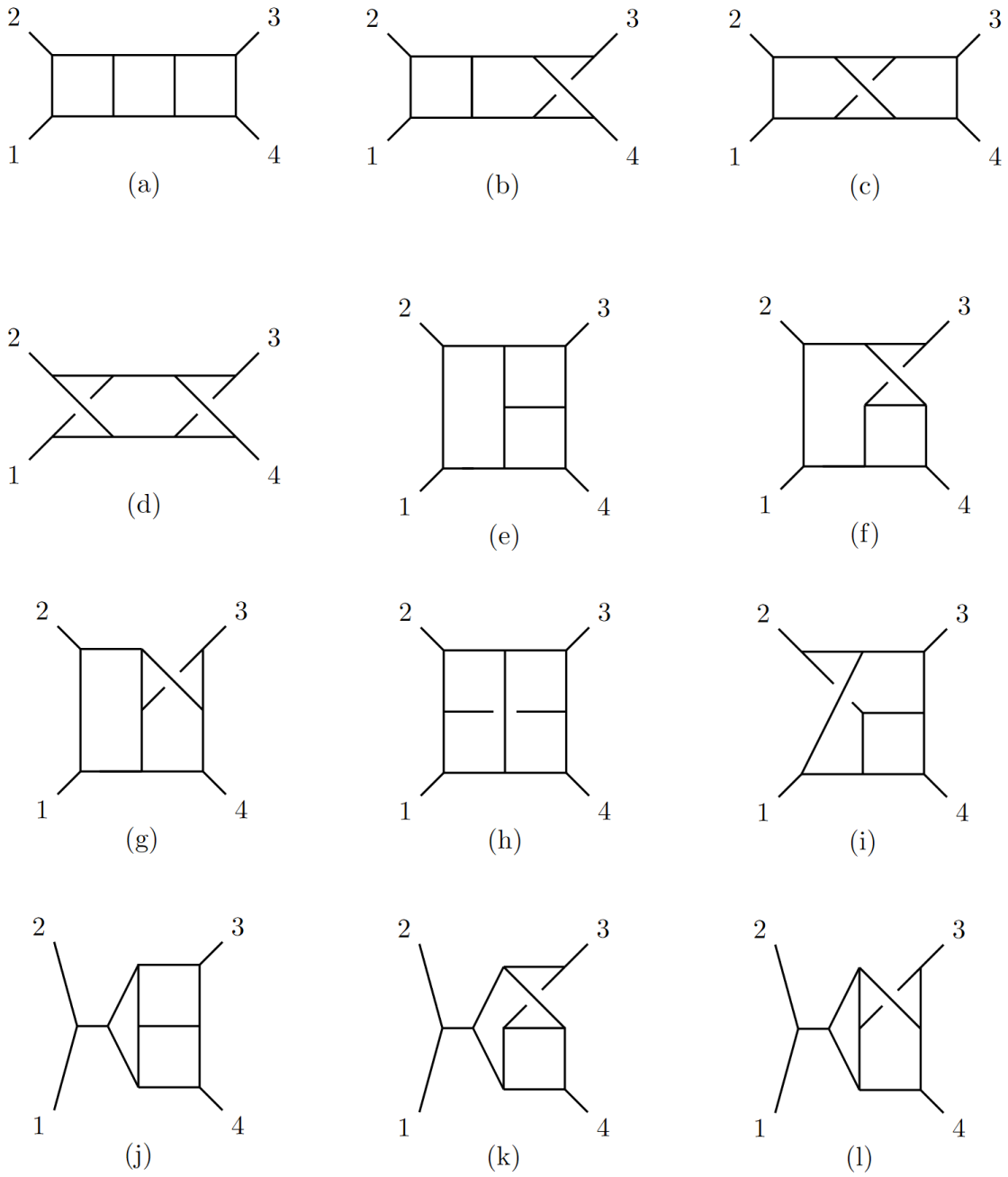

Figure 5.2: The three-loop BCJ master diagrams presented in [12].

Whilst this may seem like a laborious process, there are many shortcuts one can take in deriving all the relevant numerators. For example, not all trivalent loop diagrams *can* be cut into half-ladders, for any assignment of the loop momenta, which can be seen relatively quickly. In figure 5.2 it turns out that of the 12 diagrams only 5 can actually be cut into half-ladders, which are graphs (a), (c), (f), (g) and (h). Moreover, for any such graph one can assign an 'outside loop' on which the loop momentum ℓ_1 must lie (if the end-points of the half-ladders are chosen to be 1^+ and 1^-). Finally, for any half-ladder which *is not*

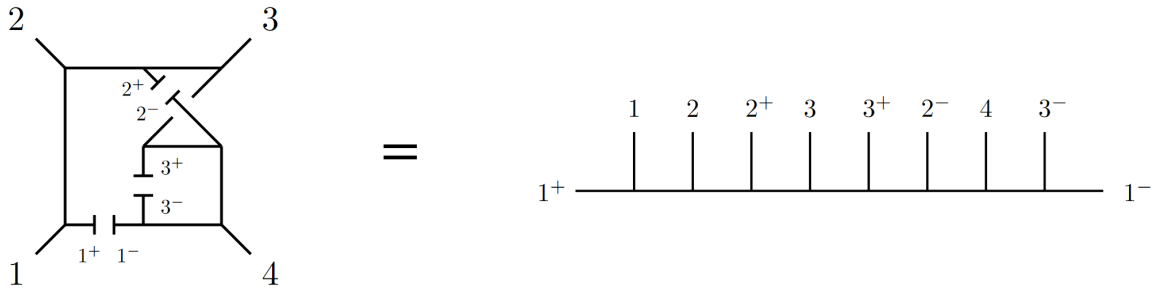

Figure 5.3: An example of obtaining the numerator at three-loops for a diagram with a specific assignment of the loop momenta. In this case, cutting the diagram at the loop-placements brings it directly to a half-ladder diagram with end-points 1^+ and 1^-; therefore the numerator for this diagram corresponds to one of our master numerators.

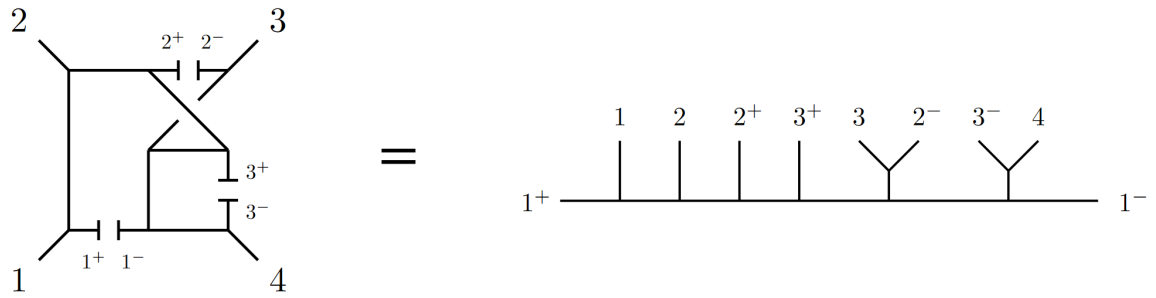

Figure 5.4: Another example of the same diagram, here with a different loop assignment. In this case, cutting the diagram at the endpoints does *not* result in a half-ladder diagram, so we do not include it when calculating the master numerators (instead, it is determined *by* the master numerators, via Jacobi identities).

obtained by this process, the corresponding numerator is set to 0.

To give an example of how this is done explicitly, figures 5.3 and 5.4 show part of this procedure in the case of considering diagram (f). This is formally part of stage (*ii*) in constructing the numerators above. Notice that with the choice of loop placements, the diagram in figure 5.3 is 'cut' into a half-ladder diagram, whereas in figure 5.4 the resulting diagram is not directly a half-ladder. Consequently, in stage (*iii*) of obtaining the numerators, the diagram in figure 5.3 is 'collected'; its half-ladder corresponds to the permutation $(1, 2, 2^+, 3, 3^+, 2^-, 4, 3^-, 1^-)$ and therefore its numerator is read off from [12] to be

$$N^{(3)}(1, 2, 2^+, 3, 3^+, 2^-, 4, 3^-, 1^-)$$
$$= \frac{1}{3}\left[-s_{12}^2 + s_{13}\,(2\ell_1 \cdot (k_2 + k_3)) - s_{14}\,(2\ell_1 \cdot (k_2 + k_4)) + s_{12}\,(2\ell_1 \cdot (-k_3 + k_4) + s_{14})\right]. \tag{5.3.1}$$

It is in this way that the numerators of the expansion (5.2.1) are calculated. Of course, this can also be applied to loop integrands at any order, particularly two-loops. Following the discussion at the end of section 5.2.1, the two-loop numerators $N^{(2)}$ could have been calculated precisely this way, concluding that the two-loop superstring result $\mathcal{Y}_{\mathbb{S}}^{(2)}$ could have been solely obtained from field theory using the strategy presented in section 5.2.

In the three-loop case, this is how we obtain the numerators for all permutations in the

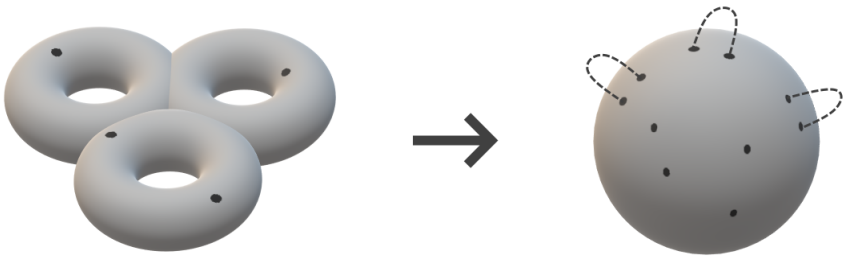

Figure 5.5: The expected degeneration of the genus-three surface to the tri-nodal sphere.

expansion (5.2.1). From the discussion above, most of the numerators (out of a possible $(4+4)! = 40,320$) are equal to zero, in line with the 'no triangle' conjecture of maximally supersymmetric Yang-Mills and gravity. To be more precise, there are 6,528 non-zero numerators, but these all follow from only 34 non-zero numerators up to appropriate relabellings of the external and loop momenta[9]. With this procedure, the expansion (5.2.1) at three-loops has been attained, and we can proceed to step (2) of our strategy.

5.3.2 Aspects of the genus-three ambitwistor string and the hyperelliptic locus

With the three-loop numerators obtained via the method presented in the last section, we can continue with our strategy at three-loops. As at two-loops, let us point out some details on what to expect from the genus-three ambitwistor string. The purpose of this is to obtain the Jacobian in $\mathcal{J}^{(3)}$, which has a crucial new feature in comparison to two-loops. Firstly, note that for $g = 3$ there are six independent components of the period matrix to integrate over as part of the moduli space integration. Three of these are expected to be used, via the scattering equations, in the global residue theorem to degenerate the genus-three surface onto a 'tri-nodal sphere'; see figure 5.5. The remaining three, in the degeneration limit, provide the measure for the nodal points via (5.1.10). Specifically in the degeneration limit these variables become

$$q_{12} = \frac{\sigma_{1^+2^+}\sigma_{1^-2^-}}{\sigma_{1^+2^-}\sigma_{1^-2^+}}\,, \qquad q_{23} = \frac{\sigma_{2^+3^+}\sigma_{2^-3^-}}{\sigma_{2^+3^-}\sigma_{2^-3^+}}\,, \qquad q_{13} = \frac{\sigma_{1^+3^+}\sigma_{1^-3^-}}{\sigma_{1^+3^-}\sigma_{1^-3^+}}\,, \tag{5.3.2}$$

so that one obtains the Jacobian through the change of variables in the measure,

$$\frac{dq_{12}\,dq_{23}\,dq_{13}}{q_{12}\,q_{23}\,q_{13}} = \frac{J^{(3)}}{\text{vol SL}(2,\mathbb{C})}\prod_{I^\pm} d\sigma_{I^\pm}\,, \tag{5.3.3}$$

with $I = 1, 2, 3$. This change of variables also results of course in a Jacobian coming from the scattering equations,

$$\bar{\delta}(\tilde{u}^{12})\bar{\delta}(\tilde{u}^{23})\bar{\delta}(\tilde{u}^{13}) = J^{(3)}\prod_{I^\pm}\bar{\delta}(\mathcal{E}_{I^\pm})\,. \tag{5.3.4}$$

[9]Specifically, there is a factor 4! from the permutations of the external particles, and a factor of $2\times2\times2$ from relabellings $2^+ \leftrightarrow 2^-$, $3^+ \leftrightarrow 3^-$ and $2^\pm \leftrightarrow 3^\pm$, giving $34\times4!\times8 = 6,528$. At the level of the numerators, other relabellings (such as $2^+ \leftrightarrow 3^-$) are not possible, since they would correspond to numerators of diagrams which do not appear in the loop integrand.

As mentioned in section 5.1.1 these two Jacobians turn out to be the same, and have the form

$$J^{(3)} = J_{\text{hyp}} \frac{\prod_I \sigma_{I^+I^-}}{\prod_{I<J} \sigma_{I^+J^+}\sigma_{I^+J^-}\sigma_{I^-J^+}\sigma_{I^-J^-}} \tag{5.3.5}$$

where

$$J_{\text{hyp}} = \sigma_{1^+2^-}\sigma_{2^+3^-}\sigma_{3^+1^-} - \sigma_{1^+3^-}\sigma_{3^+2^-}\sigma_{2^+1^-} \,, \tag{5.3.6}$$

the subscript referring to *hyperelliptic*, which we shall soon elaborate on. For now let us comment on one thing that we skipped in the above analysis. The process of obtaining the measure (5.3.3) will in principle require the inclusion of cross-ratios into the integrand, much like at two-loops. There is also the question of what the scattering equations resulting from (5.3.4) will precisely be. Since we are not working directly from the genus-three ambitwistor string, we cannot derive these cross-ratios nor the scattering equations from first principles. However, there is a way to infer what they can be by choosing which kinematic poles to manifest from the three-loop vacuum diagrams. We will not go into details here, where we expect these to be presented in future work, but we will mention that the set of cross-ratios given by

$$\begin{aligned} c^{(3)} &= \frac{1}{1-q_{12}}\frac{1}{1-q_{23}}\frac{1}{1-q_{13}}\frac{q_{23}}{q_{23}-1} \\ &= \frac{\sigma_{1^+2^-}\sigma_{1^-2^+}}{\sigma_{1^+1^-}\sigma_{2^+2^-}}\frac{\sigma_{2^+3^-}\sigma_{2^-3^+}}{\sigma_{2^+2^-}\sigma_{3^+3^-}}\frac{\sigma_{1^+3^-}\sigma_{1^-3^+}}{\sigma_{1^+1^-}\sigma_{3^+3^-}}\frac{\sigma_{2^+3^+}\sigma_{2^-3^-}}{\sigma_{2^+2^-}\sigma_{3^+3^-}} \,, \end{aligned} \tag{5.3.7}$$

is a consistent choice for the scattering equations derivable from the residues of the meromorphic quadratic differential

$$\mathfrak{P}_3 = P^2(\sigma) - \ell^{I\,2}\omega_I^2(\sigma) + (\ell_1^2+\ell_2^2)\,\omega_1(\sigma)\,\omega_2(\sigma) + (\ell_1^2+\ell_3^2)\,\omega_1(\sigma)\,\omega_3(\sigma) - \ell_1^2\,\omega_2(\sigma)\,\omega_3(\sigma) \tag{5.3.8}$$

at the marked points. These are not totally important in our goal of obtaining (5.2.1) since (*a*) the cross-ratios do not appear, and (*b*) it should be independent of the scattering equations.

In this respect we have obtained everything we need to try and construct $\mathcal{Y}^{(3)}$ in (5.2.1), that is the numerators $N^{(3)}$ and the Jacobian $\mathcal{J}^{(3)}$. However there seems to be a peculiarity with the latter, namely what happens when $J_{\text{hyp}} = 0$. From (5.3.6) this occurs when the nodal points are in special configurations. We will refer to being in this configuration as being in the *hyperelliptic sector*. The origin of this terminology stems from the following. All Riemann surfaces of genus $g \leq 2$ are hyperelliptic[10], but for $g = 3$ only a codimension-$1_{\mathbb{C}}$ subset of surfaces are hyperelliptic. On the genus-three surface there exists a modular form Ψ_9 of weight 9, defined in terms of even Jacobi theta constants[11] as

$$\Psi_9 = \sqrt{-\prod_{\delta}\theta[\delta](0)} \tag{5.3.9}$$

where the product is over the $2^{g-1}(2^g+1) = 36$ even spin structures for $g = 3$. In the degeneration limit ($q_{II} \to 0$) it has the leading behaviour

$$\Psi_9 \to \left(\prod_I q_{II}^2\right)\psi_9 + \cdots \,, \qquad \psi_9 = 2^{14} J_{\text{hyp}} \frac{\left(\prod_I \sigma_{I^+I^-}\right)^3}{\prod_{I<J}\sigma_{I^+J^+}\sigma_{I^+J^-}\sigma_{I^-J^+}\sigma_{I^-J^-}} \,. \tag{5.3.10}$$

[10] Though a genus-one surface is called elliptic, as algebraic curves they satisfy the definition of being hyperelliptic.

[11] The modular weight follows from $\prod_\delta \theta[\delta](0)$ having modular weight 18.

The hyperelliptic surfaces at genus-three are characterised by the vanishing of the modular form Ψ_9 [209], and therefore the condition $J_{\text{hyp}} = 0$ identifies the hyperelliptic sector. The set of such surfaces in the context of points in the moduli space is referred to as the *hyperelliptic locus*.

For our purposes this is important for one reason. A priori there is no reason for the four-point integrand to vanish in the hyperelliptic sector, though it may naively seem so from (5.2.1). Therefore, any ansatz for $\mathcal{Y}^{(3)}$ must take this into account, leading to further restrictions in its construction. With the details presented in this section, we can begin this construction.

5.3.3 A proposal for the three-loop four-point superstring amplitude

The subtleties described in the last section have important implications in trying to construct the four-point string integrand at three-loops. We will discuss these when they arise, but for now let us proceed with the aforementioned construction.

As mentioned in section 5.3.1, the four-point numerators appearing at three-loops are linear in the loop momentum, so we can decompose the corresponding superstring integrand into

$$2\pi i\, \mathcal{Y}^{(3)}_{\mathbb{S}} = \mathcal{Y}_0 + 2\pi i\, \ell^I_\mu\, \mathcal{Y}^\mu_I \tag{5.3.11}$$

to capture both parts separately; the factors of $2\pi i$ are placed for convenience in future expressions. The part linear in the loop momentum, corresponding to $\mathcal{Y}^\mu_I$, turns out to be the simplest. Natural objects to consider in this case are for example $\ell^I \omega_I(\sigma)$ and $\Delta^{(3)}_{ijk}$, since the former is a modular invariant and the latter has modular weight -1, and so together they provide the correct modular weight for $\mathcal{Y}^{(3)}_{\mathbb{S}}$ in accordance with (5.1.25). These objects form the basis for the construction of $\mathcal{Y}^\mu_I$. An ansatz with these ingredients would take the form

$$\alpha^\mu_1\, \omega_I(z_1)\, \Delta_{234} + \text{cyc}(1234) \tag{5.3.12}$$

where as usual we denote coordinates on the higher-genus surface by z, and the coefficients α^μ_i are determined by permutation invariance to be e.g.

$$\alpha^\mu_1 = k^\mu_2\, (k_3 - k_4) \cdot k_1 + \text{cyc}(234)\,. \tag{5.3.13}$$

This ansatz can be compared to the RHS of (5.2.1) which is linear in the loop momentum, and it turns out to match up to an overall coefficient,

$$\mathcal{Y}^\mu_I = \frac{2}{3}\left(\alpha^\mu_1\, \omega_I(z_1)\, \Delta^{(3)}_{234} + \text{cyc}(1234)\right)\,. \tag{5.3.14}$$

This contribution when multiplied by $J^{(3)}$ vanishes on the hyperelliptic sector, which will be important momentarily. The part independent of the loop momenta, $\mathcal{Y}_0$, turns out to be more intricate. For simplicity we will extract the kinematic dependence via

$$\mathcal{Y}_0 = s_{13}s_{14}Y_{12,34} + \text{cyc}(234) \tag{5.3.15}$$

such that $J^{(3)}Y_{12,34}$ depends only on the marked points in such a way that it is symmetric under exchanging $\sigma_1 \leftrightarrow \sigma_2$, $\sigma_3 \leftrightarrow \sigma_4$ and $\{\sigma_1, \sigma_2\} \leftrightarrow \{\sigma_3, \sigma_4\}$ in the degeneration limit, consistent with its kinematic coefficient. Now, one can check from the expansion (5.2.1) that $J^{(3)}Y_{12,34}$ does *not* vanish on the hyperelliptic sector, however it is possible to extract the part of it which does; we will denote this part of $Y_{12,34}$ as $\mathcal{D}_{12,34}$. This part has the

correct structure to be expressed in terms of the $\Delta^{(3)}_{ijk}$, which provides the correct modular weight. Its coefficients must then be modular invariant and have the correct $\mathrm{SL}(2,\mathbb{C})$ weights on the nodal sphere. These turn out to be Abelian differentials of the third kind,

$$\mathcal{D}_{12,34} = \frac{1}{3}\left(\omega_{3,4}(z_1)\,\Delta^{(3)}_{234} + \omega_{3,4}(z_2)\,\Delta^{(3)}_{134} + \omega_{1,2}(z_3)\,\Delta^{(3)}_{412} + \omega_{1,2}(z_4)\,\Delta^{(3)}_{312}\right), \tag{5.3.16}$$

which are defined in appendix A. The expressions (5.3.14) and (5.3.16) both vanish in the hyperelliptic sector, and in fact the combination is homology invariant[12], which provides a consistency check on the expressions and their relative numerical coefficients. In fact, (5.3.16) could have been deduced directly from (5.3.14) based on homology invariance.

The remaining part of $J^{(3)}Y_{12,34}$ remains strictly finite on the hyperelliptic sector. That means in the degeneration limit it must be proportional an object which cancels J_{hyp}. It is natural to suppose that this object is $1/\Psi_9$ from (5.3.10), which provides this cancellation directly. Since $1/\Psi_9$ has modular weight -9, we require that it is supplemented by an object which has modular weight 8 in order for the integrand to have the correct modular weight -1. Modular forms at genus-three have been well-studied [211–213] and there are in general a multitude of ways of obtaining an expression with modular weight 8.

Such a modular form has been proposed for the 'chiral measure' for the genus-three superstring in [214]. Their proposal is given by

$$d\mu^{(3)}[\delta] = c_3' \frac{\Xi_8[\delta]}{\Psi_9} \prod_{I\leq J} d\Omega_{IJ} \tag{5.3.17}$$

for c_3' a numerical constant and δ a spin structure (note that the modular form Ψ_9 implicitly also depends on δ). This follows a similar proposal in [213], and its uniqueness is shown in [215]. Our proposal above for the part of the four-point integrand non-vanishing on the hyperelliptic locus being proportional to $1/\Psi_9$ is supported by the conjecture (5.3.17). The object $\Xi_8[\delta]$ is the one of interest to us. The definition of this object is not straightforward, and we point the reader to [214] where it was defined, and expect details on this object to be explained in future work. Utilising this modular form, the remaining parts of $Y_{12,34}$, aside from the overarching $1/\Psi_9$, can be written in terms of the following combinations[13] of $\Xi_8[\delta]$ and Szegö kernels as

$$\begin{aligned}\mathcal{S}^{(a)}_{12,34} = \sum_{\delta} \Xi_8[\delta] \big(&S_\delta(z_1,z_2)S_\delta(z_2,z_3)S_\delta(z_3,z_4)S_\delta(z_4,z_1) \\ &+S_\delta(z_1,z_3)S_\delta(z_3,z_4)S_\delta(z_4,z_2)S_\delta(z_2,z_1)\big)\,,\end{aligned} \tag{5.3.18}$$

$$\mathcal{S}^{(b)}_{12,34} = \sum_{\delta} \Xi_8[\delta]\, S_\delta(z_1,z_2)^2 S_\delta(s_3,s_4)^2\,, \tag{5.3.19}$$

where the sums run over the 36 even spin structures at genus-three. The full result of $Y_{12,34}$ can therefore be expressed as

$$Y_{12,34} = \frac{1}{3}\mathcal{D}_{12,34} - \frac{1}{15\Psi_9}\left(\mathcal{S}^{(a)}_{12,34} - \frac{1}{8}\mathcal{S}^{(b)}_{12,34}\right). \tag{5.3.20}$$

[12] For discussions on homology invariance, see e.g. [207, 210].

[13] Four-point expressions of the form $S_\delta(z_1,z_3)^2 S_\delta(z_2,z_4)^2 + S_\delta(z_1,z_4)^2 S_\delta(z_2,z_3)^2$ are also consistent with the symmetries of $Y_{12,34}$, however this sum produces twice the sum in $S^{(b)}$ in the degeneration limit; we expect that this holds more generally.

In total, it is conjectured that the four-point type II superstring integrand at genus-three takes the form (5.3.11), with the objects therein determined by equations (5.3.14), (5.3.15) and (5.3.20). Unfortunately we could not find simplified expressions for $\mathcal{S}^{(a)}_{12,34}$ and $\mathcal{S}^{(b)}_{12,34}$ in (5.3.18) and (5.3.19), so it has been left explicitly in terms of a sum over even spin structures.

As a consistency check that we have obtained the correct expression for $\Xi_8[\delta]$ and the Szegö kernels, we have verified the following identities

$$\sum_{\delta} \Xi_8[\delta] = 0 \tag{5.3.21}$$

$$\sum_{\delta} \Xi_8[\delta] S_\delta(z_1, z_2)^2 = 0 \tag{5.3.22}$$

$$\sum_{\delta} \Xi_8[\delta] S_\delta(z_1, z_2) S_\delta(z_2, z_3) S_\delta(z_3, z_1) = 15(2\pi i)^3 \, \Psi_9 \, \Delta^{(3)}_{123} \tag{5.3.23}$$

to order q_{II}^2. Equation (5.3.21) gives the result of the zero-point function, which provides the vanishing of the cosmological constant. This is a vital requisite since it is well-understood that the superstring should provide a vanishing cosmological constant, due to the number of bosonic and fermionic contributions cancelling each other [214]. Equations (5.3.22) and (5.3.23) give the two- and three-point functions respectively, which at lower genus have been shown to vanish pointwise on moduli space [179]. At genus-three it has already been discussed how the two-point function (5.3.22) vanishes [216], however the three-point function has been shown only to vanish on the hyperelliptic locus for genus $g \geq 3$ [217], indicating that there are other pieces required in the calculation. Indeed, the former point is also demonstrated here in (5.3.23) with the presence of Ψ_9, and here we have managed to obtain the previously unknown coefficient $15(2\pi i)^3$ for equation (8) of [217].

The proposal we have given is consistent with some of the previous results of the genus-three superstring; in particular it works in conjunction with the proposal for the chiral measure of [214]. Whilst the nature of chiral splitting of the amplitude at genus-three still requires a detailed analysis, the conjecture presented in this section provides an indication at four-points.

5.4 Discussion

The discovery of worldsheet formulae at loop-level owes much to the study of the superstring at higher genus. In this chapter we have attempted to pay back the favour by offering a strategy which allow proposals for the loop-level amplitudes of massless states in the superstring to be constructed from the corresponding results in field theory. This is possible because of the connection that the ambitwistor string, with the scattering equations, provides between these two.

We first discussed the relation between expressions for four-point scattering in the superstring and the ambitwistor string at genus $g = 2, 3$, as well as the relation between the resulting worldsheet formulae and the corresponding field theory formulae. Here we gave our initial assumption for the genus-three expression of the superstring. We then discussed the degeneration of the worldsheet in the ambitwistor string via the scattering equations at genus $g = 2, 3$, where the dimension of the moduli space and the number of independent components of the period matrix coincide. The main proposal of this chapter follows from a strategy we laid out in section 5.2. In particular, it details that by translating a field

theory result possessing a BCJ representation into a worldsheet formula, this formula can in principle be uplifted to the higher-genus surface in the ambitwistor string, allowing one to infer the chiral integrand that appears in the superstring. This strategy was demonstrated at two-loops, exactly reproducing the known genus-two results [51, 179, 180]. This requires knowledge of how to determine the KK expansion in the worldsheet formula, so we detail how this can be done in section 5.3.1. Finally, we used the strategy to give a proposal for the four-point massless amplitude of the superstring at genus three.

We note that, in principle, the result obtained at genus-three could be imported into the heterotic string, as at genus-two [179, 207]. A natural extension would see the use of the strategy presented here for higher-point results. We believe the ongoing work of [207,218,219] studying the five-point genus-two superstring amplitude, as well as [162] which provide the corresponding BCJ numerators in $\mathcal{N} = 8$ supergravity, would be quite useful in providing a test of the stratagem. Despite the issues presented by the Schottky problem, much work has been done on the superstring at higher-genus, particularly regarding the chiral measure [220–225], which played a fundamental role for us at genus-three[14]. The connection established between superstring and field theory results, via the ambitwistor string, could mean that a study of the scattering equations at higher-loops could provide insights for obtaining results on the higher-genus surface, and vice versa. In either case, we expect the strategy presented here to be useful in this endeavour, given that BCJ numerators are known up to five loops[15] [165].

[14] Interestingly, the ansatz for the chiral measures for genus-four were shown to have non-vanishing two-point functions [226], and thus require corrections above this genus. The work of [227] has proposed a modified ansatz at genus-five which gives the correct vanishing two-point function at genus-four, but also claims that there cannot be an ansatz at genus-six which has the desired properties of a superstring measure.

[15] The five-loop case would be particularly challenging: on the field theory side a generalisation of the BCJ representation is required [165], and on the string theory side as mentioned before there is known to be a problem with the reduction of the supermoduli space [195].

Concluding remarks

In this thesis we have explored loop-level extensions of worldsheet models based on the scattering equation formalism. These extensions were made possible by the ambitwistor string whose origins trace back from CHY to the twistor string, as well as from the BCJ colour-kinematics duality to the KLT relations in string theory.

We have presented new and different formalisms at one, two and three loops, whose motivation and execution hinged on the scattering equations. We will briefly give a summary of the main results therein. At one-loop we have formulated a new form of BCFW integrand recursion in momentum space, as well as new one-loop scattering equations which can be used in worldsheet formulae to give one-loop integrands with quadratic propagators. Neither of these are solely restricted to planar theories, or necessarily to four-dimensions. At two-loops we have constructed n-point two-loop integrands for non-supersymmetric Yang-Mills and gravity, motivated by the forward-limit interpretation of loop-integrands arising from these worldsheet models. These results are calculated algorithmically and are valid in any number of dimensions. At three-loops we have given a proposal for the genus-three massless four-point superstring amplitude, a result which has not been calculated before, based on a strategy to obtain superstring loop amplitudes from results in quantum field theory.

Each of the relevant chapters have been concluded with a discussion summarising the results and an outlook regarding several topics of research that can possibly further these formalisms. Many of the potential areas of research in these chapters can be coupled with the work of other chapters. An extension of the ℓ^2-deformed scattering equations would greatly enhance the results we have presented at two-loops. Of course, such a procedure would be much more delicate at two-loops, and a better understanding is first required at one-loop. The strategy presented in chapter 5 could be used to obtain higher-point results in the two-loop superstring. This would not only be beneficial for the superstring, but also in clarifying some of the results we obtained in chapter 4 for the supersymmetric theories, such as how to simplify the Pfaffian structures and how the forward-limit can be more easily realised. Though a string description seems far away, it would also be interesting to perform the treatment of chapter 4 at three-loops, in the sense of a triple forward limit, and compare with field theory results. This might help identify any further potential subtleties for three-loop worldsheet formulae, on top of those we have already discussed in chapter 5.

We would like to take a moment to describe some of the other areas of research in ambitwistor string theory that have occurred. Whilst we have often utilised a representation valid in any number of dimensions, there exist ambitwistor string formulations specifically in four [89, 228], five [229], six [114, 230], ten and eleven [115] dimensions. Both these and the pure spinor formulations of the ambitwistor string [45, 180, 186] allow calculations with supersymmetry manifest. Recent work has also attempted to understand *celestial amplitudes* using corresponding worldsheet formulae [231, 232]. Moreover, much work has been done in understanding the ambitwistor in curved and non-trivial backgrounds [44–49], where for

example it is known that the equations of motion for supergravity arise from demanding that the corresponding worldsheet theory is free of anomalies [44].

Finally, we would like to conclude with some comments and open questions regarding the larger picture. Firstly, let us mention that the precise connection between the scattering equations and string theory is still yet to be understood. Indeed, the scattering equations can be seen as arising from string theory in both the limit $\alpha' \to 0$ [43] and $\alpha' \to \infty$ [56], indicating that there is something more, perhaps about the latter, that is not currently understood. As for open questions regarding the grander scheme of things, we offer here simply a few. How can the scattering equations help us better understand how BCJ works at loop-level, and can worldsheet models help us understand the colour-kinematics more geometrically? How can these worldsheet models help us understand string theory, QFT, as well as the connection between them better? Finally, why do these worldsheet models work, and (to reiterate a question we introduced at the beginning of this thesis) what is the S-matrix?

We firmly believe that the future of theoretical physics holds many surprises that will unlock the answers to these questions, as well as many others regarding the understanding of nature.

Appendix A

Objects defined on higher-genus Riemann surfaces

Here we define certain objects used throughout that are commonplace in calculations on higher-genus Riemann surfaces. Further details of these definitions, as well as other objects, can be found in e.g. [51, 207]. In the discussion here, we will be referring to surfaces with non-zero genus, $g > 0$.

A genus-g Riemann surface Σ contains $2g$ non-contractible cycles up to homology. One can define a homology basis of cycles by A_I, B_I $(I = 1, \cdots, g)$ such that its intersection form is canonical, $\#(A_I, B_I) = -\#(B_I, A_I) = \delta_{IJ}$. Modular transformations act on this basis as in (5.1.16). The genus-g surface admits g holomorphic 1-forms by the Riemann-Roch theorem, denoted as ω_I, which are called *Abelian differentials of the first kind*. Chosen to have normalised A_I periods, their integration around B_I cycles define the *period matrix* Ω_{IJ},

$$\oint_{A_I} \omega_J = \delta_{IJ}\,, \qquad\qquad \oint_{B_I} \omega_J = \Omega_{IJ}\,. \tag{A.1}$$

The period matrix Ω_{IJ} can be shown to be symmetric and have positive-definite imaginary part by the Riemann relations.

The Abelian differentials of the first kind also define the Abel map, which is used in various functions on the higher-genus surface. The Abel map defines a map from the Riemann surface to its Jacobian variety $J(\Sigma)$, where $J(\Sigma) \cong \mathbb{C}^g/(\mathbb{Z}^g + \Omega\mathbb{Z}^g)$ is the complex g-plane modulo the Jacobian lattice defined by the period matrix. Specifically, given a point or a divisor $d_1 z_1 + d_2 z_2 + \cdots d_n$ on Σ, the Abel map acts as

$$d_1 z_1 + d_2 z_2 + \cdots d_n z_n \mapsto \sum_{i=1}^{n} d_i \int_{z_0}^{z_i} \omega_I\,, \tag{A.2}$$

where z_0 is an arbitrary reference point on Σ. To be single-valued, this map acts modulo A_I or B_I cycles, and therefore is understood as a map into the Jacobian variety described above.

Using this we can define for example *theta functions*,

$$\vartheta[\kappa](\zeta) = \sum_{n\in\mathbb{Z}^g} \exp\left(i\pi(n+\kappa')^T\Omega\,(n+\kappa') + 2\pi i(n+\kappa')^T(\zeta+\kappa'')\right)\,, \tag{A.3}$$

where $\zeta \in \mathbb{C}^g$ is defined through the Abel map above, and $\kappa = (\kappa'|\kappa'')$ is called the theta *characteristic*. Of particular interest are characteristics corresponding to *spin structures*,

which label whether worldsheet spinors are periodic or anti-periodic around the A_I and B_I cycles[1]. For spin structures $\kappa', \kappa'' \in (\mathbb{Z}/2\mathbb{Z})^g$, the parity of the theta functions

$$\vartheta[\kappa](-\zeta) = (-1)^{4\kappa'\cdot\kappa''}\vartheta[\kappa](\zeta) \tag{A.4}$$

distinguishes between *even* and *odd* spin structures, according to whether $4\kappa' \cdot \kappa''$ is even or odd respectively. Even spin structures are often denoted as δ, and odd spin structures are often denoted as ν. On a genus-g surface, there are a total of 2^{2g} spin structures, consistent with the boundary conditions described above, of which $2^{g-1}(2^g+1)$ will be even and $2^{g-1}(2^g-1)$ will be odd[2]. In a superstring (and also ambitwistor string) correlation function, the GSO projection enforces a sum over spin-structures, which is required for modular invariance of the amplitude.

The theta functions are used to define objects that appear in superstring scattering amplitudes. For any odd spin structure ν, the square-root of the 1-form $\sum_{I=1}^{g}\partial_I\vartheta[\nu](0)\,\omega_I$ defines a $(1/2)$-form h_ν up to a sign. The *prime form* is then defined as

$$E(z,w) = \frac{\vartheta[\nu](z-w)}{h_\nu(z)h_\nu(w)} \tag{A.5}$$

which is independent of the odd spin structure ν chosen. Note that the argument $z-w$ is understood in terms of the Abel map, so that it is really $z-w \mapsto \int_z^w \omega_I$ from (A.2).

From the prime form one can define the *Szegö kernels*. For any even spin structure δ, the Szegö kernel is defined as

$$S_\delta(z,w) = \frac{\vartheta[\delta](z-w)}{\vartheta[\delta](0)\,E(z,w)} \tag{A.6}$$

which appears in the fermionic path integrals of the ambitwistor string, e.g.

$$\langle\Psi_\mu(z)\Psi_\nu(w)\rangle_\delta = \eta_{\mu\nu}\,S_\delta(z,w)\,. \tag{A.7}$$

The prime form can also be used to define other objects of interest. For example, the *Abelian differential of the second kind* is defined as

$$\omega(z,w) = dz\,dw\,\partial_z\partial_w E(z,w) \tag{A.8}$$

which produces a double-pole as $z \to w$ but is elsewhere holomorphic. It is symmetric under the exchange of z and w, $\omega(z,w) = \omega(w,z)$.

Finally, the *Abelian differential of the third kind* is defined as

$$\omega_{w_1,w_2}(z) = dz\,\partial_z \ln\frac{E(z,w_1)}{E(z,w_2)}\,, \tag{A.9}$$

which produces a simple pole with residues $+1$ and -1 as $z \to w_1$ and $z \to w_2$ respectively. The Abelian differentials of the first and third kind are very important in our study of the ambitwistor string on Riemann surfaces of genus $g > 0$, as evidenced by their appearance in the solution of P (4.2.3) at any genus.

[1] The connection between theta functions and the spin bundle on Σ is based on Riemann's vanishing theorem; see e.g. [233].

[2] There can be relations between these spin structures, e.g. in [191].

Appendix B

Two-loop partition functions and Szegö kernels on the Riemann sphere

Here we detail, for completeness, the partition functions and Szegö kernels for the NS sector present in section 4.3.1 in the degeneration limit. These follow from calculations in [51], which rigorously studied the ambitwistor string at genus-two. The NS partition functions entering in the kinematic integrand $\mathcal{I}^{(2)}_{\text{susy-kin}}$ of (4.3.6) are

$$\mathcal{Z}^{(-1,-1)}_{\text{NS}} = \frac{\sqrt{\mathrm{d}x_1\mathrm{d}x_2}}{x_1-x_2}\frac{q_3^{-2}}{\omega_{1^+1^-}(x_1)\,\omega_{1^+1^-}(x_2)\,\omega_{2^+2^-}(x_1)\,\omega_{2^+2^-}(x_2)}\,, \tag{B.1a}$$

$$\mathcal{Z}^{(-1,0)}_{\text{NS}} = \frac{\sqrt{\mathrm{d}x_1\mathrm{d}x_2}}{x_1-x_2}\frac{q_3^{-1}}{\omega_{1^+1^-}(x_1)\,\omega_{1^+1^-}(x_2)}Z_8^{(-1,0)}\,, \tag{B.1b}$$

$$\mathcal{Z}^{(0,-1)}_{\text{NS}} = \frac{\sqrt{\mathrm{d}x_1\mathrm{d}x_2}}{x_1-x_2}\frac{q_3^{-1}}{\omega_{2^+2^-}(x_1)\,\omega_{2^+2^-}(x_2)}Z_8^{(0,-1)}\,, \tag{B.1c}$$

$$\mathcal{Z}^{(0,0)}_{\text{NS}} = 10\,q_3\big(1+3q_3+q_3^2\big)\,\mathcal{Z}^{(-1,-1)}_{\text{NS}} + \frac{\sqrt{\mathrm{d}x_1\mathrm{d}x_2}}{x_1-x_2}\Big(2Z_3^{(-1,0)}Z_3^{(0,-1)}-Z^{(0,0)}\Big)\,, \tag{B.1d}$$

where $q_3 = q_{12}$ is the cross-ratio

$$q_3 = \frac{\sigma_{1^+2^+}\sigma_{1^-2^-}}{\sigma_{1^+2^-}\sigma_{1^-2^+}}\,, \tag{B.2}$$

and the factors of $Z_a^{(-1,0)}$, $Z_a^{(0,-1)}$ and $Z^{(0,0)}$ are given by

$$Z_a^{(-1,0)} = \frac{a}{\omega_{2^+2^-}(x_1)\omega_{2^+2^-}(x_2)} - \frac{\big((x_1-\sigma_{2^+})(x_2-\sigma_{2^+})\,\sigma_{2^-1^+}\sigma_{2^-1^-} - \big(\sigma_{2^+}\leftrightarrow\sigma_{2^-}\big)\big)^2}{\sigma^2_{2^+2^-}\sigma_{1^+2^+}\sigma_{1^+2^-}\sigma_{1^-2^+}\sigma_{1^-2^-}\ \mathrm{d}x_1\mathrm{d}x_2}\,,$$

$$Z_a^{(0,-1)} = \frac{a}{\omega_{1^+1^-}(x_1)\omega_{1^+1^-}(x_2)} - \frac{\big((x_1-\sigma_{1^+})(x_2-\sigma_{1^+})\,\sigma_{1^-2^+}\sigma_{1^-2^-} - \big(\sigma_{1^+}\leftrightarrow\sigma_{1^-}\big)\big)^2}{\sigma^2_{1^+1^-}\sigma_{1^+2^+}\sigma_{1^+2^-}\sigma_{1^-2^+}\sigma_{1^-2^-}\ \mathrm{d}x_1\mathrm{d}x_2}\,,$$

$$Z^{(0,0)} = \frac{\Big(\prod_{a=1^+,2^+}\big((x_1-\sigma_a)(x_2-\sigma_a)\,\sigma^2_{1^-2^-}\big)^2 + \text{perm(nodes)}\Big)}{\sigma^2_{1^+1^-}\sigma^2_{1^+1^-}\,\sigma_{1^+2^+}\sigma_{1^+2^-}\sigma_{1^-2^+}\sigma_{1^-2^-}\ \mathrm{d}x_1^2\mathrm{d}x_2^2}\,.$$

Here, perm(nodes) indicates the set of permutations of the nodal points given by $\left(\sigma_{1^+} \leftrightarrow \sigma_{1^-}\right)$, $\left(\sigma_{2^+} \leftrightarrow \sigma_{2^-}\right)$ and $\left(\sigma_{1^+} \leftrightarrow \sigma_{1^-}, \sigma_{2^+} \leftrightarrow \sigma_{2^-}\right)$. Though these depend explicitly on the auxiliary points x_1 and x_2, the final formulae are independent of these, as shown in [51]. The two-loop Szegö kernels are defined as

$$S_{\mathrm{NS}}^{(0,0)}(z,w) = \frac{\sqrt{\mathrm{d}z\,\mathrm{d}w}}{z-w},, \tag{B.3a}$$

$$S_{\mathrm{NS}}^{(1,0)}(z,w) = q_3 \frac{\sigma_{1^+1^-}^2\,(z-w)\,\sqrt{\mathrm{d}z\,\mathrm{d}w}}{(z-\sigma_{1^+})(z-\sigma_{1^-})(w-\sigma_{1^+})(w-\sigma_{1^-})}\,, \tag{B.3b}$$

$$S_{\mathrm{NS}}^{(0,1)}(z,w) = q_3 \frac{\sigma_{2^+2^-}^2\,(z-w)\,\sqrt{\mathrm{d}z\,\mathrm{d}w}}{(z-\sigma_{2^+})(z-\sigma_{2^-})(w-\sigma_{2^+})(w-\sigma_{2^-})}\,, \tag{B.3c}$$

$$\begin{aligned} S_{\mathrm{NS}}^{(1,1)}(z,w) = q_3^2\, S_{\mathrm{NS}}^{(1,0)}(z,w) S_{\mathrm{NS}}^{(0,1)}(z,w) \\ \times \frac{\left((z-\sigma_{1^+})(w-\sigma_{2^+})\,\sigma_{1^-2^-} + (z-\sigma_{2^-})(w-\sigma_{1^-})\,\sigma_{1^+2^+}\right)^2}{\sigma_{1^+2^+}\sigma_{1^-2^-}\sigma_{1^+2^-}\sigma_{1^-2^+}\,(z-w)\,\sqrt{\mathrm{d}z\,\mathrm{d}w}}\,. \end{aligned} \tag{B.3d}$$

References

[1] Joseph A. Farrow, Yvonne Geyer, Arthur E. Lipstein, Ricardo Monteiro, and Ricardo Stark-Muchão. Propagators, BCFW recursion and new scattering equations at one loop. *JHEP*, 10:074, 2020. arXiv:2007.00623 [hep-th].

[2] Yvonne Geyer, Ricardo Monteiro, and Ricardo Stark-Muchão. Two-Loop Scattering Amplitudes: Double-Forward Limit and Colour-Kinematics Duality. *JHEP*, 12:049, 2019. arXiv:1908.05221 [hep-th].

[3] Yvonne Geyer, Ricardo Monteiro, and Ricardo Stark-Muchão. Superstring loop amplitudes from the field theory limit. 6 2021. arXiv:2106.03968 [hep-th].

[4] Nadia Bahjat-Abbas, Ricardo Stark-Muchão, and Chris D. White. Biadjoint wires. *Phys. Lett. B*, 788:274–279, 2019. arXiv:1810.08118 [hep-th].

[5] Nadia Bahjat-Abbas, Ricardo Stark-Muchão, and Chris D. White. Monopoles, shockwaves and the classical double copy. *JHEP*, 04:102, 2020. arXiv:2001.09918 [hep-th].

[6] Michelangelo L. Mangano and Stephen J. Parke. Multiparton amplitudes in gauge theories. *Phys. Rept.*, 200:301–367, 1991. arXiv:hep-th/0509223.

[7] Stephen J. Parke and T. R. Taylor. An Amplitude for n Gluon Scattering. *Phys. Rev. Lett.*, 56:2459, 1986.

[8] H. Kawai, D.C. Lewellen, and S.H.H. Tye. A Relation Between Tree Amplitudes of Closed and Open Strings. *Nucl. Phys. B*, 269:1–23, 1986.

[9] Z. Bern, J.J.M. Carrasco, and Henrik Johansson. New Relations for Gauge-Theory Amplitudes. *Phys. Rev. D*, 78:085011, 2008. arXiv:0805.3993 [hep-ph].

[10] Zvi Bern, John Joseph Carrasco, Marco Chiodaroli, Henrik Johansson, and Radu Roiban. The Duality Between Color and Kinematics and its Applications. 9 2019. arXiv:1909.01358 [hep-th].

[11] Zvi Bern, Tristan Dennen, Yu-tin Huang, and Michael Kiermaier. Gravity as the Square of Gauge Theory. *Phys. Rev. D*, 82:065003, 2010. arXiv:1004.0693 [hep-th].

[12] Zvi Bern, John Joseph M. Carrasco, and Henrik Johansson. Perturbative Quantum Gravity as a Double Copy of Gauge Theory. *Phys. Rev. Lett.*, 105:061602, 2010. arXiv:1004.0476 [hep-th].

[13] Rutger H. Boels and Reinke Sven Isermann. On powercounting in perturbative quantum gravity theories through color-kinematic duality. *JHEP*, 06:017, 2013. arXiv:1212.3473 [hep-th].

[14] Simon Badger, Gustav Mogull, Alexander Ochirov, and Donal O'Connell. A Complete Two-Loop, Five-Gluon Helicity Amplitude in Yang-Mills Theory. *JHEP*, 10:064, 2015. arXiv:1507.08797 [hep-ph].

[15] David Chester. Bern-Carrasco-Johansson relations for one-loop QCD integral coefficients. *Phys. Rev. D*, 93(6):065047, 2016. arXiv:1601.00235 [hep-th].

[16] Amedeo Primo and William J. Torres Bobadilla. BCJ Identities and d-Dimensional Generalized Unitarity. *JHEP*, 04:125, 2016. arXiv:1602.03161 [hep-ph].

[17] Clifford Cheung, Ira Z. Rothstein, and Mikhail P. Solon. From Scattering Amplitudes to Classical Potentials in the Post-Minkowskian Expansion. *Phys. Rev. Lett.*, 121(25):251101, 2018. arXiv:1808.02489 [hep-th].

[18] David A. Kosower, Ben Maybee, and Donal O'Connell. Amplitudes, Observables, and Classical Scattering. *JHEP*, 02:137, 2019. arXiv:1811.10950 [hep-th].

[19] Zvi Bern, Clifford Cheung, Radu Roiban, Chia-Hsien Shen, Mikhail P. Solon, and Mao Zeng. Scattering Amplitudes and the Conservative Hamiltonian for Binary Systems at Third Post-Minkowskian Order. *Phys. Rev. Lett.*, 122(20):201603, 2019. arXiv:1901.04424 [hep-th].

[20] Zvi Bern, Clifford Cheung, Radu Roiban, Chia-Hsien Shen, Mikhail P. Solon, and Mao Zeng. Black Hole Binary Dynamics from the Double Copy and Effective Theory. *JHEP*, 10:206, 2019. arXiv:1908.01493 [hep-th].

[21] Edward Witten. Perturbative gauge theory as a string theory in twistor space. *Commun. Math. Phys.*, 252:189–258, 2004. arXiv:hep-th/0312171.

[22] Radu Roiban, Marcus Spradlin, and Anastasia Volovich. On the tree level S matrix of Yang-Mills theory. *Phys. Rev. D*, 70:026009, 2004. arXiv:hep-th/0403190.

[23] Simone Giombi, Riccardo Ricci, Daniel Robles-Llana, and Diego Trancanelli. A Note on twistor gravity amplitudes. *JHEP*, 07:059, 2004. arXiv:hep-th/0405086.

[24] Mohab Abou-Zeid, Christopher M. Hull, and L. J. Mason. Einstein Supergravity and New Twistor String Theories. *Commun. Math. Phys.*, 282:519–573, 2008. arXiv:hep-th/0606272.

[25] Tim Adamo and Lionel Mason. Einstein supergravity amplitudes from twistor-string theory. *Class. Quant. Grav.*, 29:145010, 2012. arXiv:1203.1026 [hep-th].

[26] Freddy Cachazo and Yvonne Geyer. A 'Twistor String' Inspired Formula For Tree-Level Scattering Amplitudes in N=8 SUGRA. 6 2012. arXiv:1206.6511 [hep-th].

[27] Tim Adamo and Lionel Mason. Twistor-strings and gravity tree amplitudes. *Class. Quant. Grav.*, 30:075020, 2013. arXiv:1207.3602 [hep-th].

[28] David Skinner. Twistor strings for $\mathcal{N} = 8$ supergravity. *JHEP*, 04:047, 2020. arXiv:1301.0868 [hep-th].

[29] Freddy Cachazo, Peter Svrcek, and Edward Witten. MHV vertices and tree amplitudes in gauge theory. *JHEP*, 09:006, 2004. arXiv:hep-th/0403047.

[30] Rutger Boels, L. J. Mason, and David Skinner. Supersymmetric Gauge Theories in Twistor Space. *JHEP*, 02:014, 2007. arXiv:hep-th/0604040.

[31] Rutger Boels, L. J. Mason, and David Skinner. From twistor actions to MHV diagrams. *Phys. Lett. B*, 648:90–96, 2007. arXiv:hep-th/0702035.

[32] L. J. Mason and David Skinner. Scattering Amplitudes and BCFW Recursion in Twistor Space. *JHEP*, 01:064, 2010. arXiv:0903.2083 [hep-th].

[33] Nima Arkani-Hamed, Freddy Cachazo, Clifford Cheung, and Jared Kaplan. The S-Matrix in Twistor Space. *JHEP*, 03:110, 2010. arXiv:0903.2110 [hep-th].

[34] David Skinner. A Direct Proof of BCFW Recursion for Twistor-Strings. *JHEP*, 01:072, 2011. arXiv:1007.0195 [hep-th].

[35] Tim Adamo and Lionel Mason. MHV diagrams in twistor space and the twistor action. *Phys. Rev. D*, 86:065019, 2012. arXiv:1103.1352 [hep-th].

[36] Freddy Cachazo and David Skinner. Gravity from Rational Curves in Twistor Space. *Phys. Rev. Lett.*, 110(16):161301, 2013. arXiv:1207.0741 [hep-th].

[37] Freddy Cachazo, Song He, and Ellis Ye Yuan. Scattering equations and Kawai-Lewellen-Tye orthogonality. *Phys. Rev. D*, 90(6):065001, 2014. arXiv:1306.6575 [hep-th].

[38] Freddy Cachazo, Song He, and Ellis Ye Yuan. Scattering of Massless Particles in Arbitrary Dimensions. *Phys. Rev. Lett.*, 113(17):171601, 2014. arXiv:1307.2199 [hep-th].

[39] Freddy Cachazo, Song He, and Ellis Ye Yuan. Scattering of Massless Particles: Scalars, Gluons and Gravitons. *JHEP*, 07:033, 2014. arXiv:1309.0885 [hep-th].

[40] Christian Baadsgaard, N. E. J. Bjerrum-Bohr, Jacob L. Bourjaily, and Poul H. Damgaard. Scattering Equations and Feynman Diagrams. *JHEP*, 09:136, 2015. arXiv:1507.00997 [hep-th].

[41] Freddy Cachazo, Song He, and Ellis Ye Yuan. Einstein-Yang-Mills Scattering Amplitudes From Scattering Equations. *JHEP*, 01:121, 2015. arXiv:1409.8256 [hep-th].

[42] Freddy Cachazo, Song He, and Ellis Ye Yuan. Scattering Equations and Matrices: From Einstein To Yang-Mills, DBI and NLSM. *JHEP*, 07:149, 2015. arXiv:1412.3479 [hep-th].

[43] Lionel Mason and David Skinner. Ambitwistor strings and the scattering equations. *JHEP*, 07:048, 2014. arXiv:1311.2564 [hep-th].

[44] Tim Adamo, Eduardo Casali, and David Skinner. A Worldsheet Theory for Supergravity. *JHEP*, 02:116, 2015. arXiv:1409.5656 [hep-th].

[45] Osvaldo Chandia and Brenno Carlini Vallilo. Ambitwistor pure spinor string in a type II supergravity background. *JHEP*, 06:206, 2015. arXiv:1505.05122 [hep-th].

[46] Tim Adamo, Eduardo Casali, Lionel Mason, and Stefan Nekovar. Amplitudes on plane waves from ambitwistor strings. *JHEP*, 11:160, 2017. arXiv:1708.09249 [hep-th].

[47] Tim Adamo, Eduardo Casali, and Stefan Nekovar. Ambitwistor string vertex operators on curved backgrounds. *JHEP*, 01:213, 2019. arXiv:1809.04489 [hep-th].

[48] Stefan Nekovar. *Ambitwistor strings and amplitudes in curved backgrounds*. PhD thesis, Oxford U., 2018.

[49] Kai Roehrig and David Skinner. Ambitwistor Strings and the Scattering Equations on $AdS_3 \times S^3$. 7 2020. arXiv:2007.07234 [hep-th].

[50] Tim Adamo, Eduardo Casali, and David Skinner. Ambitwistor strings and the scattering equations at one loop. *JHEP*, 04:104, 2014. arXiv:1312.3828 [hep-th].

[51] Yvonne Geyer and Ricardo Monteiro. Two-Loop Scattering Amplitudes from Ambitwistor Strings: from Genus Two to the Nodal Riemann Sphere. *JHEP*, 11:008, 2018. arXiv:1805.05344 [hep-th].

[52] Chih-Hao Fu, Yi-Jian Du, Rijun Huang, and Bo Feng. Expansion of Einstein-Yang-Mills Amplitude. *JHEP*, 09:021, 2017. arXiv:1702.08158 [hep-th].

[53] D. B. Fairlie and D. E. Roberts. Dual models without tachyons - a new approach. 7 1972.

[54] D. B. Fairlie. *Mathematical structure of dual amplitudes*. PhD thesis, Durham University, 1972.

[55] David B. Fairlie. A Coding of Real Null Four-Momenta into World-Sheet Coordinates. *Adv. Math. Phys.*, 2009:284689, 2009. arXiv:0805.2263 [hep-th].

[56] David J. Gross and Paul F. Mende. String Theory Beyond the Planck Scale. *Nucl. Phys. B*, 303:407–454, 1988.

[57] Louise Dolan and Peter Goddard. The Polynomial Form of the Scattering Equations. *JHEP*, 07:029, 2014. arXiv:1402.7374 [hep-th].

[58] Freddy Cachazo, Song He, and Ellis Ye Yuan. Scattering in Three Dimensions from Rational Maps. *JHEP*, 10:141, 2013. arXiv:1306.2962 [hep-th].

[59] Louise Dolan and Peter Goddard. General Solution of the Scattering Equations. *JHEP*, 10:149, 2016. arXiv:1511.09441 [hep-th].

[60] Stefan Weinzierl. On the solutions of the scattering equations. *JHEP*, 04:092, 2014. arXiv:1402.2516 [hep-th].

[61] Andrew Hodges. New expressions for gravitational scattering amplitudes. *JHEP*, 07:075, 2013. arXiv:1108.2227 [hep-th].

[62] Andrew Hodges. A simple formula for gravitational MHV amplitudes. 4 2012. arXiv:1204.1930 [hep-th].

[63] Clifford Cheung, Chia-Hsien Shen, and Congkao Wen. Unifying Relations for Scattering Amplitudes. *JHEP*, 02:095, 2018. arXiv:1705.03025 [hep-th].

[64] Clifford Cheung, Grant N. Remmen, Chia-Hsien Shen, and Congkao Wen. Pions as Gluons in Higher Dimensions. *JHEP*, 04:129, 2018. arXiv:1709.04932 [hep-th].

[65] John Joseph M. Carrasco and Laurentiu Rodina. UV considerations on scattering amplitudes in a web of theories. *Phys. Rev. D*, 100(12):125007, 2019. arXiv:1908.08033 [hep-th].

[66] Pieter-Jan De Smet and Chris D. White. Extended solutions for the biadjoint scalar field. *Phys. Lett. B*, 775:163–167, 2017. arXiv:1708.01103 [hep-th].

[67] Chris D. White. The double copy: gravity from gluons. *Contemp. Phys.*, 59:109, 2018. arXiv:1708.07056 [hep-th].

[68] David S. Berman, Erick Chacón, Andrés Luna, and Chris D. White. The self-dual classical double copy, and the Eguchi-Hanson instanton. *JHEP*, 01:107, 2019. arXiv:1809.04063 [hep-th].

[69] Mariana Carrillo González, Brandon Melcher, Kenneth Ratliff, Scott Watson, and Chris D. White. The classical double copy in three spacetime dimensions. *JHEP*, 07:167, 2019. arXiv:1904.11001 [hep-th].

[70] Erick Chacón, Hugo García-Compeán, Andrés Luna, Ricardo Monteiro, and Chris D. White. New heavenly double copies. *JHEP*, 03:247, 2021. arXiv:2008.09603 [hep-th].

[71] Yvonne Geyer and Ricardo Monteiro. Gluons and gravitons at one loop from ambitwistor strings. *JHEP*, 03:068, 2018. arXiv:1711.09923 [hep-th].

[72] N. E. J. Bjerrum-Bohr, Jacob L. Bourjaily, Poul H. Damgaard, and Bo Feng. Manifesting Color-Kinematics Duality in the Scattering Equation Formalism. *JHEP*, 09:094, 2016. arXiv:1608.00006 [hep-th].

[73] Vittorio Del Duca, Lance J. Dixon, and Fabio Maltoni. New color decompositions for gauge amplitudes at tree and loop level. *Nucl. Phys. B*, 571:51–70, 2000. arXiv:hep-ph/9910563.

[74] Z. Bern, Lance J. Dixon, M. Perelstein, and J. S. Rozowsky. Multileg one loop gravity amplitudes from gauge theory. *Nucl. Phys. B*, 546:423–479, 1999. arXiv:hep-th/9811140.

[75] N. E. J. Bjerrum-Bohr, Poul H. Damgaard, Thomas Sondergaard, and Pierre Vanhove. The Momentum Kernel of Gauge and Gravity Theories. *JHEP*, 01:001, 2011. arXiv:1010.3933 [hep-th].

[76] Carlos R. Mafra. Berends-Giele recursion for double-color-ordered amplitudes. *JHEP*, 07:080, 2016. arXiv:1603.09731 [hep-th].

[77] Sebastian Mizera. Inverse of the String Theory KLT Kernel. *JHEP*, 06:084, 2017. arXiv:1610.04230 [hep-th].

[78] Hadleigh Frost, Carlos R. Mafra, and Lionel Mason. A Lie bracket for the momentum kernel. 12 2020. arXiv:2012.00519 [hep-th].

[79] Christian Baadsgaard, N.E.J. Bjerrum-Bohr, Jacob L. Bourjaily, and Poul H. Damgaard. Integration Rules for Scattering Equations. *JHEP*, 09:129, 2015. arXiv:1506.06137 [hep-th].

[80] C. S. Lam and York-Peng Yao. Evaluation of the Cachazo-He-Yuan gauge amplitude. *Phys. Rev. D*, 93(10):105008, 2016. arXiv:1602.06419 [hep-th].

[81] Rijun Huang, Bo Feng, Ming-xing Luo, and Chuan-Jie Zhu. Feynman Rules of Higher-order Poles in CHY Construction. *JHEP*, 06:013, 2016. arXiv:1604.07314 [hep-th].

[82] Carlos Cardona, Bo Feng, Humberto Gomez, and Rijun Huang. Cross-ratio Identities and Higher-order Poles of CHY-integrand. *JHEP*, 09:133, 2016. arXiv:1606.00670 [hep-th].

[83] Christian Baadsgaard, N.E.J. Bjerrum-Bohr, Jacob L. Bourjaily, Poul H. Damgaard, and Bo Feng. Integration Rules for Loop Scattering Equations. *JHEP*, 11:080, 2015. arXiv:1508.03627 [hep-th].

[84] Song He and Ellis Ye Yuan. One-loop Scattering Equations and Amplitudes from Forward Limit. *Phys. Rev. D*, 92(10):105004, 2015. arXiv:1508.06027 [hep-th].

[85] Carlos Cardona and Humberto Gomez. CHY-Graphs on a Torus. *JHEP*, 10:116, 2016. arXiv:1607.01871 [hep-th].

[86] Roger Penrose and Wolfgang Rindler. *Spinors and Space-Time*, volume 1 of *Cambridge Monographs on Mathematical Physics*. Cambridge University Press, 1984.

[87] Roger Penrose and Wolfgang Rindler. *Spinors and Space-Time*, volume 2 of *Cambridge Monographs on Mathematical Physics*. Cambridge University Press, 1986.

[88] C R LeBrun. Ambi-twistors and Einstein's equations. *Classical and Quantum Gravity*, 2(4):555–563, Jul 1985.

[89] Yvonne Geyer, Arthur E. Lipstein, and Lionel J. Mason. Ambitwistor Strings in Four Dimensions. *Phys. Rev. Lett.*, 113(8):081602, 2014. arXiv:1404.6219 [hep-th].

[90] J. Polchinski. *String theory. Vol. 1: An introduction to the bosonic string*. Cambridge Monographs on Mathematical Physics. Cambridge University Press, 12 2007.

[91] Serge Lazzarini. The role of the Beltrami parametrization of complex structures in 2-d Free Conformal Field Theory. `https://arxiv.org/abs/math-ph/0509073`, 1998.

[92] Eduardo Casali, Yvonne Geyer, Lionel Mason, Ricardo Monteiro, and Kai A. Roehrig. New Ambitwistor String Theories. *JHEP*, 11:038, 2015. arXiv:1506.08771 [hep-th].

[93] David Skinner. "Ambitwistor Space". Talk at Nottingham Workshop on Geometry of Graviton Scattering Amplitudes, July 2015.

[94] Thales Azevedo and Oluf Tang Engelund. Ambitwistor formulations of R^2 gravity and $(DF)^2$ gauge theories. *JHEP*, 11:052, 2017. arXiv:1707.02192 [hep-th].

[95] Henrik Johansson and Josh Nohle. Conformal Gravity from Gauge Theory. 7 2017. arXiv:1707.02965 [hep-th].

[96] M. Nakahara. *Geometry, topology and physics*. 2003.

[97] Kai A. Roehrig and David Skinner. A Gluing Operator for the Ambitwistor String. *JHEP*, 01:069, 2018. arXiv:1709.03262 [hep-th].

[98] Daniel Friedan, Emil J. Martinec, and Stephen H. Shenker. Conformal Invariance, Supersymmetry and String Theory. *Nucl. Phys.*, B271:93–165, 1986.

[99] J. Polchinski. *String theory. Vol. 2: Superstring theory and beyond*. Cambridge Monographs on Mathematical Physics. Cambridge University Press, 12 2007.

[100] Alexander M. Polyakov. Quantum Geometry of Bosonic Strings. *Phys. Lett. B*, 103:207–210, 1981.

[101] Alexander M. Polyakov. Quantum Geometry of Fermionic Strings. *Phys. Lett. B*, 103:211–213, 1981.

[102] Kantaro Ohmori. Worldsheet Geometries of Ambitwistor String. *JHEP*, 06:075, 2015. arXiv:1504.02675 [hep-th].

[103] Yvonne Geyer, Lionel Mason, Ricardo Monteiro, and Piotr Tourkine. Loop Integrands for Scattering Amplitudes from the Riemann Sphere. *Phys. Rev. Lett.*, 115(12):121603, 2015. arXiv:1507.00321 [hep-th].

[104] Yvonne Geyer, Lionel Mason, Ricardo Monteiro, and Piotr Tourkine. One-loop amplitudes on the Riemann sphere. *JHEP*, 03:114, 2016. arXiv:1511.06315 [hep-th].

[105] Yvonne Geyer, Lionel Mason, Ricardo Monteiro, and Piotr Tourkine. Two-Loop Scattering Amplitudes from the Riemann Sphere. *Phys. Rev. D*, 94(12):125029, 2016. arXiv:1607.08887 [hep-th].

[106] Freddy Cachazo, Song He, and Ellis Ye Yuan. One-Loop Corrections from Higher Dimensional Tree Amplitudes. *JHEP*, 08:008, 2016. arXiv:1512.05001 [hep-th].

[107] Piotr Tourkine and Pierre Vanhove. One-loop four-graviton amplitudes in $\mathcal{N} = 4$ supergravity models. *Phys. Rev. D*, 87(4):045001, 2013. arXiv:1208.1255 [hep-th].

[108] Louise Dolan and Peter Goddard. Proof of the Formula of Cachazo, He and Yuan for Yang-Mills Tree Amplitudes in Arbitrary Dimension. *JHEP*, 05:010, 2014. arXiv:1311.5200 [hep-th].

[109] Stephen G. Naculich. Scattering equations and BCJ relations for gauge and gravitational amplitudes with massive scalar particles. *JHEP*, 09:029, 2014. arXiv:1407.7836 [hep-th].

[110] N. Emil J. Bjerrum-Bohr, Poul Henrik Damgaard, Piotr Tourkine, and Pierre Vanhove. Scattering Equations and String Theory Amplitudes. *Phys. Rev. D*, 90(10):106002, 2014. arXiv:1403.4553 [hep-th].

[111] Stephen G. Naculich. CHY representations for gauge theory and gravity amplitudes with up to three massive particles. *JHEP*, 05:050, 2015. arXiv:1501.03500 [hep-th].

[112] Stephen G. Naculich. Amplitudes for massive vector and scalar bosons in spontaneously-broken gauge theory from the CHY representation. *JHEP*, 09:122, 2015. arXiv:1506.06134 [hep-th].

[113] C.S. Lam and York-Peng Yao. Off-Shell CHY Amplitudes. *Nucl. Phys. B*, 907:678–694, 2016. arXiv:1511.05050 [hep-th].

[114] Giulia Albonico, Yvonne Geyer, and Lionel Mason. Recursion and worldsheet formulae for 6d superamplitudes. *JHEP*, 08:066, 2020. arXiv:2001.05928 [hep-th].

[115] Yvonne Geyer and Lionel Mason. Supersymmetric S-matrices from the worldsheet in 10 \& 11d. *Phys. Lett. B*, 804:135361, 2020. arXiv:1901.00134 [hep-th].

[116] Christian Baadsgaard, N.E.J. Bjerrum-Bohr, Jacob L. Bourjaily, Simon Caron-Huot, Poul H. Damgaard, and Bo Feng. New Representations of the Perturbative S-Matrix. *Phys. Rev. Lett.*, 116(6):061601, 2016. arXiv:1509.02169 [hep-th].

[117] Humberto Gomez. Quadratic Feynman Loop Integrands From Massless Scattering Equations. *Phys. Rev. D*, 95(10):106006, 2017. arXiv:1703.04714 [hep-th].

[118] Humberto Gomez, Cristhiam Lopez-Arcos, and Pedro Talavera. One-loop Parke-Taylor factors for quadratic propagators from massless scattering equations. *JHEP*, 10:175, 2017. arXiv:1707.08584 [hep-th].

[119] Naser Ahmadiniaz, Humberto Gomez, and Cristhiam Lopez-Arcos. Non-planar one-loop Parke-Taylor factors in the CHY approach for quadratic propagators. *JHEP*, 05:055, 2018. arXiv:1802.00015 [hep-th].

[120] Ruth Britto, Freddy Cachazo, and Bo Feng. New recursion relations for tree amplitudes of gluons. *Nucl. Phys. B*, 715:499–522, 2005. arXiv:hep-th/0412308.

[121] Ruth Britto, Freddy Cachazo, Bo Feng, and Edward Witten. Direct proof of tree-level recursion relation in Yang-Mills theory. *Phys. Rev. Lett.*, 94:181602, 2005. arXiv:hep-th/0501052.

[122] James Bedford, Andreas Brandhuber, Bill J. Spence, and Gabriele Travaglini. A Recursion relation for gravity amplitudes. *Nucl. Phys. B*, 721:98–110, 2005. arXiv:hep-th/0502146.

[123] Freddy Cachazo and Peter Svrcek. Tree level recursion relations in general relativity. 2 2005. arXiv:hep-th/0502160.

[124] Freddy Cachazo, Lionel Mason, and David Skinner. Gravity in Twistor Space and its Grassmannian Formulation. *SIGMA*, 10:051, 2014. arXiv:1207.4712 [hep-th].

[125] Nima Arkani-Hamed and Jaroslav Trnka. The Amplituhedron. *JHEP*, 10:030, 2014. arXiv:1312.2007 [hep-th].

[126] Nima Arkani-Hamed, Yuntao Bai, Song He, and Gongwang Yan. Scattering Forms and the Positive Geometry of Kinematics, Color and the Worldsheet. *JHEP*, 05:096, 2018. arXiv:1711.09102 [hep-th].

[127] Nima Arkani-Hamed, Freddy Cachazo, and Jared Kaplan. What is the Simplest Quantum Field Theory? *JHEP*, 09:016, 2010. arXiv:0808.1446 [hep-th].

[128] Nima Arkani-Hamed, Freddy Cachazo, Clifford Cheung, and Jared Kaplan. A Duality For The S Matrix. *JHEP*, 03:020, 2010. arXiv:0907.5418 [hep-th].

[129] Nima Arkani-Hamed, Jacob L. Bourjaily, Freddy Cachazo, Simon Caron-Huot, and Jaroslav Trnka. The All-Loop Integrand For Scattering Amplitudes in Planar N=4 SYM. *JHEP*, 01:041, 2011. arXiv:1008.2958 [hep-th].

[130] Nima Arkani-Hamed, Jacob Bourjaily, Freddy Cachazo, Alexander Goncharov, Alexander Postnikov, and Jaroslav Trnka. *Grassmannian Geometry of Scattering Amplitudes*. Cambridge University Press, 2016.

[131] Lorenzo Bianchi, Andreas Brandhuber, Rodolfo Panerai, and Gabriele Travaglini. Form factor recursion relations at loop level. *JHEP*, 02:182, 2019. arXiv:1812.09001 [hep-th].

[132] Alex Edison, Enrico Herrmann, Julio Parra-Martinez, and Jaroslav Trnka. Gravity loop integrands from the ultraviolet. *SciPost Phys.*, 10:016, 2021. arXiv:1909.02003 [hep-th].

[133] Zvi Bern, Lance J. Dixon, and David A. Kosower. On-shell recurrence relations for one-loop QCD amplitudes. *Phys. Rev. D*, 71:105013, 2005. arXiv:hep-th/0501240.

[134] Andreas Brandhuber, Bill Spence, and Gabriele Travaglini. From trees to loops and back. *JHEP*, 01:142, 2006. arXiv:hep-th/0510253.

[135] Rutger H. Boels. On BCFW shifts of integrands and integrals. *JHEP*, 11:113, 2010. arXiv:1008.3101 [hep-th].

[136] Rutger H. Boels and Reinke Sven Isermann. Yang-Mills amplitude relations at loop level from non-adjacent BCFW shifts. *JHEP*, 03:051, 2012. arXiv:1110.4462 [hep-th].

[137] Rutger H. Boels and Hui Luo. On-shell recursion relations for generic integrands. 10 2016. arXiv:1610.05283 [hep-th].

[138] J. M. Drummond, J. Henn, V. A. Smirnov, and E. Sokatchev. Magic identities for conformal four-point integrals. *JHEP*, 01:064, 2007. arXiv:hep-th/0607160.

[139] J. M. Drummond, G. P. Korchemsky, and E. Sokatchev. Conformal properties of four-gluon planar amplitudes and Wilson loops. *Nucl. Phys. B*, 795:385–408, 2008. arXiv:0707.0243 [hep-th].

[140] J. M. Drummond, J. Henn, G. P. Korchemsky, and E. Sokatchev. Dual superconformal symmetry of scattering amplitudes in N=4 super-Yang-Mills theory. *Nucl. Phys. B*, 828:317–374, 2010. arXiv:0807.1095 [hep-th].

[141] Vittorio Del Duca, Lance J. Dixon, James M. Drummond, Claude Duhr, Johannes M. Henn, and Vladimir A. Smirnov. The one-loop six-dimensional hexagon integral with three massive corners. *Phys. Rev. D*, 84:045017, 2011. arXiv:1105.2011 [hep-th].

[142] Johannes M. Henn. Dual conformal symmetry at loop level: massive regularization. *J. Phys. A*, 44:454011, 2011. arXiv:1103.1016 [hep-th].

[143] Zvi Bern, Michael Enciso, Harald Ita, and Mao Zeng. Dual Conformal Symmetry, Integration-by-Parts Reduction, Differential Equations and the Nonplanar Sector. *Phys. Rev. D*, 96(9):096017, 2017. arXiv:1709.06055 [hep-th].

[144] James M. Drummond, Johannes M. Henn, and Jan Plefka. Yangian symmetry of scattering amplitudes in N=4 super Yang-Mills theory. *JHEP*, 05:046, 2009. arXiv:0902.2987 [hep-th].

[145] J. M. Drummond and L. Ferro. Yangians, Grassmannians and T-duality. *JHEP*, 07:027, 2010. arXiv:1001.3348 [hep-th].

[146] Niklas Beisert, Johannes Henn, Tristan McLoughlin, and Jan Plefka. One-Loop Superconformal and Yangian Symmetries of Scattering Amplitudes in N=4 Super Yang-Mills. *JHEP*, 04:085, 2010. arXiv:1002.1733 [hep-th].

[147] J. M. Drummond and L. Ferro. The Yangian origin of the Grassmannian integral. *JHEP*, 12:010, 2010. arXiv:1002.4622 [hep-th].

[148] Henriette Elvang and Yu-tin Huang. *Scattering Amplitudes in Gauge Theory and Gravity*. Cambridge University Press, 2015.

[149] Song He, Ricardo Monteiro, and Oliver Schlotterer. String-inspired BCJ numerators for one-loop MHV amplitudes. *JHEP*, 01:171, 2016. arXiv:1507.06288 [hep-th].

[150] Rutger H. Boels. No triangles on the moduli space of maximally supersymmetric gauge theory. *JHEP*, 05:046, 2010. arXiv:1003.2989 [hep-th].

[151] Ricardo Monteiro and Donal O'Connell. The Kinematic Algebra From the Self-Dual Sector. *JHEP*, 07:007, 2011. arXiv:1105.2565 [hep-th].

[152] N. E. J. Bjerrum-Bohr, Poul H. Damgaard, Ricardo Monteiro, and Donal O'Connell. Algebras for Amplitudes. *JHEP*, 06:061, 2012. arXiv:1203.0944 [hep-th].

[153] Ricardo Monteiro and Donal O'Connell. The Kinematic Algebras from the Scattering Equations. *JHEP*, 03:110, 2014. arXiv:1311.1151 [hep-th].

[154] Zvi Bern, Lance J. Dixon, David C. Dunbar, and David A. Kosower. One loop selfdual and N=4 superYang-Mills. *Phys. Lett. B*, 394:105–115, 1997. arXiv:hep-th/9611127.

[155] Song He, Yu-tin Huang, and Congkao Wen. Loop Corrections to Soft Theorems in Gauge Theories and Gravity. *JHEP*, 12:115, 2014. arXiv:1405.1410 [hep-th].

[156] Rutger H. Boels, Reinke Sven Isermann, Ricardo Monteiro, and Donal O'Connell. Colour-Kinematics Duality for One-Loop Rational Amplitudes. *JHEP*, 04:107, 2013. arXiv:1301.4165 [hep-th].

[157] Andreas Brandhuber, Bill Spence, and Gabriele Travaglini. Amplitudes in Pure Yang-Mills and MHV Diagrams. *JHEP*, 02:088, 2007. arXiv:hep-th/0612007.

[158] Carlos R. Mafra and Oliver Schlotterer. Towards one-loop SYM amplitudes from the pure spinor BRST cohomology. *Fortsch. Phys.*, 63(2):105–131, 2015. arXiv:1410.0668 [hep-th].

[159] Marcus Berg, Igor Buchberger, and Oliver Schlotterer. String-motivated one-loop amplitudes in gauge theories with half-maximal supersymmetry. *JHEP*, 07:138, 2017. arXiv:1611.03459 [hep-th].

[160] Giulio Salvatori. 1-loop Amplitudes from the Halohedron. *JHEP*, 12:074, 2019. arXiv:1806.01842 [hep-th].

[161] Nikhil Kalyanapuram and Raghav G. Jha. Positive Geometries for all Scalar Theories from Twisted Intersection Theory. *Phys. Rev. Res.*, 2(3):033119, 2020. arXiv:2006.15359 [hep-th].

[162] John Joseph M. Carrasco and Henrik Johansson. Five-Point Amplitudes in N=4 Super-Yang-Mills Theory and N=8 Supergravity. *Phys. Rev. D*, 85:025006, 2012. arXiv:1106.4711 [hep-th].

[163] Z. Bern, J. J. M. Carrasco, L. J. Dixon, H. Johansson, and R. Roiban. Simplifying Multiloop Integrands and Ultraviolet Divergences of Gauge Theory and Gravity Amplitudes. *Phys. Rev. D*, 85:105014, 2012. arXiv:1201.5366 [hep-th].

[164] J. J. M. Carrasco, R. Kallosh, R. Roiban, and A. A. Tseytlin. On the U(1) duality anomaly and the S-matrix of N=4 supergravity. *JHEP*, 07:029, 2013. arXiv:1303.6219 [hep-th].

[165] Zvi Bern, John Joseph M. Carrasco, Wei-Ming Chen, Henrik Johansson, Radu Roiban, and Mao Zeng. Five-loop four-point integrand of $N = 8$ supergravity as a generalized double copy. *Phys. Rev. D*, 96(12):126012, 2017. arXiv:1708.06807 [hep-th].

[166] Zvi Bern, John Joseph Carrasco, Wei-Ming Chen, Henrik Johansson, and Radu Roiban. Gravity Amplitudes as Generalized Double Copies of Gauge-Theory Amplitudes. *Phys. Rev. Lett.*, 118(18):181602, 2017. arXiv:1701.02519 [hep-th].

[167] Z. Bern, Lance J. Dixon, D. C. Dunbar, M. Perelstein, and J. S. Rozowsky. On the relationship between Yang-Mills theory and gravity and its implication for ultraviolet divergences. *Nucl. Phys. B*, 530:401–456, 1998. arXiv:hep-th/9802162.

[168] Pierre Vanhove. The Critical ultraviolet behaviour of N=8 supergravity amplitudes. 4 2010. arXiv:1004.1392 [hep-th].

[169] Jonas Bjornsson and Michael B. Green. 5 loops in 24/5 dimensions. *JHEP*, 08:132, 2010. arXiv:1004.2692 [hep-th].

[170] Zvi Bern, John Joseph Carrasco, Wei-Ming Chen, Alex Edison, Henrik Johansson, Julio Parra-Martinez, Radu Roiban, and Mao Zeng. Ultraviolet Properties of $\mathcal{N} = 8$ Supergravity at Five Loops. *Phys. Rev. D*, 98(8):086021, 2018. arXiv:1804.09311 [hep-th].

[171] R. Feynman. Closed loop and tree diagrams. 1972.

[172] A. Brandhuber, B. Spence, and G. Travaglini. From trees to loops and back. *Journal of High Energy Physics*, 2006:142–142, 2006.

[173] Simon Caron-Huot. Loops and trees. *JHEP*, 05:080, 2011. arXiv:1007.3224 [hep-ph].

[174] N. Emil J. Bjerrum-Bohr, Tristan Dennen, Ricardo Monteiro, and Donal O'Connell. Integrand Oxidation and One-Loop Colour-Dual Numerators in N=4 Gauge Theory. *JHEP*, 07:092, 2013. arXiv:1303.2913 [hep-th].

[175] Marco Chiodaroli, Qingjun Jin, and Radu Roiban. Color/kinematics duality for general abelian orbifolds of N=4 super Yang-Mills theory. *JHEP*, 01:152, 2014. arXiv:1311.3600 [hep-th].

[176] Alex Edison, Song He, Oliver Schlotterer, and Fei Teng. One-loop Correlators and BCJ Numerators from Forward Limits. *JHEP*, 09:079, 2020. arXiv:2005.03639 [hep-th].

[177] Elliot Bridges and Carlos R. Mafra. Local BCJ numerators for ten-dimensional SYM at one loop. *JHEP*, 07:031, 2021. arXiv:2102.12943 [hep-th].

[178] Carlos R. Mafra. Color-dressed string disk amplitudes and the descent algebra. 8 2021. arXiv:2108.01081 [hep-th].

[179] Eric D'Hoker and D. H. Phong. Two-loop superstrings VI: Non-renormalization theorems and the 4-point function. *Nucl. Phys. B*, 715:3–90, 2005. arXiv:hep-th/0501197.

[180] Tim Adamo and Eduardo Casali. Scattering equations, supergravity integrands, and pure spinors. *JHEP*, 05:120, 2015. arXiv:1502.06826 [hep-th].

[181] Valeriya Talovikova. Riemann-Roch Theorem. `https://www.math.uchicago.edu/~may/VIGRE/VIGRE2009/REUPapers/Talovikova.pdf`, Aug 2009.

[182] Bo Feng, Rijun Huang, and Yin Jia. Gauge Amplitude Identities by On-shell Recursion Relation in S-matrix Program. *Phys. Lett. B*, 695:350–353, 2011. arXiv:1004.3417 [hep-th].

[183] Yin Jia, Rijun Huang, and Chang-Yong Liu. $U(1)$-decoupling, KK and BCJ relations in $\mathcal{N} = 4$ SYM. *Phys. Rev. D*, 82:065001, 2010. arXiv:1005.1821 [hep-th].

[184] N. E. J. Bjerrum-Bohr, Poul H. Damgaard, Bo Feng, and Thomas Sondergaard. Proof of Gravity and Yang-Mills Amplitude Relations. *JHEP*, 09:067, 2010. arXiv:1007.3111 [hep-th].

[185] Z. Bern, Lance J. Dixon, and D. A. Kosower. A Two loop four gluon helicity amplitude in QCD. *JHEP*, 01:027, 2000. arXiv:hep-ph/0001001.

[186] Nathan Berkovits. Infinite Tension Limit of the Pure Spinor Superstring. *JHEP*, 03:017, 2014. arXiv:1311.4156 [hep-th].

[187] Osvaldo Chandia and Brenno Carlini Vallilo. Ambitwistor superstring in the Green–Schwarz formulation. *Eur. Phys. J. C*, 77(7):473, 2017. arXiv:1612.01806 [hep-th].

[188] Eric D'Hoker and D. H. Phong. Two loop superstrings. 1. Main formulas. *Phys. Lett. B*, 529:241–255, 2002. arXiv:hep-th/0110247.

[189] Eric D'Hoker and D. H. Phong. Two loop superstrings. 2. The Chiral measure on moduli space. *Nucl. Phys. B*, 636:3–60, 2002. arXiv:hep-th/0110283.

[190] Eric D'Hoker and D. H. Phong. Two loop superstrings. 3. Slice independence and absence of ambiguities. *Nucl. Phys. B*, 636:61–79, 2002. arXiv:hep-th/0111016.

[191] Eric D'Hoker and D. H. Phong. Two loop superstrings 4: The Cosmological constant and modular forms. *Nucl. Phys. B*, 639:129–181, 2002. arXiv:hep-th/0111040.

[192] Eric D'Hoker and D. H. Phong. Two-loop superstrings. V. Gauge slice independence of the N-point function. *Nucl. Phys. B*, 715:91–119, 2005. arXiv:hep-th/0501196.

[193] Eric D'Hoker and D. H. Phong. Conformal Scalar Fields and Chiral Splitting on Superriemann Surfaces. *Commun. Math. Phys.*, 125:469, 1989.

[194] Nikhil Kalyanapuram. On Chiral Splitting and the Ambitwistor String. 3 2021. arXiv:2103.08584 [hep-th].

[195] Ron Donagi and Edward Witten. Supermoduli Space Is Not Projected. *Proc. Symp. Pure Math.*, 90:19–72, 2015. arXiv:1304.7798 [hep-th].

[196] Michael B. Green, John H. Schwarz, and Edward Witten. *Superstring Theory: 25th Anniversary Edition*, volume 1 of *Cambridge Monographs on Mathematical Physics*. Cambridge University Press, 2012.

[197] Humberto Gomez and Carlos R. Mafra. The closed-string 3-loop amplitude and S-duality. *JHEP*, 10:217, 2013. arXiv:1308.6567 [hep-th].

[198] Nathan Berkovits. New higher-derivative R**4 theorems. *Phys. Rev. Lett.*, 98:211601, 2007. arXiv:hep-th/0609006.

[199] John D. Fay. Theta functions on riemann surfaces. 1973.

[200] Zvi Bern, Scott Davies, and Tristan Dennen. The Ultraviolet Structure of Half-Maximal Supergravity with Matter Multiplets at Two and Three Loops. *Phys. Rev. D*, 88:065007, 2013. arXiv:1305.4876 [hep-th].

[201] Gustav Mogull and Donal O'Connell. Overcoming Obstacles to Colour-Kinematics Duality at Two Loops. *JHEP*, 12:135, 2015. arXiv:1511.06652 [hep-th].

[202] Gang Yang. Color-kinematics duality and Sudakov form factor at five loops for N=4 supersymmetric Yang-Mills theory. *Phys. Rev. Lett.*, 117(27):271602, 2016. arXiv:1610.02394 [hep-th].

[203] Rutger H. Boels, Tobias Huber, and Gang Yang. Four-Loop Nonplanar Cusp Anomalous Dimension in N=4 Supersymmetric Yang-Mills Theory. *Phys. Rev. Lett.*, 119(20):201601, 2017. arXiv:1705.03444 [hep-th].

[204] Song He, Oliver Schlotterer, and Yong Zhang. New BCJ representations for one-loop amplitudes in gauge theories and gravity. *Nucl. Phys. B*, 930:328–383, 2018. arXiv:1706.00640 [hep-th].

[205] Josua Faller and Jan Plefka. Positive helicity Einstein-Yang-Mills amplitudes from the double copy method. *Phys. Rev. D*, 99(4):046008, 2019. arXiv:1812.04053 [hep-th].

[206] Nathan Berkovits. Super-Poincare covariant two-loop superstring amplitudes. *JHEP*, 01:005, 2006. arXiv:hep-th/0503197.

[207] Eric D'Hoker, Carlos R. Mafra, Boris Pioline, and Oliver Schlotterer. Two-loop superstring five-point amplitudes. Part I. Construction via chiral splitting and pure spinors. *JHEP*, 08:135, 2020. arXiv:2006.05270 [hep-th].

[208] John H. Schwarz. Superstring theory. *Physics Reports*, 89(3):223–322, 1982.

[209] Cris Poor. The hyperelliptic locus. *Duke Mathematical Journal*, 76(3):809 – 884, 1994.

[210] Eric D'Hoker and D. H. Phong. The geometry of string perturbation theory. *Rev. Mod. Phys.*, 60:917–1065, Oct 1988.

[211] Shigeaki Tsuyumine. On siegel modular forms of degree three. *American Journal of Mathematics*, 108(4):755–862, 1986.

[212] Eric D'Hoker and D. H. Phong. Asyzygies, modular forms, and the superstring measure. I. *Nucl. Phys. B*, 710:58–82, 2005. arXiv:hep-th/0411159.

[213] Eric D'Hoker and D. H. Phong. Asyzygies, modular forms, and the superstring measure II. *Nucl. Phys. B*, 710:83–116, 2005. arXiv:hep-th/0411182.

[214] Sergio L. Cacciatori, Francesco Dalla Piazza, and Bert van Geemen. Modular Forms and Three Loop Superstring Amplitudes. *Nucl. Phys. B*, 800:565–590, 2008. arXiv:0801.2543 [hep-th].

[215] Francesco Dalla Piazza and Bert van Geemen. Siegel modular forms and finite symplectic groups. *Adv. Theor. Math. Phys.*, 13(6):1771–1814, 2009. arXiv:0804.3769 [math.AG].

[216] Samuel Grushevsky and Riccardo Salvati Manni. The Vanishing of two-point functions for three-loop superstring scattering amplitudes. *Commun. Math. Phys.*, 294:343–352, 2010. arXiv:0806.0354 [hep-th].

[217] Marco Matone and Roberto Volpato. Superstring measure and non-renormalization of the three-point amplitude. *Nucl. Phys. B*, 806:735–747, 2009. arXiv:0806.4370 [hep-th].

[218] Eric D'Hoker, Carlos R. Mafra, Boris Pioline, and Oliver Schlotterer. Two-loop superstring five-point amplitudes. Part II. Low energy expansion and S-duality. *JHEP*, 02:139, 2021. arXiv:2008.08687 [hep-th].

[219] Eric D'Hoker and Oliver Schlotterer. Two-loop superstring five-point amplitudes III, construction via the RNS formulation: even spin structures. 8 2021. arXiv:2108.01104 [hep-th].

[220] Samuel Grushevsky. Superstring scattering amplitudes in higher genus. *Commun. Math. Phys.*, 287:749–767, 2009. arXiv:0803.3469 [hep-th].

[221] Riccardo Salvati-Manni. Remarks on Superstring amplitudes in higher genus. *Nucl. Phys. B*, 801:163–173, 2008. arXiv:0804.0512 [hep-th].

[222] Sergio L. Cacciatori, Francesco Dalla Piazza, and Bert van Geemen. Genus four superstring measures. *Lett. Math. Phys.*, 85:185–193, 2008. arXiv:0804.0457 [hep-th].

[223] Francesco Dalla Piazza. More on superstring chiral measures. *Nucl. Phys. B*, 844:471–499, 2011. arXiv:0809.0854 [hep-th].

[224] Samuel Grushevsky and Riccardo Salvati Manni. The superstring cosmological constant and the Schottky form in genus 5. *Am. J. Math.*, 133:1007–1027, 2011. arXiv:0809.1391 [math.AG].

[225] Francesco Dalla Piazza. Construction of chiral superstring measure. In *18th SIGRAV Conference*, 9 2009.

[226] Marco Matone and Roberto Volpato. Getting superstring amplitudes by degenerating Riemann surfaces. *Nucl. Phys. B*, 839:21–51, 2010. arXiv:1003.3452 [hep-th].

[227] Petr Dunin-Barkowski, Alexey Sleptsov, and Abel Stern. NSR superstring measures in genus 5. *Nucl. Phys. B*, 872:106–126, 2013. arXiv:1208.2324 [hep-th].

[228] Joseph A. Farrow and Arthur E. Lipstein. From 4d Ambitwistor Strings to On Shell Diagrams and Back. *JHEP*, 07:114, 2017. arXiv:1705.07087 [hep-th].

[229] Yvonne Geyer, Lionel Mason, and David Skinner. Ambitwistor Strings in Six and Five Dimensions. 12 2020. arXiv:2012.15172 [hep-th].

[230] Yvonne Geyer and Lionel Mason. Polarized Scattering Equations for 6D Superamplitudes. *Phys. Rev. Lett.*, 122(10):101601, 2019. arXiv:1812.05548 [hep-th].

[231] Tim Adamo, Lionel Mason, and Atul Sharma. Celestial amplitudes and conformal soft theorems. *Class. Quant. Grav.*, 36(20):205018, 2019. arXiv:1905.09224 [hep-th].

[232] Eduardo Casali and Atul Sharma. Celestial double copy from the worldsheet. *JHEP*, 05:157, 2021. arXiv:2011.10052 [hep-th].

[233] Luis Alvarez-Gaume, Gregory W. Moore, and Cumrun Vafa. Theta Functions, Modular Invariance and Strings. *Commun. Math. Phys.*, 106:1–40, 1986.